PLACE IN RETURN BOX to remove this checkout from your record.
TO AVOID FINES return on or before date due.
MAY BE RECALLED with earlier due date if requested.

DATE DUE	DATE DUE	DATE DUE
JAN 1 0 2011		
~~AUG 3 1 2012~~		
1107 13		

6/07 p:/CIRC/DateDue.indd-p.1

MAPPING AND MODELING GLACIAL LAKE ALGONQUIN IN NORTHERN MICHIGAN AND WESTERN ONTARIO WITH MODELS OF UNCERTAINTY

by

Scott A. Drzyzga

A DISSERTATION

Submitted to
Michigan State University
in partial fulfillment of the requirements
for the degree of

DOCTOR OF PHILOSOPHY

Department of Geography

2007

ABSTRACT

MAPPING AND MODELING GLACIAL LAKE ALGONQUIN
IN NORTHERN MICHIGAN AND WESTERN ONTARIO
WITH MODELS OF UNCERTAINTY

By

Scott A. Drzyzga

This dissertation is the first work to map the "Upper Group" sequence of glacial Lake Algonquin water planes in northern Michigan and western Ontario. Position data were collected from relict shoreline features, which were uplifted during isostatic readjustment after deglaciation. Geostatistical models were built to describe regional uplift trends and reconstruct the now warped water planes associated with the Main, Ardtrea, Upper Orillia and Lower Orillia phases. Each water plane model was used to adjust a digital contemporary elevation model and create a digital pro-glacial elevation model, which reflected both local topography and the regional pattern of isostatic depression that existed during that particular lake phase. Data were subjected to accuracy assessments that permitted models of uncertainty about input data errors to be included in each landscape reconstruction process. Accordingly, each map depicts the extent of a former lake phase and expresses two components of uncertainty about predicted paleoshoreline locations: one associated with the precision of the predicted water

plane elevation; and another associated with co-located uncertainty about error in the digital contemporary elevation model.

Important findings of this work include, but are not limited to: a) Main phase and lower shorelines found on Cockburn Island, Ontario, suggest the island was deglaciated before the outlet at North Bay, Ontario was opened; b) relict features at Beaver Island, Michigan, indicate the Main and Ardtrea phases extended into the Michigan basin, but data collected near Little Traverse Bay, Michigan, suggest many "highest" glacial Lake Algonquin shorelines in the Michigan basin do not correlate with the Main phase; and c) similarities between isobases mapped during this work and recently published isobases that show contemporary uplift rates suggest that the regional pattern of isostatic readjustment have not changed much during the last 11,000 years.

This study also found evidence of convergence between the Main and Ardtrea water planes, which suggests differential uplift relative to the Fenelon Falls outlet was the cause of shoreline deformation and tilt during these phases. This study does not resolve the question, however, of where glacial Lake Algonquin stood in the southern parts of the Huron and Michigan basins.

Copyright by
SCOTT A. DRZYZGA
2006

ACKNOWLEDGEMENTS

I owe a special thanks to Ashton Shortridge for accepting the responsibility of advising me during his first and busy years at Michigan State University, and for his time and commitment ever since. Not only has he encouraged me to think in new ways and supported my professional endeavors, he has encouraged me to express my opinions in my writing and to not conceal them behind the curtain of absolute objectivity.

I am grateful for each member of my doctoral committee. I thank Randy Schaetzl for recruiting me into his Seminar in Physical Geography; the experience truly inspired this work and provided me with valuable opportunities to publish early in my career. I thank Judy Olson for helping me to think through many mapping problems; not the least was learning to understand how map projections and coordinate systems really work. From Judy, I also learned the values of knowing your audience and good map design. And, I am grateful for the many conversations I shared with Alan Arbogast; particularly one on a hot day at Ludington State Park. We climbed atop a large sand dune and looked over many others situated between Lake Michigan and Hamlin Lake. Alan talked about how he could see the landscape evolve in his mind's eye. He could see winds, changes in water level, stabilization and destabilization, and sands burying soils. At the time, I just stood there and wondered because I saw

only sand and junipers. That conversation stuck with me, however, because it let me realize I needed to "see" Lake Algonquin as Alan had "seen" his dunes if I were to be successful in this work, and for it to be accepted by others. That moment fully arrived while I, alone on an uninhabited island, was standing on a relict offshore bar and looking at a relict wave-cut bluff; I could see those ancient waves break and those waters swash where today no water is present. I see those waves still and have owned my research ever since.

I thank Dr. Grahame Larson, of the Department of Geology, for serving as the Dean of the College of Social Science's representative at my dissertation defense. His questions helped me to identify and recognize valuable findings that I had overlooked. I enjoyed learning from him.

I extend gratitude and thanks to Mr. L. Avra, of the Huron Timber Company of Thessalon, Ontario; my work at Cockburn Island would not have been possible without his permission or the assistance provided to me by his foreman and crew. I also thank Mr. H. McQuarrie, a retired logger and seasonal resident of Cockburn Island, who gave me his hand-drafted map of properties, logging roads and foot trails. Funding for fieldwork was provided by the Association of American Geographers via a Doctoral Dissertation Improvement Grant, and a Graduate Research Fellowship from the Department of Geography at Michigan State University.

I extend gratitude and thanks to Drs. P. F. Karrow, W. R. Cowan and C. F. M. Lewis, and to Kevin Kincare and Beth Weisenborn, for sharing data and insights regarding glacial Lake Algonquin.

I thank Rick and Janis Herman, my wonderful cousins, for graciously providing me a home while I was in Michigan and conducting field work. I will always remember our morning coffees, and those afternoons when Rick would help me clear my head with a round of golf and a cold beer.

Last but not least, I thank Cathryn Dowd for supporting me while we were in Illinois and I was getting my research off the ground, for helping me return to Michigan to conduct fieldwork, and for putting up with me while we were in Pennsylvania and I was trying simultaneously to finish my dissertation and start a new career. I owe a tremendous debt to her.

TABLE OF CONTENTS

LIST OF TABLES xi

LIST OF FIGURES xiv

CHAPTER 1: INTRODUCTION 1
- Background about glacial Lake Algonquin 2
- Statement of problem 4
- Statement of purpose and research objectives 5
- Definitions of key terms 6
  - Error 7
  - Accuracy 7
  - Precision 7
  - Uncertainty 8
  - Elevation 8
  - Location 9
  - Position 9
- Justification for research 9
- Organization of the dissertation 11

CHAPTER 2: LAKE LEVELS AND SHORELINES 14
- Introduction 14
- A word about shorelines 16
- Glacial Lake Algonquin 17
- Relict shoreline indicators and water level proxies 27
- Variation in Great Lakes water levels 36
  - Short-term events 38
  - Cyclic fluctuations 40
  - Long-term trends 43
  - Summary 44
- Summary 46

CHAPTER 3: METHODS AND FIELD CAMPAIGNS 48
- Introduction 48
- The initial glacial Lake Algonquin dataset 48
- Opportunities to improve the glacial Lake Algonquin dataset 51
- Shoreline identification, bluff selection, and sampling methods 53
- Data processing 58
- Summary of prior mapping campaigns 61
- Mapping campaigns conducted for this work 64

Cockburn Island, Ontario 67
Sugar Island, Michigan 74
Rexford, Michigan 76
The Munuscong Islands 79
Kincheloe, Michigan 82
Mackinac Island, Michigan 83
The Douglas Lake area, Michigan 87
Beaver Island, Michigan 92
From Petoskey to Traverse City, Michigan 99
The Leelanau Peninsula, Michigan 104
From Mullet Lake to Alpena, Michigan 108
From Alpena to the Au Sable River, Michigan 110
From the Au Sable River to Saganing, Michigan 112
Summary 116

CHAPTER 4: ACCURACY ASSESSMENTS 126
Introduction 126
Two datasets 127
Assessment of the glacial Lake Algonquin dataset 129
Analysis of potential selection errors 130
Ground control 131
Analysis of measurement errors 134
Cumulative elevation errors in paleoshoreline data 140
Assessment of the National Elevation Dataset 142
Geoprocessing the NED 145
Hypsometric analysis 146
Ground control 150
Select results of the first exploratory analysis 152
Complete results of the second exploratory analysis 157
Covariation with location, elevation, and slope 164
Spatial autocorrelation 170
Summary 170

CHAPTER 5: THE SPATIAL MODEL 175
Introduction 175
Modeling outcomes of a spatial random process 176
Building the spatial model 187
Models of elevation errors in the paleoshoreline elevation data 192
Assumed model of selection errors 192
Empirical model of measurement errors 194
Model of cumulative errors 195
Models of differentially upwarped water planes 197
A note about coordinate transformation 201
Main phase 202

Ardtrea phase..... 207
Upper Orillia phase..... 212
Lower Orillia phase..... 217
Cedar Point phase..... 221
Models of errors in the digital elevation model..... 223
Variography..... 225
Making predictions..... 230
Running the spatial model..... 232
Summary..... 236

CHAPTER 6: MAPPING THE RESULTS..... 241
Introduction..... 241
Summary of results obtained from the spatial model..... 241
Maps of glacial Lake Algonquin shorelines..... 246
The Main phase..... 253
The Ardtrea phase..... 256
The Upper Orillia phase..... 258
The Lower Orillia phase..... 260
Maps of glacial Lake Algonquin shorelines that reveal uncertainty..... 261
Composites map of Main Lake Algonquin and the Upper Group..... 264
Summary..... 279

CHAPTER 7: CONCLUSIONS..... 283
Introduction..... 283
Re-evaluation of research objectives..... 284
To find and survey relict shoreline features that best serve as 284
To reconstruct water planes associated with glacial Lake Algonquin 290
To reconstruct the landscape associated with each lake phases and 295
To express the degree of uncertainty with which each glacial Lake 296
Future research..... 297
Glacial Lake Algonquin..... 298
Topographic map analysis..... 300
Visualizing uncertainty..... 300
Global climate change and sea-level rise..... 301
Final thoughts..... 302

APPENDICES..... 297
Appendix A: The glacial Lake Algonquin dataset..... 298
Appendix B: Scripts written for use with R..... 317

REFERENCES..... 326

LIST OF TABLES

Table 2.1: Glacial Lake Algonquin lake phases with time frames. Lake phases are listed in descending order in terms of both contemporary elevation and age. Radiocarbon dates are from Karrow et al. (1975)..... 25

Table 2.2: Seasonal variation in contemporary Great Lakes water levels (Quinn, 2002; NOAA, 2006)..... 37

Table 2.3: Potential range of Great Lakes water-level fluctuations (see text for references)..... 45

Table 3.1: Approximate elevations for glacial Lake Algonquin water planes and the Nipissing water plane at Sault Ste. Marie and Manitoulin Island, Ontario (Cowan, 1985)..... 62

Table 3.2: Lake level elevations for glacial Lake Algonquin water planes and the Nipissing water plane at the southern end of proto-St. Joseph Island, Ontario (Karrow, 1987)..... 63

Table 3.3: Approximate elevations of glacial Lake Algonquin water planes at Cockburn Island, Ontario..... 72

Table 3.4: Approximate elevations of glacial Lake Algonquin water planes and the Nipissing water plane measured in western Chippewa County..... 78

Table 3.5: Approximate elevations of glacial Lake Algonquin water planes measured in the Munuscong Islands region..... 82

Table 3.6: Approximate elevations of glacial Lake Algonquin water planes measured at Mackinac Island, Michigan..... 87

Table 3.7: Approximate elevations of glacial Lake Algonquin water planes and the Nipissing water plane measured in the Douglas Lake area..... 91

Table 3.8: Approximate elevations of glacial Lake Algonquin water planes measured at Beaver Island, Michigan..... 99

Table 4.1: Vertical differences between measured and published heights. NGS bench marks are indicated by their Permanent Identifiers (PIDs)..... 133

Table 4.2: Summary statistics that describe the set of differences between measured and published bench mark elevations..... 135

Table 4.3: Results of Kendall's non-parametric tests for associations between position and elevation error..... 139

Table 4.4: Horizontal differences between measured and published NGS benchmark locations..... 140

Table 4.5: Summary statistics that describe differences between actual and co-located elevations in the original and corrected DEM surfaces..... 154

Table 4.6: Summary statistics that describe differences between actual and co-located DEM elevations..... 159

Table 4.7: Results of two-sample difference-of-means tests among DEM subsets..... 163

Table 4.8: Results of Kendall's tests for association between easy-to-measure landscape variables and: a) signed error and b) unsigned error..... 166

Table 5.1: Main phase trend parameters estimated via ordinary least squares. 203

Table 5.2: Summary of Main surface residuals obtained via ordinary least squares (OLS), cross-validated universal kriging with a nugget model only (CV.NUG), and cross-validated universal kriging with a Matern model of spatial structure (CV.MAT)..... 203

Table 5.3: Ardtrea phase trend parameters estimated via ordinary least squares (OLS), and generalized least squares (GLS)..... 209

Table 5.4: Summary statistics for residuals (n=41) obtained from Ardtrea water plane models predicted via ordinary least squares (OLS), generalized least squares (GLS), and cross-validated universal kriging (CV.NUG)..... 210

Table 5.5: Upper Orillia phase trend parameters estimated via ordinary least squares..... 214

Table 5.6: Summary statistics for residuals (n=33) obtained from Upper Orillia elevation trend models obtained via ordinary least squares (OLS), cross-validated universal kriging with pure nugget model (CV.NUG) and cross-validated universal kriging with anisotropic covariance model (CV.MAT)..... 214

Table 5.7: Lower Orillia phase trend model parameters estimated via ordinary least squares (OLS), and generalized least squares (GLS)..... 218

Table 5.8: Summary statistics for residuals (n=16) obtained from Lower Orillia water plane models predicted via ordinary least squares (OLS), generalized least squares (GLS) and cross-validated universal kriging (CV.UK)..... 219

Table 5.9: Cedar Point phase trend parameters estimated via ordinary least squares (OLS)..... 222

Table 6.1: Estimates of total land area under water during each lake phase. Percentages of contemporary land area under water are indicated in parentheses..... 246

Table A.1: The glacial Lake Algonquin datatset..... 298

LIST OF FIGURES

Figure 1.1: The extents of glacial Lake Algonquin hypothesized by Hough (1958) and Larsen (1987)..... 3

Figure 2.1: Terms used to describe morphologic features along the beach profile (adapted from Komar, 1998)..... 15

Figure 2.2: Baedke et al. (2004) used buried foreshore deposits as shoreline indicators. Figure adapted from descriptions in their text and from Figure 2.6 in Johnston (2004)..... 32

Figure 2.3: Schaetzl et al. (2002) used bouldery/gravelly lags at the bases of wave-cut bluffs as shoreline indicators. Figure was adapted from their Figure 2b (p.405)..... 34

Figure 3.1: The study area explored by Schaetzl et al. (2002), points in the original glacial Lake Algonquin dataset, and the extent of the Main phase of glacial Lake Algonquin as they had determined it. Figure adapted from their Figure 1..... 50

Figure 3.2: Map of the current study area with names of places and features mentioned in the text. County boundaries and names added for reference..... 52

Figure 3.3: Schaetzl et al. (2002) used bouldery/gravelly lags at the bases of wave-cut bluffs as shoreline indicators. Figure was adapted from their Figure 2b (p.405)..... 54

Figure 3.4: Index map for smaller-scaled maps that show field campaigns and field sites mentioned in this chapter..... 66

Figure 3.5: Relict bluff sites at Cockburn Island, Ontario. Sites are labeled with a unique site identification number and an elevation value (e.g., 642: 200 m)..... 68

Figure 3.6: Image of a relict bluff on the south side of McCaigs Hill, Cockburn Island, Ontario..... 70

Figure 3.7: Diagram of the relict bluff shown in Figure 3.6. Shoreline positions were measured at gravel lag situated at the base of the bluff..... 70

Figure 3.8: Apparent contours across the Main Lake Algonquin water plane.. 73

Figure 3.9: Relict bluff sites at Sugar Island, Michigan. Sites are labeled with a unique site identification number and an elevation value (e.g., 642: 200 m). Also shown are the locations of features surveyed by Cowan (1985)..... 75

Figure 3.10: Relict bluff sites near Rexford, Michigan. Sites are labeled with a unique site identification number and an elevation value (e.g., 642: 200 m).. 77

Figure 3.11: Relict bluff sites in the Munuscong Islands region. Sites are labeled with a unique site identification number and an elevation value (e.g., 642: 200 m)..... 81

Figure 3.12: Relict bluff sites at Mackinac Island. Sites are labeled with a unique site identification number and an elevation value (e.g., 642: 200 m).... 85

Figure 3.13: Relict bluff sites in the Douglas Lake area. Sites are labeled with a unique site identification number and an elevation value (e.g., 642: 200 m)... 90

Figure 3.14: Relict bluff sites on Beaver Island, Michigan. Sites are labeled with a unique site identification number and an elevation value (e.g., 642: 200 m)..... 94

Figure 3.15: Exposed sediment profile in a gravel pit located near the southern end of proto-Beaver Island. A 2-foot carpenter's level is shown for scale..... 98

Figure 3.16: Relict bluff sites near Petoskey, Michigan. Sites are labeled with a unique site identification number and an elevation value (e.g., 642: 200 m)... 100

Figure 3.17: Relict bluff sites on the Leelanau Peninsula. Sites are labeled with a unique site identification number and an elevation value (e.g., 642: 200 m)..... 103

Figure 3.18: Relict bluff sites in the Black Lake area. Sites are labeled with a unique site identification number and an elevation value (e.g., 642: 200 m).... 108

Figure 3.19: Relict bluff sites in the Long Lake area. Sites are labeled with a unique site identification number and an elevation value (e.g., 642: 200 m).... 109

Figure 3.20: Relict bluff sites near Alpena, Michigan. Sites are labeled with a unique site identification number and an elevation value (e.g., 642: 200 m)..... 111

Figure 3.21: Relict bluff sites in near Harrisville, Michigan. Sites are labeled with a unique site identification number and an elevation value (e.g., 642: 200 m)..... 112

Figure 3.22: Relict bluff sites in near Oscoda, Michigan. Sites are labeled with a unique site identification number and an elevation value (e.g., 642: 200 m)..... 114

Figure 4.1: Distribution of error in sampled bench mark elevations: a) Stem and leaf plot - solid line denotes the decimal place; and b) q-q plot of standardized errors with a one-to-one line and 90% confidence envelope..... 135

Figure 4.2: Scatterplots of signed error in sampled bench mark elevations and position. Errors and elevations are reported in meters. Latitude and Longitude values are reported in decimal degrees..... 137

Figure 4.3: Scatterplots of unsigned error in sampled bench mark elevations and position. Errors and elevations are reported in meters. Latitude and Longitude values are reported in decimal degrees..... 138

Figure 4.4: Frequency histograms of elevation. Bin width is one meter..... 148

Figure 4.5: Histograms of: a) 529 check point elevations; and b) all DEM elevations in the study area. The difference between frequency scales is the results of unequal sample sizes..... 152

Figure 4.6: Scatterplots of DEM-reported and actual elevations for the (a) original DEM and for (b) the corrected DEM..... 153

Figure 4.7: Scatterplots of DEM error and the linear components of slope aspect..... 155

Figure 4.8: Map of DEM errors at control point locations. The map reveals no global pattern but suggests error values exhibit some spatial continuity at short distances. The image is presented in color..... 158

Figure 4.9: Histograms of elevation errors in the DEM..... 160

Figure 4.10: Q-Q plots of standardized elevation errors in the DEM..... 161

Figure 4.11: Scatterplots of: a) signed error and slope gradient; and b) unsigned error and slope gradient. Black lines drawn to emphasize zero error..... 169

Figure 4.12: Map and scatterplot of ground control locations used to assess error in the Ontario subset..... 169

Figure 5.1: The spatial model Schaetzl et al. (2002) used to reconstruct landscapes in northern Michigan associated with glacial Lake Algonquin..... 188

Figure 5.2: The spatial model used in this work to digitally reconstruct water planes and landscapes in northern Michigan and western Ontario that were associated with glacial Lake Algonquin. The model was run 100 times for each water plane, which produced a set of 100 results that were summarized to reveal the influences of input data errors..... 191

Figure 5.3: Histograms of errors generated randomly. Error values are binned in 0.25 m intervals..... 195

Figure 5.4: Histogram of cumulative paleoshoreline elevation errors. Error values are binned in 0.25 m intervals. Frequency scale is different than that used in Figure 5.2..... 197

Figure 5.5: Empirical variograms of Main trend surface residuals generated via ordinary least squares. Solid lines represent fitted variogram models..... 205

Figure 5.6: The Main Algonquin water plane: a) predicted elevations are contoured with a 10-meter interval; and b) greater uncertainties are expressed with darker gray tones. Sample sites are shown as black dots..... 207

Figure 5.7: Empirical variogram model fitted to the spatial structure of Ardtrea water plane residuals generated during ordinary least squares..... 210

Figure 5.8: The Ardtrea phase water plane: a) predicted elevations are contoured with a 10-meter interval; and b) greater uncertainties are expressed with darker gray tones. Sample sites are shown as black dots..... 211

Figure 5.9: Spatial structure of residuals obtained during attempts to model the Upper Orillia water plane via ordinary least squares..... 215

Figure 5.10: The Upper Orillia phase water plane: a) predicted elevations are contoured with a 10-meter interval; and b) greater prediction uncertainties are expressed with darker gray tones. Sample sites are shown as black dots... 217

Figure 5.11: Spatial structure of OLS residuals generated during attempts to model the Lower Orillia water plane..... 219

Figure 5.12: The Lower Orillia phase water plane: a) predicted elevations are contoured with a 10-meter interval; and b) greater prediction uncertainties are expressed with darker gray tones. Sample sites are shown as black dots... 221

Figure 5.13: Empirical semi-variograms and variogram models for DEM subsets..... 227

Figure 5.14: Composite surface of predicted DEM errors. The image in this dissertation is presented in color..... 231

Figure 5.15: Uncertainty in the surface of predicted DEM errors. Darker tones are associated with larger confidence intervals and hence greater uncertainties. Areas shown in white were masked from analysis to facilitate computation..... 232

Figure 5.16: Composite surfaces of DEM errors. Cells shown in gray were masked from analysis to facilitate computation, but later set to zero. The image in this dissertation is presented in color..... 234

Figure 5.17: Contemporary uplift rates (cm/century) derived from the ICE-3G geophysical model (Tushingham and Peltier, 1991). Figure adapted from Tushingham (1992: 445)..... 238

Figure 5.18: Contemporary uplift rates (cm/century) derived from historical lake gauge data. Figure adapted from Mainville and Craymer (2005: 1077).... 239

Figure 6.1: Predicted shorelines of the Main phase of glacial Lake Algonquin in the study area. Shorelines are represented as blackened areas; greater widths imply greater uncertainty about shoreline location..... 248

Figure 6.2: Predicted shorelines of the Ardtrea phase of glacial Lake Algonquin in the study area. Shorelines are represented as blackened areas; greater widths imply greater uncertainty about shoreline location..... 249

Figure 6.3: Predicted shorelines of the Upper Orillia phase of glacial Lake Algonquin in the study area. Shorelines are represented as blackened areas; greater widths imply greater uncertainty about shoreline location..... 250

Figure 6.4: Predicted shorelines of the Lower Orillia phase of glacial Lake Algonquin in the study area. Shorelines are represented as blackened areas; greater widths imply greater uncertainty about shoreline location..... 251

Figure 6.5: The Main phase of glacial Lake Algonquin. Darker tones indicated greater uncertainties about the predicted water plane. The image in this dissertation is presented in color 265

Figure 6.6: The Ardtrea phase of glacial Lake Algonquin. Darker tones indicated greater uncertainties about the predicted water plane. The image in this dissertation is presented in color 266

Figure 6.7: The Upper Orillia phase of glacial Lake Algonquin. Darker tones indicated greater uncertainties about the predicted water plane. The image in this dissertation is presented in color 267

Figure 6.8: The Lower Orillia phase of glacial Lake Algonquin. Darker tones indicated greater uncertainties about the predicted water plane. The image in this dissertation is presented in color 267

Figure 6.9: The Main (dark gray), Ardtrea (pink), Upper Orillia (purple), and Lower Orillia (green) phases of Lake Algonquin. The image in this dissertation is presented in color..... 269

Figure 6.10: Areas on Cockburn Island that were predicted to be above glacial Lake Algonquin water levels. The extent of this figure corresponds with the extent of Figure 3.5. The image in this dissertation is in color..... 270

Figure 6.11: Areas in the Munuscong Island region that were predicted to be above glacial Lake Algonquin water levels. The extent of this figure corresponds with the extent of Figure 3.11. The image in this dissertation is in color..... 271

Figure 6.12: Areas in the Douglas Lake area that were predicted to be above glacial Lake Algonquin water levels. This extent of this figure corresponds with the extent of Figure 3.13. The image in this dissertation is presented in color..... 272

Figure 6.13: Areas near Charlevoix that were predicted to be above glacial Lake Algonquin water levels. This extent of this figure corresponds with the extent of Figure 3.16. The image in this dissertation is presented in color..... 274

Figure 6.14: Areas south of Alpena, Michigan, predicted to be above glacial Lake Algonquin water levels. This extent of this figure corresponds with the extent of Figure 3.20. The image in this dissertation is presented in color..... 275

Figure 6.15: Areas near Oscoda, Michigan, predicted to be above glacial Lake Algonquin water levels. This extent of this figure corresponds with the extent of Figure 3.22. The apparent line west of Oscoda marks the southern limit of the study area. The image in this dissertation is presented in color.... 276

Figure 6.16. The Rapid River outwash fan/delta during the: a) Main; b) Ardtrea; c) Upper Orillia; and d) Lower Orillia phases. Pictured is a portion of the USGS 1:24,000 Torch River 7.5 Minute Series Quadrangle, but rescaled to 1:63,500 for display. Darkened areas are predicted to have been under water at with 90% confidence. The image in this dissertation is presented in color..... 277

Figure 6.17. Pullup Lake and the surrounding area during the : a) Main; b) Ardtrea; c) Upper Orillia; and d) Lower Orillia phases. Pictured is a composite of the USGS 1:24,000 Gilchrist and Roberts Corner 7.5 Minute Series Quadrangles, but rescaled to 1:63,500 for display. Darkened areas are predicted to have been under water with 90% confidence. The image in this dissertation is presented in color..... 278

CHAPTER 1: INTRODUCTION

This dissertation reports research about reconstructing and visualizing a sequence of pro-glacial lakes that existed in the Great Lakes basin more than 10,000 years ago. The sequence, known as glacial Lake Algonquin, cannot be observed directly, but its existence is inferred from relict shoreline features perched above contemporary lake levels.

The tasks of mapping relict shoreline features and drawing lines on maps to reconnect them are made difficult by several factors: some features exhibit evidence of many water levels while others exhibit evidence of only one; long distances separate many relict features; and the earth's surface has been differentially lifted and tilted in the Great Lakes region, so different features created along the perimeter of the same water surface might no longer be situated along the same plane of elevation. Accordingly, there is some confusion in the literature regarding the numbers of water levels and lake phases that existed, and which shoreline features belong to which lake phase (Schaetzl et al., 2002). This work enlists the power of computers and geostatistical methods to explore and analyze paleoshoreline data, to build and test spatial models of differential uplift and tilt, and to reconstruct some of these ancient landscapes.

This research is much more than reconnecting old bits of shorelines; it is about working with imperfect data and dealing with uncertainties that propagate through spatial models and into results. Moreover, shorelines are not static like

the lines drawn on maps to represent them. They are dynamic over multiple spatial and temporal scales. This research attempts to describe completely what is known and knowable about shoreline locations. Ultimately, this work develops a new way of looking at the land-water interface and offers a stochastic representation --- a fundamental breakthrough in the way shorelines can be visualized.

Brief background about glacial Lake Algonquin

Glacial Lake Algonquin was a sequence of pro-glacial lakes in the Great Lakes basin (Figure 1.1). It maintained relative high water levels from 11,200 to 10,400 yr BP [1] (see Figure 12 in Karrow, 1975) and developed conspicuous shoreline features (Larson and Schaetzl, 2001). As the Laurentide glacier receded from the basin, lower outlets were uncovered and lake levels fell in stages (Larson and Schaetzl, 2001). The land surface rebounded upward as the weight of the ice was removed; the adjustment process is called *isostatic rebound.* Locations in northern Michigan and Ontario, which are closer to the former centers of ice loading, have rebounded at rates faster than locations in southern Michigan (The Coordinating Committee on Great Lakes Basic Hydraulic and Hydrologic Data, 1977, 2001). Consequently, landforms associated with the sequence have become differentially lifted and tilted.

---

[1] Conventional radiocarbon ages are reported in years before present (yr BP). The datum, 0 yr BP, corresponds to calendar year 1950 AD.

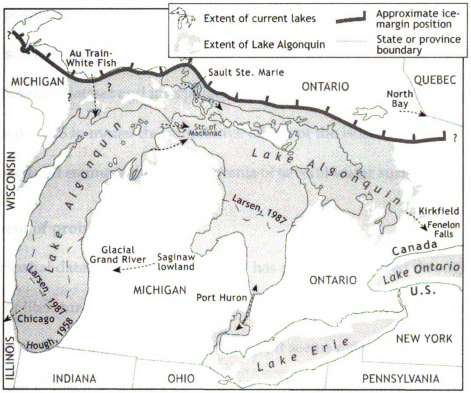


Figure 1.1: The extents of glacial Lake Algonquin hypothesized by Hough (1958) and Larsen (1987).

Much has been written about how glacial Lake Algonquin was formed (Spencer, 1891; Gilbert, 1898; Goldthwait, 1908; Leverett and Taylor, 1915; and Stanley, 1936), but little agreement exists about the elevations and spatial extents of its water surfaces (Hough, 1958; Futyma, 1981; Larsen, 1987; and see Figure 1.1). Little agreement exists because the earth's surface has been lifted and tilted over the past 10,000 years and many relict landforms have been altered by natural and human processes; some were buried or reworked by later lake transgressions. Uncertainty about the timing and extents of this lake sequence prompted an extensive survey by Schaetzl et al. (2002). The authors employed

global positioning technology to measure positions along relict Lake Algonquin features. They used a GIS and a digital elevation model to analyze their paleoshoreline dataset and interpolate unknown shoreline locations. In brief, they used a GIS to model the cumulative effects of the isostatic rebound process over space and estimate the spatial extents of several water surfaces.

Statement of problem

Spatial data quality is a theme that has ebbed and flowed through the course of literature devoted to Geographic Information Systems (GIS) and Geographic Information Science (GISc). Yet, it seems many people are indifferent to this line of work because the same warnings have been issued time and time again. For example, Goodchild and Gopal (1989) claimed virtually all spatial datasets stored in a GIS are, to some extent, contaminated by error. Thirteen years later, Heuvelink and Burrough repeated the same message: "data stored in a spatial database are rarely, if ever, truly free of error" (Heuvelink and Burrough, 2002: 111).

Burrough (1992) once baited the spatial modeling community to include assessments of spatial data quality and error propagation as ingredients of *intelligent* spatial model design. The community at large did not take the bait and Heuvelink (1998) was compelled to reiterate the dangers in work that utilizes GIS yet fails to assess errors inherent in the data sets used or propagated through the spatial models employed. Together, Heuvelink and Burrough (2002)

have argued it is crucial "to know how accurate the data contained in spatial databases really are" (p.111), because without that knowledge neither the true value of the information derived, nor the correctness of the decisions they support can be evaluated.

Assessing spatial data quality and decontaminating spatial datasets are difficult and often tedious and frustrating tasks for in most cases only imperfect knowledge exists about the amount of error contained in any one observation, let alone among any set of observations. Data errors, inaccuracies, or imprecision, even when acknowledged, are often absorbed into analyses; their impacts on results left unexamined and potential consequences ignored. A need exists to demonstrate the value of assessing spatial data quality and uncertainty propagation in work that utilizes GIS. Perhaps Motro summarized this need best when he wrote:

> Uncertainty permeates our understanding of the real world. The purpose of information systems is to model the real world. Hence information systems must be able to deal with uncertainty (Motro, 1993, cited in Parsons, 1996: 2).

Statement of purpose and research objectives

The purpose of this research is to demonstrate the value of assessing spatial data quality, incorporating information and uncertainty about input data errors into spatial model design, and visualizing uncertainties propagated

through work accomplished within a GIS environment. To achieve this end, this work reconstructs the paleolandscapes of glacial Lake Algonquin, and shows by example how accuracy assessments, uncertainty models, and visualizations of uncertainty can be used to aide and improve such an undertaking. Accordingly, this research has the following objectives:

1. To find and survey relict shoreline features that best serve as indicators of former lake levels;
2. To conflate new paleoshoreline data with data collected during previous mapping campaigns;
3. To reconstruct water planes associated with the various phases of glacial Lake Algonquin;
4. To reconstruct the landscape associated with each lake phase and map the distribution of shorelines;
5. And, to express the degree of uncertainty with which each shoreline location has been mapped.

Definitions of key terms

Many data quality concepts are commonly, but erroneously, used inter-changeably. This work relies heavily on several of these concepts, so I offer definitions for them below.

Error

Error is the difference between an attribute value and its measured representation. All measured values contain error because the precisions of human ability and equipment are finite. The term error includes not only mistakes, bias, and blunders, but the statistical concept of variation.

Accuracy

Accuracy refers to the quality of a measurement and indicates whether or not it contains an acceptable amount of error. A measurement is accurate if it contains an acceptable amount of error (or less); it is inaccurate if it contains more. Although accuracy can be considered a binary condition (i.e., being one of only two possible states), it is used more commonly to refer to the degree of conformity between measured and true values (Wolf and Dewitt, 2000). Such use permits the accuracy of one measurement to be compared to the accuracy of another in relative terms (e.g., measurement x is more accurate than measurement y).

Precision

Precision refers to the quality of a measurement process and is commonly used to indicate the exactness of values obtained by that process. According to Wolf and Dewitt (2000), precision can be assessed by taking repeated measurements of a single quantity and examining the variance. The process, and the exactness of values obtained from it, is considered imprecise if the variance exceeds a predetermined threshold. The process, and the exactness of values

obtained from it, is considered precise if repeated measurements vary less than the threshold.

Uncertainty

Western science idealizes prefect data and information because they support rational thought and quick decisions, but uncertainty lurks as an intrinsic property of many concepts, ideas, and data (Couclelis, 2003). According to MacEachren (2005: 140), "when inaccuracy is known objectively, it can be expressed as error; when it is not known, the term *uncertainty* applies." Yet, there is no generally agreed-upon definition of uncertainty, so it is most often treated as a multi-faceted characterization that embodies related concepts including error, accuracy, precision, validity, variability, noise, fuzziness, vagueness, completeness, and reliability (Buttenfield, 1993; Pang, 2001; MacEachren, 2005). I use the term to connote the degree of confidence with which something can be known given available data or information. According to Christakos (2000), determinations and reports of uncertainty are the hallmarks of geostatistical analysis and important to processes related to risk assessment and decision-making.

This research also relies heavily on the terms elevation, location and position. I define them below.

Elevation

Elevation is a 1-dimensional measure of vertical distance, or height. All elevations in this work are referenced to the WGS84 ellipsoid and GEOID03

geoid models, which are used to specify the familiar concept of mean sea level in and around the United States.

Location

Location refers to a 2-dimensional measure of horizontal distances between a point and the origin of a coordinate system. The system can be geographic, in which case locations are specified with pairs of longitude and latitude values. All geographic coordinates in this work are referenced to the WGS84 and NAD83 geographic coordinate systems, which are used interchangeably. The system can be planar, in which case locations are expressed as pairs of easting and northing values. Unless noted otherwise, all planar coordinates are referenced to the Michigan GEOREF planar coordinate system.

Position

Position refers to a 3-dimensional specification of a point in space and includes specifications of both elevation and location (see above).

Justification for research

This research continues the exploration and mapping traditions of Geographic research and offers new and original contributions. For example, this work offers the first known maps of the Upper Orillia and Lower Orillia shorelines (Deane, 1950) of glacial Lake Algonquin. And, this work offers the first reported survey of relict shoreline features at Cockburn Island, Ontario. Other contributions are incremental because they build upon the

geomorphologic research and data collection activities initiated more than a century ago by Spencer (1891), Lawson (1891), and others. For example, this research expands upon the work of Schaetzl et al. (2002) and Drzyzga et al. (2002) by offering updated reinterpretations of extant paleoshoreline data, updated water plane reconstructions, and maps of Lake Algonquin shorelines that cover a geographic area broader than they had studied. New data points also fill some of the large data gaps that Cowan (1985) had mentioned; there be fewer dragons on the map now (Blake, 1999).

This research also provides the field of Geography with a fundamental contribution -- a new way of looking at the land-water interface. A stochastic representation of a shoreline embodies variation in water levels and, hence, the degree of confidence with which the location of a shoreline, as it is traditionally conceptualized, can be known. While the application of this new method is limited in this research to the reconstruction of ancient lakes in the Great Lake basin, it can also be applied to other paleolimnologic reconstructions and adapted for use in contemporary applications that focus on riparian and coastal land use issues.

This research is intrinsically geographic because it synthesizes concepts, knowledge, and tools from multiple disciplines to study a portion of the Earth. It employs methods developed in the field of Geographic Information Science to address a long-standing physiographic and paleolimnologic problem. Some geomorphologists might find issue with the lack of stratigraphy or rheology in

this work, for example, and geostatisticians will not find any new theories here, just applications of existing methods. But, it is the synthesis and novel application of ideas borrowed from multiple disciplines to address a long-standing problem that forms the basis of my contribution.

As an aside, the idea of large pro-glacial lakes and icy waters washing over vast areas of land we now call Ontario or Michigan is both fascinating and unnerving because it forces the mind to visualize a landscape unlike any that can be seen on earth. It prompts consideration of a landscape with large glaciers and without anthropogenic modifications; a cold, wet, windy, and dangerous place. Yet, glacial Lake Algonquin has inherent value beyond prompting the imagination in such wild ways -- it places the contemporary Great Lakes system into a context of landform evolution. Knowing glacial Lake Algonquin existed reminds us that the Great Lakes have evolved through a history of greater great lakes and are evolving still.

Organization of the dissertation

The work reported here follows two interleaved threads of research: the first thread is associated with Objectives 1 and 2 and focuses on my efforts to find, survey, and correlate relict shoreline features with known glacial Lake Algonquin lake phases; the second thread is associated with satisfying Objectives 3, 4 and 5 and focuses on my efforts to digitally reconstruct glacial Lake Algonquin water planes and landscapes, and to estimate the degree of

uncertainty with which interpolated shorelines have been mapped. Because each thread provides a context for examining the other, some reviews of literature, descriptions of methods, and reports of results are arranged in a noncontiguous way.

This dissertation is organized into seven chapters. As is traditional, the first chapter, this one, identifies the scope of the research (i.e., background materials, the research problem, research questions, and the context and justification for the work). Chapter 2 reviews the known history of glacial Lake Algonquin and provides a discussion that recognizes uncertainty as an intrinsic property of lake levels and shorelines. I also make a case for incorporating the dynamic nature of shorelines into a study of ancient lakes. Chapter 3 describes methods used and field campaigns conducted to collect data about Lake Algonquin lake phases. I document the methods used survey, process, and classify paleoshoreline data. Because Objectives 1 and 2 needed to be satisfied before work on Objects 3, 4 and 5 could begin, correlations among collected paleoshoreline data and Lake Algonquin lake phases are also reported in Chapter 3. It just made sense to report relict shoreline features and their correlations with lake phases in one place rather than force the reader to mentally dovetail multiple landform descriptions and lake phase correlations that, if reported in the traditional way, would have spanned multiple chapters. Readers familiar with the seminal work of Leverett and Taylor (1915) will recognize my attempt to describe fieldwork, features, and correlations as they

had done. The narrative style of writing is less formal than I use in other chapters, but it lends itself to others who might use the text as a field guide during future research. Chapter 4 offers a comprehensive assessment of the principal datasets I employ in my analysis: the glacial Lake Algonquin dataset and a digital elevation model. Relevant literature and methods for assessing the accuracy of these data are also presented. Chapter 5 presents the crux of the work. I report work to build uncertainty models that accommodate errors in my datasets, build geostatistical models of four differentially upwarped water planes, and incorporate all of this information into a spatial model that predicts whether or not locations in the area of interest were above or below each water plane. Relevant literature is also reviewed. Chapter 6 delivers the results; maps that illustrate paleoshorelines associated with the Main and "Upper Group" phases of glacial Lake Algonquin, as well as areas where the locations of these shorelines remain uncertain. Figure 6.10 is a large-format map that shows the locations of data points in the glacial Lake Algonquin dataset as well as the predicted shoreline locations for the entire Upper Group sequence of water levels. Chapter 7 summarizes the work and identifies goals worth pursuing in future research. Finally, Appendix A lists every record in the glacial Lake Algonquin dataset as well as every record in the supplemental database that holds surveyed features that were retained for future analysis.

CHAPTER 2: LAKE LEVELS AND SHORELINES

Introduction

This chapter provides a context for surveying, mapping, and modeling a sequence of differentially-uplifted water planes associated with glacial Lake Algonquin. I begin the chapter by introducing glacial Lake Algonquin and providing an abridged history of processes and events that lead to its formation, lake-level changes through time, and demise. Next, I review work that employs coastal landforms as shoreline indicators and uses measurements taken from these landforms as proxies for former water levels. Special attention is given to the pioneering work of Lawson (1891), who established a precedent for mapping glacial Lake Algonquin features and correlating sequences stranded at different locations. Last, I offer a discussion of variation in contemporary Great Lakes water levels, which is used to infer variation in glacial Lake Algonquin water levels. The discussion serves two purposes: (1) to estimate the precision with which an average water level can be measured by taking a spot measurement from a relict shoreline feature, and (2) to estimate the precision with which two successive lake phases can be discriminated on the basis of such measurements.

I adopted Komar's (1976, 1998) nomenclature for describing shorezone morphology (Figure 2.1). Larsen (1994) employed Komar's system of names in his work about glacial Lake Algonquin, so it seems reasonable to continue using it. Readers are referred to Komar's latest text (1998) for complete definitions.

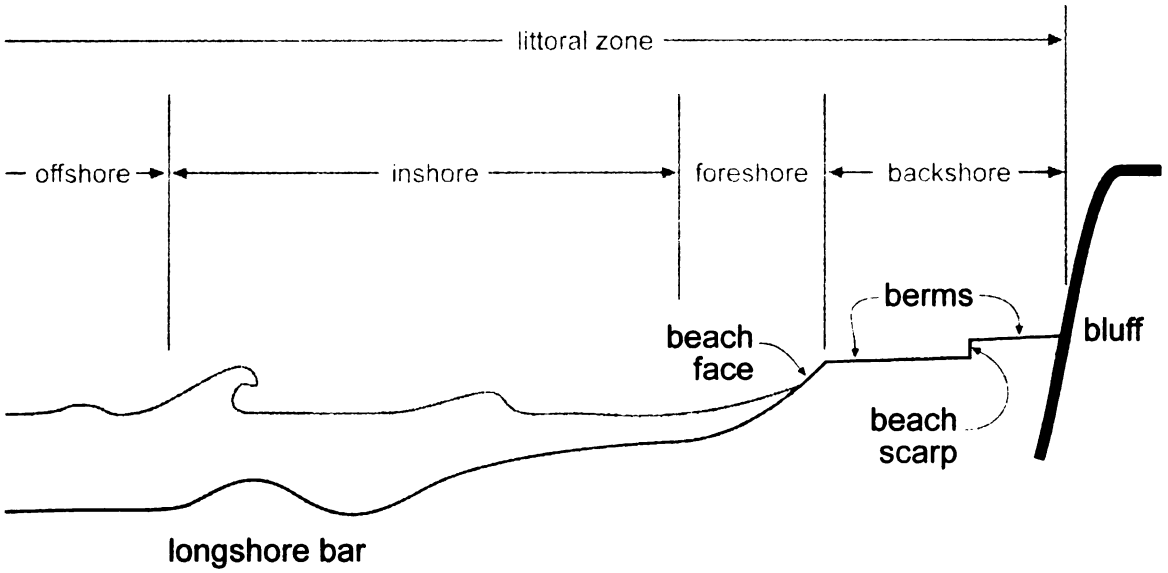


Figure 2.1: Terms used to describe morphologic features along the beach profile (adapted from Komar, 1998).

The landforms illustrated in Figure 2.1 are based on a discrete model of geographic space. A continuous zone of the earth's surface is partitioned into discrete conceptual entities (e.g., longshore bar, beach face, berm, or bluff) according to sets of relative geomorphometric (e.g., slope aspect, gradient, curvature), spatial (e.g., landward of *a*, or seaward of *b*) or sedimentologic characteristics (e.g., parent material, grain size). Discrete conceptual entities can be represented by cartographic objects (i.e., points, lines, and areas) and located with respect to a known spatial reference system. Digital forms of mapped objects can be attributed, stored, edited, manipulated, queried, analyzed and displayed within a GIS environment.

A word about shorelines

A shoreline is a conceptual entity that generalizes a dynamic intersection among bodies of air, land, and water into a simple geometric construct. The word *shoreline* connotes an infinitely thin line along the shore, and thus a high-degree of precision, which lends itself to efficient representation in a visually manageable form. This connotation is evident in Komar's (1998) definition:

> "**Shoreline**: The line of demarcation between the water and the exposed beach. The water's edge." (p.47).

In one sense, Komar's definition is useful because it reduces a complex phenomenon to an object that can be discussed and analyzed; it facilitates scientific inquiry and efficient representation on maps or within a GIS environment. The problem with the definition, however, is that practitioners do not always agree on how to identify a shoreline in the field (Graham et al., 2003), and when they do, it is nonetheless difficult to identify and measure consistently (Parker, 2003).

This research recognizes that a line object is an imprecise representation of a shoreline because it fails to capture intrinsic variations inherent to the dynamic air, land, and water interface over the long term. Shorelines move landward as water levels rise, and they move lakeward as water levels fall. The more gentle the beach slope, the greater the horizontal movement. Shorelines do not move horizontally only when beach slope is infinite (i.e., a vertical cliff or wall). This

research attempts to mitigate this imprecision problem by employing a representation that captures the range of locations (i.e., the area) over which interface movements occur given variability in water levels. Extant research about contemporary and historic Great Lakes water-level fluctuations can be used to condition an expectation about variability in glacial Lake Algonquin water levels.

Glacial Lake Algonquin

Much of what is known today about glacial Lake Algonquin, its shorelines, and its water levels was established at the turn of the twentieth century on the basis of pioneering land surveys and geomorphic reconnaissance missions. Spencer (1891a) is credited as the first person to attach the Algonquin moniker to conspicuous bluff relicts and shoreline strands located "above the eastern rim of Lake Huron" (Schaetzl et al., 2002:399). The work of Leverett and Taylor (1915), however, is generally considered the first authoritative history of glacial Lake Algonquin. They integrated a set of previous and disparately located works conducted by themselves and others (e.g., Lawson, 1891; Spencer, 1891a; Leverett, 1897; Taylor, 1894 and 1897) in order to make generalizations about the glacial and post-glacial history of the Great Lakes region. The authors report included hypotheses and claims about outlet locations, outlet chronologies, correlations among features at disparate field sites, enduring lake stages, and general patterns of differential crustal deformation. Extant research

(e.g., Farrand and Eschman, 1974; Schaetzl et al., 2002), this work included, continues to recognize the value of Leverett and Taylor's (1915) synthesis.

Two major contributions have synthesized and thus improved the collective understanding of Great Lakes evolution: Hough's (1958) *Geology of the Great Lakes;* and Karrow and Calkin's (1985) *Quaternary Evolution of the Great Lakes*. The later represents a collection of individual works that update the lake-level and outlet histories in each of the lake basins. More recent works by Pengelly et al. (1997) and Larson and Schaetzl (2001) offer new summaries of Great Lakes evolution. Another review is warranted here.

Water basins in the Great Lakes region are largely products of repeated scouring and erosion as continental glaciers advanced, oscillated, and retreated during the last 2.4 million years; ice flows tended to follow bedrock valley systems that existed before glaciation (Larson and Schaetzl, 2001). Many sites in Michigan and Ontario, as well as others in adjacent states, show geomorphic and stratigraphic evidence of multiple glaciations. Large morainic systems (e.g., the Lake Border, Port Huron or Munising morainic systems) mark the limits of particular glacial advances. The last major glacial advance of the Laurentide ice sheet began 26 ka, covered the entire watershed, and reached a maximum extent 18 ka (Larson and Schaetzl, 2001). After oscillating at the maximum extent for a few thousand years, the ice sheet margin retreated northward, "but that retreat was interrupted by several readvances at about 15.5, 13.0, 11.8, and 10.0 ka" (Larson and Schaetzl, 2001: 537). As the southern margin of the Laurentide ice

sheet retreated, large pro-glacial lakes formed in topographic sinks where waters were impounded by glacial ice to the north and high topography elsewhere. Relict shoreline features (e.g., wave-cut bluffs, beach ridges, spits, and deltas) mark the limits of pro- and post-glacial lakes that formed during glacial retreats. Lake waters were displaced during readvances and shoreline features were overridden or destroyed by glacial ice. The Laurentide ice sheet withdrew from the watershed roughly 9000 years ago (Larson and Schaetzl, 2001).

The highest set of relict shoreline features north of Georgian Bay was identified by Spencer (1891a) as remnants of the earliest knowable lake to occupy the Lake Huron, Michigan and Superior basins simultaneously (Eschman and Karrow, 1985; Larsen, 1987). Other highest shoreline features were discovered in the region and reported to occur at progressively lower altitudes from north to south (Larsen, 1987). Lawson (1891), Taylor (1894, 1895, 1897), Leverett (1913) and Goldthwait (1908, 1910) surveyed relict shoreline features, made correlations among features stranded at disparate locations, and mapped former lake extents. They also reported lower shorelines that marked lower and younger lakes. According to Leverett and Taylor (1915), the four highest shorelines occurred at progressively lower elevations until they converged at a point south of Traverse City, Michigan.

Larsen (1987) described how converging shorelines and spatial patterns of shoreline deformation and tilt provided grist for opposing theories of crustal movement during the late 1800s. Gilbert (1890), for example, believed tilted

shorelines in the Great Lakes region bore similarities to tilted shorelines found elsewhere in Utah and, thus, the earth's crust in the Great Lakes region had been depressed by the massive weight of a continental ice sheet during glacial advance and rebounded as the weight of ice diminished during retreat. Gilbert (1890) adopted an elastic model of crustal movement; patterns of shoreline deformation and tilt reflected a continuous process of differential isostatic adjustment since glaciation. Goldthwait (1908, 1910) adopted an alternative model -- a rigid model of crustal movement -- that required a stable southern region and a tectonically active northern region; a hinge line model represented the boundary between these two regions. Goldthwait (1908) assumed crustal stability in the southern region allowed the glacial Lake Algonquin shoreline to remain horizontal while episodic tectonic movements somewhere in the northern region forced crustal uplift. The hinge metaphor provided an explanation for how a single shoreline could split into multiple shorelines and diverge with increasing distance, and it suggested rates of episodic movement increased with distance from the hinge line. Leverett and Taylor (1915) adopted the hinge line model for use in their landmark manuscript[1], which, in effect, installed the rigid model of crustal movement as the proper geologic context for conducting

[1] Leverett and Taylor (1915) claimed Lake Algonquin attained its greatest extent before a "great uplift" (p410) had warped the land.

subsequent geomorphic research and interpreting relict shorelines during the next fifty years (e.g., Stanley, 1936; Deane, 1950; and Hough, 1958).

Not until the 1970s did works like Clarke and Persoage (1970) and the Coordinating Committee on Great Lakes Basic Hydraulic and Hydrologic Data (1977) report the entire Great Lakes watershed was undergoing differential vertical movements associated with postglacial rebound - and not only those locations situated north of a supposed hinge. The spatial isostatic adjustment pattern was smooth, continuous, and tended to increase from southwest to northeast and towards the former centers of ice loading. Locations along the southern shore of Lake Michigan were adjusting at slower rates than locations near the Port Huron outlet - but adjusting nonetheless. The Coordinating Committee published a second report (Coordinating Committee, 2001) confirming the process was ongoing and noting water levels along the southern shores of the Great Lakes were rising (i.e., transgressing) slowly over time. Others (e.g., Tushingham, 1992; Clark et al., 1994; Mainville and Craymer, 2005) have either repeated the experiment or conducted similar work, and all obtained similar results. These reports debunk Goldthwait's (1908) rigid earth model. Kaszycki (1985) and Larsen (1987) have since offered evidence that conflicts with the hinge line model and suggested glacial Lake Algonquin shorelines plunge below contemporary lake levels in the supposed southern region.

The glacial readvance of 11.8 ka covered the northern half of the Michigan basin and the northwestern end of the Huron basin, and it blocked the Straits of

Mackinac that, at times, had allowed water to flow from one basin to the other (Hansel and Mickelson, 1988; Larson and Schaetzl, 2001). Broecker and Farrand (1963) reported a radiocarbon date (11,850 yr BP) obtained from a forest near Two Rivers, Wisconsin, that was overridden and buried by this advance. It is generally believed that pro-glacial Lake Chicago formed in the southern Michigan basin and drained via an outlet near Chicago, Illinois (Leverett, 1897; Hansel and Mickelson, 1988), and pro-glacial Lake Algonquin formed in the southern Huron basin and drained via the Fenelon Falls outlet near Kirkfield, Ontario (Finamore, 1985; Hansel and Mickelson, 1988). Differential isostatic rebound changed the relationship between land surface elevations and each field of equal gravitational potential along which each lake surface rested. For example, Hansel and Mickelson (1988) reported lake transgression occurred during the Calumet phase of Lake Chicago as land was uplifted, and Larson and Schaetzl (2001) reported a contemporaneous lake transgression occurred in the southern end of the Huron basin as the Fenelon Falls outlet was uplifted at a faster rate.

As glacial ice retreated from the maximum extent of 11.8 ka, lakes in the Michigan and Huron basins expanded into sinks formerly occupied by ice. The lakes were joined when retreating ice uncovered the Indian River lowlands and, slightly later, the Straits of Mackinac (11,200 yr BP according to Larsen, 1987). Upon joining, water levels in glacial Lake Chicago dropped to the glacial Lake Algonquin level (Hansel et al., 1985) and left the outlet at Chicago abandoned

(Larson and Schaetzl, 2001). The magnitude of the drop is unknown (Kaszycki, 1985). Continued ice margin retreat allowed glacial Lake Algonquin to enter the Superior basin (Cowan, 1985; Larson and Schaetzl, 2001). The northern extent of glacial Lake Algonquin is not known, however, because many shoreline features in the Superior basin were overridden or destroyed during the next glacial advance (Cowan, 1985; Farrand and Drexler, 1985).

Differential isostatic rebound continued to change the relationship between land surface elevations and the field of equal gravitational potential along which the large surface of glacial Lake Algonquin rested. Eschman and Karrow (1985: 89) remarked the "Main Algonquin beach south of the [Fenelon Falls] outlet represents the maximum of a transgressing water level" whereas north of the outlet it represents just one of several regressing water levels. Larson and Schaetzl (2001) noted debate exists regarding whether or not transgressing waters reached the Port Huron outlet. For example, Pengelly et al. (1997) insisted that the excavation of the lowest portion of the Niagara Gorge (between the Erie and Ontario basins) cannot be explained if the Erie basin did not receive inflow from the Huron basin, but Mothersill and Schurer (2004) claimed Lake Huron waters bypassed Lake Erie, which allowed extensive plant-choked swamps to form in Lake Erie's western sediment basins. In either case, a combination of continued ice margin retreat and continued uplift ultimately shifted outflow away from the Fenelon Falls outlet and to the Fossmill outlets that spilled water into the Ottawa River valley Eschman and Farrand, 1985).

The sequence of descending shorelines in the northern Great Lakes region marks a sequence of progressively younger lake phases. In descending order (Table 2.1), the sequence is comprised of the highest or *Main phase* of Lake Algonquin (Spencer, 1891a; Leverett and Taylor, 1915); an *Upper Group* containing the Ardtrea, Upper Orillia and Lower Orillia shorelines/phases that Deane (1950) identified in Ontario's Lake Simcoe district; a *Lower Group* containing the Wyebridge, Penetang, Cedar Point and Payette shorelines/phases that Stanley (1936) identified on Ontario's Penetanguishene Peninsula; and the very low Sheguiandah and Korah shorelines/phases that Hough (1958) identified near Sault Ste. Marie, Ontario. Both Karrow (1987) and Larsen (1987) have noted the controversy that has surrounded these shorelines because it is not yet known whether glacial Lake Algonquin water levels dropped abruptly as new outlets were uncovered, or the land surface was differentially lifted above the field of equal gravitational potential along which the lake surface rested. Karrow (pers. comm.) recently correlated a sequence of descending outlets with the sequence of descending lake phases, but his results remain unpublished. Nevertheless, it seems reasonable to consider that a sequence of discrete short-term outlet change events occurred during the same period as the continuous long-term process of isostatic readjustment; the cumulative impacts of both sequences could produce a very complicated lake-level history.

Glacial Lake Algonquin ended when the North Bay outlet was deglaciated (Hansel et al., 1985) and the large lake drained leaving three pools: Lake

Chippewa in the Michigan basin (Hough, 1955; Hansel et al., 1985; Larson and Schaetzl, 2001), Lake Stanley in the Huron basin (Hough, 1955; Hansel et al., 1985; Larson and Schaetzl, 2001), and Lake Hough in the Georgian Bay basin (Lewis, 1969; Larson and Schaetzl, 2001). Karrow et al. (1975) reported radiocarbon dates that indicate glacial Lake Algonquin, from the Main phase to the lowest, existed between 11,200 yr BP and 10,400 yr BP. Individual lake phase initiations and durations, however, have not yet been dated (Table 2.1).

Table 2.1: Glacial Lake Algonquin lake phases and time frames. Lake phases are listed in descending order in terms of both contemporary elevation and age. Radiocarbon dates are from Karrow et al. (1975).

Name of lake phase	Time frame
The Main phase (Spencer, 1891)	11,200 yr BP - ?
The *Upper Group* (Deane, 1950)	
Ardtrea	? - ?
Upper Orillia	? - ?
Lower Orillia	? - ?
The *Lower Group* (Stanley, 1936)	
Wyebridge	? - ?
Penetang	? - ?
Cedar Point	? - ?
Payette	? - ?
Sheguiandah (Hough, 1958)	? - ?
Korah (Hough, 1958)	? - 10,400 yr BP

In summary, glacial Lake Algonquin was a sequence of pro-glacial lakes in the Great Lakes basin (Figure 1.1). It maintained relative high water levels from 11,200 to 10,400 BP (Karrow et al., 1975; Larson and Schaetzl, 2001). Each

water level is assumed to have rested along a field of equal gravitational potential that can be approximated by a horizontal plane (Clarke et al., 1990). Assuming the same kinds of erosional and depositional processes that occur today also occurred during glacial Lake Algonquin times, wave-action at the perimeter of each lake phase formed shoreline features at or near the horizontal plane. Observations of stranded sets of descending shoreline features support the theory that lake levels fell in discrete stages (Lawson, 1891; Spencer, 1891b). The sequence of descending shorelines was attributed to a series of lake phases (Leverett and Taylor, 1915; Stanley, 1936; Deane, 1950; Hough, 1958). Observations of tilt among relict shorelines support the theory that water planes, and hence the entire land surface, were differentially uplifted as the glacier retreated and the weight of ice diminished (Gilbert, 1898; Schaetzl et al., 2002). Observations of greater tilt at northern locations and lesser tilt at southern locations support the theory that the former ice sheet originated in the north and, after reaching maxima extents, retreated to the north. Observations of greater tilt rates among higher shorelines and lesser tilt rates among lower shorelines support the theory that rates of differential uplift have decreased over time (Larsen, 1987). Together, these theories and the observations that support them provide an explanation for the origin of the contemporary Great Lakes: they evolved through a history of greater great lakes. They also provide the basis for reconstructing glacial Lake Algonquin water planes.

Relict shoreline indicators and water level proxies

Lawson's (1891) study of abandoned shorelines along the north side of Lake Superior seems to have established a precedent for mapping relict shorelines and correlating stranded sequences across space. Although Taylor (1897:111) did not agree with many of his interpretations, he did praise "the high value of Prof. Lawson's observations." Lawson's data collection methods, as well as the statements he made about data uncertainty, have particular relevance to this work about mapping and modeling paleolake levels and shorelines, so several excerpts are examined below.

Lawson (1891) was interested in the cumulative effects of isostatic rebound on glacial Lake Algonquin shorelines. His purpose was to ascertain "what evidences the ancient strand lines of Lake Superior afford of differential crustal movements" (p.185) and to determine whether or not the ancient strand lines "maintained their original horizontality or had been thrown into inclined altitudes" (p.186). Lawson's (1891:186) objective was to "secure accurate data as to the altitude of the various strand lines at as many points as possible and to gather evidence which would help to trace particular strands around the coast." With his purpose and objective in mind Lawson wrote:

> [It] was clearly recognized at the outset that it would be hopeless, owing to the merely local development of shore features, to settle the question by attempting to trace out continuously any single

> strand line or any set of such strands. It was, however, believed that the strands of different vertical series could be correlated, unless there had been rather complex movements, by carefully comparing the intervals between them (Lawson, 1891:230-231).

He continued:

> In order to effect such a correlation the most accurate possible data were necessary, and steps were accordingly taken to ascertain the elevations of the various features indicative of shore lines by precise engineering methods. (Lawson, 1891:231)

Lawson (1891) was concerned about two types of error in his work: measurement and selection. The quote above implies concern about the taking of accurate and precise measurements, yet throughout his work the author voiced confidence about his team's ability to conduct an accurate and precise survey[2]. Lawson dwelled considerably, however, on selection error, for he was very concerned about his ability to interpret relict shorelines consistently and to select points that indicate former water-levels accurately. He wrote:

> The figures [i.e., measured elevations -*author's inclusion*] do not represent always the actual level of the water. The crest of a beach

[2] Unfortunately, he could not reference his survey to an absolute datum, so no way exists to assess the absolute accuracy of his measurement technique.

> is always above the level of the water line at which it is formed; the rear of a terrace may be sometimes above the actual water line and occasionally it may be below it, so that in nearly all cases a correction has to be made for the actual water level. The amount of this correction is never definitely known so it has been thought best not to apply it, but to give the figures for the actual observations. In this connection it is well to note that many of the apparent discrepancies in strand lines ... are doubtless due to the varying value of this correction. (Lawson, 1891:231)

Lawson was concerned about uncertainty. He tried to mitigate uncertainty about estimating former water plane positions by making observations of modern beach features encountered at the base of each topographic profile he measured. For example, Lawson (1891:231) noted, "the base of a sea-cliff is commonly one or two feet above the calm water, though occasionally it coincides with the lake-level closely, and the rear of terraces forming at the mouths of streams is usually below lake-level." Ultimately, Lawson's observations lead him to rely primarily on the bases of stranded sea-cliffs and lake bluffs to be the best shoreline indicators; elevations taken at the bases to be the best proxies for water levels.

Prompted by debate and uncertainty in the contemporary literature, Morton and Speed (1998) sought to determine which shore features best serve as monitors of average water levels and shoreline positions. The authors studied a

wave-dominated and micro-tidal environment near Galveston, Texas, and measured water levels and positions along morphological features on several sandy beaches. The Great Lakes are considered to be a wave-dominated and atidal environment, so their findings have some application here.

Morton and Speed (1998) argued random fluctuations in water level behavior can inhibit the taking of accurate measurements of long-term shoreline positions, but such fluctuations can be mitigated by using "a stable beach feature" (p.1381) as an indicator. They found that, for shores composed of erodable materials, "the stability of shoreline features increases landward and the frequency of movement of a shoreline feature increases seaward" (p.1381). For example, the toe of a wave-cut bluff is a more stable indicator of shoreline position than a berm crest or beach ridge along the same shore. The authors also report discrepancies between measured and actual water levels tend to be "greatest on low-gradient sandy beaches along a microtidal and wave-dominated coast", and, "in such settings, the mean highest high water line consistently plots ... far seaward of the berm crest" (p.1383). Their work suggests that the average water-level, which by definition is lower in elevation than the mean highest high water line, also tends to occur far seaward of the berm crest - likely farther. Given this finding, high-gradient shorezones composed of materials that are less erodable than beach sand (e.g., glacial till, gravel, or bedrock) may offer better environments for taking accurate measurements of water levels and shoreline positions than do low-gradient and

sandy shorezones. The authors suggest using stable features like erosional bluffs or scarps, or a vegetation line as indicators. In related work, Moore (2000: p.116 after Morton, 1991) argued that "where beach morphology permits ... the bluff/cliff toe or a vegetation line may be a better choice for shoreline analysis" than other beach features. The recent findings of Morton and Speed (1998) and Moore (2000) support the observations and choices that Lawson (1891) made a century before.

In work on reconstructing late Holocene lake-levels, Thompson (1992) and others (Baedke et al., 2004; Johnston, 2004; and Thompson and Baedke, 1995; 1997; 1999) focused on sandy depositional features in protected post-glacial embayments. Relatively coarse foreshore deposits between successive beach ridges were used as shoreline indicators; elevations taken from them were used as proxies for water levels (Figure 2.2).

Baedke and Thompson (2004) provided the most recent description of Thompson's sampling technique, so I offer a summary of their description here. A search is made along a horizontal strandplain of beach ridges. Soil and buried sediments are excavated via coring at "the change in slope that occurs along the lakeward side of the beach ridge" (Baedke et al., 2004: 440). Core site elevations are surveyed with sub-centimeter precision. Organic deposits are collected from the landward swale of the same beach ridge. In a laboratory, cores are analyzed and summarized in terms of grain size distributions, biological components, and physical structures. Abrupt and gradational grain-size changes within each

vertical core are used to infer the contact between relatively coarse foreshore deposits and other deposits. The vertical point of contact is assumed to be the coarsest portion of the horizontal foreshore and related to plunge-point deposits that occur "at or very near the still-water elevation of the lake" (Baedke et al., 2004: 439).[3] Radiocarbon age determinations are made of the organic deposits.

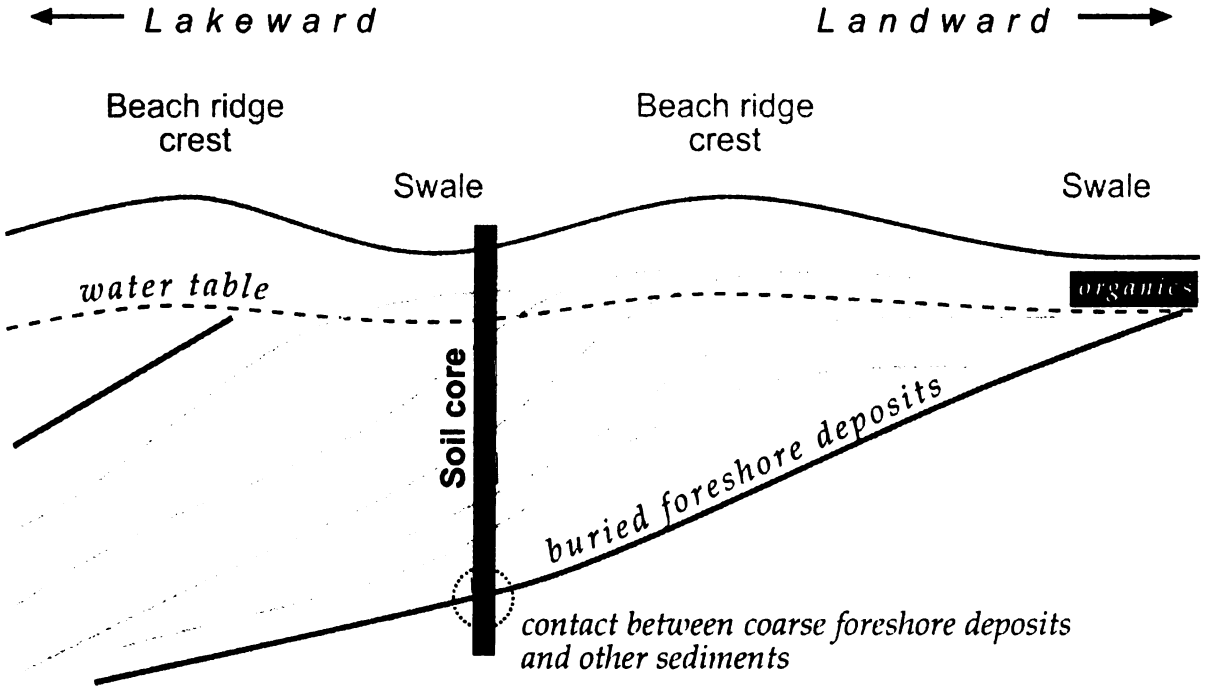


Figure 2.2: Baedke et al. (2004) used buried foreshore deposits as shoreline indicators. Figure adapted from descriptions in their text and from Figure 2.6 in Johnston (2004).

[3] Neither Thompson (1992) nor Baedke et al. (2004) have offered evidence to suggest the location of the "change in slope" on the land surface is an accurate indicator of the location of the coarsest portion (a.k.a. plunge-point) of a buried foreshore.

Building on Thompson's early work, Larsen (1994) documented a record of relative lake-level changes among three locations (Whitefish Point, MI; Sturgeon Bay, WI; and the Gary Airport, IN) by correlating dated beach ridge sequences. Like Thompson, Larsen studied beach ridges because they "preserve continuous geomorphic and stratigraphic records of lake-level change" (p.108). But unlike Thompson (vis a vis Baedke et al., 2004), Larsen recognized elevation data taken from buried geomorphic features should be interpreted as possible outcomes of a fluctuating lake system and not as highly-accurate sedimentary indicators of statistical mean lake levels (+/- 0.003 m). Moreover, Larsen (1994) claimed buried foreshore deposits usually indicate levels within the upper range of lake levels and, so, not average lake levels. When considered within the context of the range of contemporary Great Lakes water level fluctuations (Table 2.2), elevations taken from individual beach ridges could overestimate average lake-levels by 2.7 meters or more. Larsen's (1994) argument was later supported indirectly by Argyilan et al. (2005), who claimed beach ridges preferentially reflect high water levels.

In work related to this research, Schaetzl et al. (2002) reported concern about their abilities to identify relict shorelines consistently in the field and to select points that indicate former water-levels accurately. Like Lawson (1891), they recognized that different kinds of features, which are formed by different process, have differing abilities to indicate average paleowater planes consistently. For example, they reported offshore bars are typically formed

below a lake surface whereas a spit crest might rise several meters above it; elevations taken from these features would underestimate or overestimate average water levels, respectively. Schaetzl et al. (2002) observed that postlacustrine debris is often located on the surfaces of benches just below the bases of wave-cut bluffs and claimed, where present, bouldery/gravelly lags provide "the most credible estimation of mean water level" (p.405). Figure 2.3 illustrates their observation.

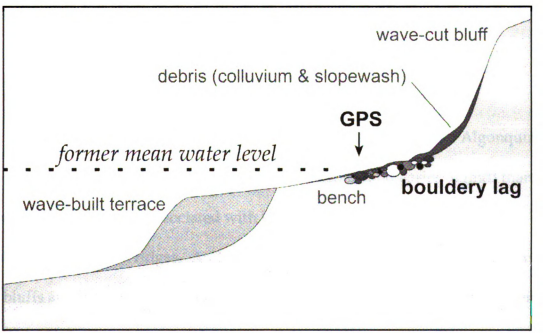


Figure 2.3: Schaetzl et al. (2002) used bouldery/gravelly lags at the bases of wave-cut bluffs as shoreline indicators. Figure was adapted from their Figure 2b (p.405).

Where present, the bouldery/gravelly lags at the bases of wave-cut bluffs and the foreshore deposits buried beneath beach ridges have been used effectively as geomorphic indicators of relict shoreline positions. Both are

effective indicators because each consists of relatively coarse-sized sediments that physically mark the sorting action of swashing and back swashing waters. Wave-cut bluffs form in erosional environments. Beach ridges form in depositional environments. In terms of surveying and mapping relict shoreline features of glacial Lake Algonquin, however, the bouldery/gravelly lags at the bases of wave-cut bluffs seem to offer two distinct advantages. First, glacial Lake Algonquin refers to a sequence of descending lake phases that occurred during a period of "strong (hurricane-force) winds" (Krist and Schaetzl, 2001: 11) and "exceedingly strong waves and currents" (Krist and Schaetzl, 2001: 13), which suggests wind and wave conditions that favored erosional processes likely prevailed over gentler conditions that favored depositional processes. Consequently, I expected erosional landforms associated with Lake Algonquin shorelines, like wave-cut bluffs, to be more numerous (and easier to find) than depositional landforms associated with Lake Algonquin shorelines, like strandplains of beach ridges. And second, for practical purposes, bases of wave-cut bluffs are more accessible than buried foreshore deposits because wave-cut bluffs typically do not require trenching or deep coring to reach them in the field. Therefore, based on the long tradition of glacial Lake Algonquin research, Lawson's (1891) observations, the recent findings of Morton and Speed (1998) and Moore (2000), and the related work of Schaetzl et al. (2002), this research relies on the bouldery/gravelly lags that form at the bases of wave-cut bluffs to be the best indicators of glacial Lake Algonquin shorelines. And, using words

modified from Lawson (1891), it is understood that measured elevations do not represent actual water levels, but simply the elevations of shore features "from which the actual water levels may be inferred, within certain considerable limits of error" (Lawson, 1891: 231-232).

Variation in Great Lakes water levels

Contemporary Great Lakes water levels are generally resistant to change because the bodies of water are deep, have large surface areas, have small drainage basins relative to lake areas, and are controlled by relatively small outlets. Under *ceteris paribus* conditions, the surface of each lake is expected to rest along a field of equal gravitational potential (Clarke et al., 1990). Yet, variations in precipitation, air temperature, in-flow, and out-flow force the water surface to fluctuate and compensate, so lake gauge stations are used to capture, and statistical techniques are used to summarize, variability in water levels over time.

The historical water level record provides grist for scientific inquiry. Quinn (2002), for example, analyzed seasonal variation in the record; Table 2.2 lists average lake levels and portions of Quinn's summary (Quinn, 2002: Table 1 on page 455). Bishop also (1990) analyzed inter-annual variation and found, "the ranges in measured mean monthly levels for Lakes Michigan-Huron and Erie are approximately 2.4 m and 1.8 m, respectively" (Bishop, 1990: 406). And Changnon's (2004) analysis of the lake-level record for Lakes Superior, Michigan-

Huron, and Erie found "record highs or record lows were being set on one or more lakes during nearly half the time over the 141-year period" (Changnon, 2004: 197). So, although generally resistant, Great Lakes water levels are not immune to change and change differently over time.

Table 2.2: Seasonal variation in contemporary Great Lakes water levels (Quinn, 2002; NOAA, 2006). [4]

Lake	Average lake level (m a.s.l.)	Seasonal range (m)	Standard deviation (m)	Time period
Superior	183.5	0.30	0.11	1980-2000
Michigan	176.5	0.27	0.12	1987-2000
Huron	176.5	0.27	0.12	1987-2000
Erie	174.1	0.46	0.15	1861-2000
Ontario	74.6	0.55	0.20	1960-2000

Fluctuations around, or deviations from, long-term average water levels are generalized into three categories or scales: short-term events (i.e., short time frames that range from less than one hour to several days and, thus, considered as events); cycles (i.e., various periods), and long-term trends (i.e., multi-year). The following sections describe each scale in terms of the contemporary Great Lakes, and attempt to place them within the context of the relatively large spatial and temporal domains once occupied by glacial Lake Algonquin. Estimating a

[4] Quinn (2002) did not report average lake levels, so I estimated average lake levels for a twenty-year period between January 1, 1980 and January 1, 2000 using NOAA's Center for Operational Oceanographic Products and Services data (NOAA, 2006). Data from the lake gauge situated nearest to each outlet was summarized.

likely range of glacial Lake Algonquin water-level fluctuations is important because the range can serve as a guiding threshold for discriminating evidences of different lake surfaces in the field. For example, given a field site with two instances of a relict coastal landform and a vertical distance between them that is less than the threshold value, it is reasonable to conclude, based on the observed difference between elevations alone, that both features were shaped by the same lake phase operating around the same mean water level. Conversely, given a field site with two instances of a relict coastal landform but a vertical distance between them that is greater than the threshold value, it is reasonable to conclude, based on the difference between elevations alone, that each feature was shaped by a different lake phase operating around a different mean water level.

Short-term events

Short-term events are the results of differential wind conditions (i.e., speed, direction, and fetch) or barometric pressures, which force localized and temporary imbalances along a water surface. Energy obtained from the atmosphere is dispersed across the water surface and delivered to the shore in waves. Wood et al. (1994) studied waves in Lake Michigan and reported most are one-meter high or less; the maximum observed was approximately six meters. Gabriel et al. (1997) and Brown et al. (2005) claim storm-generated waves and seiches can upset water levels by as much as several meters for several hours. Such short-term events effect local and temporary deviations from, but no permanent changes to, long-term average water levels.

When considered in the context of an entire lake surface and over a long time frame (e.g., decades), chaotic or noisy variations in lake level associated with all short-term events can be summarized over both space and time. Accordingly, the large-space and long-term distribution of water-level fluctuations associated with short-term disturbances on the contemporary Great Lakes is characterized in this work as the result of an unbiased and unstructured random process with a zero mean. Although the true variance is unknown, the quantitative information provided by Wood et al. (1994) suggests the average deviation is one meter or less.

Storms and storm-generated waves occurred on glacial Lake Algonquin. Krist and Schaetzl's (2001) treatment of Lake Algonquin type spits, for example, provides evidence of coastal erosion and longshore transport processes that were associated with "exceedingly strong waves and currents" (p. 13) driven by "frequent and intense cyclonic storms and their associated wind fields" (p.14). The modern Great Lakes are not commonly subjected to" strong (hurricane-force) winds" (p.11) as was glacial Lake Algonquin, so this work infers from Krist and Schaetzl's (2001) findings that average and maximum wave heights were likely greater during glacial Lake Algonquin times than they are today. The large spatio-temporal distribution of water-level fluctuations associated with short-term disturbances on glacial Lake Algonquin can be characterized as the result of an unbiased and unstructured random process with a zero mean and an average deviation that was at least as great or greater than one meter.

Cyclic fluctuations

Lenters (2001) analyzed the historical lake gauge record (from 1860 to 1998) for each Great Lake. His analysis of intra-annual variations revealed the influences of the annual hydrologic cycle that has been reported by many others (e.g., Fairchild, 1926; Bishop, 1990; and Angel, 1995). Peak lake levels are associated with peaks in spring run-off and precipitation, and typically occur in June (Lakes Huron, Michigan and Superior) or July (Lakes Erie and Ontario); winter lows, which are associated with precipitation lows, precipitation stored on land as snow, and evaporation, typically occur in late March or early April. And, according to Angel (1995), the annual hydrologic cycle generates fluctuations that range from 20 to 40 cm in any given year.

Lenters' (2001) analysis of inter-annual variation also revealed changes in the annual water-level cycle. Each Great Lake has exhibited a trend of increasing high spring levels and decreasing low autumn levels, although only trends associated with Lakes Erie and Ontario could be characterized as statistically significant. Quinn (2002) analyzed water level data for the period between 1860 and 2000, found similar shifts, and concluded that all of the lakes have "experienced changes in their seasonal cycle over the past 140 years" (Quinn, 2002: 464).

Todd Thompson, by himself (Thompson, 1992) and through work with others (Thompson et al., 1991; Thompson and Baedke, 1995, 1997 and1999; Baedke and Thompson, 2000; and Baedke et al., 2004), has developed a research

program to investigate periodicity in lake-levels in the upper Great Lakes. The program is designed to focus not only on historical lake gauge data, but on sandy depositional features in protected, post-glacial embayments. Thompson searches the local geologic record for preserved evidence of lake level history. For now, the longest history observed extends to approximately 4,700 BP. Baedke and Thompson (2000) identified quasi-periodic lake-level fluctuations that occur at 29 to 38 yr intervals with an average amplitude of 0.5 meters, and a longer-term fluctuation that occurs over durations between 120 and 180 years and with average amplitudes between 0.5 and 1.5 meters. More recently, Quinn and Sellinger (2006) found supporting evidence for such quasi-periodic extreme lake levels in their analysis of dendrochronologic data, which they linked to coincident changes in air temperature and precipitation.

The record of glacial Lake Algonquin water level fluctuations is not known, but it is reasonable to expect that, then, water levels were subject to cyclic deviations forced by cyclic changes in air temperature or precipitation. Moreover, glacial Lake Algonquin was bounded to the north by a retreating ice sheet (Karrow, 1987; Farrand, 1967/1998). Fluctuations associated with glacial discharge and advances or retreats in ice-margin position likely occurred and, perhaps, were substantial. Tinkler and Pengally (1995) simulated outbursts from Lake Agassiz into the Upper Great Lakes and found water levels would have risen between 2 and 20 m; the largest would have required nearly three years for the Upper Great Lakes to re-attain equilibrium. Disagreement exists, however,

about whether or not outflow from Lake Agassiz actually entered the Upper Great Lakes during Algonquin times (see e.g., the correspondence between Karrow, 2002 and Teller, 2002). Yet, given the large size of the ice sheet and the amount of water it probably relinquished during the summer seasons, it is reasonable to speculate that such variations were greater than, perhaps much greater than, those contained within the historical lake gauge record, Quinn and Sellinger's (2006) tree-ring record, or Baedke and Thompson's (2000) beach-ridge record.

Cyclic processes are important catalysts for local coastal erosion processes (e.g., Loope and Arbogast, 2000; Zurek et al., 2003). When considered in the global context of the large surface area and the long time frame associated with glacial Lake Algonquin, variation associated with cyclic processes can be summarized over space and time. The large spatiotemporal distribution of cyclic lake-level deviations is characterized in this work as the result of an unbiased and unstructured random process with a zero mean. Given the quantitative evidence provided by Lenters (2001) and Baedke and Thompson (2000), and given the assumption that cyclic water-level fluctuations during glacial Lake Algonquin times were greater than modern fluctuations, then the range of cyclic water-level deviations associated with glacial Lake Algonquin lake phases may easily have exceeded two meters or more.

Long-term trends

Many studies have examined a long-term trend that impacts lake levels, which is generally thought to be caused by differential vertical movements of the earth's crust across the Great Lakes basin (e.g., Coordinating Committee of Great Lakes Hydraulic and Hydrologic Data, 2001 and 1977; Tushingham, 1992; Clarke et al., 1994; and Mainville and Craymer, 2005). Quinn and Sellinger (1990) provide a summary of the process:

> "A tremendous weight such as a regional glacier can theoretically force localized land masses downward into the crust until a compensatory equilibrium is achieved. Once that weight is removed, as in a glacial retreat, the landmass will rebound upward to once again achieve equilibrium. The Laurentide glacier of the Pleistocene Epoch depressed the crust in the Great Lakes area differentially because the thickest ice was to the northeast ... Due to the varying thicknesses of ice cover over the Great Lakes region, differential isostatic rebound rates are location specific." (Quinn and Sellinger, 1990: 134)

Differential isostatic rebound continues today with land at northern locations rebounding faster than land at southern locations. Lee and Southam (1994: 409) report, for example, that land at Michipicoten, Ontario is currently rising 0.525 m/century faster than land at Duluth, MN, and land at Pt. Iroquois, MI is rising

0.122 m/century with respect to Marquette, MI (from Table 1 on p.410). Ongoing crustal movement results in differential changes in the relationship between the land surface that holds water bodies and the fields of gravity that act on the surfaces of those water bodies. Consequently, isostatic rebound results in differential changes in the relationship between the elevations of contemporary shoreline features and relict shoreline features.

Although differential isostatic rebound in the Great Lakes region has been well studied, little agreement exists about the behavior of the phenomenon, rates of change in the behavior of the phenomenon since deglaciation, or the amount of cumulative effect it has had on individual water planes and relict shorelines. For the purposes of discussion, however, it is important to note that the isostatic rebound process cannot be characterized as another unbiased and unstructured random process with a mean of zero; rather, as a spatially structured process with a non-stationary mean amount of uplift that increases toward the northeast. Models of isostatic rebound are presented in Chapter 5.

Summary

Apparent random behavior in water-level fluctuations reflects the superposition of short-term events onto longer-term cyclic processes, which interact in ways that can produce record highs and lows. In terms of the contemporary Great Lakes, the cumulative distribution of water-level fluctuations likely includes deviations from the long-term average that exceed 2.7 meters (see Table 2.3). Quinn (1999) cautions, however, that our understanding

of modern lake-level behavior is limited because the current regime may produce "high and low lake levels with extremes significantly higher than our present measurements would indicate" (p.4).

Table 2.3: Potential range of Great Lakes water-level fluctuations (see text for references).

Process and duration	Typical deviation (m)
Storms or waves	
~from seconds to several hours	±1.0
Seasonal hydrologic cycle	
~1 year	0.2
Baedke and Thompson (2000)	
~33-year cycle	0.5
~150-year cycle	1.0
Differential isostatic rebound	
(varies with location)	?
Total	± 2.7 m

The range of historic water-level fluctuations is important because it suggests the precision with which average water levels (statistical quantities subject to variation) can be estimated from spot elevations (measured quantities) taken from static landforms. As explained above, this research relies on the gravel lags that form at the bases of wave-cut bluffs to be geomorphic indicators of shoreline events because they tend to form at or near the land-water interface and where wave energies are relatively high. Elevations taken from the tops of these lags serve as proxies for average water levels (Schaetzl et al., 2002). Because beach sediments and shoreline features can move in response to water level fluctuations, I must recognize that estimates of glacial Lake Algonquin water

levels based on geomorphic proxies are subject to uncertainty. Fortunately, the range of contemporary Great Lakes water-level fluctuations (Table 2.3) provides a convenient (albeit rough) estimate of this uncertainty. This research proceeds by assuming the minimum vertical difference between two gravel lags that can be used to discriminate two average glacial Lake Algonquin water levels is 3 meters.

Summary

Lake levels and shorelines are results of complex and dynamic interactions among bodies of air, land and water, and gravitational forces. Such interactions can occur over multiple spatial and temporal scales. Changes in lake level, as well as rates of change in lake level, are generally recognized as important controls on shoreline position, coastal processes, and coastal landform changes. In general, shorelines migrate upward and landward as water levels increase, and migrate downward and lakeward as water levels decrease. Statistical techniques are usually required to summarize the distributions of historic or contemporary lake-level fluctuations in terms of average lake levels.

Researchers interested in mapping and modeling paleolakes and paleoshorelines must deal with difficulties associated with estimating statistical lake levels by taking elevation measurements from relict shoreline features. The precision of this method can be influenced by the choice of shoreline indicator as

well as the legacies of earth processes that have modified the landscape or moved relict shoreline features since they were formed.

This research relies on the bouldery/gravelly lags that formed at the bases of relict wave-cut bluffs to be indicators of former shoreline positions (Schaetzl et al., 2002). It is understood, however, given natural variability among local site conditions, different lags that formed along the edge of the same lake surface might have elevations that vary. The tradition of glacial Lake Algonquin research and the later work of Morton and Speed (1998) and Moore (2000) suggest the precision with which a lake level can be established by the elevation of a wave-cut bluff alone is likely sub-meter, but knowledge about contemporary water-level behavior indicates the precision may be, at the extreme, no better than three meters. Accordingly, this research recognizes imprecision as a form of uncertainty and proceeds by assuming the precision with which a former lake level can be established by the elevation of a gravel lag situated at the base of a wave-cut bluff is one meter, and the minimum vertical distance that can be used to confidently discriminate different lake levels is three meters.

CHAPTER 3: METHODS AND FIELD CAMPAIGNS

Introduction

This chapter describes methods used to collect relict shoreline data and build a glacial Lake Algonquin dataset. I begin by summarizing the work of Schaetzl et al. (2002), which established a relevant methodology and produced an initial dataset, which I inherited. I continue by recognizing opportunities to improve upon the work they had done. Next, I review the prior mapping campaigns led by Cowan (1985) and Karrow (1987) and describe how data they collected were conflated with data collected during this work. I then report new data I collected during a series of field campaigns designed to expand and improve the geographic distribution of sampled shorelines. My report of relict features at Cockburn Island, Ontario, for example, is a significant contribution to the literature for no other report describes these features in detail. And, in light of new data and recently published work, I offer reinterpretations of old data.

The initial glacial Lake Algonquin dataset

Uncertainty about the elevations, timing and extents of glacial Lake Algonquin lake phases prompted Schaetzl et al. (2002) to conduct an extensive survey of relict coastal landforms in northern Michigan. They targeted more than 200 sites and were guided by descriptions of relict landforms in the literature (e.g., Leverett and Taylor, 1915; Futyma, 1981; Farrand and Drexler, 1985; Schaetzl et al., 2002; and Krist and Schaetzl, 2001) and their interpretations

of features on 7.5-minute USGS topographic maps. The authors investigated sites to determine whether or not each one contains a relict wave-cut bluff suitable for sampling. At suitable sites, Schaetzl et al. (2002) measured bluff positions, rather than accept any previously published elevation values, because the literature provides: a) few detailed descriptions about where previously reported position measurements were actually made; b) few references to the spatial reference systems employed (i.e., either the horizontal or vertical datum was unspecified); and c) no assessments of data quality. Without such metadata, the authors felt they could not assess confidently whether or not any previously reported elevation value was valid, commensurate with other published data, or acceptable for inclusion in further analysis. Their dataset contains 146 records (Figure 3.1). Individually, each record represents the position of a relict shoreline feature. In aggregate, their data reveal the spatial extents of four, possibly five, glacial Lake Algonquin lake phases in northern Michigan (Schaetzl et al., 2002). Schaetzl et al. (2002) concluded that pro- and postglacial lake levels can be effectively identified, reconstructed, and correlated via examinations of elevation data collected from wave-cut bluffs. They claimed their rebound curves and isobase maps are more accurate than those published previously, but suggested more geomorphologic and stratigraphic research is needed beyond their area of study.

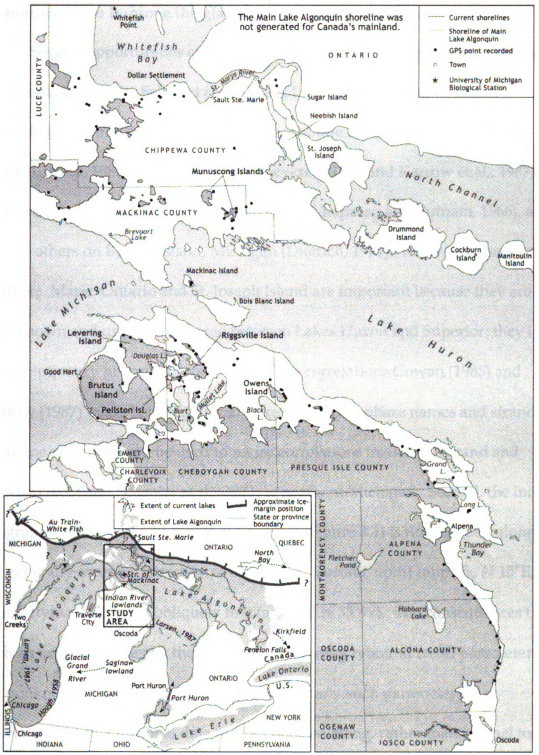


Figure 3.1: The study area explored by Schaetzl et al. (2002), points in the original glacial Lake Algonquin dataset, and the extent of the Main phase of glacial Lake Algonquin as they had determined it. Figure adapted from their Figure 1.

Opportunities to improve the glacial Lake Algonquin dataset

Several opportunities existed to substantially yet efficiently improve the initial dataset built by Schaetzl et al. (2002); I capitalized on three. First, I expanded the study area (see Figure 3.2) to include relict features at Sault Ste. Marie (Cowan, 1985), St. Joseph Island (Leverett, 1913 and Karrow et al., 1987) and Cockburn Island, Ontario (Leverett, 1913; Chapman and Putnam, 1966), as well as others on Beaver Island, Michigan (Dietrich, 1978). Relict bluff features at Sault Ste. Marie, Ontario and St. Joseph Island are important because they are well-known and uniquely situated between Lakes Huron and Superior; they link the evolutionary histories of these lakes. The correlations Cowan (1985) and Karrow (1987) made between glacial Lake Algonquin phase names and stranded shoreline elevations can be used to revise correlations made by Farrand and Drexler (1985) and Schaetzl et al. (2002) in northern Michigan. Second, the initial geographic distribution of sampled positions (Figure 3.1) is not oriented along the generally accepted direction of differential isostatic uplift (approx. N 15°E; after Futyma, 1981), but obliquely to it (approx. N 35°W). The consequences that such an orientation has on the process of estimating rebound trend parameters are not known, but it seems reasonable to treat any such parameters as provisional until additional data can be collected along, rather than normal to, the uplift trend. Collecting and integrating data from the islands mentioned above adds important features to the glacial Lake Algonquin dataset and much needed support to unsampled sectors along the former water planes.

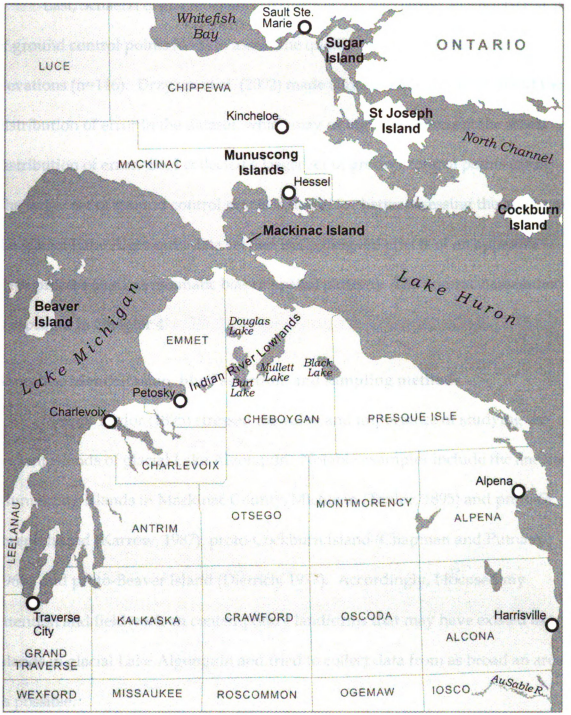


Figure 3.2: Map of the current study area with names of places and features mentioned in the text. County boundaries and names added for reference.

Last, Schaetzl et al. (2002) and Drzyzga et al. (2002) used an undersized set of ground control points (n=8) to assess the quality of sampled shoreline elevations (n=146). Drzyzga et al. (2002) made simplistic assumptions about the distribution of error in the dataset, which may or may not represent the actual distribution of error. So, I collected a larger set of ground control points (n=24). The larger set of ground control points is useful for better assessing the quality of the glacial Lake Algonquin data set and mitigating the effects of an apparent error process (e.g., a systematic bias or spatial pattern). The accuracy assessment is reported in Chapter 4.

Shoreline identification, bluff selection, and sampling methods

Frank Taylor (1895) stressed the value and importance of studying the ancient islands of glacial Lake Algonquin. Notable examples include the ancient Munuscong Islands in Mackinac County, Michigan (Taylor, 1895) and proto-St. Joseph Island (Karrow, 1987), proto-Cockburn Island (Chapman and Putnam, 1966), and proto-Beaver Island (Dietrich, 1977). Accordingly, I focused my attention and fieldwork on contemporary landforms that may have existed as islands in glacial Lake Algonquin and tried to collect data from as broad an area as possible.

I inherited the dataset and employed the same set of shoreline identification and bluff selection methods used by Schaetzl et al. (2002: 405-406). And, like they did, I relied on the bouldery/gravelly lags that form at the bases

of wave-cut bluffs to be geomorphic indicators of ancient shorelines (Figure 3.3). Using the same indicator ensures similar reliability and consistency characteristics between data collected during their campaign and new data collected during mine. Similarities notwithstanding, I provide a summary of methods below because several differences do exist between the GPS leveling technique and data processing methods I used and those that Schaetzl et al. (2002) used. For example, I take advantage of the latest geoid model (GEOID03, Roman et al., 2004) that is a better approximation of mean sea level throughout the United States than the GEOID96 geoid model (Smith and Milbert, 1999) they used.

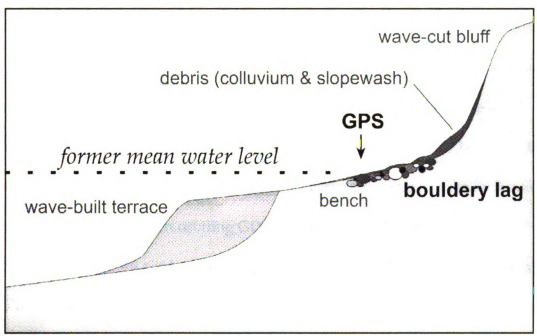


Figure 3.3: Schaetzl et al. (2002) used bouldery/gravelly lags at the bases of wave-cut bluffs as shoreline indicators. Figure was adapted from their Figure 2b (p.405).

First, I collected 7.5-minute USGS topographic map sheets for all locations within the study area. I also collected 1:50,000 Canadian Topographic Map sheets to supplement coverage of Cockburn Island, St. Joseph Island, and Sault Ste. Marie, Ontario. Field notes taken during previous campaigns as well as extant literature (e.g., Leverett and Taylor, 1915; Hough, 1958; Dietrich, 1978; and Karrow, 1987) were used as guides for targeting likely sites with relict wave-cut bluffs. Initial selections were limited to only those features that are landward of, and higher than, the generally accepted Nipissing water surface (Goldthwait, 1910). I plotted extant data and new potential bluff targets on topographic map sheets to identify areas with little data.

Next, I visited targeted sites. A target was selected for sampling if it exhibited a conspicuous bluff-to-beach morphology and presented a well-defined bluff toe. If a target exhibited a conspicuous bluff-to-beach morphology but not a well-defined toe, then I traveled along the feature (for up to several hundred meters in either direction of the initial site) in search of a "best" site that contained a well-defined toe and a relative paucity of forest cover (to facilitate radio signal reception from orbiting GPS satellites). Locations that evinced anthropogenic change or bluff failure are not suitable locations for sampling and, so, were not sampled.

Third, an initial position was selected along the bluff toe. Soil was excavated with a bucket auger to a maximum depth of 1.5 meters. If a bouldery/gravelly lag (Figure 3.3) could not be detected, then sampling

proceeded down slope at successively lower locations until a buried lag was found. (Fortunately, at many sites a conspicuous boulder lag is present below the bluff.) Field notes were taken at the ultimate location to describe the site and record depth to the buried gravel lag. Elevation measurements, which were taken at the land surface, were adjusted downward to account for the vertical distance between the land surface and the buried lag. Also, when weather permitted, an image of the site was recorded with a digital camera.

And fourth, real-time differential Global Positioning System (GPS) technology was employed to measure relict shoreline positions. When used correctly, GPS leveling offers at least five distinct advantages over other field methods: a) on average, position measurements {x,y,z triplets} can be made quickly and with sub-meter errors; b) position values collected among scattered field sites can be georeferenced to the same spatial reference system; c) field equipment is light-weight and portable; d) fieldwork can be conducted effectively and efficiently by one person, which precludes the need for a second person to work the other end of a level line; and e) all position data are recorded and stored in digital form, which facilitates translation into data formats that can be analyzed within a GIS or spreadsheet environments.

I planned and organized data collection activities in three important ways to take best advantage of GPS technology. First, the field season was limited to leaf-off conditions (i.e., late fall) because summer-time leaf canopies can obfuscate, perturb, or block GPS radio signals. The winter leaf-off season was

also avoided, however, because regional winter snow blankets ground features and inhibits exploration. In the field, the GPS receiver was mounted onto a tripod and raised two meters above the ground. Second, all data were collected during temporal windows that framed optimal GPS satellite constellation configurations (i.e., VDOP ≤ 3.0)[1]. GPS receiver software can manipulate and tumble numbers under a plethora of constellation configurations, but relatively few configurations offer geometries sufficient for taking accurate and precise vertical measurements. Trimble's *Quick Plan* software (Trimble Navigation Limited, 2002) and current satellite ephemeris data were used to identify and select suitable VDOP windows. Data collection activities were scheduled and limited to these windows only. And third, a point-averaging technique was used to estimate position at each site. The point-averaging technique requires

---

[1] A Dilution of Precision (DOP) value is an estimate of the quality of a GPS position. For a given point in time, the DOP value takes into account the location of each GPS satellite relative to the locations of others in the constellation, and their geometry in relation to the GPS receiver (Reilly, 2002). A low DOP value suggests a relatively high probability of taking an accurate measurement. A low VDOP (Vertical Dilution of Precision) suggests a relatively high probability of taking an accurate vertical measurement. Because this research is concerned with taking accurate vertical measurements, primary emphasis is placed on obtaining low VDOP values during data collection activities. Most satellite-viewer geometries that are optimal for taking accurate vertical measurements also allow taking accurate horizontal measurements.

multiple measurements of the same feature to be made. Collecting a sample of measurements and summarizing it in terms of average coordinate values and precisions, rather than collecting a single measurement, reduces the risk of accepting data with large random errors. Schaetzl et al. (2002) used the point averaging technique and collected a sample of no less than 100 position measurements at each bluff site. They achieved reliable results with the technique, but had to discard some valuable data because, for some sites, many of the 100+ measurements were deleted during data processing (pers. comm.). Collecting a larger sample at each site would have helped preserve their data. So, for this work, I collected a larger sample of no less than 300 position measurements at each bluff site. All horizontal locations are referenced to the North American Datum of 1983 (NAD83). All elevations were referenced first to the World Geodetic System 1984 (WGS84/G873) ellipsoid model and later converted to orthometric heights (see below).

Data processing

Data files (one sample of shoreline measurements per file) were processed using Trimble *Pathfinder Office* (GPS) and Microsoft *Excel* (spreadsheet) software. Data processing followed this model:

First, each file was assigned to one of two groups: those with position data that were differentially corrected in the field, and those that were not. The radio link between a GPS receiver and the satellite that delivers OMNIStar's real-time

correction service is sometimes lost behind local obstructions (e.g., a massive bluff or a dense forest condition). Each file with uncorrected data required post-processing using differential-correction data made available via the network of National Geodetic Survey, Continuously Operating Reference Stations (CORS).

Next, the spatial distribution of individual position measurements collected at each bluff was examined using a scatterplot matrix. The 3-D distribution was examined and filtered of positions associated with conspicuous multi-path errors (i.e., a linear pattern of sequential measurements that drifted over distances greater than one meter and suggested the incoming radio signal was bouncing off a nearby object) or indicators of poor satellite geometries (i.e., VDOP values > 3.0). The remaining set of acceptable positions was summarized geometrically to support average x, y and z coordinate values and measures of precision (i.e., standard deviation).

Elevation values were processed one step further to convert heights referenced to the WGS84 ellipsoid to orthometric heights, which are referenced to the North American Vertical Datum of 1988 (NAVD88) and tied to the familiar notion of mean sea-level. Orthometric height (H) is calculated as:

$$H = h - N \qquad \text{[Eq. 1]}$$

where: h is the average of sampled heights above the WGS84 ellipsoid as obtained from GPS leveling; and N is the geoidal undulation at that location and

obtained from the GEOID03 model (Roman et al., 2004). In Michigan, users of GEOID03 are able to convert GPS-measured ellipsoid heights to orthometric heights to within 2.7 cm of traditional land-based geodetic measurements (Roman et al., 2004: 11, Table 1).

Last, field notes, digital images, and feature positions were reviewed a final time. Each elevation value was adjusted downward to account for the tripod height (two meters) any distance between the land surface and the buried gravel lag. Feature positions associated with conspicuous wave-cut bluffs were added as records to the glacial Lake Algonquin dataset and exported to an ASCII text file, which is readable by common GIS or spreadsheet applications. Feature positions not associated with conspicuous wave-cut bluffs are retained in a supplemental database.

This research employs the same sets of selection criteria, GPS equipment (Trimble XRS receiver, antenna and software) and real-time differential correction procedures used by Schaetzl et al. (2002). So, by following the same data collection methods and using the same field equipment, it is reasonable to assume that the data collected during this exercise can be conflated with data collected during the previous work. Yet, to ensure data are conflated properly in every manner, I utilized the original and unprocessed set of GPS data files collected by Schaetzl et al. (2002), which I inherited, and processed each according to the model describe above. The only notable difference in methods was that Schaetzl et al. (2002) employed the GEOID96 geoid model (Milbert and

Smith, 1996) and this work uses the current GEOID03 geoid model (Roman et al., 2004) to convert heights measured above the ellipsoid to elevations tied to the NAVD88. The current geoid model is considered the most accurate available.

Summary of prior mapping campaigns

Sly and Lewis (1972), Cowan (1985), and Karrow (1987) collected paleoshoreline data at Manitoulin Island, Sault Ste. Marie and St. Joseph Island, Ontario, respectively, and correlated their features with Algonquin lake phases named by Deane (1950: Ardtrea, Upper Orillia and Lower Orillia), Stanley (1936: Wyebridge, Penetang, Cedar Point and Payette) and Hough (1958: Sheguiandah and Korah). Their campaigns relied on the bases of wave-cut bluffs to be indicators of former lake levels and they employed survey-grade equipment to measure paleoshoreline elevations precisely and accurately. Moreover, features at Sault Ste. Marie and St. Joseph Island are situated near others surveyed in Northern Michigan, so I used them to inform my classification of relict features in Northern Michigan and, in effect, revise some previous classifications proposed by Farrand and Drexler (1985) and Schaetzl et al. (2002).

Cowan (1985) mapped Quaternary sediments at Sault Ste. Marie, Ontario, and concluded the sandy terrain situated between the exposed Canadian Shield (to the north) and St. Marys River (to the south) exhibits a descending sequence of stranded shoreline features. He associated the uppermost (at 309 m) with the Main phase of glacial Lake Algonquin. Although Cowan reported elevations, he

did not report the locations of features he surveyed, so readers of his report cannot use it as a field guide. I contacted Dr. Cowan to inquire about the locations of bluff features he surveyed and, graciously, he sent me copies of his field notes and data. He also sent copies of topographic maps, on which he marked the locations of benchmarks, level lines and relict bluffs. Given this wealth of information, I was able to combine his surveyed elevation data (z) with corresponding location data (x,y) that I interpolated from each topographic map. According to Cowan (1985), his elevation data are accurate to within 30 centimeters. The location data I interpolated from topographic maps are accurate to within 25 meters. Table 3.1 summarizes Cowan's (1985) results (Table 1, p34).

Table 3.1: Approximate elevations for glacial Lake Algonquin water planes and the Nipissing water plane at Sault Ste. Marie and Manitoulin Island, Ontario (Cowan, 1985).

Elevation at Sault Ste. Marie (m)	Elevation at Manitoulin Island (m)	Lake phase
309	309	Main
302?	-	Ardtrea
295	287-296	Upper Orillia
?	-	Lower Orillia
275?	271-276	Wyebridge
265	267	Penetang
257	259	Cedar Point
247	244	Payette
233±	233	Sheguiandah
210	212	Korah
198	198	Nipissing

Karrow (1987) mapped Quaternary sediments at St. Joseph Island, Ontario and surveyed stranded shoreline features. Specifically, he measured the elevations of wave-cut bluffs and the tops of beach bars. He projected his surveyed elevation data onto a line of profile oriented along the presumed direction of maximum uplift (N15°E; after Futyma, 1981). Karrow compared his projected elevation data to the set of previously named water planes (Hough, 1958; Sly and Lewis, 1972; and Cowan, 1985) and concluded, despite some inconsistencies, that all but the central hill of St. Joseph Island was submerged by the Main phase of glacial Lake Algonquin. I summarize Karrow's Figure 5 (p116-117) as Table 3.2 to facilitate comparison with data I collected in this work.

Table 3.2: Lake level elevations for glacial Lake Algonquin water planes and the Nipissing water plane at the southern end of proto-St. Joseph Island, Ontario (Karrow, 1987).

Elevation (m)	Association
280	Main Algonquin
272?	Ardtrea
266?	Upper Orillia
258?	Lower Orillia
240?	Wyebridge
232	Penetang
225	Cedar Point
212	Payette
200	Sheguiandah
-	Korah
196	Nipissing

Readers of Karrow's (1987) report cannot use it as a field guide, so I contacted him to inquire about the locations of the bluff features he surveyed.

He graciously sent me copies of his survey data and marked topographic maps with the locations of relict wave-cut bluffs he surveyed. Given this information, I was able to combine his surveyed elevations (z) with corresponding location data (x,y) that I interpolated from topographic maps (Figure . In related work, Karrow (1988) indicates his surveying method yield elevations with decimeter-level accuracy. The location data I interpolated from topographic maps are accurate to within 25 meters, which is the precision afforded by the width of a printed contour line at the 1:50,000 scale.

Mapping campaigns conducted for this work

Frank Taylor stressed the importance of ancient islands when he wrote:

> "...[they] can hardly be overestimated, especially if they are situated well out from the mainland. Each one furnishes a new point of support for the restoration of the water plane and must prove valuable in the ultimate study of the earth's history as disclosed in the deformation of former water levels" (Taylor, 1895: 28)

Accordingly, I focused much of my attention and fieldwork on contemporary landforms that may have existed as islands in glacial Lake Algonquin. I visited sites with potential bluff features between June 2000 and December 2003. The subsections that follow document features and observations I made during these visits. In the text I provide maps and refer to field sites using a system of unique

site identification numbers (e.g., SID642) and report features elevations in meters. Figure 3.4 can be used to reference each of the smaller-scaled area maps. Last but not least, I report correlations I made between elevations taken from relict wave-cut bluffs and named glacial Lake Algonquin lake phases.

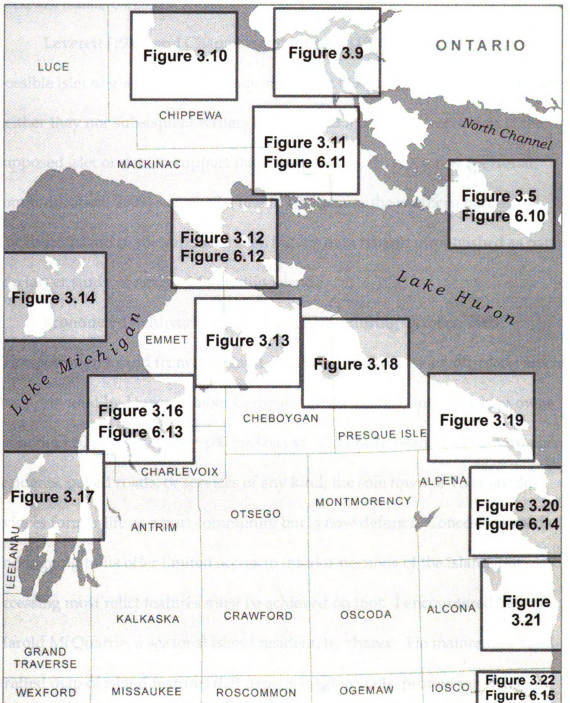


Figure 3.4: Index map for smaller-scaled maps that show field campaigns and field sites mentioned in this chapter.

Cockburn Island, Ontario

Leverett (1913) and Chapman and Putnam (1966) mentioned that a possible islet of glacial Lake Algonquin exists at Cockburn Island, Ontario, but neither they nor subsequent writers have offered a detailed description of the supposed islet or data to support their observations. P. F. Karrow (personal communication, 2003) surveyed a line in 1991 across the northern part of Cockburn Island to the supposed islet, but his data remain unpublished as part of a larger study of nearby Manitoulin Island.

I conducted fieldwork on Cockburn Island during October, 2003. Transportation to and from the Island, lodging, and access to an off-road vehicle were provided by Huron Timber Company of Thessalon, Ontario, which owns more than 80 percent of the ~100 km^2 island. Cockburn Island has no permanent residents, paved roads, or services of any kind; the sole town of Tolsmaville evinces former life as a port community but is now defunct. Concession roads and logging trails offer limited access to interior portions of the island, but accessing most relict features must be achieved on foot. I encountered Mr. Harold McQuarrie, a seasonal island resident, by chance. He maintains a hand-drafted map of island features that depicts logging trails, property ownership boundaries, concession- and patent-holder names, and basic hydrographic features. Mr. McQuarrie's map (McQuarrie, 2000) greatly facilitated my efforts to traverse the Island and approach bluff targets. Figure 3.5 shows Cockburn Island and identifies field sites visited and discussed in the text.

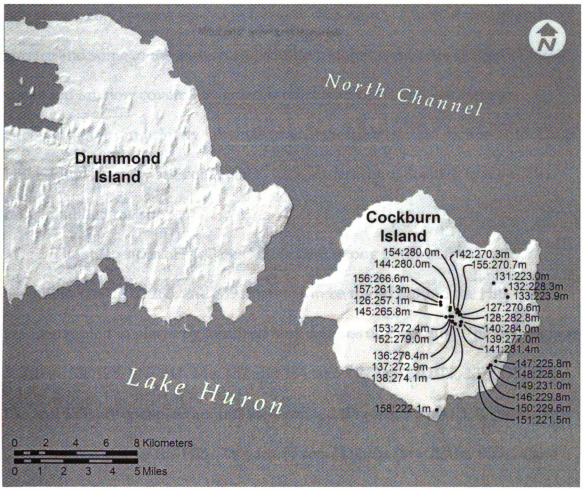


Figure 3.5: Relict bluff sites at Cockburn Island, Ontario. Sites are labeled with a unique site identification number and an elevation value (e.g., 642: 200 m).

I focused attention on a small upland called McCaigs Hill. McCaigs Hill is the highest feature on Cockburn Island, approximately 2 km^2 in size, composed of unconsolidated sediments, and divided roughly into quadrants by two intersecting concession roads. McCaigs Hill exhibits a relatively smooth surface that dips visibly southward; only a shallow saddle, which trends NNE-SSW, and scattered well-rounded boulders interrupt the surface. Soil samples taken along the surface (to a maximum depth of 1.5 meters) revealed red-brown sands and

few stones; clay content tended to increase with depth. Much of the upland surface and some of the eastern and southern slopes were once cleared of forest cover and are now covered by grasses; relict landforms in these areas are exposed plainly and clearly. A small area in the northeastern section of McCaigs Hill is known locally as Scotch Block, for a settlement of Scottish families that once inhabited the site.

The steep sides of McCaigs Hill exhibit strong bluffs at four distinct elevations (280, 272, 266, and 259 m); two can be traced around the Hill, but all are interrupted in places by localized bluff failures or road cuts. The two highest (~280 m: SID128, 136, 141, 144, 152 and 154; and ~272 m: SID127, 137, 138, 142, 153 and 155) are conspicuous and well-defined (Figures 3.6 and 3.7), particularly in the eastern side of the Hill. Two lower sets of bluffs (at ~259 m: SID126 and 157; and at ~266 m: SID145 and 156) are also conspicuous and well-defined, but on the northwestern side of the Hill only. The bluff at 259 m (height >16 m) is well preserved, but shrouded by dense tree cover along most of its length. All other bluffs are absent where this bluff is strongest; it visibly truncates the next higher bluff (266 m) and, perhaps, an intermediate bench. The bluff changes character rapidly, for it shortens into a low bluff and then degrades into three wave-cut scarps or bars that run in a south-southeasterly direction away from northwestern side of the upland. The bars are composed of rounded gravels and are relatively tall, narrow and compactly spaced at locations near the bluff site, but tend to shorten, widen and separate as they curve away from the Hill.



Figure 3.6: Image of a relict bluff on the south side of McCaigs Hill, Cockburn Island, Ontario.

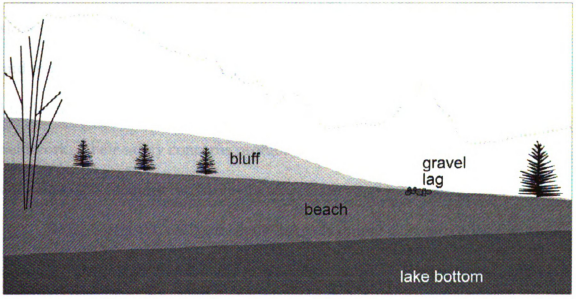


Figure 3.7: Diagram of the relict bluff shown in Figure 3.6. Shoreline positions were measured at gravel lag situated at the base of the bluff.

A pair of lower shorelines is also present (at ~230 m: SID132, 146, 149 and 150; and at ~222 m: SID131, 133, 147, 148, 151 and 158). They are situated several kilometers from McCaigs Hill and outline what must have been younger and larger proto-Cockburn Islands. I characterize these two shorelines as a pair because each occurs in close proximity to the other. For example, at some locations these features present as a set of gravelly bars, with one situated several meters higher than the other. At other locations they appear as a combination of erosional bluff and bar or as a set of erosional bluffs. Incidentally, this pair is the highest set of relict shoreline features connected to bedrock outcrops. I found small dolomite outcrops at the northern and southern tips of this ancient island which might have supplied the parent material for the gravelly bars.

Cedar swamps sandwich narrow hardwood stands situated along the sloping sands and gravels between the bluffs at the 222 m and 230 m elevations and might hold organic material suitable for radiocarbon analysis and dating. Lumbermen were harvesting hardwoods in this area and during the time of fieldwork. Their safety concerns prohibited me from accessing features at these worksites, so I consider the survey of relict features as incomplete.

Relict bluffs at Cockburn Island have elevations that correspond with the elevations of relict bluffs stranded at Sault Ste. Marie, St. Joseph Island, and Manitoulin Island as well as others in the eastern half of Michigan's Upper Peninsula. Table 3.3 lists the elevations of relict bluffs at Cockburn Island and the names of coplanar water levels at nearby St. Joseph Island.

Table 3.3: Approximate elevations of glacial Lake Algonquin water planes measured at Cockburn Island, Ontario.

Approximate elevation (m)	Water plane/lake phase
280	Main
272	Ardtrea
266	Upper Orillia
259	Lower Orillia
230	Penetang
222	Cedar Point

Cowan (1985) describes relict shoreline features at Sault Ste. Marie, Ontario and argues they are directly comparable with others at Little Current, Ontario (Sly and Lewis, 1972), because respective interpretations of both "Main Algonquin and Nipissing levels are within one meter of each other" (p.36). If Cowan's argument is correct, then both locations have experienced similar rates of, and cumulative amounts of, isostatic recovery over time. Cartographically, an isoline of paleolake-plane elevation can be drawn to represent the apparent connection between these two locations (Figure 3.8, 309 m). Such a line is oriented similarly to other isolines drawn by Goldthwait (1910:38), Leverett and Taylor (1915:429), Hough (1958:256) and Clark and Persoage (1970).

Cockburn Island is situated south of the isoline drawn between Sault Ste. Marie and Little Current, Ontario (Figure 3.8). Given the generally accepted trend of increasing isostatic rebound across the region (N15°E; Futyma, 1981) and given the relative location of Cockburn Island with respect to this isoline, it is reasonable to expect that intersections between glacial Lake Algonquin water

planes and the Cockburn Island land surface occur today at elevations lower than those measured at Sault Ste. Marie and Little Current, ON (309 m, after Cowan, 1985: p. 34). The highest shoreline measured at Cockburn Island is at 280.2 m, which is lower than the highest shorelines found at Sault Ste. Marie and Little Current, and proximate to the highest shorelines found at St. Joseph Island, ON (280 - 285 m, after Karrow, 1987) and in northern Michigan (282 - 285 m, after Schaetzl et al., 2002). The highest shorelines at St. Joseph Island and in northern Michigan are associated with the Main phase of glacial Lake Algonquin, so it seems reasonable to infer from the near-equivalent elevation of the highest shoreline at Cockburn Island that McCaigs Hill, a small upland, was an ancient islet of the Main phase of glacial Lake Algonquin.

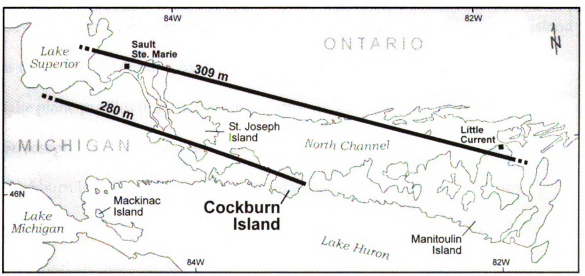


Figure 3.8: Apparent contours across the Main Lake Algonquin water plane.

Interpretation of lower shorelines is problematic, however, because they cannot be correlated consistently with water planes named at nearby places. For example, Schaetzl et al. (2002) argued that only the Main, Ardtrea, Wyebridge and Payette phases can be interpreted consistently among the data they collected in Michigan. This set of four lake phases is not sufficient for interpreting the six water planes I observed at Cockburn Island. Based on their isoline maps of bluff elevations (Schaetzl et al., 2002:411) bluffs at Cockburn Island that occur at 280, 272, and 266 m correlate closely with their Main, Ardtrea and Wyebridge phases, respectively, the bluffs stranded at 259, 230, and 222 m have no correlates. Karrow (1987:118) reports many relict shoreline features on St. Joseph Island that appear to correspond to Upper Group and Lower Group beaches, but he claims his data are insufficient "to clearly distinguish particularly consistent and well-developed water planes" below the highest one. Yet, assuming St. Joseph Island is to Cockburn Island as Sault Ste. Marie is to Manitoulin Island, I use Karrow's lake plane profiles (Figure 5, p116-117) to extrapolate named water levels from St. Joseph Island to Cockburn Island. In descending order, paleoshorelines at Cockburn Island correspond with the Main, Ardtrea, Upper Orillia, Lower Orillia, Penetang and Cedar Point water planes.

Sugar Island, Michigan

Schaetzl et al. (2002) surveyed two relict features at Sugar Island, which is situated in the St. Marys River and between Sault Ste. Marie and St. Joseph

Island, Ontario (Figure 3.9). The authors measured a high feature twice (240 m: SID395 and 407) and correlated it with the Payette phase. They measured a low feature twice (228 m: SID396 and 453) but correlated one measurement with Lake Minong phase of Lake Superior and attributed the other to an unnamed "lower" phase of Lake Huron. In light of data available in nearby Canada, I believe the lower feature is best correlated with the Sheguiandah phase.

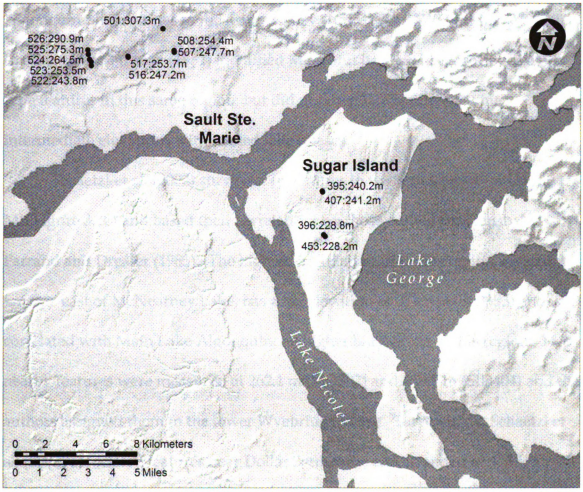


Figure 3.9: Relict bluff sites at Sugar Island, Michigan. Sites are labeled with a unique site identification number and an elevation value (e.g., 642: 200 m). Also shown are the locations of features surveyed by Cowan (1985).

Rexford, Michigan

Main Algonquin occupied a "sizeable part of Whitefish Bay in eastern Lake Superior" (Cowan, 1985: 34). Farrand and Drexler (1985) recognized several post-Algonquin lakes, "at least through Sheguiandah" (p30), that transgressed into the Superior basin; they correlated features found near Pendills Bay with the Wyebridge and Payette phases. A careful read suggests, however, that Farrand and Drexler (1985) were not fully confident in their assignments of Algonquin phase names to the features they studied (i.e., "Wyebridge(?)", p29). In other work, Futyma (1981) identified Main and Battlefield (now deprecated) type features in this same region, but did not correlate features having intermediate elevations with named lake phases.

Schaetzl et al. (2002) surveyed 16 features in western Chippewa County, MI (Figure 3.10) and based their correlations on those named previously by Farrand and Drexler (1985). The highest stranded bluff in this region, located 3 km due east of McNearney Lake, has a toe elevation of 281.9 m (SID393) and is correlated with Main Lake Algonquin; no higher bluff exists in this region. Two nearby features were measured at 262.1 m (SID392) and 259.5 m (SID404) and the authors assigned them to the lower Wyebridge phase. Surprisingly, Schaetzl et al. (2002) associated features near Dollar Settlement and stranded at ~232 m with Lake Minong. Farrand and Drexler clearly describe a bench near Dollar Settlement "at 213 to 219 m" to be "a good candidate for the Minong shoreline" because it occurs in the Pendills Lake embayment immediately west of Nadoway

Point and does not occur "to the east on the Lake Huron slope" (Farrand and Drexler, 1985: 29). Confusion about these features prompted me to reinterpret them.

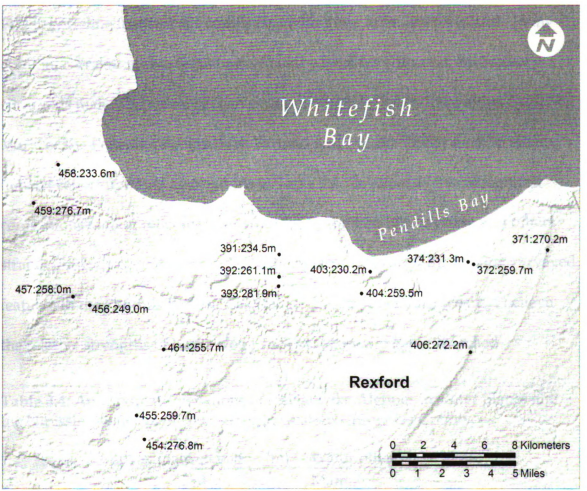


Figure 3.10: Relict bluff sites near Rexford, Michigan. Sites are labeled with a unique site identification number and an elevation value (e.g., 642: 200 m).

The highest stranded shoreline in this region has an elevation of 281.9 m. Nearby features associated with the Nipissing water plane rest at 198 m. The elevations of Main Algonquin and Nipissing features correspond very closely

with those measured at St. Joseph Island and do not correspond with those located, for example, north of Sault Ste. Marie (see Figure 3.2). Assuming St. Joseph Island is to the Pendills Bay area as Manitoulin Island is to Sault Ste. Marie (after Cowan, 1985), I used Karrow's lake plane profiles (Figure 5, p116-117) to correlate features at Pendills Bay with those at St. Joseph Island. In my opinion, correlating two sequences of nearby features with near equivalent elevations makes better sense than extrapolating lake levels from either Sault Ste. Marie or the Penetang Peninsula as Farrand and Drexler (1985) seem to have done. I report updated associations in Table 3.4. In effect, I have recognized connections among relict features stranded in the Pendills Bay area and others stranded at St. Joseph Island and Cockburn Island (Figure 3.5). Having surveyed features in the Pendills Bay area, as well as those at Cockburn Island, I believe the relative strengths of bluffs along each sequence are better matched.

Table 3.4: Approximate elevations of glacial Lake Algonquin water planes and the Nipissing water plane measured in western Chippewa County.

Approximate elevation (m)	Water plane/lake phase
280	Main
273	Ardtrea
-	Upper Orillia
259	Lower Orillia
240	Wyebridge
232	Penetang
198	Nipissing

The Munuscong Islands

Taylor (1895) reported observations and provisional height measurements taken along a set of Algonquin strands situated ~1.5 km north of Hessel, MI. According to Taylor, the Munuscong Islands were the only landforms that interrupted the highest Algonquin water surface "between Mackinac and the Canadian Highlands back of Sault Ste. Marie" (p28). Although the author reports that at least three islands remain, he visited only two: the one closest to Hessel and "irregular in outline" (p.26); and a smaller island situated northeast of Hessel that exhibited "precipitous cliffs of limestone 75 to 100 feet in height" (p26). Taylor did not visit the largest of the three islands he mentioned, which is situated northwest of Hessel.

Eighty-five years later, Futyma (1980) revisited the Munuscong Islands. Unfortunately, his report offers no new information about these landforms. A careful review of Appendix A (Futyma, 1980) indicates the author focused on just the one island closest to Hessel and relied only on Taylor's (1895) and Leverett and Taylor's (1915) early findings.

Twenty years after Futyma, Schaetzl et al. (2002) targeted these islands, were finally able to access and study a portion of the unvisited northwestern island, and provided new information. In all, Schaetzl et al. (2002) measured 10 positions in the Munuscong Island region. They identified shorelines associated with the Main, Ardtrea and Wyebridge phases along the central island closest to

Hessel; the Wyebridge and Payette phases along a minor islet; and the Wyebridge, Payette and lower phases along the large northwestern island.

I conducted fieldwork in the Munuscong Islands region, visited old sites, and collected five new position measurements (Figure 3.11). I focused most of my attention on the large northwestern island. The upland covers the better part of 9 km^2 and was accessible to me only via a poorly maintained two-track named Fish Road. All other points of entry, particularly the one along Criderman Road, are gated and posted. In the southern half of Sec. 14 T43N R2W, I observed two bluffs, one massive (height > 35 m) and one lesser, but only by comparison. Huge limestone boulders litter the bases of these giant bluffs. The sheer sizes of these well-rounded boulders, perched atop beach sand, clearly imply powerful water action. Unable to receive GPS radio signals at positions along the bluff toe, I traced the features northward into the northern half of Section 14. There I was able to measure positions along the upper and lower shorelines. The upper shoreline is stranded at 266.9 m (SID172) and I associate it with the Main phase. The lower shoreline is stranded at the 259.7 m (SID171) plane and, I believe, is associated with the Ardtrea phase. I measured a third shoreline position in Sec. 26 T43N R2W at the 264.3 m plane (SID169), which I believe is also associated with the Main phase. I attempted to maneuver toward the northwestern side of the large island, but nearly every pathway and trail is gated or posted. I believe the northwestern side holds additional massive bluffs, which are visually apparent from nearby Interstate 75, and I hope to study them someday.

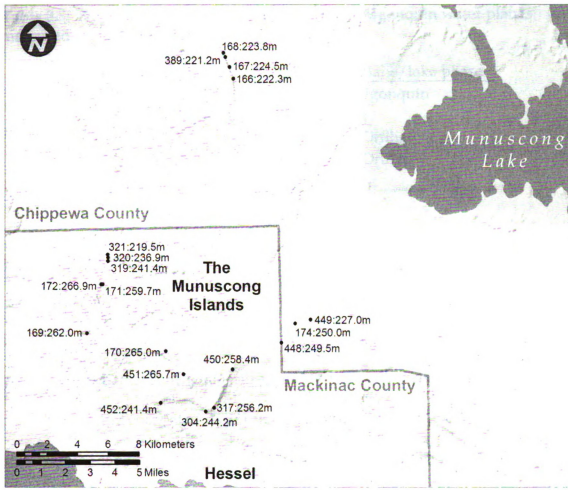


Figure 3.11: Relict bluff sites in the Munuscong Islands region. Sites are labeled with a unique site identification number and an elevation value (e.g., 642: 200 m).

An apparent fourth and easternmost island of the Munuscong Island chain remains unstudied. Much of the land area is currently held by mining interests; a large quarry occupies large portions of Sections 3 and 10 of T42N R1E and, perhaps, is the site where Taylor (1895:26) observed his "precipitous cliffs of limestone." Table 3.5 lists the glacial Lake Algonquin water planes I associated with paleoshoreline elevations in this region.

Table 3.5: Approximate elevations of glacial Lake Algonquin water planes measured in the Munuscong Islands region.

Approximate elevation (m)	Water plane/lake phase
265	Main Algonquin
258	Ardtrea
250	Upper Orillia
242	Lower Orillia
220	Penetang

Kincheloe, Michigan

The Kinross State Correctional Facility (formerly the Kincheloe Air Force Base) is situated atop a raised terrace; a conspicuous wave-cut bluff marks nearly every side. Schaetzl et al. (2002) surveyed the toe of a substantial bluff on its eastern flank and correlated its 221 m elevation with Lake Minong (SID389). I surveyed the same feature at three locations along 2 km of its length (SID166, 167 and 168) and obtained an average elevation of 223 m (Figure 3.11). Farrand and Drexler (1985), working northwest of Kincheloe, MI in the Pendills Bay area, identified Lake Minong shorelines at elevations between 213 and 219 m and contend a "Nadoway Point-Gross Cap sill" (p29) retained Minong waters in the Superior Basin until it was downcut (or breached by inflow from Lake Agassiz), thereby lowering water level even further. In light of Kincheloe's relative location with respect to the proposed Nadoway Point-Gross Cap sill and situation with respect to St. Joseph Island (~30 km), I believe the stranded bluff at Kincheloe is too high to be associated with the Minong phase of Lake Superior. I

believe this feature is better correlated with the Cedar Point water level of glacial Lake Algonquin.

Mackinac Island, Michigan

Leverett and Taylor (1915) identified an ancient island at Mackinac Island, MI, which is uniquely situated near the confluence of Lakes Michigan and Huron, and between the Munuscong Islands in Michigan's Upper Peninsula and the Pellston/Riggsville Islands region of the Lower Peninsula. They describe "splendid displays" of "all the beaches from the upper Algonquin down" (Leverett and Taylor, 1915: p424) and assigned the now deprecated Upper Group, Battlefield and Fort Brady labels, in descending order, to three groups of successively lower relict features.

Stanley (1936) studied relict shoreline features along the Penetanguishene Peninsula (a.k.a. Penetang Peninsula) of Ontario and compared water levels there with those he and Leverett and Taylor (1915) observed at Mackinac Island. I include an excerpt from his report here (Stanley, 1936:1955):

> On theoretical grounds, all the Algonquin planes here discussed should be separated by similar intervals wherever the total amount of Algonquin deformation is equal, provided that tilting between Algonquin and Nipissing times proceeded always in the same direction. For instance, on Mackinac Island there should be a shoreline about 90 feet lower than the highest Algonquin (809-812)

> in order to correlate with the Wyebridge shoreline in the Penetang area (which is 90 feet below the Algonquin in that region). The type Battlefield beach (719) on Mackinac Island fulfills this requirement exactly.

Stanley's provisional correlation of Ontario's Wyebridge type beach and Mackinac Island's Battlefield beaches required a leap of faith considering that he could not identify the Wyebridge shoreline near Wasaga Beach (see Stanley, 1936: 1938 and Table 3 on page 1951) and his work at Mackinac Island yielded, in his own words, "poor results" (p1955). He expressed uncertainty regarding "just how the lower Algonquin beaches of the Mackinac region fit in with those near Penetang" (p1955). Deane (1950: 74), working later and near Lake Simcoe, Ontario, argued Wyebridge features are "not strong" and indicate "only a short pause of Lake Algonquin at this level." He also reported elevations and relative strengths of features formed along four upper lake levels (Main, Ardtrea, Upper Orillia and Lower Orillia) and characterized the Main and Upper Orillia paleoshorelines as strongest.

Uncertainty about the elevations of features at Mackinac Island and their correlations with others prompted Schaetzl et al. (2002) to visit the island and survey relict features there; they obtained five paleoshoreline positions (Figure 3.12). Schaetzl et al. (2002) correlated the highest bluff (242.0 m: SID307) with Main Lake Algonquin, a lower observation (236.3 m: SID302) with the Ardtrea

phase, and three lower observations (~228.0 m: SID301, 305 and 306) with the Wyebridge phase. They claim paleoshorelines in the vicinity of Mackinac Island correlate well with those near the center of Deane's (1950) study area.

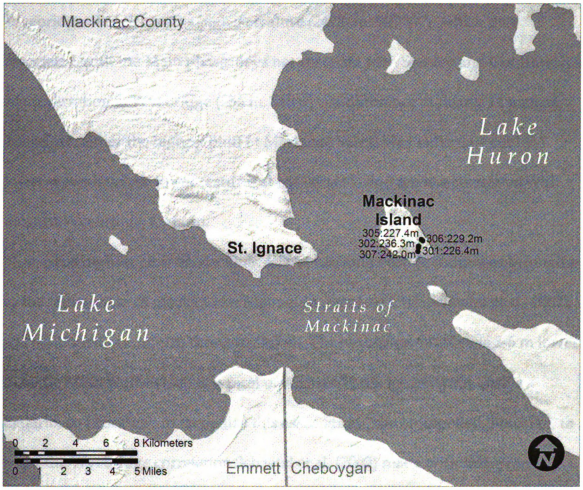


Figure 3.12: Relict bluff sites at Mackinac Island. Sites are labeled with a unique site identification number and an elevation value (e.g., 642: 200 m).

Although two paleoshorelines at Mackinac Island apparently share elevations with others located at Wyebridge, Ontrario, Schaetzl et al. (2002) did not apply Stanley or Deane's typology consistently to a third. For example, the

Nipissing plane at Mackinac Island occurs at ~193 m (634 ft) and seems to correspond with Goldthwait (1910) and Stanley's (1936) Nipissing shoreline at Wyebridge, Ontario (194 m, 637 ft). Mackinac bluffs stranded at ~228.0 m (750 ft) have elevations that correspond with Stanley's (1936) Wyebridge bluff at Wyebridge. But Schaetzl's highest feature (242.0 m: SID307), which they associated with the Main phase, does not correlate with Stanley and Goldthwait's Main elevation at Wyebridge (256 m, 840 ft) -- a difference of nearly 14 meters. Therefore, either the highest bluff at Mackinac Island was either last cut by a lower water level, or lower features at Mackinac Island are not correlated with those at Wyebridge, Ontario.

The highest bluff at Mackinac Island has long been identified as belonging to the Main phase of glacial Lake Algonquin (Stanley, 1945; Schaetzl et al., 2002), so I continue to recognize this association. The next lower bluff rests 5-6 m lower than the Main bluff, which is typical of Ardtrea bluffs located near Orillia, Ontario, so I continue to recognize this association. I am compelled, however, to reject the Wyebridge correlation Schaetzl et al. (2002) made with features stranded at 228 m. Conspicuous examples of Upper Orillia shorelines and few instances of Wyebridge shorelines are present at Sault Ste. Marie, Cockburn Island, the Munuscong Islands, the Penetang Peninsula, or in Lake Simcoe District, so it seems unlikely that Wyebridge shorelines would be expressed better at Mackinac Island than those carved elsewhere, or expressed stronger than those carved by the Upper Orillia water plane. So, in light of the elevations

and relative strengths of Upper Orillia shorelines elsewhere, and the relative location of Mackinac Island with respect to these Upper Orillia shoreline features, I correlate features at ~228 m on Mackinac Island with the Upper Orillia phase of glacial Lake Algonquin and not with the Wyebridge phase.

Table 3.6: Approximate elevations of glacial Lake Algonquin water planes measured at Mackinac Island, Michigan.

Approximate elevation (m)	Water plane/lake phase
242	Main
236	Ardtrea
228	Upper Orillia
?	Lower (observed but not surveyed)

The Douglas Lake area, Michigan

Schaetzl et al. (2002:406) began classifying their shoreline data near Douglas Lake and the University of Michigan Biological Station in Cheboygan County, MI "because only two highly distinct shorelines exist in this region." According to their work, and their interpretation of Leverett and Taylor's (1915) previous work, relict shorelines of the Main phase of glacial Lake Algonquin are expected at the 225 m elevation plane and remnants of a lower and later shoreline are expected at ~210 m. Interestingly, Spurr and Zumberge (1956) also argue that two distinct shorelines exist in this region; they accept the Main phase at 738 ft (225 m) but claim residual segments of a pre-Algonquin shoreline are stranded at 724 ft (220 m). Spurr and Zumberge (1956) make no mention of a post-Main shoreline at 210 m. Obviously, these reports differ in their

interpretations. I am disinclined to accept Spurr and Zumberge's (1956) pre-Algonquin lower shoreline hypothesis, however, because I expect that any feature composed of unconsolidated sediments (as are the ones in question) would have been buried, reshaped or reworked under the high waters of the relatively long-standing Main phase. Also, the idea that drowned shorelines simply re-emerged unscathed after several hundred years of subaqueous exposure, especially in an environment that suffered "the long fetch afforded by Lake Algonquin" and "frequent and intense cyclonic storms" (Krist and Schaetzl, 2001:14), seems unreasonable.

Before conducting fieldwork, I reviewed Schaetzl's data and plotted them on the Pellston, Indianville, and Mullet Lake MI 7.5 minute USGS topographic map sheets. Of the thirteen points they surveyed in this area, four have elevation values near 230 m, six have values near 225 m, one at 221 m, and two others at ~211 m. Given the 3-meter limit of precision I have adopted during this work, the differences among these elevation values suggest that four, not two, distinctive water levels existed in this region.

I revisited field sites at locations around Douglas Lake and surveyed other relict shorelines nearby (Figure 3.13). I started at the boat ramp located due south of Pells Island and traveled counterclockwise around the upland known as Pellston Island. In SE$\frac{1}{4}$ Sec. 30 T37N R3W, I measured the gravel lag at the base of a protruding relict bluff at 222.2 m (SID180). I then followed the base of the upland as it crosses over the Pellston Island spit (Krist and Schaetzl, 2001) and

then south and down into SE¼ Sec. 25 T37N R4W; where I measured the base of a relict bluff at 223.0 m (SID181). I continued southward and surveyed several positions along the west side of the island (unfortunately, most of these points were later discarded because each sample contained large anomalies, thus indicating the nearby tree stands or the intermittent snowfalls of the week perturbed GPS signal reception). In NE¼ SW¼ Sec. 7 T36N R3W, the base of a stranded bluff rests at 223.0 m (SID182). Schaetzl et al. (2002) measured a 221.6 m elevation at a location 1 km east of this point and along the same feature (SID328). The apparent difference in elevation between these two samples (~1.4 m) is less than the critical threshold value (3.0 m) used to distinguish distinctive lake levels, so they are considered to represent that same water plane.

I was able to observe several remnants of what I assume to be lower and later shorelines as I traveled around the north end of Burt Lake. For example, as Indian Road approaches Burt Lake, several houses are situated along a bluff cut at 187.6 m (SID184), which Spurr and Zumberge (1956:102) might associate with the Nipissing Great Lakes. On the east side of Burt Lake, a pipeline runs north-south through Sec. 12 T36N R3W and crosses two apparent shorelines. Admittedly, the bluffs here are weak but they are discernible. The higher bluff was measured at 211.8 m (SID185) and the lower at 197.0 m (SID186).

Returning to Douglas Lake, starting at South Fish Tail Bay (NE ¼ Sec. 33 T37N R3W) and working westward, a single relict shoreline and bluff can be traced along and above the southern rim of Douglas Lake. I found an instance of

a double bluff near Grapevine Point, which is located due north of the University of Michigan Biological Station campus (Sec. 28 T37N R3W). Figure 2 in Spurr and Zumberge (1956) illustrates the feature. The base of the lower bluff is cut at 220.3 m (SID179), which is 3 m higher than the average water level of Douglas Lake. The base of the upper bluff rests at 227.4 m (SID178).

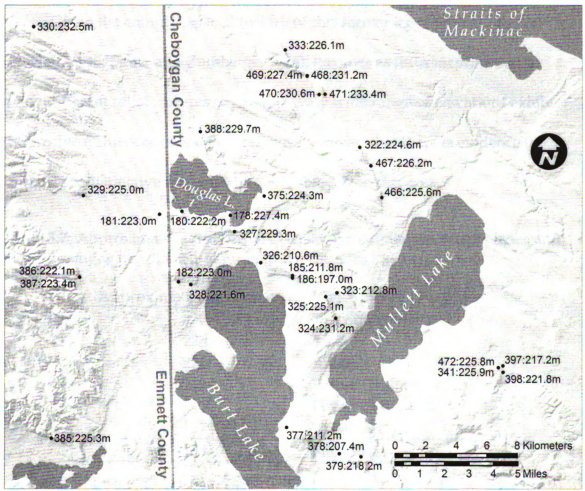


Figure 3.13: Relict bluff sites in the Douglas Lake area. Sites are labeled with a unique site identification number and an elevation value (e.g., 642: 200 m).

I surveyed other relict bluffs north of Douglas Lake (e.g., NW of North Fishtail Bay in Sec. 22 T37N R3W and SE of Lancaster Lake in Sec. 8 of the same township), but had to discard these samples because they contain highly scattered position data. My field notes indicate a heavy snow/rain mix was falling during data collection, so it is likely that precipitation interfered with GPS signal transmissions as water collected atop the antenna.

Given the complex glacial history of this former ice-marginal region (Blewett, 1995; Spurr and Zumberge, 1956), it comes as little surprise that so many different relict features over a relatively wide range of elevations exhibit the erosive influences of water. I believe, however, that there is evidence to support six distinctive water levels (see Table 3.7) in this area.

Table 3.7: Approximate elevations of glacial Lake Algonquin water planes and the Nipissing water plane measured in the Douglas Lake area.

Approximate elevation (m)	Water plane/lake phase
230	Ice-contact margin?
225	Main
221	Ardtrea
212	Upper Orillia
-	Lower Orillia
197	Uncertain
188	Nipissing

As mentioned above, I reviewed Schaetzl's data for this region and found 4 points with elevation values near 230 m (e.g., SID327), which is 5 meters higher than the generally accepted elevation (~225 m) of the Main phase (Spurr and

Zumberge, 1956; Schaetzl et al., 2002). Features at this elevation might mark an ice-contact margin described by Spurr and Zumberge (1956). I removed these points from the glacial Lake Algonquin dataset and placed them into the supplemental dataset. Among the areas covered by the Pellston, Indianville, and Mullet Lake, MI topographic map sheets, 8 samples now mark relict bluffs along the 225 m elevation plane. Given the long history of associating features at this elevation to the Main phase of glacial Lake Algonquin, I am compelled to do the same. Smaller sets of lower shoreline relicts are associated with later and lower glacial Lake Algonquin lake phases as indicated in Table 3.7; the lowest position is associated with the Nipissing Great Lakes.

Beaver Island, Michigan

Beaver Island is a part of Charlevoix County, Michigan. It is situated among a small group of islands in Lake Michigan, approximately 50 km north-northwest of the City of Charlevoix and 55 km west of Mackinac City. Leverett and Taylor (1915:425) described an upland area on Beaver Island as a "morainic tract about 4 miles long from northeast to southwest and $1\frac{1}{2}$ miles wide" with altitudes "considerably above the highest Algonquin beach." The authors explored "unusually well developed" (p.425) beaches on the north, south and west sides of this upland; they make no mention, however, of any relict coastal landforms on the eastern side of Beaver Island.

Dietrich (1978) visited Beaver Island fifty years later, examined soils and landforms around Leverett and Taylor's (1915:425) "morainic tract" and found features that "appear to be beach gravels that are well below what are generally recognized as Lake Algonquin levels" (p.287). He reasoned these beach gravels might belong to later and lower glacial Lake Algonquin lake phases because they occur at elevations higher than the expected Nipissing water plane. Furthermore, he claimed the most substantial bluff features, particularly those situated on the southern and western sides of the relict upland, were eroded by Lake Nipissing and not by Lake Algonquin - as Leverett and Taylor (1915) claimed. Dietrich (1978) continued to argue that "the island's only prominent wave-cut scarp attributable to Lake Algonquin" exists on the *eastern* side of the island "between Iron Ore Bay and Miller Marsh" (p.287). He also speculated that two small inland lakes (Fox Lake and Green's Lake) existed as bays in glacial Lake Algonquin. According to Dietrich's (1978) interpretation of Leverett and Taylor's (1915:p439) isobase map, the highest glacial Lake Algonquin water plane intersects the contemporary land surface between the 215 and 230 m planes of elevation. The highest elevation on the island surface is approximately 245 m, so it is possible that a proto-Beaver Island existed as an island in glacial Lake Algonquin. The apparent conflicts between claims made about the relationship between the highest Lake Algonquin water plane and the locations of relict lacustrine features on Beaver Island prompted me to visit the Island and examine these features.

I conducted fieldwork on Beaver Island, Michigan during late October, 2003 (Figure 3.14). I used the *Beaver Island North* and *Beaver Island South* 7.5 minute USGS topographic maps and *The Wojan-Cashman Map of Beaver Island* (Cashman and Wojan, 1977) as field guides. The provisional USGS maps provide good hypsometric information, but the topology of the local road network is better represented by the Wojan-Cashman Map. The morainic tract is situated in the southern half of the modern island.

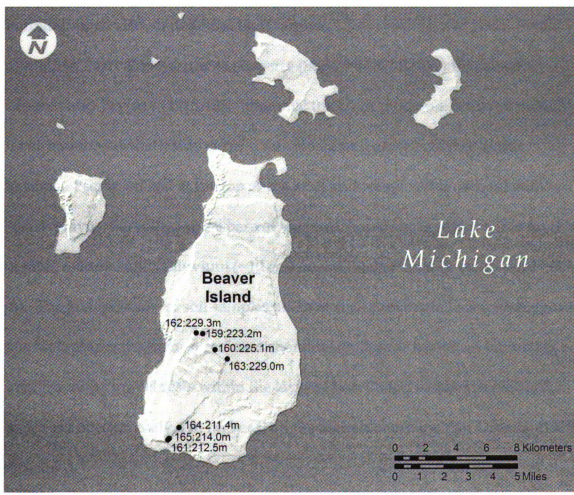


Figure 3.14: Relict bluff sites on Beaver Island, Michigan. Sites are labeled with a unique site identification number and an elevation value (e.g., 642: 200 m).

I selected an initial set of twelve potential bluff targets, which includes only those locations with elevations above the expected Nipissing water plane (189 m after Dietrich, 1978). Unfortunately, none of the maps I used illustrates the actual state of land ownership fragmentation or the maze of private in-holdings that exists within the Jordan River State Forest. Many in-holdings are fenced, gated and padlocked, so access to relict features on these properties is prohibited without permission. I was able to contact several landowners and obtain permissions to access their lands, but was unable to secure enough permissions to visit all potential bluff targets.

Mr. Larry Dawson owns property (Sec. 29 T38N R10W) that abuts Leverett and Taylor's (1915:425) "morainic tract." A moderate bluff (~6 m high) is cut into the northern side of the tract. No other feature is higher at this location. I sampled soil at the top of the bluff and found red-brown till with coarse gravel. Sampling at the base of the bluff, however, revealed a thin layer of organic material and colluvium (~10 cm) over a thicker layer of beach sand (~1 m). The juxtaposition of soil samples taken at such proximate locations suggests this bluff marks the highest remnant shoreline on Beaver Island. A buried lag of small rounded gravel rests within the layer of beach sand at 229.3 m (SID162), which is approximately 6 m higher than the highest shoreline that Dietrich (1978) measured.

I followed the bluff eastwardly and down into a wetland where it loses its distinctive toe. I continued to follow the upland tract around the southern rim of

Fox Lake where I found a second wave-cut bluff at 223.2 m (SID159). The elevation of this feature is similar to the highest elevation that Dietrich (1978) reported and is approximately 2 meters higher than the average water level of Fox Lake (as indicated on USGS topographic maps). The near coincidence between bluff and lake elevations is, perhaps, the reason why Dietrich (1978) speculated Fox Lake once existed as a bay in glacial Lake Algonquin. Sampling at this location again revealed red-brown till at the bluff top and beach sand at the bluff base. The lower relict shoreline lost its distinctive character and graded into a wetland as I traveled southeasterly along the upland tract. I could not distinguish the higher shoreline feature (229.3 m) anywhere along the southern rim of Fox Lake.

About 1.2 km farther east, the lower shoreline regains its character in the form of a very large bluff (~15 m). Sampling at the top of the bluff revealed red-brown till composed mainly of sand with some gravel. Large boulders are scattered across the surface of the bluff top. Soil sampling at the base of the bluff (SID160: 225.1 m) revealed a layer of plant detritus, which rests over a layer of peat, which rests over a layer of beach sand. An apparent relict bar sits 50 m "lakeward" of the relict bluff, which may have acted as a barrier between open water and a lagoon that allowed the peat to form.

Vegetation is dense and the ground is very wet along the base of the large bluff. So, I retreated uphill to a trail that parallels the bluff top and continued eastward. After another kilometer or so I left the trail and followed the morainic

tract as it turns south. A few hundred meters farther, I found a conspicuous wave-cut bluff cut into the eastern side of the morainic tract at 229.0 m (SID163). Beyond this site the bluff loses its distinctive toe, vegetation becomes denser and the ground gets wetter. I assume this feature is correlated with the high feature I found on Mr. Dawson's property. I could not distinguish lower shoreline features at this site.

The eastern flank of the morainic tract is very difficult to approach from the northern end. I attempted to follow the Dotty Trail as marked on the Wojan-Cashman Map of Beaver Island (Cashman and Wojan, 1977), but found the path flooded and impassible. The western flank is also very difficult to approach because almost every access road is gated and locked, or posted with a hostile message for potential trespassers. Lacking permission, I did not search for relict shoreline features along these two flanks.

The eastern and western flanks of the morainic tract converge toward the southern end of proto-Beaver Island, but the tip of the tract has apparently been truncated by Nipissing waters (Dietrich, 1978). I visited the prominent Lake Algonquin scarp Dietrich (1978) described along the eastern side and "between Iron Ore Bay and Miller Marsh" (p.287) and measured three elevations along one-kilometer of its length (214.0 [SID165], 212.5 [SID161] and 211.4 m [SID164]). Each value is within 3 m of each other, so all are considered marks along one relict shoreline. In my opinion, this feature serves to distinguish a third and lower Algonquin water plane at Beaver Island.

As a final note, the supposed morainic tract changes character halfway along its 8 km length; rough hills typical of the northern 5 kilometers give way to a relatively smooth surface typical of the southern 3 kilometers. As mentioned above, soil samples taken above the highest shoreline in the northern zone yielded red-brown tills with gravels. Sediments sampled along the smooth surface near the southern edge, however, did not reveal a red-brown till, but a sequence of well-sorted sands and gravels. A gravel pit at the southern tip of the upland reveals a profile of sorted sediments (Figure 3.15).

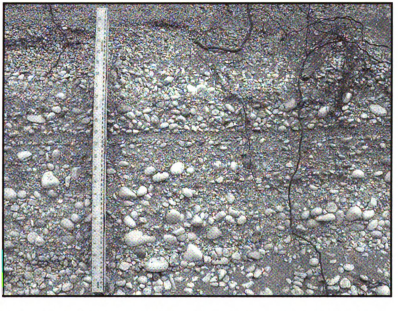


Figure 3.15: Exposed sediment profile in a gravel pit located near the southern end of proto-Beaver Island. A 2-foot carpenter's level is shown for scale.

In my opinion, the apparent differences (i.e., topographic expression and general sediment structure) between the northern and southern zones of the central upland on Beaver Island indicate the two zones were shaped by different

processes. Also, the elevation of the land surface above the gravel pit (at 220 m) is lower than the two highest shoreline elevations I measured at the north end of the upland (at ~229.0 m), so it seems reasonable to suggest the southern zone of the upland was formed, or at least shaped, under lake waters.

I measured relict shoreline features at three distinct levels of elevation on Beaver Island, MI (see Table 3.8). The highest shoreline, which is displayed best at Mr. Dawson's property, is correlated with the Main phase of glacial Lake Algonquin. Paleoshoreline elevations at Beaver Island correlate well with others stranded nearby on Leverett and Taylor's (1915) Brutus Island (Schaetzl et al., 2002). Evidence of other water planes exists at Beaver Island, particularly along the eastern and western flanks of the central upland, but the beach gravels Dietrich (1978) described are beyond the scope of this research. I believe much more can be learned from further study at Beaver Island.

Table 3.8: Approximate elevations of glacial Lake Algonquin water planes measured at Beaver Island, Michigan.

Approximate elevation (m)	Water plane/Lake phase
229	Main
223	Ardtrea
212	Wyebridge

From Petoskey to Traverse City, Michigan

The area between Petoskey and Traverse City, MI contains many upland areas that contain long and narrow lakes (e.g., Lake Charlevoix and Walloon,

Intermediate and Torch Lakes). The terrain is complex and relatively difficult to interpret. Leverett and Taylor (1915:426) speculated glacial Lake Algonquin "probably" extended up these valleys and left "distinct shorelines around Pine Lake" (now called Lake Charlevoix – see Figure 3.16) that "mark the highest Algonquin beach and some lower members of the upper group." The authors also mentioned relict features at "Undine and Hortons [*sic*] Bay" (Leverett and Taylor, 1915: 426).

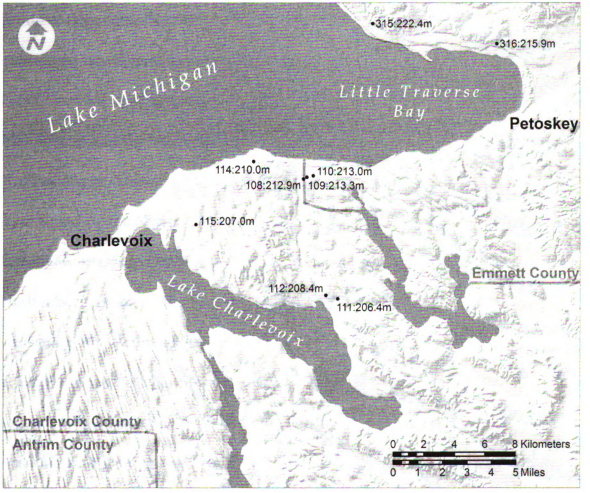


Figure 3.16: Relict bluff sites near Petoskey, Michigan. Sites are labeled with a unique site identification number and an elevation value (e.g., 642: 200 m).

A high bluff parallels the southern limit of Little Traverse Bay west of Petoskey. I studied three sites near Bay Shore and along Pincherry Road (SID108, 109 and 110). All three have ~213 m elevations. This shoreline is the highest in the region and, according to Spurr and Zumberge (1956: Figure 2), it represents the Main phase. I do not agree with this correlation, however, and attribute it to the Ardtrea phase instead. I considered the well known instance of a Main phase bluff that is situated along the north shore of Little Traverse Bay. Leverett and Taylor (1915:424) describe "the best-preserved parts" of "the upper group of Algonquin beaches" between Middle Village and Canby, MI. And, I considered that Schaetzl et al. (2002) measured bluff elevations at two sites near Good Hart, MI: the highest was at 224.4 m (SID313), which they attributed to the Main phase; and the lower one at 221.8 m (SID314), which they attributed to the Ardtrea phase. These features are well preserved (pers. obs.), where not interrupted by the Nipissing transgression and can be traced confidently for fifteen kilometers to Harbor Springs. A site situated approximately 4 km west of Harbor Springs marks the Main plane at 222.4 m (SID315); another situated 4 km west marks the Ardtrea plane at 215.9 m (SID316). Supposed "Main" shorelines at Bay Shore and Harbor Springs have elevations that differ by 9.4 m but are separated by no more than 10.5 km, thus implying a rate of uplift near 0.9 m/km. An uplift rate as large as 0.9 m/km is not expected at this location or latitude and, if proposed, would imply some kind of geologic unconformity exists. Lacking evidence of any such unconformity, I do not carry the Main phase across

Little Traverse Bay. Instead, I carry only the Ardtrea phase, which implies a 0.2 m/km rate uplift. Although such a correlation might seem provocative, I am not the first to propose it. Larsen (1987) summarized "a lack of consistency between the [Michigan and Huron] basins, indicating that the [Main] Algonquin level of Michigan is considered younger than that of Lake Huron" (p20).

Between the Undine Cemetery and Horton Bay ($SE\frac{1}{4}$ Sec. 1 T33N R7W), I measured a well-defined instance of a Nipissing shoreline; a small bluff is cut at 186.3 m (SID113), situated a few hundred meters north of Lake Charlevoix (not shown in Figure 3.16). Goldthwait (1910: Figure 4) reported a Nipissing elevation of 613 ft (186.8 m) near Burgess, MI, which is located only a few miles away.

Many houses along Boyne City Road in Horton Bay are built into a high bluff. For example, at Mr. Jim Chellis' property ($SE\frac{1}{4}$ $NE\frac{1}{4}$ Sec. 6 T33N R6W), I measured the old shoreline at 208.4 m (SID112). This shoreline is the highest apparent shoreline in the region and I correlate it with the Upper Orillia. The Horton Bay area exhibits several intermediate shorelines situated between the high bluff at Mr. Chellis' property and the current water level of Lake Charlevoix. These features are represented by a series of beach ridges that are stranded along what once was a low-gradient shorezone. These intermediate shoreline features were not surveyed because beach ridges are not always stable indicators of former water level elevations.

Leverett and Taylor (1915: 426) claimed glacial Lake Algonquin once covered "Grass, Clam, Torchlight and Elk lakes to the basin of Grand Traverse Bay" (Torchlight Lake is now known as Torch Lake). They offered, however, only one description of a relict landform:

> A mile and a half south of Elk Rapids the upper beach is marked by a strong gravel ridge and a hooked spit, and one or two of the members below it are faintly developed. It runs thence south close to the shore of East Arm, much of the way as a wave-cut bench and bluff, in which form it passes south into swampy flats (Leverett and Taylor, 1915:426).

These features are clearly illustrated on the Elk Rapids, MI and Williamsburg, MI 7.5 minute USGS topographic map sheets. Plotted contour lines indicate, however, that these features occur at elevations near 185 m, which is lower than expectations of glacial Lake Algonquin water levels but consistent with expectations of Nipissing water levels. Field observations confirm the elevations.

Further review of the topographic maps prompted me to inquire about other features in the area - particularly those situated along Torch Lake. For example, just north of French Point (Sec. 18 T29N R8W), I observed what I believe to be a set of two relict shorelines as indicated by a double bluff. The lower shoreline is situated at 185.5 m (SID119), which I correlate with the Nipissing Great Lakes. The higher bluff is situated at 193.6 m (SID117 and 118).

I traced the higher bluff both northwardly and southwardly and looked for other conspicuous instances to sample. Most of the land area along Torch Lake has been disturbed by residential and seasonal home development, which rendered several observable instances unsuitable for sampling. I did, however, find one instance situated on a vacant lot that had only been staked for development. Here, a relict shoreline is marked by a substantial bluff at 192.2 m (SID116). I found no evidence of higher or lower Algonquin water levels around Torch Lake and remain uncertain about which phase of glacial Lake Algonquin, if any, these points are associated with. So, I placed them into the supplemental database.

The Leelanau Peninsula, Michigan

Leverett and Taylor (1915) indicated the Algonquin beach is well-defined along the Leelanau Peninsula of Michigan. They identified a relict islet near Omena, a high lake cliff near Northport and several sets of lower Lake Algonquin beach ridges among several other locations. More recently, Kincare and Larson (2002) mapped the surficial geology of Northern Leelanau Peninsula and provisionally marked the locations of the uppermost Algonquin shoreline. The authors claim "isostatic uplift has elevated Algonquin shorelines from about 197 meters (646 ft) in Leland to just over 200 meters (656 ft) near Lighthouse Point." They did not, however, find any evidence of "lower Algonquin strands." Instead, Kincare and Larson (2002) suggest that the low strands that do exist likely belong to the Algoma and Nipissing Great Lakes.

I investigated sites described by Leverett and Taylor (1915) and mapped by Kincare and Larson (2002). Figure 3.17 show the area. The upper Algonquin water plane and the later Nipissing Water plane are expected to be separated by less than 20 meters of elevation. In some locations, the higher and older shoreline was obviously cut away by transgression of the lower. In other locations, both relict shorelines have been cut away by recent wave action and substantial bluffs now mark the contemporary shoreline.

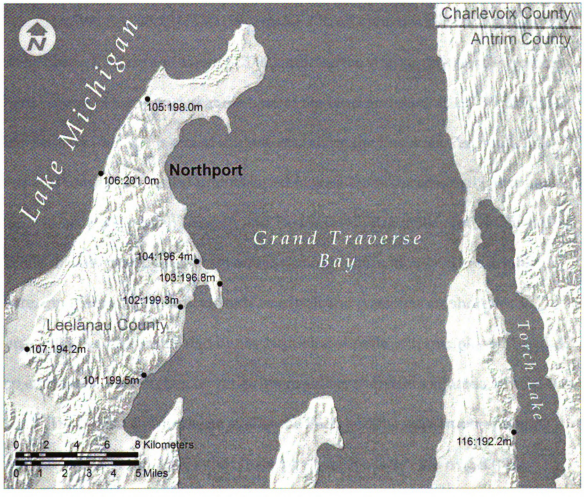


Figure 3.17: Relict bluff sites on the Leelanau Peninsula. Sites are labeled with a unique site identification number and an elevation value (e.g., 642: 200 m).

In Sec. 15 T30N R11W, I measured the base of a strong wave-cut bluff at 199.5 m (SID101); it is the highest wave-cut feature in the area. As the ground slopes away from the bluff and toward Suttons Bay it exhibits a sequence of minor ridges and terraces. The ridges run parallel to each other and the modern shoreline. While these ridges and terraces may represent agricultural modifications, they may, rather, represent relict beach ridges associated with falling water levels. Additional study is needed. A small orchard is situated at the site and trees have been planted along these terraces.

In SW$\frac{1}{4}$ Sec. 35 T31N R11W, Freeland Road switches direction to ascend a steep bluff. Kincare and Larson (2002) indicate the Algonquin shoreline occurs here. A gravel lag is buried at the base of the bluff and rests at 199.3 m (SID102). Incidentally, this site is one of the last sites along the Leelanau Peninsula that remains forested, wet, and undeveloped for residential or seasonal home uses.

I visited the knoll Leverett and Taylor (1915) described east of Omena. While the authors suggested several lower Algonquin members are exhibited here, my observations indicate only one high and conspicuous shoreline is present; it has been truncated by the Nipissing shoreline in two places. I found no evidence of any higher, lower or intermediate shorelines situated around the knoll. I surveyed the northeast side of the knoll and the uppermost shoreline was cut at 196.9 m (SID103); the Nipissing shoreline is at ~186 m (SID119).

Michigan Route 22 approaches a glacial Lake Algonquin bluff about two km north of Omena. The relict shoreline rests at 196.4 m (SID104).

Leverett and Taylor (1915) described the highest Algonquin beach as it "turns directly west across the peninsula ... about a mile north of Northport" (p.426). I visited this area and believe their description is not correct. Although the Algonquin bluff does begin to turn west north of Northport, it does not proceed directly across the peninsula. Rather, the shoreline traces the back of a small bay (Kincare and Larson, 2002) and returns east just north of Garthes Pond. From Garthes Pond, I observed the bluff to head in a northeasterly direction for another 2.2 km. It is from here that the shoreline turns west and across the peninsula. A Lake Algonquin shoreline is marked at 198.0 m (SID105) by a massive bluff near Christmas Cove (Sec. 21 T32N R11W). The bluff has been truncated by the contemporary shoreline of Lake Michigan. I did not find lower shorelines below the massive bluff and above the Nipissing water plane.

The high truncated bluff reappears south of Christmas Cove and near the Onominese Cemetery (Sec. 5 T31N R11W). I measured the shoreline and it is cut at 201.0 m (SID106). This site is cluttered by gravelly colluvium in many places below the steep bluff face, so this elevation is considered high.

As mentioned above, Kincare and Larson (2002) indicate the Algonquin shoreline is situated at "about 197 meters (646 ft) in Leland." I observed the base of a wave-cut bluff at 194.2 m (SID107: 637 ft) approximately two km east of Leland and near the eastern shore of Lake Leelanau ($SW\frac{1}{4}$ $SW\frac{1}{4}$ Sec. 11 T30N R12W). This feature is well-defined for about one km (near Wardens Point) and sheltered from westerly winds.

Schaetzl et al. (2002) followed Leverett and Taylor's (1915) descriptions of relict landforms and surveyed many in the area around Black Lake (Figure 3.18). Most have elevations that correspond with others located in the Douglas Lake area. Each water plane tends to decline as one travels south toward Alpena. Such correspondence is expected given that paleoshorelines are oriented parallel to the generally presumed isobase of isostatic rebound (after Hough, 1958).

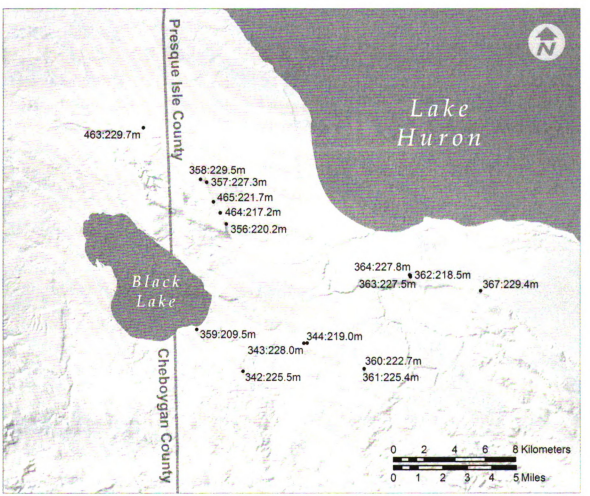


Figure 3.18: Relict bluff sites in the Black Lake area. Sites are labeled with a unique site identification number and an elevation value (e.g., 642: 200 m).

The highest paleoshoreline (227 - 222 m) is conspicuous and easily associated with Main Algonquin. A few instances of a slightly lower water plane are associated with the Ardtrea phase (222 - 217 m). In keeping with my recognition of Orillia water planes in Ontario and elsewhere in Michigan, I am compelled to update several sites that had been attributed to the lower Wyebridge phase (SID399, 410).

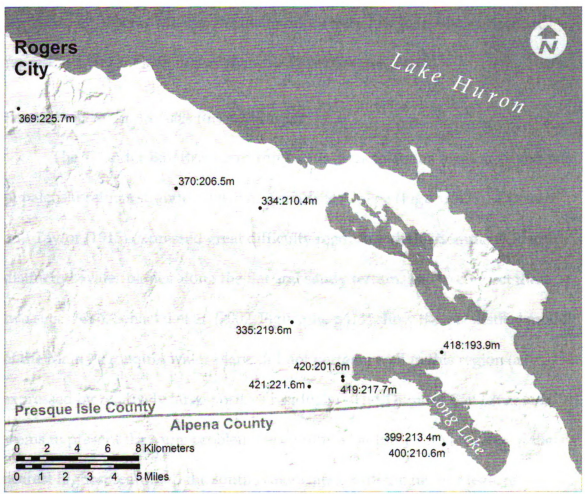


Figure 3.19: Relict bluff sites in the Long Lake area. Sites are labeled with a unique site identification number and an elevation value (e.g., 642: 200 m).

Schaetzl et al. (2002) also surveyed features in the area around Long Lake (Figure 3.19). The authors attributed a single instance of a very low paleoshoreline (201.6 m: SID420) with the Payette phase (Figure 3.19), but I do not agree with this correlation. Interpretation of Karrow (1987, Figure 5) and Stanley (1936: Figure 2) indicates the Payette water plane is expected to dip below the Nipissing water plane well before it reaches the contemporary Michigan shore; consequently, Payette shorelines are not expected to exist landward of Alpena, MI. So, the instance of a very low paleoshoreline must represent a water plane higher than the Payette water plane.

From Alpena to the Au Sable River, Michigan

The Thunder Bay River area represents a conspicuous break between sets of paleoshorelines stranded north and south of Alpena (Figure 3.20). Leverett and Taylor (1915) expressed great difficulty regarding their attempts to identify distinctive water planes along the flat and sandy terrain, and to connect these two sets. Also, Schaetzl et al. (2002: Figure 4a, p411) show their statistical model of the Main Algonquin water plane did not perform well in this region (as expressed by relatively large positive residuals). The Thunder Bay River area seems to present the same problem I encountered at Little Traverse Bay: if the nearest highest feature to the south is associated with the nearest feature attributed to the Main phase, then the local linear rate of uplift between the two sites is surprisingly high. Perhaps this is no coincidence.

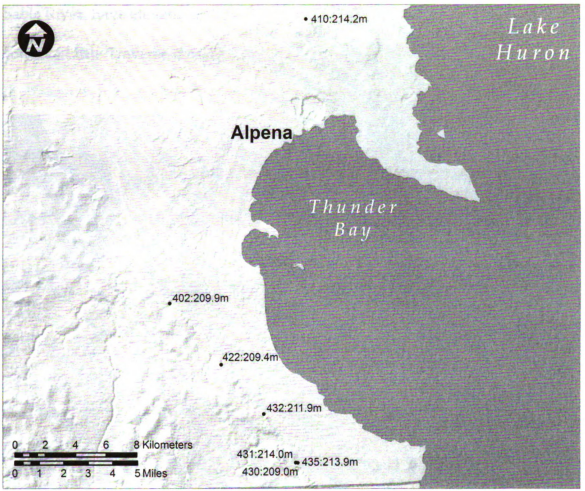


Figure 3.20: Relict bluff sites near Alpena, Michigan. Sites are labeled with a unique site identification number and an elevation value (e.g., 642: 200 m).

I think it is reasonable to speculate that features situated south of Alpena, having been worked by several converging water planes, might not express the elevation of the first water level to act upon it. Therefore, Main Lake Algonquin features may not be present here. As best as I can determine, only two sites south of Alpena express Main Lake Algonquin (214 m: SID431, 435). The balance, I believe, are associated with the Ardtrea and Upper Orillia water planes. Paleoshorelines situated near Harrisville, between Alpena and the Au

Sable River, have elevations that correspond very closely with others located south of Little Traverse Bay (Figure 3.21).

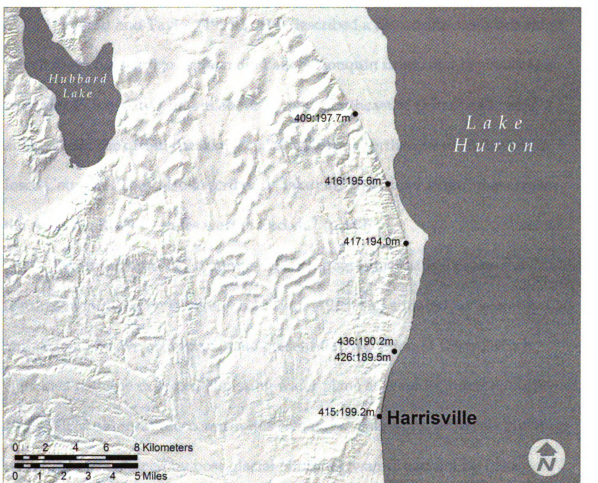


Figure 3.21: Relict bluff sites near Harrisville, Michigan. Sites are labeled with a unique site identification number and an elevation value (e.g., 642: 200 m).

From Au Sable River to Saganing, Michigan

The area between the Au Sable River and Saganing, MI is generally composed of fine lucustrine materials (Farrand and Bell, 1982) and exhibits a topography that is generally flat or slightly rolling. Two instances of end

moraines composed of fine-textured till can be found near Turner and Tawas City (Farrand and Bell, 1982), however, fewer instances of conspicuous wave-cut bluffs can be found within the region.

Leverett and Taylor (1915: p.419) described a discontinuous beach ridge, which they characterize as the main Lake Algonquin ridge, that begins near a cemetery in Bay City, "passes about $1\frac{1}{2}$ miles southeast of Omer" and "runs about a mile back from the lake [i.e., Lake Huron] northward to Alabaster, in Iosco County." They also described a "lake cliff and upper ridge" that crosses the Au Sable River "4 miles west of Oscoda" (p.420).

Recent editions of 7.5 minute USGS topographic maps indicate the features mentioned by Leverett and Taylor (1915) and situated between Bay City and Alabaster have an approximate present-day elevation of 184 m, which coincides with the expected Nipissing water plane at these locations (Goldthwait, 1910). Field observations confirm this elevation. Therefore, these relict features were likely last shaped by post-glacial Nipissing waters and not by Lake Algonquin waters.

Leverett and Taylor's (1915:p420) lake cliff, however, is well-defined on the Foote Site Village 7.5 minute USGS topographic map and rests at present-day elevations greater than 190 m, which is higher than the expected Nipissing plane at this location (Goldthwait, 1910). Burgis (1977) describes the same shore-cliff in terms of a graded deltaic sequence that formed in relatively high lake waters (she suggests Lakes Grassmere and Lundy) and was later truncated by glacial Lake

Algonquin waters. She also illustrates a lower delta (Burgis, 1977; Figure 44) that formed at the former mouth of the Au Sable River and in glacial Lake Algonquin waters. Burgis (1977) did not provide elevation data for these features.

Old logging roads provide access to the truncated delta, a portion of which rests in the Au Sable State Forest, north of the Au Sable River, and west of Oscoda, Michigan (Figure 3.22). I made observations along the base of a very strong bluff in Sections 26, 23, 14 and 11 of T24N R8E. For example, in $NW\frac{1}{4}$ $NE\frac{1}{4}$ Sec. 26, the bluff is approximately 30 m high, well-preserved and steep.

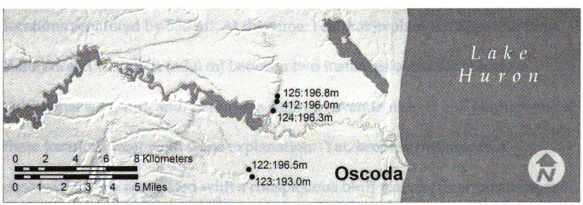


Figure 3.22: Relict bluff sites near Oscoda, Michigan. Sites are labeled with a unique site identification number and an elevation value (e.g., 642: 200 m).

Schaetzl et al. (2002) reported an elevation of 196.0 m (SID412) along the base of this bluff at a location just north of Bissonette Road ($SW\frac{1}{4}$ $NE\frac{1}{4}$ Sec. 26). I report elevation values of 196.3 m (SID124: $SE\frac{1}{4}$ $SW\frac{1}{4}$ Sec. 26) and 196.8 m (SID125: $NW\frac{1}{4}$ $NE\frac{1}{4}$ Sec. 26). As one proceeds northward into Sections 23 and 14, however, the bluff degrades into a series of benches. Two upper benches are

backed by faint scarps with basal elevations at 211.4 m (SID996) and 204.3 m (SID995). The lowest portion descends into a swamp and no conspicuous wave-cut features can be identified along its slope. The upper bench positions, which are not associated with conspicuous wave-cut bluffs, are retained in the supplemental database.

South of the Au Sable River in Sec. 10 of T23N R8E, I made observations along the bases of a weak scarp (SID999: 203.0 m - not shown), a strong scarp (SID122: 196.5 m) and a conspicuous wave-cut bluff (SID123: 193.4 m) roughly 6 m high. The two later observations were made along the same feature but at locations separated by 530 m. At this time, I cannot explain the apparent large difference in elevation (~3.0 m) between two instances of the same feature. Additional sampling and, perhaps, a rigorous examination of soil stratigraphy at these locations may yield some explanation. Yet, because the later two observations are associated with a conspicuous bluff feature, their positions are included in the shoreline dataset - as is the uncertainty that exists between them. The highest of the three positions, which is not associated with a conspicuous bluff feature, is retained in the supplemental database.

Given the substantial relief of this bluff (~30 m) and the coincidental higher elevations of scarps found at locations both north (204.3 m) and south (203.2 m) of the Au Sable River, the base of this bluff (~196 m) is likely not correlated with the highest Algonquin water level, but a subsequent and lower one. I associate the base of this bluff with the Upper Orillia water plane.

Summary

I described the methods I used to collect relict shoreline data and substantially improve the glacial Lake Algonquin dataset created by Schaetzl et al. (2002). I surveyed 88 new relict features in Northern Michigan and Western Ontario and was able to attribute 69 features to known glacial Lake Algonquin lake phases; the balance is reserved in the supplemental database.

I retained 128 of the 146 positions Schaetzl et al. (2002) collected. Four elevations taken near Douglas Lake, Michigan, mark anomalous features that rest higher than the Main water plane (~225 m). The other fourteen points not retained were taken from features that resemble offshore bars, barrier bars, or spits and, so, were not collected according to my sampling protocol; I reserve these eighteen points in the supplemental database and they await future review. Also, many of the elevation values I obtained at sites in the Munuscong Islands region, near Douglas Lake and near the Au Sable River compliment the elevation values reported previously by Schaetzl et al. (2002) - so it seems our efforts identified the same features and obtained similar elevation values from them.

I conflated well-known paleoshoreline data taken by others at Sault Ste. Marie (10) and St. Joseph Island (19). Together, the glacial Lake Algonquin dataset and the supplemental database hold 243 bluff records; Appendix A presents a complete list of them; Figure 6.10 shows bluff locations with respect to predicted shorelines. Individually, each sample marks a point along a former shoreline of glacial Lake Algonquin (although a few mark Nipissing shorelines).

In aggregate, they outline several distinct water planes within the region of interest: Main (57), Ardtrea (41), Upper Orillia (33), Lower Orillia (16), Wyebridge (12), Penetang (13), Cedar Point (17), Payette (7), Sheguiandah (3), Korah (1) and others (43). Apparent differences among water plane elevations are useful for modeling the cumulative effects of differential isostatic rebound (Chapter 5).

A major difference exists between the method Schaetzl et al. (2002) used to correlate paleoshorelines with named water planes, and the method I used. Schaetzl et al. (2002) began correlating shoreline data and Lake Algonquin lake phases in the Douglas Lake area, worked their way east and west, and then proceeded north and south. I attempted to follow that procedure, but encountered difficulties when attempting to recognize their set of four lake levels at locations north of the Straits of Mackinac - where additional water planes are clearly evident. Ultimately, I started again but began correlating paleoshoreline data with Lake Algonquin lake phases at Sault Ste. Marie instead. Sly and Lewis (1972), Cowan (1985), and Karrow (1987) correlated features in the region with respect to the Lake Algonquin lake phases named by Deane (1950: The *Upper Group* containing the Ardtrea, Upper Orillia and Lower Orillia phases), Stanley (1936: The *Lower Group* containing the Wyebridge, Penetang, Cedar Point and Payette phases) and Hough (1958: Sheguiandah and Korah), so it was relatively easy to interpret my results at Cockburn Island in terms of their findings. Having recognized the connections Cowan (1985) made between Manitoulin

Island and Sault Ste. Marie, and the apparent connections that I recognize between Cockburn Island and St. Joseph Island, it became clear that relict features in Michigan's Upper Peninsula needed to be reclassified. From these northern locations I then progressed southwestwardly and continued to recognize water planes as I went.

Relict shoreline features at Cockburn Island are particularly important features because they add much needed support near the northern rims of glacial Lake Algonquin water planes. They also provide clues about former ice margin position (Karrow, 1987). We know that the Superior Lobe of the Laurentide ice sheet retreated northeastwardly after reaching a maximum extent that covered the northern portion of Michigan's Lower Peninsula (Karrow, 1987; Larson and Schaetzl, 2001). Lakes in the Michigan and Huron basins were joined when retreating ice uncovered the Indian River lowlands and, slightly later, the Straits of Mackinac, which Larsen places at approximately 11,200 yr BP (after Hansel et al., 1985). Water levels in glacial Lake Chicago dropped to the glacial Lake Algonquin level upon joining (Hansel et al., 1985), which left the outlet at Chicago abandoned (Larson and Schaetzl, 2001) and directed all outflow to the Fenelon Falls outlets near Kirkfield, Ontario (Finamore, 1985). Thus began the Main phase of glacial Lake Algonquin. The presence of Main phase shorelines on Cockburn Island suggests that the ice sheet retreated through Cockburn Island sometime during the early portion of this lake phase; early enough to allow bluff cutting and other shoreline development processes to occur. Karrow

(1987) concluded that St. Joseph Island was deglaciated "about 11,000 yr BP or shortly thereafter" (p119). Cockburn Island is apparently situated along the same isobase that runs through St. Joseph Island (Figure 3.8), so both islands were likely deglaciated at the same time. Therefore, locations between the Straits of Mackinac and the Cockburn Island-St Joseph Island region must have been deglaciated within, roughly, a 200-year period.[2] Main phase and lower shorelines on Cockburn Island tell us that Cockburn Island was deglaciated before the Fossmill outlets at North Bay, Ontario, because lower lake phases are associated with falling water levels brought about by deglaciation of the outlets at North Bay (Kaszycki, 1985; Karrow, 1987). Karrow et al. (1975) reported radiocarbon dates that indicate glacial Lake Algonquin, from the Main phase to the lowest, existed between 11,200 yr BP and 10,400 yr BP. Relict shoreline features at Cockburn Island are important features because they help to place the ice sheet margin as well as the northern extent Main Lake Algonquin into a spatial context within this very short time frame.

---

[2] Karrow (1987) mapped a separation between areas of the Laurentide ice sheet that are known as *Superior ice* and *Algoma ice* (Figure 2, page 114). Superior ice covered the Straits of Mackinac and Algoma ice covered St. Joseph Island and Cockburn Island. This separation complicates the deglaciation history of the northern Lake Huron basin and precludes, for now, speculation about *how* glacial ice retreated in locations between the Straits of Mackinac and the St. Joseph-Cockburn Islands region.

Understanding the relict features at Mackinac Island remains a key to establishing the proper link between the Upper Peninsula and the Lower Peninsula- interpretation of these features, however, remains a crux. Proto-Mackinac Island was small and distant from other Algonquin islands, and it holds relatively few conspicuous paleoshorelines to study (despite their notoriety). Schaetzl et al. (2002) correlated features at 242 m with the Main phase, those at 236 m with the Ardtrea phase, and those at 228 m with the Wyebridge phase; they claimed features at Mackinac Island have elevations similar to others in the Lake Simcoe District of Ontario (Deane, 1950). I was compelled, however, to reinterpret these data as I attempted to integrate new data with old findings. I reviewed Deane's (1950) work and consider the work of Cowan (1985) and Karrow (1987), as well as my own, and found reasons to believe that features Schaetzl et al. (2002) correlated with the Wyebridge phase rest at elevations better correlated with the earlier Upper Orillia water plane. For example, I considered Deane's (1950) descriptions of features; he characterized Upper Orillia bluffs as strong and characterized Wyebridge features as "not strong" and indicative of "only a short pause of Lake Algonquin at this level" (Deane, 1950: 174). I considered my work at Cockburn Island - the strongest bluffs there occur at elevations that correlate very well with the Upper Orillia water plane and rest at elevations higher than the expected Wyebridge water plane. Also, I did not find features on Cockburn Island that were associated with the Wyebridge water plane. Finally, I considered the relative location of

Mackinac Island with respect to other places that mark the Upper Orillia water plane. Ultimately, I correlated features at ~228 m on Mackinac Island with the Upper Orillia phase of glacial Lake Algonquin and not with the Wyebridge phase. More study is needed here.

Making correlations between relict shoreline features and Lake Algonquin lake phases is difficult in areas near Little Traverse Bay (Lake Michigan) and Thunder Bay (Lake Huron) because paleoshorelines in these areas are oriented roughly north-south, and interrupted by contemporary water features that are oriented roughly east-west. Ever since Leverett and Taylor (1915), the highest paleoshorelines on either side of these water features have been considered as representatives of the same water level - Main Lake Algonquin. Such connections, however, implicitly require anomalous crustal deformations to have occurred in both bays. In Emmet County, for example, the highest paleoshoreline cut into the north side of Levering Island occurs at 232 m and the highest paleoshoreline cut into the south side of Brutus Island (on the north side of Little Traverse Bay) is 222 m; both shorelines are associated with the Main phase (Leverett and Taylor, 1915; Schaetzl et al., 2002). These two sites are separated by approximately 30 km, thus yielding a reasonable 0.33 m/km linear rate of elevation change along the Main water plane. Continuing southwardly, if we assume the highest paleoshoreline on the north side of Little Traverse Bay is the same as the highest paleoshoreline on the south side of Little Traverse Bay, then that would require an effective 0.90 m/km linear rate of change along the

water plane over a mere 10.5 km span. In other words, assuming the highest paleoshoreline on both sides of Little Traverse Bay are the same shorelines would require an anomaly in the isostatic rebound process at this location. A similar anomaly is required if the highest paleoshorelines north and south of the Thunder Bay River are also considered as the same. Lacking any knowledge of anomalous deformations in these two areas, I must consider that the highest paleoshorelines situated north of Little Traverse Bay/ Alpena are not correlated with the highest paleoshorelines south of Little Traverse Bay/ Alpena.

In related work, Goldthwait (1910) described features along the highest paleoshoreline in the area between Kincardine and Port Elgin, Ontario. He also reported several features occur at anomalously low elevations. Karrow (1988) surveyed this region and found that features previously identified as the highest Lake Algonquin shoreline had actually been eroded and lowered by later water levels. Consequently, the features in question indicate the action of younger lake phases and not the Main phase of glacial Lake Algonquin. I speculate that a similar pattern of erosion occurred in the areas south of Little Traverse Bay and Thunder Bay, Michigan. Both Deane (1950) and Schaetzl et al. (2002) reported Main and Ardtrea water planes seem to converge at roughly this latitude, so it is quite reasonable to speculate that later, lower, and converging water planes continued to erode bluffs that might have once held marks of the Main phase, but no longer do. The Main Lake Algonquin water plane elevation at Port Elgin, Ontario (220 m after Karrow, 1988: p159) correlates well with highest

paleoshoreline found north of Alpena and west of Long Lake (221.6 m). The elevations of lower relict features situated south of Port Elgin, Ontario (208 m after Karrow, 1988: p159) correlate well with features situated south of Alpena, Michigan (209 m). In both cases, however, the elevations of lower relict features correlate best with the younger Upper Orillia lake phase and not the higher and older Main or Ardtrea phases.

Karrow (1987) and Larsen (1987) have noted the long-standing controversy regarding whether certain water planes in the Lake Algonquin series are parallel, thus implicating changes in outlets were responsible for changes in water levels, or whether they converge toward a single outlet, which would implicate isostatic rebound as the sole cause of shoreline deformation. Stanley (1936) and Hough (1958) suggested the shorelines were parallel; each represented a new outlet. Deane (1950) and Schaetzl et al. (2002), however, found evidence of convergence between the Main and Ardtrea water planes; each shoreline represented differential uplift relative to the same (also uplifting) outlet. Larsen (1987) argued for convergence after considering historic uplift data (Clark and Persoage, 1970). This work finds some evidence of both.

Like Dean (1950) and Schaetzl et al. (2002), this study finds evidence of convergence between the Main and Ardtrea water planes. Proceeding roughly southwardly: Main and Ardtrea bluffs at Cockburn Island are vertically separated by approximately 8 m (280 and 272 m, respectively); in the Munuscong Islands region they are separated by ~7 m (265 and 258 m, respectively); on

Mackinac Island they are separated by ~6 m (242 and 236 m, respectively); and, in the Douglas Lake area, they are separated by ~4 m (225 and 221 m, respectively). Moreover, the Main and Ardtrea shorelines are difficult to differentiate at locations south of Little Traverse Bay (Lake Michigan) and Thunder Bay (Lake Huron) because they either occur within 3 m of each other or they were reworked or destroyed by younger and lower lake phases. Convergence between the Main and Ardtrea shorelines suggests differential uplift relative to the Fenelon Falls outlet was the cause of deformation and tilt during the Main and Ardtrea phases.

Upper Orillia shorelines consistently occur below Ardtrea shorelines at Cockburn Island, the Munuscong Islands, Mackinac Island, and in the Douglas Lake area, but elevation differences between them provide conflicting evidence regarding convergence. Between some locations they appear to converge toward the south, while among other locations there is evidence of parallelism.

Few sites exist that mark multiple instances of later and lower water planes. Cockburn Island and the Munuscong Islands region, for example, are the only two locations that hold instances of both the Upper Orillia and Penetang shorelines. The vertical difference between these shorelines at Cockburn Island is 36 m, whereas the difference in the Munuscong Islands region is only 30m. A decreasing separating distance with decreasing latitude suggests convergence again, hence the influence of differential rebound. A comparison between two points, however, is not sufficient for characterizing the spatial patterns of two

regional water planes, so no valid conclusion can yet be drawn about the relationship between the Upper Orillia and Penetang water planes.

Evidence of convergence or parallelism between particular water planes in northern parts of the Huron basin notwithstanding, these data cannot be used to resolve the question of where Lake Algonquin stood in the southern parts of the Huron and Michigan basins. Like Schaetzl et al. (2002), my study area did not extend into those areas.

The new elements of the glacial Lake Algonquin dataset, including those surveyed during this work (n=69) or conflated from previous work (n=29), fill large data gaps (Cowan, 1985) and furnish new points of support for the restoration of glacial Lake Algonquin water planes (Taylor, 1895).

CHAPTER 4: ACCURACY ASSESSMENTS

Introduction

All spatial data are, to some extent, contaminated by error (Foody, 2003; Burrough and McDonnell, 1998; Heuvelink and Burrough, 1993; Openshaw, 1989 and Goodchild and Gopal, 1989). Error implies a discrepancy between an attribute of an entity or phenomenon and its measured representation. A potential danger exists in work that uses spatial data because errors can propagate through analyses, render results uncertain and prompt misleading interpretations (Shortridge, 2001; Heuvelink, 1988). Heuvelink and Burrough (2002: 111) have argued the importance of knowing "how accurate the data contained within spatial databases really are" so the "value of the derived information" might be known. Accordingly, the accuracies of the datasets employed in this work need to be assessed so that knowledge about data errors can be used to improve data analysis and qualify the results.

I report exploratory data analyses and accuracy assessments of the paleoshoreline dataset and a selected portion of the National Elevation Dataset (NED: Gesch et al., 2002). I use the public-domain *R* environment for statistical computing and graphics (R Development Core Team, 2005), particularly the *geoR* (Ribeiro Jr. and Diggle, 2001), *gstat* (Pebesma 2004), *maptools* (Bivand, 2005), and *RandomFields* (Schlather, 2001) packages, to explore and analyze data and conduct statistical tests.

Two datasets

I employ two datasets: a) a primary set of paleoshoreline positions; and b) a secondary digital elevation model that covers the region of interest. Every elevation value in each dataset, however, is the result of a random measurement process and likely contains error. From the outset I expected errors in elevation to have much greater potentials for contributing uncertainty to spatial model results than errors in horizontal locations because a significant difference in scale exists between the horizontal and vertical dimensions that bound glacial Lake Algonquin shorelines. The region of interest (see Figure 1) includes the confluence of Lakes Michigan and Huron and it extends northward past Sault Ste. Marie, Ontario, southward to the Au Sable River, westward to the Leelanau Peninsula and eastward to Harrisville, MI. The north-south dimension of the study area covers approximately 240 km of terrain whereas the east-west dimension covers 195 km. If a paleoshoreline position was to contain a horizontal location error of 10 m, then the error magnitude would represent no more than 0.005% of the east-west extent or 0.004% of the north-south extent. In other words, the relative size of a 10-meter horizontal error would be very small, and if input to a spatial model, then its influence on model results would also be small. I chose the GPS leveling methods and equipment described in Chapter 3 because they typically yield horizontal coordinates with sub-meter errors. A sub-meter error is an order of magnitude less than a 10-meter error, so its relative influence is expected to be negligible.

The contemporary range of elevations associated with stranded glacial Lake Algonquin features (~133 m) is much smaller than either range of horizontal coordinate values, which is the important difference in scale mentioned above.[1] Consider a paleoshoreline position that contains a 10 m elevation error, rather than a horizontal error. A 10-meter error in elevation would represent 7.5% of the elevation range. Hypothetically, if a 10-meter elevation error were entered into a spatial model, then it would likely perturb results. By comparison, the relative impact of a 10-meter error in elevation is much greater than the impact of a 10-meter horizontal error given the substantial difference between vertical and horizontal extents. Moreover, the contemporary ranges of elevation associated with individual glacial Lake Algonquin water planes are less than 133 m, so individual water-plane models supported by such erroneous positions are subject to even greater impacts and uncertainties.[2] That is why I used differential GPS technology and designed a strict sampling protocol that limited data collection activities to occur only during temporal

---

[1] The average level of water in the contemporary Michigan-Huron basin is 176 m, below which glacial Lake Algonquin shorelines cannot be observed. The highest elevation associated with a glacial Lake Algonquin feature is approximately 309 m (Cowan, 1985).

[2] Schaetzl et al. (2002: Table 4, p412) reported three post-Main Lake Algonquin water plane elevations at Alpena, MI and Sault Ste. Marie, Ontario. The differentially warped Ardtrea, Wyebridge and Payette water planes include elevations that range 75, 77 and 51 meters, respectively, between the two sites.

windows that framed optimal satellite constellation geometries suitable for the taking of accurate and precise elevation measurements. Differential GPS technology can yield elevations with sub-meter accuracy when used properly. Yet, proper planning and use notwithstanding, it is common knowledge among the GPS community that GPS technology resolves elevation values less precisely than horizontal coordinate values. So, the set of GPS-measured paleoshoreline data, particularly the set of elevation values, might contain errors that need mitigation. I focus my attention on these. And, it is common knowledge that "elevations recorded within digital models are ... fraught with errors" (Fisher, 1998:215), so I also focus on them.

Assessment of the glacial Lake Algonquin dataset

The task of assessing accuracy is concerned with describing errors in data (Shortridge, 2001). Typical assessments begin with the assumption that each error is the result of a random measurement process, proceed by comparing a set of measured values to a set of known or higher-order values assumed to be accurate, and end with a description of the distribution of error. A higher-quality paleoshoreline dataset does not exist to assess the set of data collected during this work. Yet, rather than assume paleoshoreline data are accurate by virtue of being the highest-order available, I attempt an assessment by recognizing potential sources of error and conceptually or empirically estimating their potential values. Each shoreline sample is subject to two sources of error: a)

the limits of precision associated with the method I used to select relict shorelines in the field; and b) the limits of precision associated with the methods I employed to measure and process shoreline positions at selected sites. I address both.

Analysis of potential selection errors

As explained in Chapter 2, I rely on the gravel lags that form at the bases of wave-cut bluffs to be the set of best indicators of former water-level positions. Morton and Speed (1998) suggest the precision with which a lake level can be established by the elevation of a wave-cut bluff alone is sub-meter, but my knowledge of contemporary water-level behavior suggests the precision might be as great as three meters (see Chapter 2). Such imprecision is supported by Goldthwait (1910: Figure 2) who, when drafting profiles of uplifted water planes, used bands "6 feet broad according to the vertical scale" to represent "small scale discordances as must be expected because of the original variation" (p37) in water plane heights.

Every field site, save the few noted otherwise, exhibited a conspicuous gravel lag from which the limits of long-term wave-action can be inferred fairly confidently. A possibility exists, however, for some gravel lags to have been deposited at elevations higher than long-term water levels (e.g., during storm events). If I selected such a feature, then a probability exists for the selected elevation to overestimate the former water level. I expect such errors are rare.

Based on my experience in the field and following the research of others (e.g., Goldthwait, 1910; Morton and Speed, 1998), I expect most selection errors to be 0 m, the majority of selection error values to fall within the interval of 0 and 1 m, and, on rare occasions, extreme values to fall within the interval of 1 and 3 m.

Ground control

Measurement errors in the paleoshoreline dataset cannot be assessed directly because no paleoshoreline surveyed in this work has been surveyed independently or by higher-order methods; an indirect assessment method is needed. So, I assess the precision of the data collection and processing methods, from which I infer the accuracy of data they yield. Small sets of National Geodetic Survey (NGS) bench marks were measured during each field campaign. The protocol used to measure and process paleoshoreline position data was used to measure and process bench mark data. After each campaign, each set of bench marks was added to the pool of ground control data. Calculated discrepancies between measured and actual bench mark positions are used to assess the accuracy of paleoshoreline position data and correct any bias.

The National Geodetic Survey is the authority for determining latitude, longitude, elevation, crustal velocity and gravity throughout the United States and it serves as the depository for geodetic data of the highest-order (NGS, 1998). Geodetic data represent a network of precisely surveyed control stations with accurate position attributes (Bossler, 1984). Horizontal control stations, also

known as monuments, are established to provide users with accurate longitude and latitude values. Vertical control stations, also known as bench marks, are established to provide accurate height (elevation) information. Interestingly, not all bench marks have horizontal data of geodetic-quality and not all monuments have height data of geodetic-quality, but some do have both. The NGS maintains a geodetic datasheet (NGS, 2004) for each monument and bench mark. Datasheets are archived annually on a regional basis and those that represent control stations in Michigan were last archived in November, 2004. Datasheets contained within this archive are used to assess the precision of the data collection methods described in Chapter 3 and to assess, by inference, the accuracy of paleoshoreline position data.

Twenty-four different NGS control stations (see Table 4.1) were occupied and measured during my field campaigns, of which ten stations have geodetic longitude and latitude information. During data processing, however, I discovered six station samples to be unfit for use. Three samples (PIDs OJ0706, PK0154 and PK0165) were collected on November 13, 2003 and each contains conspicuous large errors - particularly station PK0154. Such large errors prompted me to review all field notes, field equipment and data processing methods, but I found nothing from these sources to help me explain their occurrences. I discovered, ultimately, the US Coast Guard archive of *GPS Status Message Reports* (US Coast Guard Navigation Center, 2004), which contains historic status information about the GPS space and control segments.

Table 4.1: Vertical differences between measured and published heights. NGS bench marks are indicated by their Permanent Identifiers (PIDs).

PID	GPS height (m)	NGS height (m)	Difference (m)
Observations used to assess shoreline elevation data.			
NF0260	259.86	260.26	-0.40
PK0227	193.85	194.28	-0.43
PL0361	192.20	192.21	-0.01
PL0369	190.63	190.61	0.02
PL0370	195.62	195.83	-0.21
PL0389	182.93	182.36	0.57
QJ0086	180.31	179.70	0.61
QJ0151	198.21	196.51	1.70
QK0087	185.55	184.84	0.71
QK0325	255.22	255.55	-0.33
QK0410	177.29	177.56	-0.27
QK0469	194.63	194.52	0.11
QK0470	205.24	206.60	-1.36
QK0484	232.83	232.04	0.79
RJ0161	193.20	192.37	0.83
RJ0230	236.24	234.77	1.47
RJ0644	208.01	208.49	-0.48
RJ0691	234.17	234.68	-0.51
Observations perverted by satellite malfunction (rejected).			
OJ0706	183.32	184.72	-1.40
PK0165	203.88	206.02	-2.14
PK0154	185.28	190.66	-5.38
Observations taken at bench marks with non-geodetic quality height information (rejected).			
QK0852	243.16	242.00	1.16
*	267.97	266.70	1.27
*	249.40	248.41	0.99

Several GPS status reports (USCG, 2004) revealed that a GPS satellite malfunctioned on November 13, 2003 and was broadcasting bad data for at least twenty-four hours. The GPS signal was eventually turned off, but not before I

collected data. I discarded these samples because I could not remove the influences of bad data obtained from the now decommissioned satellite. This event prompted me to review every archived status report for each day data collection activities occurred, which included the previous work accomplished by Schaetzl et al. (2002). Fortunately, I found no evidence to suggest other bench marks or any paleoshoreline data should be discarded for similar reasons.

I rejected three more control station samples because each was obtained at a site having non-geodetic quality information. For example, the datasheet that represents bench mark QK0852 contains elevation data not obtained by rigorous survey, but interpolated from an old topographic map built using the obsolete North American Vertical Datum of 1929 (NAVD29). Unfortunately, this mark is the only documented vertical control station on Beaver Island, MI. I rejected two marks collected by Schaetzl et al., 2002 (marked in Table 4.1 with an asterisk - *) because they were taken at road intersections annotated with spot heights on topographic maps (and rounded to the nearest foot), and not at bench marks with high-order geodetic information. The lesser-qualities of these three control points are insufficient for assessing the greater precision of GPS-based measurement methods or the accuracy of the data they yield, so they are rejected.

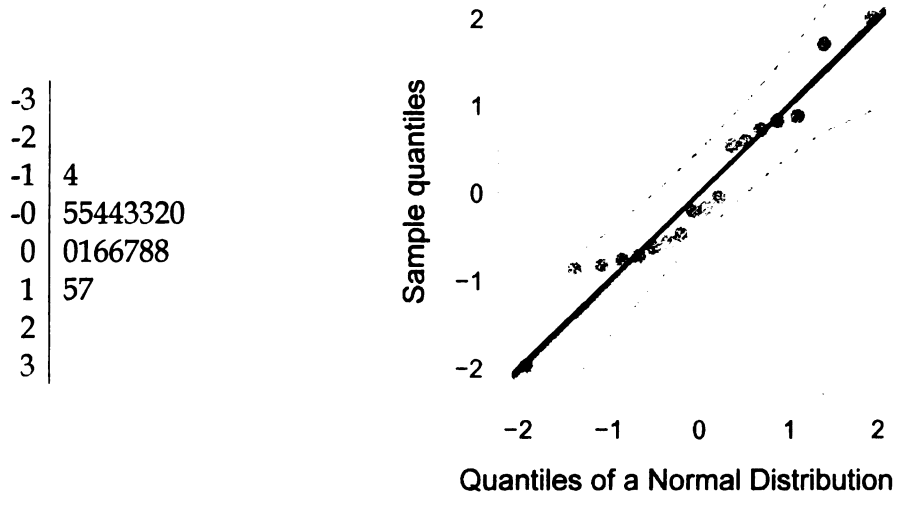
Analysis of measurement errors

Differences between measured and published elevations are listed in Table 4.1 for eighteen bench marks having geodetic-quality height information.

Summary statistics (Table 4.2) and a stem-and-leaf plot (Figure 4.1a) show measurement errors are small in magnitude; the distribution appears symmetric and centered near zero.

Table 4.2: Summary statistics that describe the set of differences between measured and published bench mark elevations.

Sample statistics	Value	Test for mean ≠ 0	Value
n	18		
minimum	-1.36 m		
median	0.00 m		
mean (bias)	0.16 m	matched-pairs t	$p = 0.4010$
standard error of mean	0.19 m		
standard deviation	0.77 m		
maximum	1.70 m		



(a) (b)

Figure 4.1: Distribution of error in sampled bench mark elevations: a) Stem and leaf plot - solid line denotes the decimal place; and b) q-q plot of standardized errors with a one-to-one line and 90% confidence envelope.

Results of a matched-pairs *t* test indicate the mean difference between measured and published elevations (0.16 m) is not statistically different than zero at the 90% confidence level. A q-q plot of standardized error values (Figure 4.1b) and results of a Shapiro-Wilk test for normality (a = 0.10: W=0.9540 and ρ = 0.4915) provide no significant evidence to suggest the sample distribution of elevation error does not fit a Normal distribution. No elevation difference exceeds 1.7 m, which is less than the three-meter threshold used to distinguish different long-term water levels. As expected, the majority of measured elevations (15 of 18, or 83%) contain sub-meter errors.

I used scatterplots to examine associations between error and position (Figures 4.2 and 4.3). I used Kendall's non-parametric *tau* statistic to test the strengths of associations because latitude and longitude values are non-linear measures of distance. Kendall's *tau* does not rely on assumptions about the underlying distribution of data. It is applied to the ranks of data (which mitigates the non-linear distance problem) and takes values ranging between -1 and +1 (which can be interpreted like Pearson's or Spearman's statistics). No plot or statistical test result provides strong evidence to suggest errors, either signed or unsigned, are associated with location or elevation.

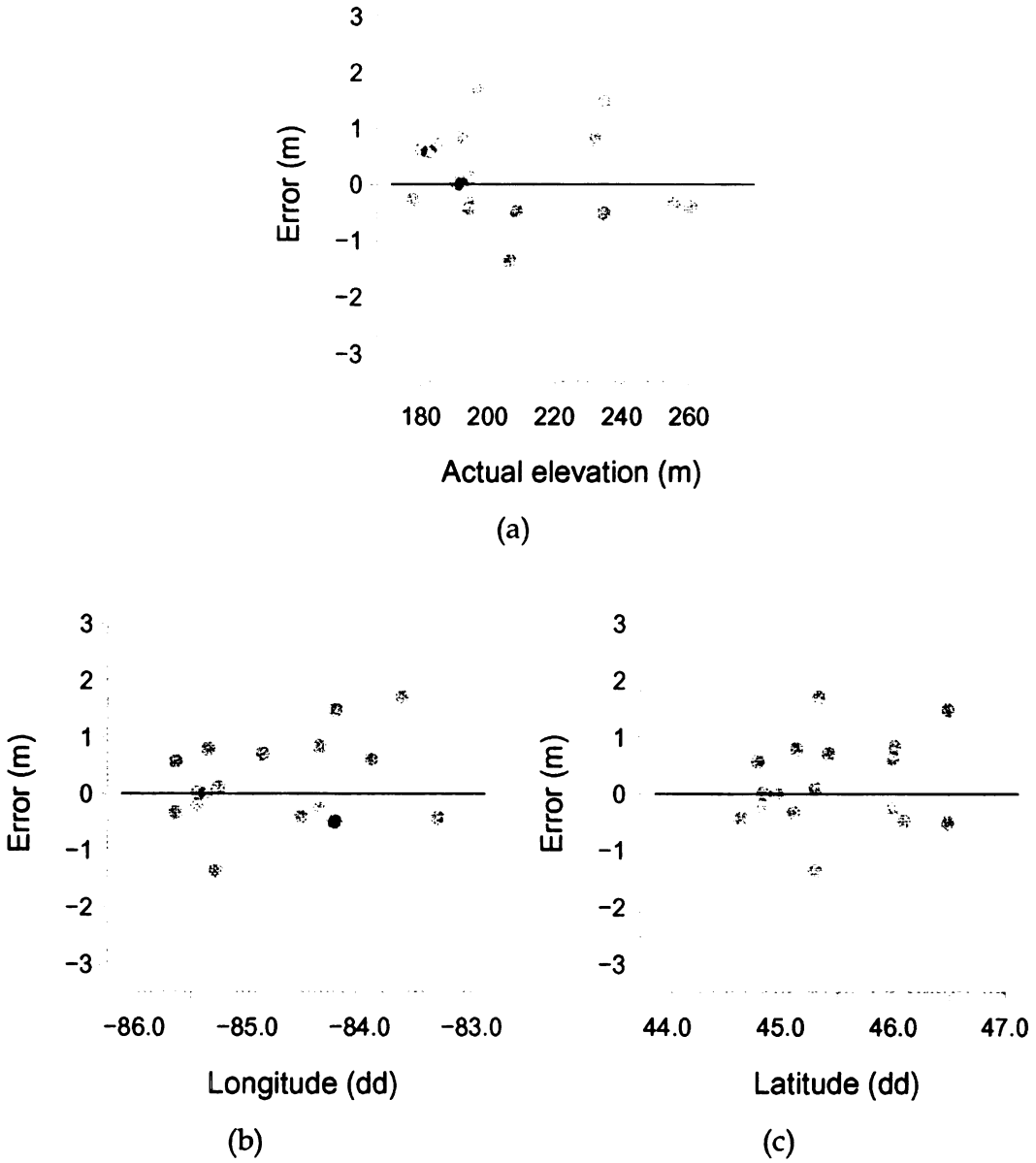


Figure 4.2: Scatterplots of signed error in sampled bench mark elevations and position. Errors and elevations are reported in meters. Latitude and Longitude values are reported in decimal degrees.

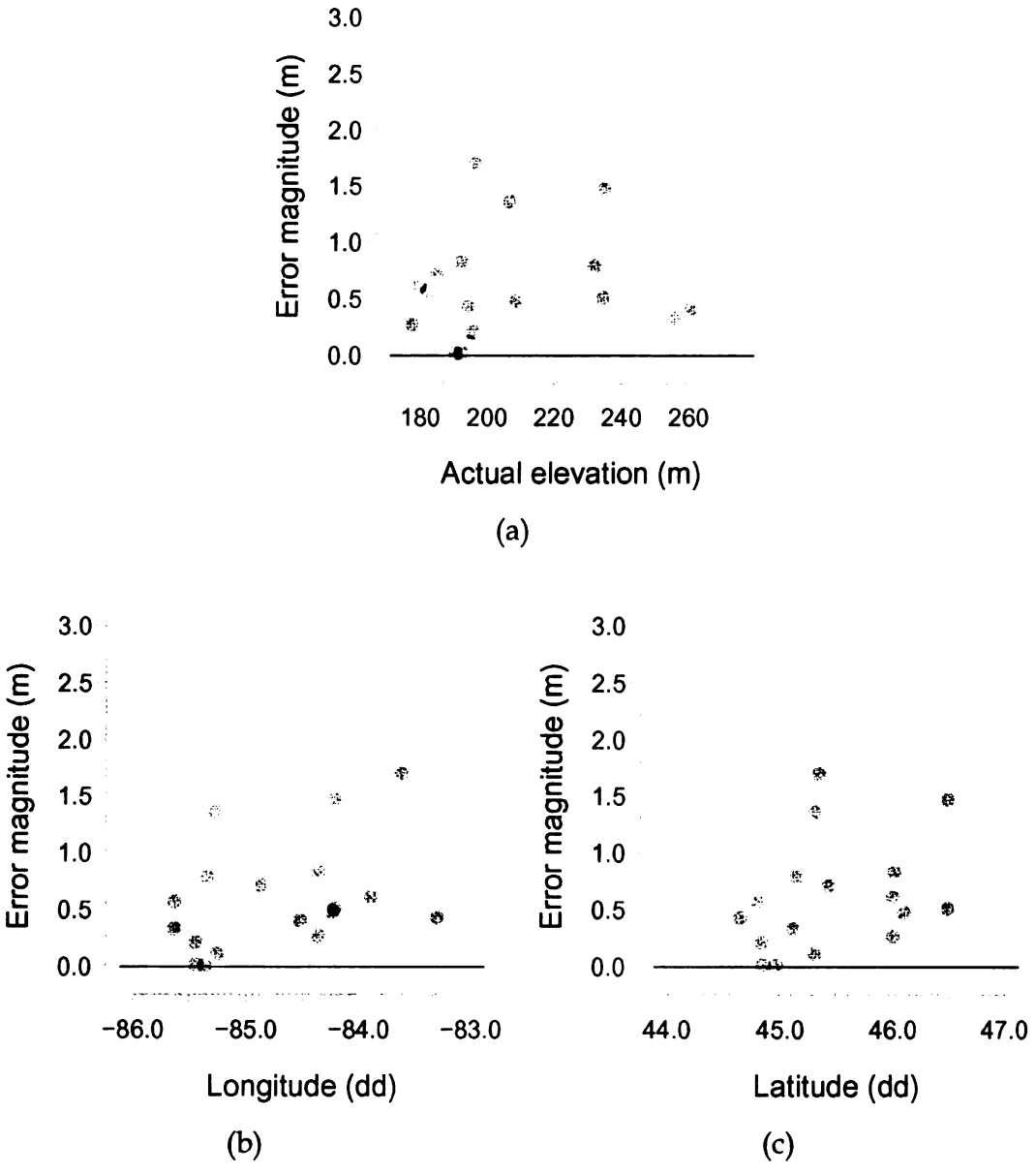


Figure 4.3: Scatterplots of unsigned error in sampled bench mark elevations and position. Errors and elevations are reported in meters. Latitude and Longitude values are reported in decimal degrees.

I used Moran's I statistic (Bailey and Gatrell, 1995: 270) to test for spatial autocorrelation. The calculated statistics for signed and unsigned errors (I = 0.047 and -0.090, respectively) are near zero and indicate no spatial

autocorrelation is present, so I infer no spatial structure exists among the errors in these bench mark elevations.

Table 4.3: Results of Kendall's non-parametric tests for associations between position and elevation error.

	Signed error		Unsigned error	
	tau	*p* value	tau	*p* value
Longitude	0.150	0.410	0.294	0.096
Latitude	0.072	0.709	0.268	0.131
Elevation	-0.163	0.369	0.137	0.454

The actual distribution of error is not known, but sampled errors appear small, random, normally-distributed and not a function of location, elevation or autocorrelation. Because the methods used to measure paleoshoreline elevations are the same as those used to measure bench mark elevations, errors in paleoshoreline elevations are inferred to be similarly small, random, normally distributed and spatially unstructured.

Calculated differences between measured and published latitude and longitude values (converted to meters) are listed in Table 4.4 for seven monuments having geodetic-quality latitude and longitude information (recall that ten were measured but three were rejected because of a satellite malfunction). All location coordinates contain sub-meter errors. On average, a measured location is typically within 0.5 m of the actual location.

Table 4.4: Horizontal differences between measured and published NGS benchmark locations.

PID	Error in Latitude (m)	Error in Longitude (m)	Distance (m)
NF0260	0.16	0.09	0.19
PL0361	-0.47	0.22	0.52
QK0325	-0.96	0.19	0.98
QK0469	-0.48	-0.41	0.63
QK0470	-0.65	-0.02	0.65
QK0484	-0.30	0.30	0.42
RJ0161	-0.03	0.21	0.21

The methods used to measure paleoshoreline locations are the same as those used to measure bench mark locations, so horizontal errors in paleoshoreline locations are inferred to be similarly small. Moreover, the maximum error observed in horizontal coordinate data (0.98 m at mark QK0325) is smaller than the widths of most gravel lags that form along contemporary Great Lakes shorelines (pers. obs.). From this observation, and given the large extent of the study area, random and small horizontal errors likely associated with measured shorelines, while likely not zero, are hereafter considered to be not meaningfully different than zero. In short, they are ignored.

Cumulative elevation errors in paleoshoreline data

Recall that each shoreline measurement is subject to two sources of error: a) the limits of precision associated with the method I used to *select* relict shorelines in the field; and b) the limits of precision associated with the methods I employed to *measure and process* shoreline positions. I have no reason to believe

that either one of these sources of error can be influenced by the presence, location, magnitude or direction of the other, so I assume that each error process operates independently of the other. Therefore, the total error in any paleoshoreline elevation is expected to be the simple sum of selection and random measurement errors. I describe in Chapter 5 the process I used to estimate total elevation error in my paleoshoreline elevation data.

Assessment of the National Elevation Dataset

The National Elevation Dataset (Gesch et al., 2002) is a digital elevation model (DEM) that provides seamless data coverage of the United States. It is produced by the US Geological Survey (USGS) and distributed in raster format. The NED represents bare earth elevations and is the best such dataset available for the area under investigation. Unlike older DEMs (e.g., the USGS 7.5-minute and 3 arc-second models) that contain elevation data tied to different spatial reference systems, the NED contains elevations that are referenced only to the North American Datum of 1983 (NAD1983) and North American Vertical Datum of 1988 (NAVD88) -- and they share a common unit of measure (meter). NED elevations are arranged on a grid and spaced at one arc-second intervals, which, at 46° N latitude, spans approximately 31 meters in the north/south direction and 22 meters in the east/west direction. When first released, most NED elevations were derived from reprocessed versions of older DEMs, but increasingly they are being derived from new and more accurate source materials. The NED is now assembled completely from 10-meter and 30-meter resolution sources and new tiles at 10-meter resolution are incorporated as they are produced (Gesch et al., 2001). The NED is updated every two months; this work employs the December 2004 release that contains new elevation data for a portion of northern Lower Michigan.

DEMs contain errors in elevation that are the cumulative results of imprecise sampling, measurement and interpolation processes (see e.g., Shortridge, 2001; Fisher, 1998; Bolstad and Stowe, 1994; Brown and Bara, 1994 and Shearer, 1990).[3] The NED has not yet been assessed for accuracy, but according to the USGS (2005), "a plan for assessing the overall accuracy of the National Elevation Dataset (NED) based on independent high-accuracy geodetic control is currently under development." The USGS (2005) suggests NED users should consult "published information on the accuracy of the source digital elevation models (DEM's) from which NED was assembled."

Spatial metadata distributed with NED data contain polygons that outline footprints of source DEMs and attribute tables with statistical summaries of error. A root mean square error (RMSE) quantifies the average mismatch between a small set of ground-based and DEM-reported elevations within each footprint. Such values are not specific to particular locations and hence cannot be used to pinpoint spots where elevations can be considered as reliable or in need of improvement (Shortridge, 2001; Kyriakidis et al., 1999). Furthermore, RMSE values represent mismatches calculated prior to NED processing, which

---

[3] Horizontal locations stored in a digital elevation model are controlled during the production process (i.e., they are selected and not measured), so digital elevation models by design do not contain horizontal errors (Maune, 1996). Admittedly, it is possible for an elevation to be assigned incorrectly to a location, but such violations still are considered elevation errors and not horizontal errors.

may be different than actual values. The NED data processing protocol includes: a) the application of large filters to remove production artifacts or smooth discontinuities along input tile boundaries; b) bilinear interpolation methods that coerce data from extant resolutions into available spots along the arc second grid; and c) geodetic transformations that change elevations formerly rounded and stored as integers (either in feet or meters) into decimal meters stored with floating point precision (USGS, 2005). Consequently, a potential mismatch exists between metadata-reported and actual RMSE values. So, while historic RMSE values associated with source files may be the best available indicators of accuracy, actual accuracy is uncertain.

The NED also contains elevation data for Canada that are situated near the US/Canada border and within the one-degree tile structure employed by the USGS (Gesch et al., 2001; Gesch et al., 2002). Canadian elevation data were not collected according to USGS protocols, but likely derived from the Digital Terrain Elevation Dataset (DTED: NIMA, USGS and NGDC, 1997). The DTED was created for large areas of the world by the former Defense Mapping Agency during the 1960s and 1970s, and used primarily for military purposes. NED metadata provide scant information about how these data were collected or processed, but metadata-reported RMSE values (10 - 29 m) indicate elevation data for Canada contain large errors relative to those associated with other sources (RMSE 1 - 7 m). Consequently, elevation data for Canada are considered a likely source of uncertainty in model results.

Geoprocessing the NED

NED data were projected onto the Michigan GEOREF planar coordinate grid and resampled to 45-meter resolution using GIS software. I was initially reluctant to reduce the horizontal precision of NED data, but was compelled by computer memory and storage limits (NED data for the study area consume nearly 0.5 GB of disk space at 30-m resolution). Nevertheless, the new resolution is an improvement over the coarser 90-m data employed in related work by Schaetzl et al. (2002) and Drzyzga et al. (2002). Also, many grid cells associated with Lakes Michigan, Huron and Superior were masked from analysis because they do not represent land surface information. The geoprocessed version of NED data is hereafter referred to as, simply, "the DEM."

I divided the DEM into three subsets: Lower Peninsula, Upper Peninsula, and Ontario. I divided Michigan data into two subsets because elevation data for the selected portion of the Lower Peninsula were derived primarily from contour lines on topographic maps, and most elevation data for the selected portion of the Upper Peninsula were derived photogrammetrically. Elevation data for Ontario were derived differently than elevation data for Michigan, so I suspected internal inconsistencies might differ as well. The literature has long recognized that differences among DEM production methods yield DEMs with different error characteristics (e.g., Wood, 1996 or Brown and Bara, 1994), so I sought to examine each subset to ascertain whether or not such differences existed wihin my data. I originally considered subsetting the DEM using source tile polygons

that were attributed with different production method data, but doing so would have fragmented the study area into many non-contiguous and hard-to-manage units. More importantly, however, the USGS can update any or all data within a source tile with elevations obtained via methods not consistent with those reported in the spatial metadata file (USGS, 2005). Consequently, footprints of NED source tiles, which indicate the extents of pre-NED production methods, may not coincide with the extents of actual production methods. This complicating factor prompted me to use simple majorities to inform my choice of three subsets.

Hypsometric analysis

Initial assessment of the DEM and each subset can be achieved by visual analysis of frequency histograms, which can reveal internal inconsistencies if any are present (Hutchinson and Gallant, 2000; Wood, 1996). The frequency distribution of my DEM elevations (Figure 4.4a) is skewed toward lower elevations and it contains several conspicuous spikes. The largest spike is situated between 176 and 181 m and represents a large number of "water" cells associated with the contemporary Lake Michigan-Huron water plane that remain in the model, as well as others associated with inland lakes Burt, Charlevoix and Mullet. A secondary peak is situated between 213 and 218 m and associated with large homogenous groups of cells that represent the elevations of Hubbard Lake (Lower Peninsula) and North Manistique Lake, Manistique Lake and South

Manistique Lake (Upper Peninsula). Several lesser spikes are also evident at 213, 244, 274 and 305 m, but these cannot be explained by known topographic regularities.

The Lower Peninsula subset is the largest of the three and its distribution (Figure 4.4b) dominates the distribution of the whole DEM as the two histograms are quite similar. High frequencies of 213, 244, 274 and 305 m elevations in the DEM are not evident in this subset. Other and lesser spikes, however, appear at three-meter intervals. Most 1:24,000 USGS topographic maps have elevation contours mapped at ten-foot intervals (roughly three meters), so it seems that artifacts associated with DEM production methods that utilized digitized contour lines have survived geoprocessing and are observable.

The Upper Peninsula histogram (Figure 4.4c) contains many low elevations that represent the characteristic lake plain topography of the area, and a small peak centered near 255 m, which represents several bedrock uplands. Two conspicuous spikes occur at 177 and 217 m: the lower is associated with "water" grid cells representing contemporary Great Lakes water level elevations; the higher is associated with a large number of small inland lakes that occur at various locations across the lake plain of the eastern Upper Peninsula. The Seney National Wildlife Area, for example, is predominantly swampland and most open water bodies situated within it were mapped with the same elevation value.

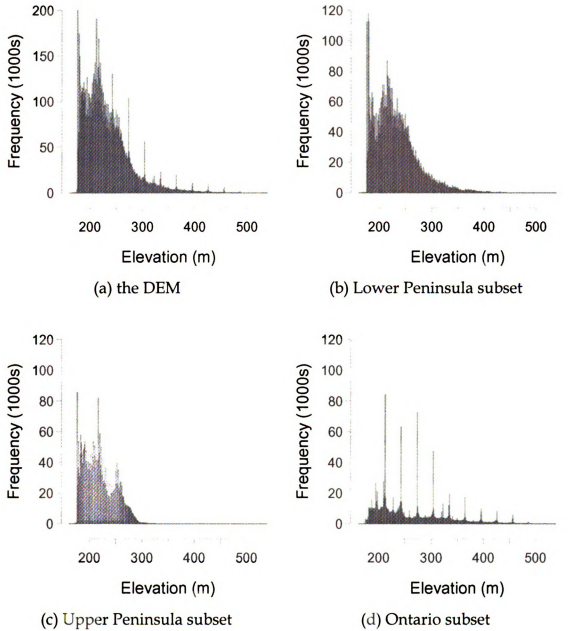


Figure 4.4: Frequency histograms of elevation. Bin width is one meter.

Large spikes at 213, 244, 274 and 305 m in the DEM histogram are not evident in the Upper Peninsula histogram. Yet, other and lesser spikes do appear at three-meter intervals. The majority of elevation data in this subset were derived

photogrammetrically yet some were derived from contours, which explains the consistent pattern of overrepresented elevations at three-meter intervals.

The Ontario subset (Figure 4.4d) is the smallest of the three but contains the full range of elevation values. Topography in the Ontario region is interesting and unique because it contains both stranded lake plains and a high and exposed portion of the Canadian Shield. Yet, irregular Shield topography does not account for the regular spikes that occur at 213, 244, 274 and 305 m or the intermediate spikes at 229, 259, and 289 m. When meters are converted to imperial feet, these spikes reveal a consistent pattern of overrepresented elevations at 100 and 50 ft intervals, respectively, and suggest a systematic and non-topographic cause (Hutchinson and Gallant, 2000; Wood, 1996). Given that 1:250,000 USGS topographic maps of the region were drafted using a 50-foot contour interval, it seems reasonable to speculate that such mapped contours were used as source materials for DTED elevations, which are the likely sources of NED elevations in Ontario. Again, NED metadata contain no information about the sources used to assemble data for locations in Ontario, so this is only speculation. Regardless of source, however, spikes in Ontario elevation data betray a likely artifact of a DEM production process and they indicate the elevation model over-represents contour elevations within this region.

Ground control

The task of assessing accuracy is concerned with describing errors in data (Shortridge, 2001). Typical assessments: begin with the assumption that each error is the result of a random measurement process; proceed by comparing a set of measured values to a set of known or higher-order values assumed to be accurate; and end with a description of the error distribution. I assembled a pool of high-order check points consisting of National Geodetic Survey (NGS) and Geodetic Division of Canada (GDC) control stations. Stations were selected if they are located within the area of interest and have geodetic-quality location and elevation information. As mentioned above, not all stations have geodetic-quality location information or geodetic-quality height information, so not all can be used for this purpose. The set of control stations was reduced further to exclude those mounted atop manmade objects (e.g., an antenna, lighthouse, range light, dock, bridge etc.) or those not mounted flush with the ground surface. Geodetic control stations are preferentially situated near engineered works (e.g., a railroad, highway, or commercial waterway) or atop accessible high points (pers. obs.; Kumler, 1994). Consequently, the set of station locations is not representative of the full range of topographic conditions in the region. I added the set of GPS-measured paleoshoreline data to the pool of check points so that locations distant from engineered works can also be assessed. Paleoshoreline data are suitable for this purpose because they contain sub-meter location errors, typically contain sub-meter errors in elevation, and are, therefore,

of a higher-order than DEM data. Like control stations, paleoshoreline positions were also preferentially selected and so, for example, do not include hill tops or river valleys, but their inclusion adds important landscape variation that is missing from the set of geodetic control station locations. Moreover, adding paleoshoreline positions to the pool enables me to ensure that agreement exists between the surface elevations I observed in the field and the surface elevations stored in the DEM (see Chapter 5). A pool of 529 check points (256 NGS control stations, 4 GDC control stations and 269 paleoshoreline positions) was used to quantitatively assess DEM elevations.

A comparison of frequency histograms reveals that the distribution of check point elevations (Figure 4.5a) is shaped and skewed like the distribution of DEM elevations (Figure 4.5b) and suggests that the sample of check point elevations is representative of the larger sample held by the DEM surface. The check point distribution lacks, however, large spikes in the lowest elevation bins because the elevations of open water bodies, which are represented in the surface, are not represented in check point data.

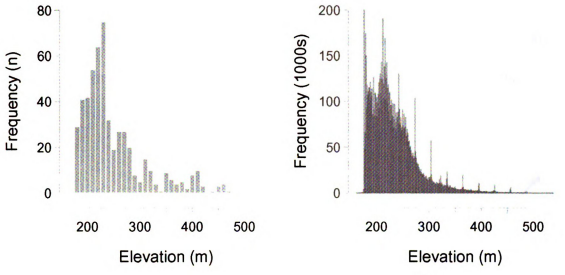


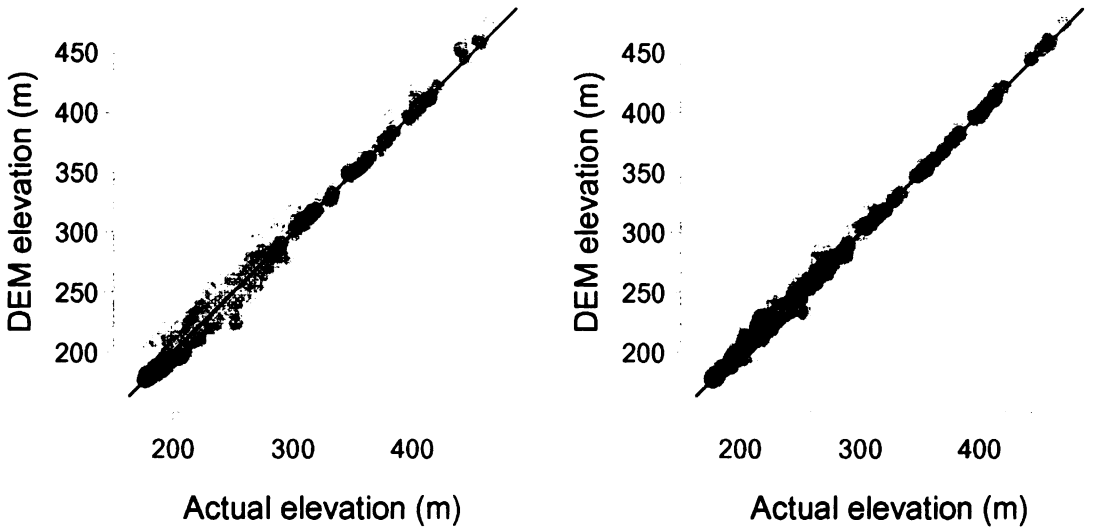
Figure 4.5: Histograms of: a) 529 check point elevations; and b) all DEM elevations in the study area. The difference between frequency scales is the results of unequal sample sizes.

Select results of the first exploratory analysis

Ultimately, I conducted two exploratory data analyses of error. The first led me to find a latent horizontal shift in the original NED– a systematic shift that propagated through geoprocessing unnoticed and perturbed my attempts to assess the distribution of error. Rather than report complete sets of results for both analyses, however, I use this section to highlight interesting characteristics of the original DEM that betrayed evidence of the shift. I use the next section to report a complete accuracy assessment of the corrected and properly-situated DEM.

Original DEM elevations were assigned to control point locations using nearest-neighbor interpolation and GIS software. A scatterplot (Figure 4.6a)

suggested DEM elevations generally agreed with actual elevations. Results of a Kendall's test for statistical association (a = 0.10: coefficient = 0.897, $p < 0.0000$) indicated a strong and significant correlation existed between the two sets.



(a) Original DEM (b) Corrected DEM

Figure 4.6: Scatterplots of DEM-reported and actual elevations of the (a) original DEM and for (b) the corrected DEM.

I estimated errors in DEM elevations by subtracting check point elevations from interpolated DEM elevations and then calculated summary statistics to describe the distribution. Table 4.5 contains the first and second sets of summary statistics. For example, the original sample mean difference ($\bar{x}$ = -0.55 m) was significantly different than zero at the 90% confidence level.

Table 4.5: Summary statistics that describe differences between actual and co-located elevations in the original and corrected DEM surfaces.

	The original DEM	The corrected DEM
n	529	529
minimum	-26.2 m	-18.6 m
median	-0.30 m	-0.02 m
mean (bias)	-0.55 m	-0.36 m
standard error of mean	0.27 m	0.18 m
standard deviation	6.79 m	4.07 m
maximum	27.8 m	19.8 m

Ultimately, I investigated possible covariates with error and was surprised to find significant associations with the linear components of slope aspect.[4] Circular measures of aspect {0 ≤ aspect < 360 degrees} were decomposed into the linear U (east-west) and V (north-south) components of a unit vector {-1, ... ,1} to facilitate linear statistical analysis. A pure south-facing slope, for example, has a V component value of -1, and a pure north-facing slope has a V component of +1. Scatterplots (Figure 4.7) and results of Kendall's tests for association both suggested error was positively and significantly correlated with the east-west component (tau = 0.199 and $p < 0.0000$), and negatively and significantly correlated with the north-south component (tau = -0.287 and $p < 0.0000$).

[4] I derived a surface of slope aspects from the grid of DEM elevations and assigned co-located values to control points using GIS software.

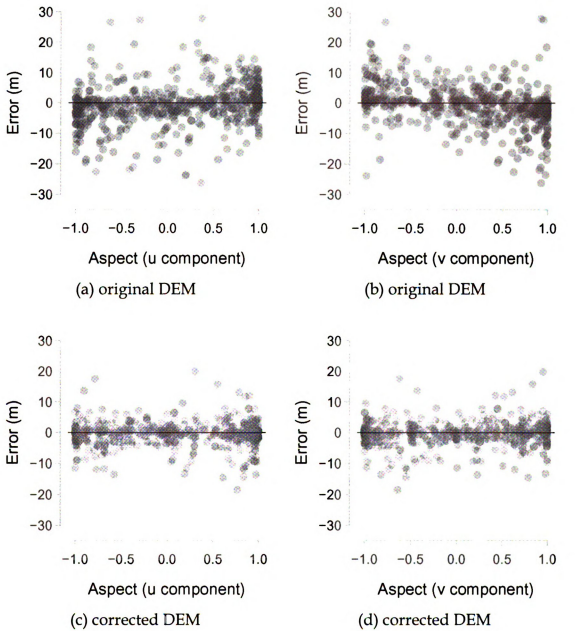


Figure 4.7: Scatterplots of DEM error and the linear components of slope aspect.

Although the statistical relationships were weak, the graphical evidence was striking (Figure 4.7a and 4.7b) and indicated elevations in the original DEM tended to overestimate elevations at locations with east- or south-facing slopes,

and underestimate elevations at locations with west- or north-facing slopes. Such results indicated clearly that the DEM was not georeferenced properly.

I visually inspected control point and DEM data simultaneously using GIS software and observed the apparent shift for the first time. Multiple attempts to estimate the correct locations of control points within the footprints of nearby grid cells yielded consistent estimates. On average, elevations in the original DEM were shifted 75 m south and 15 m east of control point locations. So, I corrected the DEM by translating the origin of the original NED surface 75 m north and 15 m west, and reprocessed the model according to the methods described above. Hereafter, any mention of "the DEM" employed in this work refer to the correctly georeferenced elevation surface.

Corrected DEM elevations were assigned to control point locations using nearest-neighbor interpolation and GIS software and I conducted a second exploratory analysis that yielded markedly improved results. For example, the association between error and slope-aspect is now considered random, uncorrelated and not indicative of any systematic bias (see Figure 4.7c and 4.7d). The association between DEM-reported and actual elevation is stronger (see Figure 4.6b) and suggests a better match ($a = 0.10$: Pearson's correlation coefficient = 0.9978, $p < 0.0000$), the sample mean and median values moved toward zero, the two extreme error values have much lesser magnitudes, and the sample variance diminished (see Table 4.5). These new results indicate that the DEM is georeferenced more accurately than before.

Complete results of the second exploratory analysis

Again, corrected DEM elevations were assigned to control point locations using nearest-neighbor interpolation and GIS software. Errors in elevation were estimated by subtracting check point elevations from interpolated elevations. A map of data postings (Figure 4.8) reveals no conspicuous trend or drift. Yet, many small errors occur near other small errors, many positive errors are situated near other positive errors and large negative errors tend to occur near other large negative errors (although, in some instances, large positive errors are situated near large negative errors). In short, differences from the sample mean (-0.36 m) seem to exhibit spatial continuity or structure. Table 4.6 contains statistical summaries of error, Figure 4.9 shows frequency histograms and Figure 4.10 shows q-q plots for the entire DEM and each subset. The calculated mean of all DEM errors ($\bar{x}$ = -0.36 m) is significantly different than zero at the 90% confidence level. Summary statistics and the frequency histogram (Figure 4.9a) suggest the distribution of error is bell-shaped, symmetric and centered near zero. The q-q plot (Figure 4.10a) reveals, however, larger-than-expected errors in both tails. Results of a Shapiro-Wilk test for normality (a = 0.10: W = 0.917 and p < 0.0000) indicate the standardized distribution of error is generally correlated with, but does not significantly fit a Normal distribution.

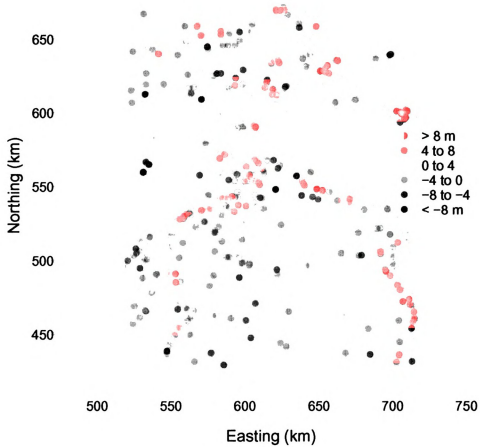
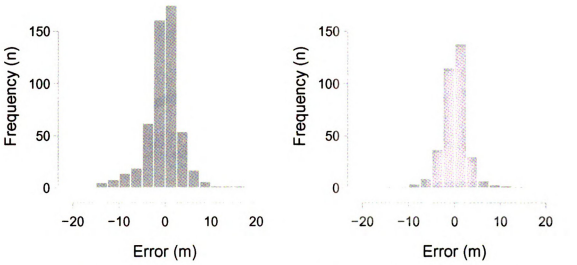


Figure 4.8: Map of DEM errors at control point locations. The map reveals no global pattern but suggests error values exhibit some spatial continuity at short distances. The image is presented in color.

Elevations in the Lower Peninsula subset were collected originally from contour lines either digitized or scanned from topographic maps. The Lower Peninsula sample mean of calculated errors ($\bar{x}$ = -0.06 m) is not significantly different than zero at the 90% confidence level.

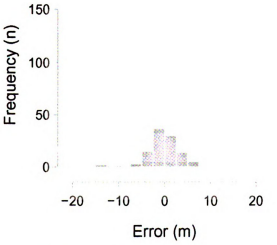
Table 4.6: Summary statistics that describe differences between actual and co-located DEM elevations.

The entire DEM	Value	Test for mean ≠ 0	Value
n	529		
minimum	-18.6 m		
median	-0.02 m		
mean (bias)	-0.36 m	matched-pairs *t*	$p = 0.043$
standard error of mean	0.18 m		
standard deviation	4.07 m		
maximum	19.8 m		
Lower Peninsula subset			
n	348		
minimum	-13.3 m		
median	0.05 m		
mean (bias)	-0.06 m	matched-pairs *t*	$p = 0.718$
standard error of mean	0.16 m		
standard deviation	2.94 m		
maximum	13.1 m		
Upper Peninsula subset			
n	108		
minimum	-13.6 m		
median	-0.30 m		
mean (bias)	-0.50 m	matched-pairs *t*	$p = 0.147$
standard error of mean	0.34 m		
standard deviation	3.57 m		
maximum	7.0 m		
Ontario subset			
n	73		
minimum	-18.6 m		
median	-2.07 m		
mean (bias)	-1.58 m	matched-pairs *t*	$p = 0.081$
standard error of mean	0.90 m		
standard deviation	7.65 m		
maximum	19.8 m		

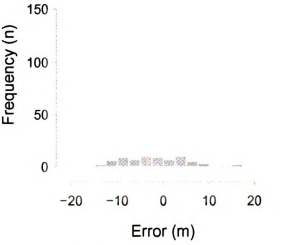


(a) entire DEM

(b) Lower Peninsula subset



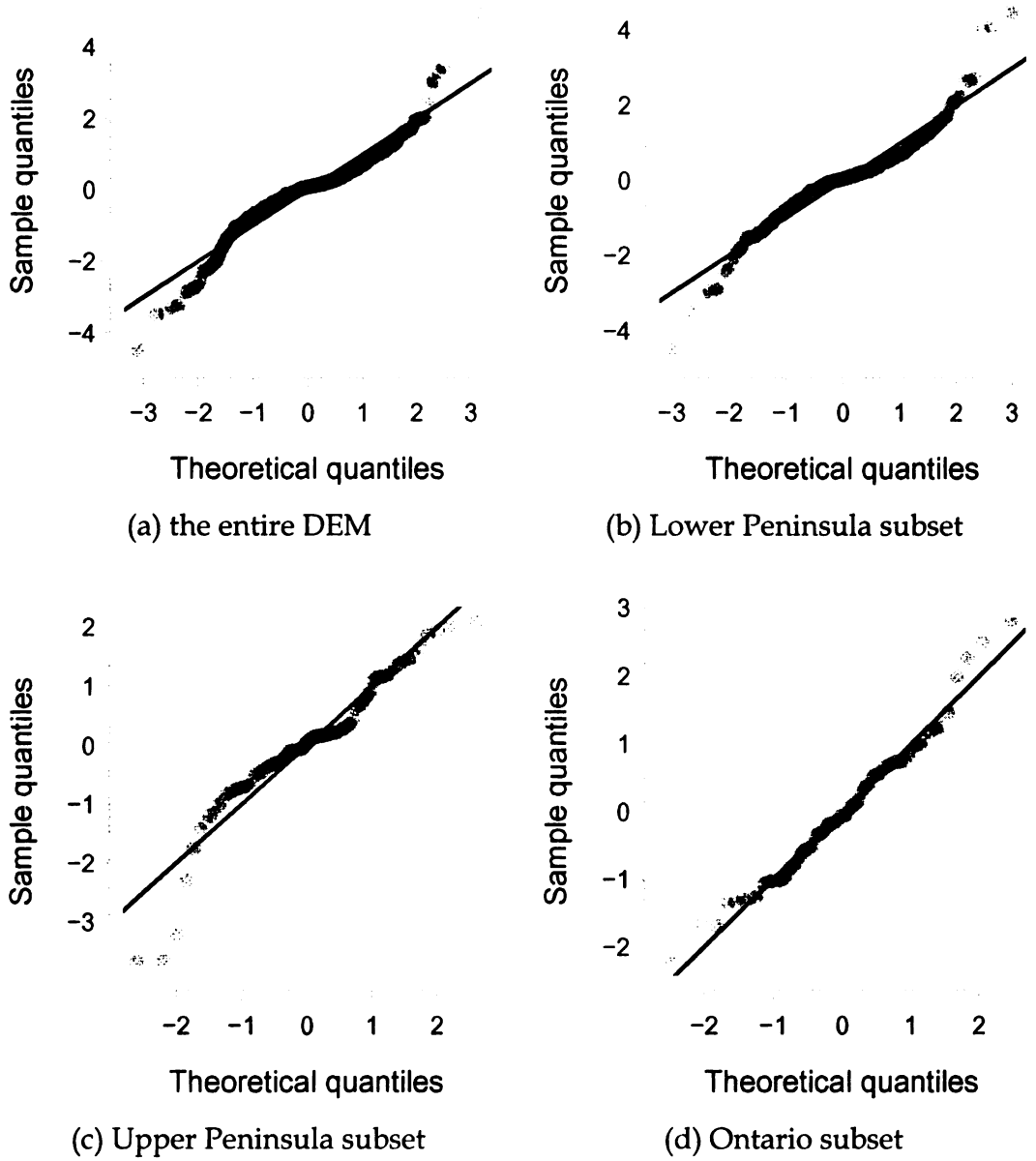
(c) Upper Peninsula subset



(d) Ontario subset

Figure 4.9: Histograms of elevation errors in the DEM.

Summary statistics and a frequency histogram (Figure 4.9b) suggest the distribution of error is bell-shaped, symmetric and centered near zero, but may contain larger-than-expected positive errors.



(a) the entire DEM

(b) Lower Peninsula subset

(c) Upper Peninsula subset

(d) Ontario subset

Figure 4.10: Q-Q plots of standardized elevation errors in the DEM.

The Lower Peninsula q-q plot (Figure 4.10b) reveals, however, larger-than-expected errors in both tails. Results of a Shapiro-Wilk test for normality (a = 0.10: W = 0.930 and $p < 0.0000$) indicate the distribution or error in the Lower Peninsula does not fit a Normal distribution.

Elevations in the Upper Peninsula were collected primarily using photogrammetric techniques. Bolstad and Stowe (1994) compared photogrammetrically-derived elevations at 42 NGS bench marks near Blacksburg, VA and reported such values tend to underestimate actual elevations. The sample mean of calculated errors ($\bar{x}$ = -0.50 m) for the Upper Peninsula subset is less than zero and so suggests this model also tends to underestimate actual elevations, but the sample mean is not significantly different than zero at the 90% confidence level. A histogram (Figure 4.9c) suggests the distribution of error is bell-shaped, but has large errors in the lower tail. A q-q plot (Figure 9.10c) indicates the lower half of the distribution is not well-behaved for it contains several values that are larger than expected should errors be distributed as Normal. Results of a Shapiro-Wilk test for normality (a = 0.10: W = 0.930 and $p < 0.0000$) indicate the distribution of error in the Upper Peninsula does not fit a Normal distribution.

Elevations in Ontario, Canada were likely derived from the DTED and coerced into the NED. Summary statistics and a frequency histogram (Figure 4.9d) suggest the distribution of DEM error is skewed left and centered below zero. The Ontario subset contains extreme values and they are the same as those associated with the entire DEM. The sample mean of calculated errors ($\bar{x}$ = -1.58 m) is significantly different than zero at the 90% confidence level and the sample standard deviation (7.65 m) is relatively large. As expected, elevation data for Ontario contain large errors and so should be considered a likely source of

uncertainty in model results. A q-q plot (Figure 4.10d) suggests that the distribution of error might not be distributed as normal, but results of a Shapiro-Wilk test for normality (a = 0.10: W = 0.982 and p = 0.364) indicate the distribution or error does fit a Normal distribution.

I partitioned the DEM into three subsets based on ancillary information about the original DEM production methods. I expected to find marked differences in the resultant behaviors of their elevations and errors. It seems, however, that subsequent geoprocessing mitigated (or obfuscated!) many of the apparent differences, for only the Ontario subset appears stands out with its relatively large mean and variance. I transformed this observation into a hypothesis and conducted three, two-sample difference-of-means tests to assess statistical differences (a = 0.1, m = 0.0 m and assuming unequal variances). All test results (Table 4.7) indicate, however, that no statistical difference exists between the means. Nevertheless, I continued to work with the three subsets because each contains data derived from different source materials.

Table 4.7: Results of two-sample difference-of-means tests among DEM subsets.

	Lower Peninsula	Upper Peninsula
Upper Peninsula	t =1.164 df = 107 p value = 0.233	
Ontario	t = 1.612 df = 72 p value = 0.201	t =1.126 df = 72 p value = 0.274

Covariations with location, elevation, and slope

Bolstad and Stowe (1994) reported large discrepancies between ground-based and DEM-reported elevations tend to occur along steep slopes and "in high-relief forested areas" (p1329), thus implying DEM errors exhibit spatial continuity and covary with other landscape elements. Such ideas about spatial continuity are not unique for others also have reported spatial patterns of error (e.g., Holmes et al., 2002, Kyriakidis et al., 1999; Hunter and Goodchild, 1997; and Veregin, 1997), but they are important because they provide grist for examining error in terms of location, elevation and other landscape attributes. Specifically, Bolstad and Stowe (1994) claim dense tree canopies negatively impact the precision of some DEM production methods, and photogrammetric image correlations can fail in areas with steep slopes. Such imprecision and failures yield inaccurate data for those locations. From this information, I plotted maps (not shown), reviewed field notes and examined datasheets for check points associated with large errors ($> |8\ m|$). Indeed, I found many that occur in high-relief or forested areas (NGS datasheets contain descriptions of the approach and area near control stations). Station RJ1215 (error = -13.6 m) is situated atop a high and forested knoll, station RJ1118 (error = -12.0 m) is mounted along a large outcrop of limestone, and station RJ0383 (error = -13.6 m) is situated near the peak of a high and steep hill of sand. Station PL0631 (error = -8.8 m), however, is situated on flat and open ground.

Of the thirty-four control points that have large absolute errors, only four are NGS control stations; the others are paleoshoreline sites. Had I not already assessed the quality of my paleoshoreline data (mean = 0.16 m, standard deviation = 0.77 m), then I might have considered this result to be an indictment of the lesser quality of my paleoshoreline data. Instead, I believe that many of the large errors (> | 8 m |) are associated with ground slope and data model imprecision. Elevations in the DEM grid are spaced at 45-meter intervals that span terrain discontinuities and cannot capture finer-scale variations in topography (Maune, 1996; Carter, 1992; Shearer, 1990). Many relict lake bluffs, for example, have steep slopes that rise from toe to top over runs less than 45 meters - all within the footprint of a single grid cell. Consequently, the DEM will, by design, contain errors that covary with such breaks or changes in slope.

Check-points have location, elevation and error attributes so relationships among these variables can be assessed easily. To assess the relationship between error and slope, however, I derived surfaces of slope gradients and slope aspects from the grid of DEM elevations and assign co-located values to control points using nearest-neighbor interpolation and GIS software. Any comparison between an elevation error and an elevation-based derivative, like slope gradient or aspect, presupposes extant errors in elevation do not influence the slope values derived for the same locations. Such a presupposition is unreasonable, especially since Carter (1992) demonstrated how gradient and aspect calculations

are sensitive to even small elevation errors, but I continued for the sake of exploration.

Table 4.8: Results of Kendall's tests for association between easy-to-measure landscape variables and: a) signed error and b) unsigned error.

	a) signed error		b) unsigned error	
The entire DEM	tau	p value	tau	p value
Easting	0.021	0.476	0.126	< 0.001
Northing	-0.037	0.204	0.178	< 0.001
Elevation	-0.053	0.067	0.074	0.011
Slope gradient	0.033	0.256	0.273	< 0.001
Slope aspect (U)	0.004	0.902	-0.007	0.804
Slope aspect (V)	0.051	0.078	0.035	0.227
Lower Peninsula subset				
Easting	0.108	0.003	0.018	0.621
Northing	-0.003	0.928	0.085	0.018
Elevation	-0.062	0.083	0.021	0.563
Slope gradient	0.039	0.275	0.308	< 0.001
Slope aspect (U)	0.024	0.498	0.019	0.598
Slope aspect (V)	0.140	< 0.001	0.050	0.160
Upper Peninsula subset				
Easting	0.050	0.444	-0.032	0.619
Northing	0.021	0.750	-0.034	0.604
Elevation	-0.062	0.344	0.176	0.007
Slope gradient	0.076	0.244	0.331	< 0.001
Slope aspect (U)	0.043	0.512	-0.017	0.799
Slope aspect (V)	-0.145	0.026	0.099	0.128
Ontario subset				
Easting	-0.424	< 0.001	0.174	0.029
Northing	0.287	< 0.001	-0.207	0.010
Elevation	-0.006	0.943	-0.046	0.567
Slope gradient	-0.168	0.036	0.051	0.520
Slope aspect (U)	-0.144	0.071	0.034	0.675
Slope aspect (V)	-0.003	0.970	0.057	0.478

I used scatterplots (not shown) and Kendall's non-parametric test for association to examine the relationships between error and location, elevation and slope. I examined unsigned errors as well. Table 4.8 lists the results. A strong association between variables is indicated when there is a large probability that the ranks of data are in the same order (tau > 0.667). Of all the relationships tested, none exhibited a strong association. Jumbled pairings (tau < 0.333) or statistically insignificant test results (p > 0.100) eliminate the need to consider most of these relationships further. A few, however, exhibit moderate (0.333 < tau < 0.667) and significant (p < 0.100) associations, so I focused on them.

Unsigned error is positively correlated with slope gradient in every set, although results for the Ontario subset are weak and not statistically significant. These results are reasonable because they suggest large errors occur in locations where elevation is hard to measure -- along steep slopes -- and they agree with results reported by Bolstad and Stowe (1994) and Hunter and Goodchild (1997). A scatterplot of this relationship offers conflicting evidence (Figure 4.11) however, for it shows the full range of error occurs at locations with relatively shallow slopes (< 5% gradient). Also, both point clouds show no linear patterns of association.

The relationship between error and slope gradient provides grist for general conclusions only. Carter's (1992) work cautions that gradient calculations are uncertain given errors in the elevation model. From these results, steep slopes can be associated with large DEM errors, but both large and

small DEM errors can occur along any slope regardless of gradient. Therefore, an error estimate cannot be reduced if the terrain is known to have a low gradient.

The only other moderate correlation among error and location is in the Ontario subset and it indicates error decreases in an easterly direction. Review of ground control data, however, provides a reason for why this test result might not be a valid result. Ground control data used to assess the Ontario portion of the DEM are highly clustered (Figure 4.12a). They contain only four GDC control stations - the balance are paleoshoreline positions collected at field sites. Paleoshoreline data near Sault Ste Marie, Ontario, for example, were collected by Cowan (1985) and his data comprise the northwestern cluster. Figure 4.12b reveals most DEM elevations tend to overestimate elevations in this cluster. Paleoshoreline data at St. Joseph Island were collected by Karrow (1987) and his data comprise the central cluster. DEM elevations tend to overestimate Karrow's elevations, but not always. And, I collected paleoshoreline data at Cockburn Island, which comprise most of the southeastern cluster. DEM elevations tend to underestimate elevations in this cluster, but not always. In short, the test for association between error and Easting is seemingly influenced by the interrelations among three distant clusters and not among seventy-three well-distributed observations (Figure 4.12b). Consequently, the test statistic has likely been overestimated and the associated p value is too small. I did not to pursue this association further.

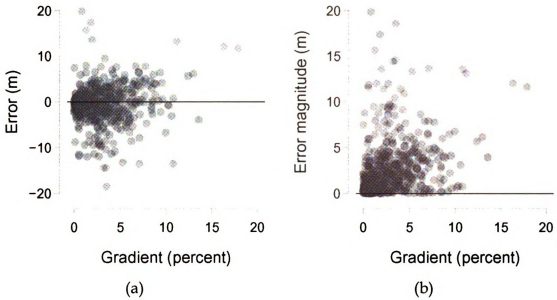


Figure 4.11: Scatterplots of: a) signed error and slope gradient; and b) unsigned error and slope gradient. Black lines drawn to emphasize zero error.

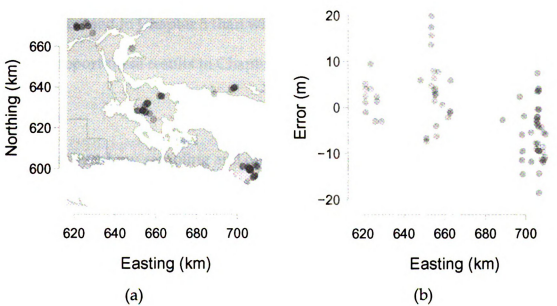


Figure 4.12: Map and scatterplot of ground control locations used to assess error in the Ontario subset.

Spatial autocorrelation

The distribution of DEM error (Figure 4.8) seems to exhibit some form of local spatial continuity or structure - meaning two errors located close to each other tend to have more similar values than two errors that are far apart (after Isaaks and Srivastava (1989:50-51). This is structure that cannot be explained by the weak associations with location, elevation or slope. The semi-variogram is a useful tool for exploring and characterizing the way in which the deviations from a mean value at different locations covary or are correlated (Bailey and Gatrell, 1995: 162). Yet successful use and interpretation of a semi-variogram of errors presupposes an understanding of regionalized variables and the assumptions of stationarity. These concepts are much more closely aligned with the spatial models discussed in Chapter 5 than with the accuracy assessments presented here, so I report these results in Chapter 5.

Summary

I designed my sampling and data processing protocols (Chapter 3, this volume) to ensure that paleoshorelines were measured as accurately as possible given the lesser precision of GPS technology relative to traditional yet more labor-intensive technologies. Careful planning and diligent use has yielded a set of measured positions that closely match actual positions. Measurement errors in elevation are random, typically sub-meter and always less than two meters; the distribution is centered near zero and Normal. Horizontal errors are

negligible. There is no evidence of any remaining gross or systematic error that can or should be mitigated.

Selection errors in paleoshoreline data present a problem because they cannot be easily identified or redressed. Gravel lags are the best indicators of former shorelines, but using them as indicators of shoreline elevation is imprecise. I suspect such errors are often ignored during spatial modeling and analysis. In this case, however, the range of possible selection errors is large enough to exceed the three-meter critical threshold I adopted for distinguishing different water levels, and so they warrant further consideration. A position with a three-meter selection error is not acceptable for use, but I do not know if any of my data contain such an error. Consequently, my only recourse is to add the information I do have about possible selection errors to my spatial model. In short, I need to simulate their existence in order to ascertain how they might impact my results.

The US Coast Guard archive of *GPS Status Message Reports* (US Coast Guard Navigation Center, 2004) is a valuable resource; I did not know it existed until after I collected data and began analysis. The US Coast Guard posts status reports that list planned outages and system changes as well as recent and unexpected satellite behaviors (such as the one I encountered). This kind of information will impose additional constraints on future planning missions, but it will add value to any data I collect with GPS in the future.

The NED is the best available source of ground surface elevation data for the region of interest. Unfortunately, these data contain both large and small errors that are the results of a long and complex geoprocessing history. Analysis of the NED has provided the biggest surprise for I did not expect to find a systematic bias in location. I translated the NED surface 75 m north and 15 m west and, subsequently, removed a systematic pattern of elevation errors and reduced the sample mean, median and variance of errors. Simultaneous visualization of the corrected surface and check point data provides solid evidence of a better fit. I have since revisited all NED-related documents on the USGS website and scoured the literature for any report that might address the shift I observed, but I have found no report that does so. I forwarded my results to the USGS, but have not yet received a reply.

Although corrected, the DEM still holds a pool of variations associated with topography, artifacts of DEM production methods, and adulterations imposed by various geoprocessing algorithms. Partitioning the model into three subsets has proven useful for it has allowed me to isolate some of these variations and consider their impacts. The distribution of elevations in the Ontario subset, for example, is clearly dominated by artifacts of a data production process. Had I not subset the model, the non-topographic pattern of spikes in the Ontario histogram would have remained largely hidden in the histogram of DEM elevations. Elevations in the Lower and Upper Peninsula subsets also exhibit artifacts of data production processes, but these appear mild

by comparison. By and large, the Lower and Upper Peninsula subsets contain elevations that represent surface topography.

Mapped errors in DEM elevations exhibit evidence of local spatial continuity as positive errors tend to occur near other positive errors and negative errors tend to occur near other negative errors. Yet, correlation test results demonstrate DEM error, either signed or unsigned, does not covary with location coordinates, elevation, or slope. Moreover, trend surface analyses (not reported) provided no statistical power to suggest otherwise. The apparent association between unsigned error and slope gradient is acknowledged but the parameters that might define its behavior are uncertain because gradient calculations are so sensitive to errors in elevation (Carter, 1992) and the DEM employed in this work certainly contains errors in elevation. In my opinion, no correlation is sufficiently strong to advocate using knowledge about it to improve estimates of error at unsampled locations. While it would be convenient to have found a strong and significant association between error and location, elevation, or slope - or any other cheap-to-measure landscape variable for that matter - other means of qualifying spatial continuity are necessary. I take up this issue again in Chapter 5.

Absolute errors in DEM elevations often exceed three meters and, in Ontario, can reach almost twenty meters. Such errors far exceed the critical threshold I've adopted for distinguishing different water levels. The DEM, as is, is not fit for my use. Unfortunately, the current DEM is the best one available,

and so I must use it. My only recourse is to add the information I do have about DEM errors to my spatial model. In short, I need to fix the elevations errors where I know they occur, and I need to simulate the presence of error at locations between check point locations. Doing so will enable me to ascertain how they might impact my results.

CHAPTER 5: THE SPATIAL MODEL

Introduction

This chapter describes a spatial model for digitally reconstructing ancient landscapes associated with glacial Lake Algonquin. The model has two parts. The first part reconstructs water planes that have been upwarped by differential isostatic rebound over the past 11,000 years. Initial reconstructions are supported by paleoshoreline data (described in Chapter 3) and parameters that describe the upwarped surface are estimated via least squares. Water planes are reconstructed ultimately via universal kriging, which yields both a prediction surface and an estimate of uncertainty at each predicted location. The second part of the spatial model addresses error and uncertainty about error in a contemporary digital elevation model (DEM), which is used to represent ground surface form for the region of interest. A set of control points and information about elevation errors at control point locations is used to condition the DEM and, via ordinary kriging and Monte Carlo simulation techniques, to generate alternate possible realizations of the ground surface. Finally, results of the two parts (a predicted water plane and a set of alternate possible DEMs) are combined to allow locations within the area of interest to be characterized as: above water plane; below water plane; or uncertain. Four landscapes are reconstructed and they are associated with the Main, Ardtrea, Upper Orillia, and Lower Orillia phases of glacial Lake Algonquin.

I offer a review of geostatistical concepts that underlie general spatial prediction and kriging before presenting the spatial model and its two parts. My review summarizes essential points related to the theory of spatial prediction, but does so in a user-friendly format. Formal treatments of these theories and methods are presented by Journel and Huijbregts (1978), Isaaks and Srivastava (1989), Bailey and Gatrell (1995) and Gringarten and Deutsch (2001).

Modeling outcomes of a spatial random process

A *field* is a conceptual model that is useful for representing an attribute of a phenomenon that varies over space. Elevation, for example, is an attribute of terrain and it varies over space. Similarly, relative humidity and air temperature are attributes of the atmosphere that vary over space. A field model typically represents space by employing a tessellation of discrete spatial elements (e.g., points, grid cells, facets etc.) that are assigned values taken from the phenomenon of interest. This work utilizes a two-dimensional tessellation of discrete grid cells. Field models are always approximate because "we cannot store an infinite number of locations" (Cova and Goodchild, 2002:511) and we cannot collect or store attributes with infinite precision.

Any procedure or process used to take measurements of a phenomenon has finite precision, so data obtained from measurements are imperfect. The difference between a measured value and the actual value is error. The amount of error in any measured value is always unknown, however, because the true

value exists beyond the limits of equipment or procedural precisions. Because of this inescapable error, the amount of error in a measured value is considered a random variable. An elevation value obtained from measurement is also considered a random variable because it contains a component of fixed truth and a component of random error. A process that generates a random variable is a random process. Accordingly, a process for measuring elevations at locations over a region of interest is considered a spatial random process.

Other spatial processes can influence the outcomes of a spatial random process. Consider, for example, an instance of terrain that is flat, easy to access during calm weather and, so, relatively easy to measure given equipment provided (i.e., conditions for taking measurements are optimal). An elevation value taken under such conditions might be expected to contain random error associated only with variation that occurs beyond the limits of equipment or procedural precision. Alternatively, consider an instance of terrain that is rough, difficult to access during stormy weather and, so, very difficult to measure given the equipment provided (i.e., conditions are not optimal). An elevation value taken under such conditions might be expected to contain an error greater than that generated by equipment precision alone because external forces upset the measurement process. Using these two instances as "straw men," it is easy to imagine spatial gradients of terrain (from flat to rough) and weather (from calm to stormy) and how they might interact across space and time and, so, differentially perturb the measurement process from one location and one

moment to a next. Consequently, a random measurement process can generate a field of random variables that contain noisy errors associated with equipment precision as well as spatial patterns of error introduced by external phenomena that differentially upset the process. Unfortunately, we do not always know where or when a spatial error process (or processes) exists or how such a process might alter our best efforts to collect data in the field or lab.

A *random field* is a conceptual model that is useful for representing the outcomes of a random spatial process.[1] Use of a random field assumes variation over space can be expressed as the sum of three components: a deterministic component akin to either a constant mean or spatial trend (Journel and Huijbregts, 1978: p40, prefer the term "drift"); a random and spatially structured error component; and a random but spatially unstructured error component (i.e., noise). In short, the outcome at each location is considered a random variable, the set of all random variables across the region of interest comprises a random field, and a specific set of measured outcomes within the region of interest is

---

[1] Many geostatisticians use the phrases *regionalized variable* (Journel and Huijbregts, 1978; Burrough, 1991) or *random function* (see Kyriakidis et al., 1999; Goovaerts ,1997; or Issaks and Srivastava, 1989), but I prefer to use the phrase *random field* (see Diggle and Ribeiro Jr, 2002; or Ehlschlaeger, 2002) because it provides an explicit link to the *field* data model (Couclelis, 1992; Cova and Goodchild, 2002), and doing so averts confusion with other uses of the term *function*.

considered a realization of that random field. Following Burrough (1991), a random field is expressed as:

$$Z(\mathbf{u}) = m(\mathbf{u}) + \varepsilon'(\mathbf{u}) + \varepsilon'', \qquad \forall\, \mathbf{u} \in R \qquad \text{[Eq. 1]}$$

where $Z(\mathbf{u})$ is the random field, $m(\mathbf{u})$ is either the constant mean or spatial trend component, $\varepsilon'(\mathbf{u})$ is the random and spatially structured error component, ε'' is the random and spatially unstructured error component, and $\mathbf{u}$ is the set of all locations in the region of interest R. Let $\mathbf{u}_i$, $i = 1,\ldots,n$, represent a set of n locations where the random field $Z(\mathbf{u})$ has been observed in region R, and let $\mathbf{u}_0$ represent unsampled locations in region R.

The probability density function (pdf) of a random field $Z(\mathbf{u})$ is a model of possible values that z can take at locations $\mathbf{u}$ and their associated probabilities:

$$f(\mathbf{u}; z) = \text{Prob}\{ Z(\mathbf{u}) = z \}, \quad \forall\ z \qquad \text{[Eq. 2]}$$

Because the probability at a single point in a continuous distribution is always zero, a pdf is, for practical purposes, often expressed in terms of the integral between two points in the distribution.

The cumulative distribution function (cdf) is a model that defines the probability that outcomes of $Z(\mathbf{u})$ do not exceed a given threshold z :

$$F(\mathbf{u}; z) = \text{Prob}\{ Z(\mathbf{u}) \leq z \}, \quad \forall\ z \qquad \text{[Eq. 3]}$$

If additional information exists and can be used to condition the random field, then the conditional cumulative distribution function (ccdf) of the random field $Z(\mathbf{u})$ defines the probability that outcomes do not exceed threshold z given this information:

$$F(\mathbf{u}; z \mid (\text{info})) = \text{Prob}\{ Z(\mathbf{u}) \leq z \mid (\text{info}) \}, \quad \forall\ z \qquad \text{[Eq. 4]}$$

The expected value or spatial trend $m(\mathbf{u})$ and spatially unstructured error ε'' components are models covered in many statistical texts, so another review here would be redundant. I focus instead on the basis geostatistics provides for exploring and modeling the random and spatially structured component $\varepsilon'(\mathbf{u})$. Spatial structure implies a relationship between proximity and similarity of outcomes: two outcomes located close to each other will tend to have values more similar than two outcomes that are farther apart (after Isaaks and Srivastava, 1989). According to Bailey and Gatrell (1995), if we expect a random field to exhibit spatial structure, then we can anticipate "observing positive covariance or correlation at short distances and lower covariance or correlation at greater distances" (p 162). Covariance $C()$ is a measure of similarity between outcomes $\mathbf{u}_i$ and $\mathbf{u}_j$ and can be expressed as:

$$C(\mathbf{u}_i, \mathbf{u}_j) = \text{E}\{ (Z(\mathbf{u}_i) - m(\mathbf{u}_i)) \cdot (Z(\mathbf{u}_j) - m(\mathbf{u}_j)) \} \qquad \text{[Eq. 5]}$$

Modeling the spatial component of a random field often requires adopting one or more assumptions when complete knowledge is not available for all locations within the region of interest. For example, it is not always possible to estimate the cdf at a given location because, typically, at most only one observation is available at that location (Shortridge, 2001). So, we must adopt assumptions about the cdf if we want to proceed with sparse data. The assumption of stationarity, for example, holds the expected value and variance of the random field $Z(\mathbf{u})$ are independent of location, or $m(\mathbf{u}) = m$ and $\sigma^2(\mathbf{u}) = \sigma^2$. Adopting this assumption allows the cdf at any location to be characterized by the cdf of the random field. A more commonly used but weaker assumption is intrinsic stationarity, which assumes a constant mean and a constant variance in "the differences between values at locations separated by a given distance and direction" (Bailey and Gatrell, 1995:162). In geostatistical notation:

$$E\,[Z(\mathbf{u}) - Z(\mathbf{u} + \mathbf{h})] = 0 \qquad \text{[Eq. 6]}$$

$$\text{Var}\,[Z(\mathbf{u}) - Z(\mathbf{u} + \mathbf{h})] = E\,\{\,[Z(\mathbf{u}) - Z(\mathbf{u} + \mathbf{h})]^{\,2}\,\} \qquad \text{[Eq. 7]}$$

where $\mathbf{h}$ is a vector of distances (or distances and directions) that separate pairs of outcomes. Adopting the weaker assumption removes focus from the absolute locations of data and estimating joint cdfs that are supported by few observations and, rather, places focus on the more-numerous distance vectors that separate pairs of random variables. In this sense, spatial structure implies two outcomes

located close to each other will tend to have more similar values than two outcomes far apart (after Isaaks and Srivastava (1989:50-51) - *regardless of absolute locations*. Covariance between outcomes (Eq. 5) can be re-characterized in terms of separating distances:

$$C(\mathbf{h}) = E\{Z(\mathbf{u}) \cdot Z(\mathbf{u}+\mathbf{h})\} - E\{Z(\mathbf{u})\} \cdot E\{Z(\mathbf{u}+\mathbf{h})\} \qquad \text{[Eq. 8]}$$

or, by assuming intrinsic stationarity and substituting a constant mean, m, as:

$$C(\mathbf{h}) = E[Z(\mathbf{u}) - Z(\mathbf{u}+\mathbf{h})] - m^2 \qquad \text{[Eq. 9]}$$

Note, stationarity and intrinsic stationarity are not properties of any phenomenon, but modeling decisions that provide reasonable means of analyzing a random field given sparse data or scant information about data.

A variogram $2\gamma(\mathbf{h})$ is the expected squared difference between data values separated by vector $\mathbf{h}$ (Gringarten and Deutsch, 2001). A variogram can be expressed as:

$$2\gamma(\mathbf{h}) = \text{Var}[Z(\mathbf{u}) - Z(\mathbf{u}+\mathbf{h})] = E\{[Z(\mathbf{u}) - Z(\mathbf{u}+\mathbf{h})]^2\} \qquad \text{[Eq. 10]}$$

The semi-variogram $\gamma(\mathbf{h})$ is one-half the variogram $2\gamma(\mathbf{h})$ and a measure of *variability* used commonly to explore spatial structure in data. Semi-variance

values increase as outcomes become dissimilar and tend towards zero as outcomes become similar.

Again, covariance $C()$ is a statistical measure of *similarity* and, under the assumption of intrinsic stationarity, inversely related to semi-variance. By definition, the covariance at $\mathbf{h} = 0$, or $C(\mathbf{0})$, is the variance σ^2 (Gringarten and Deutsch, 2001). Covariance $C(\mathbf{h})$ is 0 when values separated by $\mathbf{h}$ are not correlated. Combining these relations and the concepts embodied in Equations 9 and 10, the link between semi-variance and covariance is:

$$\gamma(\mathbf{h}) = C(\mathbf{0}) - C(\mathbf{h}) \quad \text{or} \quad C(\mathbf{h}) = \sigma^2 - \gamma(\mathbf{h}) \qquad \text{[Eq. 11]}$$

The link between semi-variance and covariance provides the basis for interpreting a semi-variogram. The "sill" of a variogram represents the variance σ^2 of the random field and it corresponds with no spatial correlation. If $Z(\mathbf{u})$ and $Z(\mathbf{u} + \mathbf{h})$ are positively correlated, then corresponding semi-variance values are less than the variance, or sill. If $Z(\mathbf{u})$ and $Z(\mathbf{u} + \mathbf{h})$ are negatively correlated, however, then corresponding semi-variance values are greater than the variance, or sill. The "range" of a semi-variogram is the distance h at which observed semi-variance reaches the sill and spatial correlation no longer occurs. Also, a "nugget" effect might be observed at very short distances. A nugget effect is interpreted as random chaotic or nonlinear variations "that have no spatial autocorrelation structure" (Gringarten and Deutsch, 2001: 509)

For computation, the semi-variogram is expressed as:

$$\gamma(\mathbf{h}) = \frac{1}{2n(\mathbf{h})} \sum_{i=1}^{n(\mathbf{h})} [z(\mathbf{u}_i) - z(\mathbf{u}_i + \mathbf{h})]^2 \qquad \text{[Eq. 12]}$$

where $n(\mathbf{h})$ is the number of outcomes separated by each distance (or direction) in vector $\mathbf{h}$. Given sparse data, however, values of $\mathbf{h}$ typically represent lags or small ranges of distances approximately equal to $\mathbf{h}$ (i.e., within some tolerance).

When used within a kriging framework, the theory of random fields and spatial structure can be employed to predict outcomes at unsampled locations (i.e., interpolation). According to Bailey and Gatrell (1995), if covariance exists between observed outcomes, then outcomes at unsampled locations "are not entirely unpredictable" (p183). A kriging framework accomplishes spatial prediction by modeling unsampled outcomes as weighted linear combinations of sampled outcomes. In practice, kriging weights are assigned with respect to: a) a model of covariances observed among sampled outcomes; and b) a model of covariances expected between sampled and unsampled locations. Kriging weights are subject to linear constraints that ensure the expected squared prediction error is zero. In geostatistical notation, a set of kriging weights is:

$$\lambda(\mathbf{u}_{i,0}) = \mathbf{C}^{-1}\mathbf{c}(\mathbf{u}_{i,0}) \qquad \text{[Eq. 13]}$$

where $\lambda(\mathbf{u}_{i,0})$ is the set of weights; C^{-1} is the inverse of a matrix holding covariances between sampled outcomes; and $c(\mathbf{u}_{i,0})$ is the set of expected covariances between sampled and unsampled locations $\mathbf{u}_0$. In practice, expected covariances $C(\mathbf{h})$ between sampled and unsampled locations are modeled as a function of distance between $\mathbf{u}_0$ and nearby $\mathbf{u}_i$. Given a sample, distances between sampled and unsampled locations, and information about the spatial structure of covariance over space, the set of predicted outcomes at unsampled locations becomes:

$$Z(\mathbf{u}_0) = \sum_{i=1}^{n} \lambda(\mathbf{u}_{i,0}) Z(\mathbf{u}_i) \qquad \text{[Eq. 14]}$$

A kriging framework can be used to model uncertainty at predicted locations. The mean square prediction error (a.k.a. kriging variance, σ_0^2) is modeled by removing the portion of variance explained by spatial structure from the total variance σ^2. As the amount of variance explained by spatial structure approaches zero, the kriging variance approaches the total variance σ^2. This link can be expressed as:

$$\sigma_0^2 = \sigma^2 - c^T(\mathbf{u}_{i,0}) C^{-1} c(\mathbf{u}_{i,0}) \qquad \text{[Eq. 15]}$$

or, by substituting kriging weights (Eq. 13) for $\boldsymbol{C}^{-1}\boldsymbol{c}(\mathbf{u}_{i,0})$, as:

$$\sigma_0^2 = \sigma^2 - \boldsymbol{c}^T(\mathbf{u}_{i,0})\lambda(\mathbf{u}_{i,0}) \qquad \text{[Eq. 16]}$$

An expected value $z(u_i)$ and a kriging variance σ_0^2 are sufficient for specifying a cdf at each location (if we also assume the distribution of values at each location is distributed as Normal). Furthermore, information provided by nearby random variables allows a ccdf to be specified. Therefore, alternate possible realizations can be generated at each location in the region of interest by drawing values randomly from each ccdf.

Sequential Gaussian simulation (sGs) is a technique for generating alternate realizations of a random field that can be used as inputs to a spatial model. According to Goovaerts (1998:4),

> "sequential simulation amounts to modelling the conditional cumulative distribution function (ccdf), ... ,then sampling it at each of the grid nodes visited along a random sequence. To ensure reproduction of the z-variogram model, each ccdf is made conditional not only to the original n data but also all values simulated at previously visited locations."

The promise of using not a single realization, but multiple alternate realizations of a random field is the ability to reveal uncertainty in results of a spatial model

given uncertainty about errors in data. When used within a Monte Carlo simulation framework, sequential Gaussian simulation can reveal uncertainty in results accurately and precisely (Goovaerts, 1998).

Monte Carlo simulation is a computer-intensive framework that is useful for revealing contributions of input data errors to results, differences among uncertainties across a geographic region of interest (Burrough and McDonnell, 1998) and uncertainties that lurk in spatial model results. In essence, a typical simulation consists of evaluating a spatial model many times, each time using input data that have been modified randomly via a model that expresses an error distribution or makes assumptions about error behavior. Parameters of the model are derived with respect to known or assumed information about errors in the input data. After a set of n input realizations is generated, the spatial model is run n times and the set of n spatial model results is summarized to determine the range of possible outcomes at each location.

Building the spatial model

Schaetzl et al. (2002) built a spatial model for interpolating paleoshorelines along four glacial Lake Algonquin water planes; Figure 5.1 diagrams their workflow. In essence, a differentially upwarped water plane was modeled as a function of location using paleoshoreline position data and a second-order polynomial surface model with parameters estimated via ordinary least squares. The minimum measured paleoshoreline elevation value was subtracted from the

upwarped surface and the result represented differential warping relative to the lowest sampled feature.

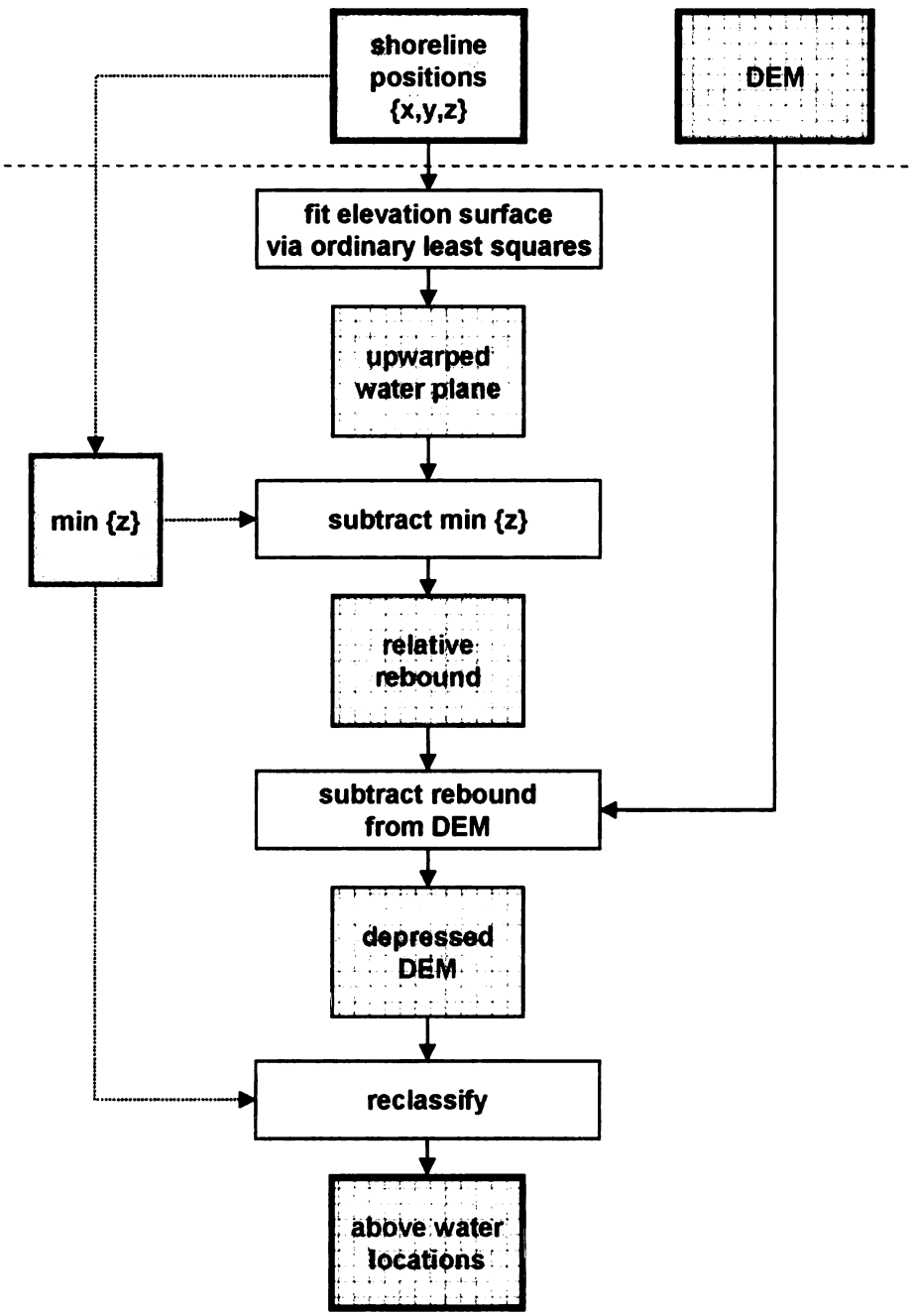


Figure 5.1: The spatial model Schaetzl et al. (2002) used to reconstruct landscapes in northern Michigan associated with glacial Lake Algonquin.

Next, the relative rebound surface was subtracted from a contemporary digital elevation model (DEM), thereby generating a topographic surface that was down-warped (i.e. differentially depressed) by the immense weight of the Laurentide ice sheet; this is similar to the method used by Krist and Schaetzl (2001). Finally, adjusted elevation values were classified with respect to the aforementioned lowest feature; DEM cells with elevation values greater than the lowest feature were classified *above water* and the balance was classified *not above water*. The binary classification scheme served to cartographically flood the depressed landscape, reveal the extent of the modeled water plane as constrained by topography and, hence, interpolate paleoshorelines at locations between measured paleoshoreline positions.

Others have built similar models for reconstructing ancient water planes in Scotland (e.g., Smith, Cullingford and Firth, 2000; Firth, Smith and Cullingford, 1993) and interpolating paleoshorelines in Canada (e.g., Leverington and Teller, 2003; Leverington, Teller and Mann, 2002), but each assumed paleoshoreline data do not contain measurement errors (Poole and O'Farrell, 1971), which in my experience is not always the case. Consequently, their results are deterministic and do not convey any imprecision or uncertainty.

I use a model similar to the one built by Schaetzl et al. (2002), but instead of generating a single deterministic result, I employ kriging methods and sequential Gaussian simulation (sGs) within a Monte Carlo framework to take advantage of information I have about random errors in my paleoshoreline data

and digital elevation model, respectively. Figure 5.2 diagrams my workflow. The enhanced spatial model allows me to identify locations in my results that are subject to greater or lesser uncertainties. Knowing which locations suffer greater uncertainties is useful for qualifying my results (and prescribing limited uses) and for focusing subsequent fieldwork.

Below I present the two major parts of the paleoshoreline interpolation model. The first part acknowledges possible errors that lurk in the paleoshoreline dataset and limitations associated with using ordinary least squares (OLS) to estimate upwarped water plane elevations. The second part acknowledges errors that lurk in the DEM and describes the models I use to generate alternate possible realizations of the contemporary ground surface. Ultimately, the results of these two parts are combined so that a comparison can be made at every DEM grid cell location between the elevation of the contemporary land surface and the elevation of the differentially-upwarped water plane. Unsampled locations with ground surface elevations equal to, or very near to, the co-located water plane elevation are identified as candidates for having unsampled paleoshorelines.

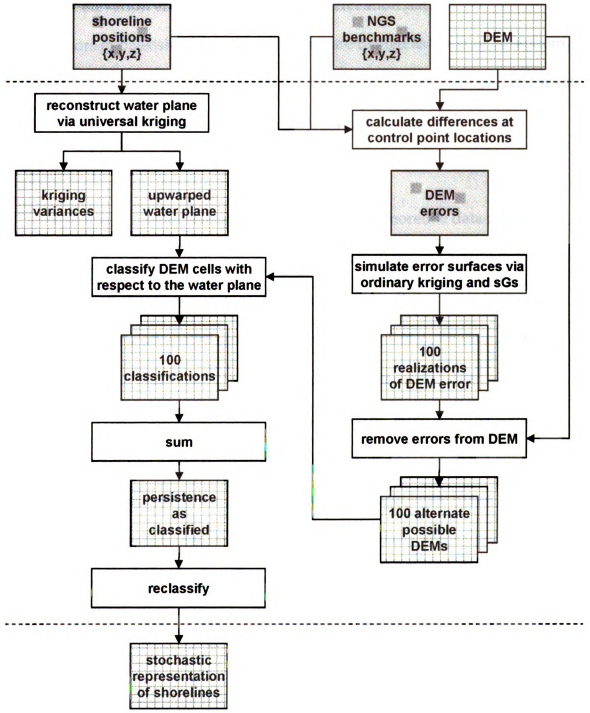


Figure 5.2: The spatial model used in this work to digitally reconstruct water planes and landscapes in northern Michigan and western Ontario that were associated with glacial Lake Algonquin. The model was run 100 times for each water plane, which produced a set of 100 results that were summarized to reveal the influences of input data errors.

Models of elevation errors in paleoshoreline elevation data

Errors in paleoshoreline elevation data are treated as the sum of random and independent and selection errors and measurement errors. I use a statistical model to express these errors and mitigate their influence.

Assumed model of selection errors

Uncertainty about selection errors in my paleoshoreline data can be addressed by adopting assumptions about selection error and employing a model based on those assumptions (Shortridge, 2001). Based on my experience in the field and via an analysis of the research of others (e.g., Lawson, 1891; Goldthwait, 1910; Morton and Speed, 1998), I expect most surveyed elevations are accurate proxies for former water levels. I expect, however, that some measured elevations might overestimate water levels because: a) the base of a wave-cut bluff typically forms at or slightly above water level; b) the bouldery/gravelly lags that form at the bases of wave-cut bluffs vary in width (pers. obs.) according to local wave conditions and water levels fluctuations (Chapter 2); and c) I began my search for the bouldery/gravelly lag at the highest point along each base. Accordingly, my search method preferentially selects the highest portion of each the bouldery/gravelly lag. Therefore, there is a possibility that the highest measurable point on a particular bouldery/gravelly lag might overestimate average water.

I assume most selection errors to be 0 m because I expect most surveyed features represent water levels. Wherever errors do occur, I assume most will be small and fall within the interval of 0 and 1 m. I must recognize that, on rare occasions, an extreme error might exist and I assume it will fall within the interval of 1 and 3 m. I do not have reason to expect any selection error will exceed three meters. Selection error at any paleoshoreline location can be modeled as a random variable that is distributed as Exponential. I chose the Exponential distribution for its convenience: it can be adapted easily to describe the expectations and assumptions I have about selection errors (i.e., bounded by zero and decreasing probabilities with increasing error values). The Exponential probability density function is expressed as:

$$f(x) = \frac{1}{\beta} e^{-(x-\mu)/\beta} \qquad x \geq \mu; \beta > 0 \qquad \text{[Eq. 17]}$$

where: x is a value in the distribution; μ is the mode of the distribution; and β is the mean of the distribution. The specific selection error model employed here assumes an Exponential distribution with parameters μ = 0.0 m and β = 0.33 m.

$$f(x) = 3e^{-(x)/0.33} \qquad \text{[Eq. 18]}$$

Selection errors are assumed to be spatially unstructured. A histogram (Figure 5.3a) shows one realization of 529 selection errors (one for each paleoshoreline

sample I have) that were generated using the Exponential model. Note the distribution is bounded by a value of zero and the frequency of a particular selection error occurring decreases with an increase in value.

Empirical model of measurement errors

Uncertainty in measurement error can be addressed by characterizing the measurement process and employing a model based on the characterization (Shortridge, 2001). In Chapter 3, I reported elevation errors measured at NGS control stations. From my assessment of these values, measurement error is modeled as a random variable that is distributed as Normal. The Normal probability density function is characterized as:

$$f(x) = \frac{e^{-(x-\mu)^2/(2\sigma^2)}}{\sigma\sqrt{2\pi}} \qquad \text{[Eq. 19]}$$

where: x is a value in the distribution; μ is the mean of the distribution; and σ is the standard deviation. The specific measurement error model (Eq. 20) assumes a Normal distribution with parameters taken from the sample of control station errors: μ = 0.16 m and σ = 0.77 m.

$$f(x) = \frac{e^{-(x-0.16)^2/1.1858}}{1.9301} \qquad \text{[Eq. 20]}$$

A second histogram (Figure 5.3b) shows a realization of 529 measurement errors, which is the same number of ground control points that I have available, that were generated using the Normal model and parameters described above.

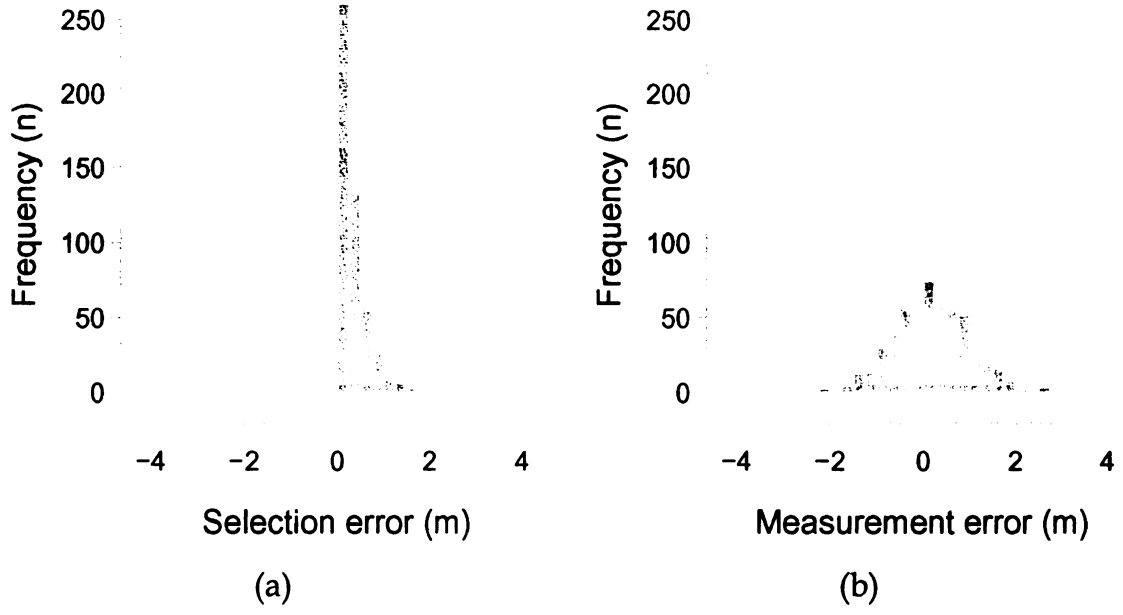


Figure 5.3: Histograms of errors generated randomly. Error values are binned in 0.25 m intervals.

Model of cumulative errors

Paleoshoreline elevation data are subject to the limits of precision associated with the method I used to select relict shorelines and the limits of precision associated with the method I used to measure relict shorelines. I assume selection errors are not spatially structured, since I have found no evidence that suggests they are. Moreover, I assume each spatial error process exists independently of the other, for I have no reason to believe they do not.

Therefore, the cumulative error in any paleoshoreline elevation can be modeled as the sum of assumed selection and inferred measurement errors. The expected value (i.e., mean) of the sum of two or more random variables is the sum of the respective means. In this case, the expected selection error is 0.33 m and the expected measurement error is 0.16 meters, therefore, the expected cumulative error is 0.49 m. The variance of the sum of two or more random variables is equal to the sum of the variances when the random variables are independent - as selection and measurement errors are assumed to be. In this case, the expected variance of selection error is 0.11 m and the expected variance of measurement error is 0.77 m, therefore the expected variance of cumulative error is 0.88 m. To complete my illustration, Figure 5.4 shows a histogram of 529 simulated cumulative errors in paleoshoreline elevations.

It is assumed that paleoshoreline elevation data contain relatively small cumulative errors that are spatially unstructured. At this time, the best estimate of error at any location is the expected cumulative error (0.49 m), so 0.49 m was subtracted from each observed paleoshoreline elevation value.

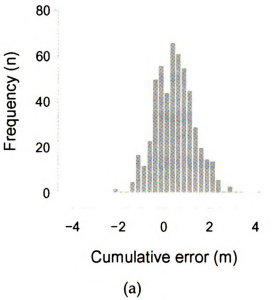


Figure 5.4: Histogram of cumulative paleoshoreline elevation errors. Error values are binned in 0.25 m intervals. Frequency scale is different than that used in Figure 5.2.

Models of differentially upwarped water planes

My data are sufficient to support reconstructions of four glacial Lake Algonquin water planes: Main, Ardtrea, Upper Orillia and Lower Orillia. The later three are known as the "Upper Group" (after Deane, 1950). Field evidence exists for several lower, and presumably younger, water planes in Ontario and the Upper Peninsula (e.g., Penetang, Cedar Point and Payette). Although I discuss the Cedar Point phase briefly, I do not have enough data to support a reconstruction or enough data to support reconstructions of any phase belonging to the "Lower Group" (after Stanley, 1936).

Water plane elevations are modeled as a random field:

$$H_{phase}(\mathbf{u}) = m_{phase}(\mathbf{u}) + \varepsilon'_{phase}(\mathbf{u}) + \varepsilon''_{phase}(\mathbf{u}), \quad \forall \mathbf{u} \in R \qquad \text{[Eq. 21]}$$

where: *phase* denotes the Main, Ardtrea, Upper Orillia or Lower Orillia water plane, $m_{phase}(\mathbf{u})$ represents the expected elevation trend of that plane; $\varepsilon'_{phase}(\mathbf{u})$ represents random and spatially-structured deviations from the uplift trend; and $\varepsilon''_{phase}(\mathbf{u})$ represents random and spatially unstructured errors.

It is reasonable to model upwarped water planes as random fields because each water plane can be considered in terms of the three components of a random field. As discussed previously, former water planes are differentially upwarped in a manner that elevation increases "exponentially toward the former ice centers" (Larsen, 1987: p11). The regional uplift pattern can be modeled as an elevation trend with a non-stationary mean elevation. Localized deviations from the regional trend are associated with differences among site conditions. Goldthwait (1908), for example, allowed for "five feet" (1.5 m) of discordance for "original variations in height ... due to local conditions under which [relict shoreline features - *author's inclusion*] were constructed or cut" (p.463). Alternatively, localized deviations from the general water-plane trend can be modeled as random and spatially-structured covariations. And finally, unexplained or chaotic deviations from the combination of the global trend and regional structure components can be captured by a random and spatially

unstructured error component. Chapter 2 describes short-term and cyclic influences that effect random and chaotic behavior in water-levels.

Water planes were reconstructed initially using the general spatial prediction protocol outlined by Bailey and Gatrell (1995:189-190). The protocol stipulates: a) fit a suitable trend surface model to data using ordinary least squares and obtain residuals; b) if residuals evince spatial structure, then conduct a variography and select a suitable variogram model to capture the structure; c) re-fit a suitable trend surface model to data using generalized least squares to accommodate both the spatial trend component [$m_{phase}(\mathbf{u})$]and the random and spatially structured error component [$\varepsilon'_{phase}(\mathbf{u})$]; d) examine the new set of residuals [$\varepsilon''_{phase}(\mathbf{u})$] for anomalies or any remaining spatial structure; and, if needed, e) iterate through steps b and c until stability is achieved.

Universal kriging is mathematically similar to the general spatial prediction protocol outlined above, except the set of trend parameters are estimated implicitly "and not made explicit in the results" (Bailey and Gatrell, 1995: 196). I made the modeling decision to use universal kriging during the final model run because I am most interested in the final prediction surface and, for now, less interested in the parameters that describe uplift. This decision also allowed me to take advantage of the variography and cross-validation assessment tools already available in the *geoR* (Ribeiro and Diggle, 2001) and

gstat (Pebesma, 2004) packages made for the R environment for statistical computing (R Development Core Team, 2005).

Isaaks and Srivastava (1989) and Bailey and Gatrell (1995) suggest using cross-validation to assess spatial prediction models for dangerous warning signs before proceeding onto a final model run. Bailey and Gatrell provide a concise summary:

> "Each sample point ... is deleted in turn and its value predicted from the rest of the data, using the chosen variogram model and the chosen form of the trend component. This results in an observed set of n prediction errors between the predicted and true values at each sample site. These prediction errors can then be studied in order to evaluate the overall prediction process and possibly identify necessary adjustments to either the variogram model or the form of the trend." (Bailey and Gatrell, 1995: 191)

I employed cross-validated universal kriging to get a sense of how well (or poorly) each ad-hoc combination of trend, spatial structure, and aspatial noise components behaved. I examined cross-validated residuals for large errors, bias and any remaining spatial structure. If I found such evidence, then I would review data for any misclassified features and return to the spatial prediction protocol. According to Isaaks and Srivastava (1989), cross-validation provides a valuable "dress rehearsal" (p533) for a final model run because it can

identify poor model performance. They warn, however, that cross-validation does not guarantee best model performance and should be used cautiously when adjusting a variogram model. In this work, if a dress rehearsal did not reveal dangerous warning signs, then I proceeded to a final run and reconstructed the differentially warped water plane via universal kriging. I report only the set of final water plane models.

A note about coordinate transformation

Before reporting my final water plane models, however, I note that all coordinate values were transformed from the Michigan GEOREF planar coordinate system to a local coordinate system. Coordinate transformation involved rescaling from the meter to the kilometer unit of measure, and translating the origin from outside the State of Michigan to a location at Traverse City, Michigan. I rescaled coordinate values after building an initial set of models and obtaining unstable results (not reported). Although my initial models seemed reasonable at first, I found they suffered from rounding errors created by computer word overflows (Burrough and McDonnell, 1998: see Box 9.2 on page 228) - especially when coordinate values were raised to powers greater than 1 during trend surface analysis. Translation of the origin to Traverse City, MI serves two purposes. First, it reduces further the magnitudes of values needed to represent bluff locations and, so, further mitigates problems associated with computer word overflows. And second, it places the origin inside the study

area, which allows the intercept term of each trend surface model to serve as a useful, rather than useless, estimate of water plane elevation. Locations in Traverse City were not sampled during this work, so placing a false origin there conveniently allows water plane elevations to be predicted at the site.

Main phase

The spatial distribution of Main water plane elevations is modeled as a random field $\{H_{main}(\mathbf{u}_i), \mathbf{u}_i \in R\}$, which is a set of spatially-structured random variables $\{H_{main}(\mathbf{u}_i), i = 1,...,N\}$ each defined at the center of one of N grid cells in the region of interest R. The set of sampled paleoshoreline elevations associated with the Main phase of glacial Lake Algonquin $\{h_{main}(\mathbf{u}_a), a = 1,...,n\}$ is considered one possible realization of n corresponding random variables. The set of 59 samples I assembled $\{h_{main}(\mathbf{u}_a), a = 1,...,59\}$ is considered a joint realization of 59 corresponding random variables.

Polynomial trend surface models were fit to elevation data via ordinary least squares (OLS) to capture the expected northeastward trend $m_{main}(\mathbf{u})$. Trend models were checked for goodness of fit and overall significance. Parameter coefficients were tested for significance, and outliers and observations that might have unduly leveraged results were removed. Ultimately, a reduced second-order polynomial provided the best statistical fit (Table 5.1). Coefficients of the y^2 and interaction (x*y) parameters are both positive in sign and support

the expectation that water plane elevations increase toward the northeast. A summary of residuals is listed in Table 5.2.

OLS residuals are generally small and well-behaved (e.g., non-normality was not evident, they were not correlated with predicted values or independent variables), but they exhibit spatial structure (maps used for rummaging through these data are not shown).

Table 5.1: Main phase trend parameters estimated via ordinary least squares.

OLS	Estimate	Standard error	Probability
Intercept	212.3	1.3	< 0.0001
x_{km}	-0.2405	0.0260	< 0.0001
x_{km}* y_{km}	0.001838	0.0001	< 0.0001
x_{km}^2	0.001213	0.0001	< 0.0001
y_{km}^2	0.001743	< 0.0001	< 0.0001
		Adjusted R^2	0.9930
		F-statistic	1973
		p-value	< 0.0001
		Residual standard error	2.01 m

Table 5.2: Summary of Main surface residuals obtained via ordinary least squares (OLS), cross-validated universal kriging with a nugget model only (CV.NUG), and cross-validated universal kriging with a Matern model of spatial structure (CV.MAT).

Residuals	OLS	CV.NUG	CV.MAT
minimum	-3.66 m	-4.17 m	-3.14 m
median	-0.18 m	0.19 m	-0.26 m
mean (bias)	0.00 m	0.04 m	0.00 m
RMSE	1.92 m	2.12 m	1.66 m
maximum	4.54 m	4.77 m	3.43 m

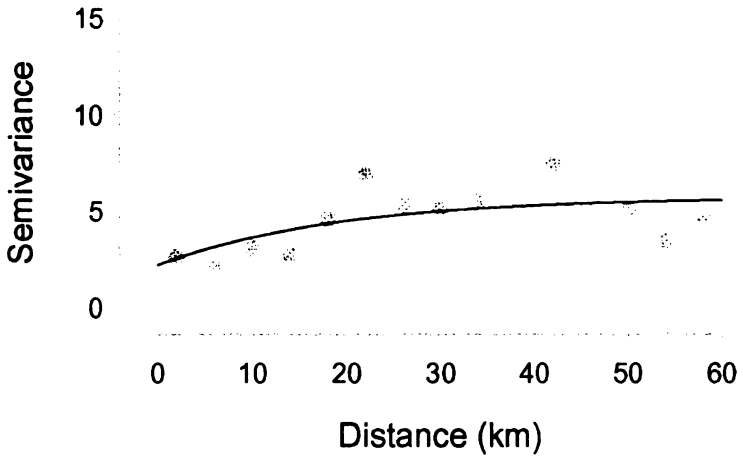
A variography revealed an anisotropic association between semi-variance and distance.[2] The strongest spatial correlation structure occurs along an azimuth of 20 degrees (Figure 5.5a). No spatial structure is apparent along an azimuth of 110 degrees (Figure 5.5b). Not incidentally, the axis of strongest spatial structure coincides with the general direction of glacial retreat (N15°E, after Futyma, 1981). Such a coincidence might suggest the trend model does not capture the uplift trend completely. Yet, semi-variance along this axis does not increase monotonically with distance, which suggests a localized process, and not a global process, is acting. Semi-variance values reach a sill between the 20 and 30 km lags, beyond which no spatial structure is apparent. The ad-hoc division of large-scale trend, smaller-scaled spatial structure, and aspatial noise, seems reasonable, so I moved forward.

I did not fit a trend to data via generalized least squares because I could not build a suitable anisotropic covariance matrix. Instead, I relied on the cross validation tools available in the *gstat* package, which can accommodate anisotropic spatial structures. I assessed two water plane models via cross-validated universal kriging. The first employed the global trend and an aspatial

---

[2] All semi-variograms were calculated using 4 km lags, or bins, and constrained to a minimum of 6 pairs of observations in each lag. Directional variograms were calculated using a 45-degree tolerance angle. Efforts to assess semi-variance at distances shorter than 4 km proved futile because I could not capture sufficient numbers of paired observations in every lag or obtain interpretable results.

noise component (pure nugget). The other employed the global trend, an anisotropic variogram model of spatial structure and an aspatial noise component (Figure 5.5). Comparing sets of residuals generated by these two universal kriging models allowed me to asses whether or not the anisotropic spatial component served to better the prediction process.



n: 59

Model: Matern

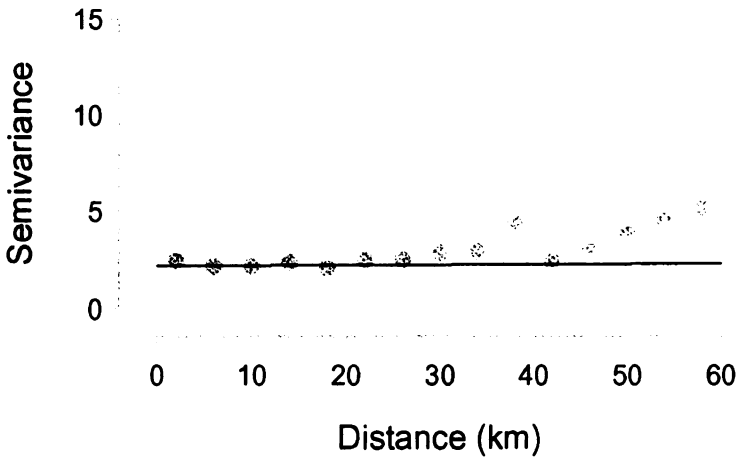
Sill: 3.5 m^2

Range: 19 km

Kappa: 0.5

Nugget: 2.2

a) 20 degrees azimuth



n: 59

Model: Pure nugget

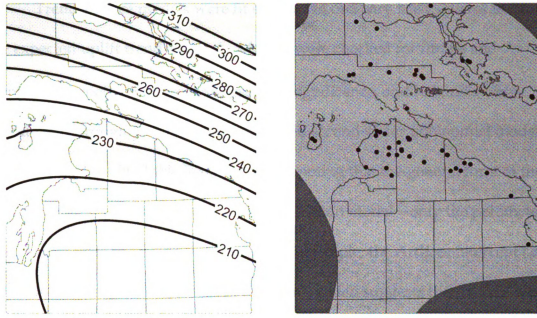
Nugget: 2.2

b) 110 degrees azimuth

Figure 5.5: Empirical variograms of Main trend surface residuals generated via ordinary least squares. Solid lines represent fitted variogram models.

Neither kriging model generated residuals that evince bias, extreme values, or warning signs that suggests the trend model should be refined further. The model that employed only the aspatial noise component generated the largest residuals. The model that employed both anisotropic covariance and aspatial noise components performed best and generated residuals smaller than those generated via OLS, which suggests the model compensated for missing data and offers good predictive ability.

I reconstructed the final Main glacial Lake Algonquin water plane via universal kriging using the anisotropic variogram model described above. Figure 5.6a shows the final prediction surface, which illustrates the uplift trend toward the former center of ice loading. Figure 5.6b shows the surface of confidence intervals (at the 95% confidence level) about the predictions. The spatial pattern of uncertainty reflects the distribution of available data for confidence intervals tend to increase with distance from sampled locations. Note, there are no data to support the curve expressed by the 210 m contour line.



(a) Predicted elevations (b) Uncertainty in the predictions

Figure 5.6: The Main Lake Algonquin water plane: a) predicted elevations are contoured with a 10-meter interval; and b) greater uncertainties are expressed with darker gray tones. Sample sites are shown as black dots.

Ardtrea phase

The spatial distribution of Ardtrea water plane elevations is modeled as a random field $\{H_{ard}(\mathbf{u}_i), \mathbf{u}_i \in R\}$, which is a set of spatially-structured random variables $\{H_{ard}(\mathbf{u}_i), i = 1,...,N\}$ each defined at the center of one of N grid cells in the region of interest R. The set of paleoshoreline elevations associated with the Ardtrea phase of glacial Lake Algonquin $\{h_{ard}(\mathbf{u}_a), a = 1,...,n\}$ is considered one possible joint realization of n corresponding random variables. The set of 41 samples I assembled $\{h_{ard}(\mathbf{u}_a), a = 1,...,41\}$ is considered a joint realization of 41 corresponding random variables.

Trend surface models were fit to data via ordinary least squares to capture the expected uplift trend $m_{ard}(\mathbf{u})$. Models were checked for fitness and significance, coefficients were assessed for significance, and residuals were examined thoroughly. Ultimately, a reduced second-order polynomial model provided the best fit (Table 5.3). It is worth noting that the general form of the Ardtrea model is the same as the form of the Main model - only the parameters that specify rates of uplift are different. For example, the Ardtrea intercept (208.3 m) is lower than the Main intercept (212.3 m), which suggests the Ardtrea water plane is below the Main water plane at Traverse City. Also, each rate of uplift in the Ardtrea trend model is less than its respective counterpart in the Main trend model, which indicates the Ardtrea water plane is warped less than the Main plane. A summary of residuals is listed in Table 5.4. OLS residuals are small and well behaved (e.g., non-normality is not evident, they are not correlated with either sets of predicted values or independent variables), and they evince no spatial structure (maps used for rummaging through these data are not shown). I conducted a variography to explore the spatial structure of OLS residuals (e.g., Figure 5.7), but found none.

I calculated an inter-distance matrix and used a pure nugget variogram model to convert it into a covariance matrix. The trend surface model was then re-fit to data via generalized least squares; the inverse of the covariance matrix was used as a spatial weights matrix. Model parameters are organized in Table 5.3 and a summary of residuals is given in Table 5.4. As expected, the

generalized model provides a fit identical to the ordinary model. The pure nugget component does not alter the overall fit or significance of the model; rather, it inflates the standard error associated with each parameter estimate. Nevertheless, all coefficients remain significant at the 95% confidence level.

Table 5.3: Ardtrea phase trend parameters estimated via ordinary least squares (OLS), and generalized least squares (GLS).

OLS	Estimate	Standard error	Probability
Intercept	208.3	0.9	< 0.0001
x_{km}	-0.2008	0.0201	< 0.0001
x_{km}* y_{km}	0.001645	< 0.0001	< 0.0001
x_{km}^2	0.001026	< 0.0001	< 0.0001
y_{km}^2	0.001667	< 0.0001	< 0.0001
		Adjusted R^2	0.9961
		F-statistic	2547
		p-value	< 0.0001
		Residual standard error	1.42 m

GLS	Estimate	Standard error	Probability
Intercept	208.3	1.3	< 0.0001
x_{km}	-0.2008	0.0273	< 0.0001
x_{km}* y_{km}	0.001645	0.0001	< 0.0001
x_{km}^2	0.001026	0.0001	< 0.0001
y_{km}^2	0.001667	< 0.0001	< 0.0001
		Adjusted R^2	0.9961
		F-statistic	2547
		p-value	< 0.0001
		Residual standard error	1.42 m

Table 5.4: Summary statistics for residuals (n=41) obtained from Ardtrea water plane models predicted via ordinary least squares (OLS), generalized least squares (GLS), and cross-validated universal kriging (CV.NUG).

Residuals	OLS	GLS	CV.NUG
minimum	-2.73 m	-2.73 m	-2.96 m
median	0.03 m	0.03 m	0.04 m
mean (bias)	0.00 m	0.00 m	-0.01 m
RMSE	1.33 m	1.33 m	1.55 m
maximum	2.82 m	2.82 m	3.35 m

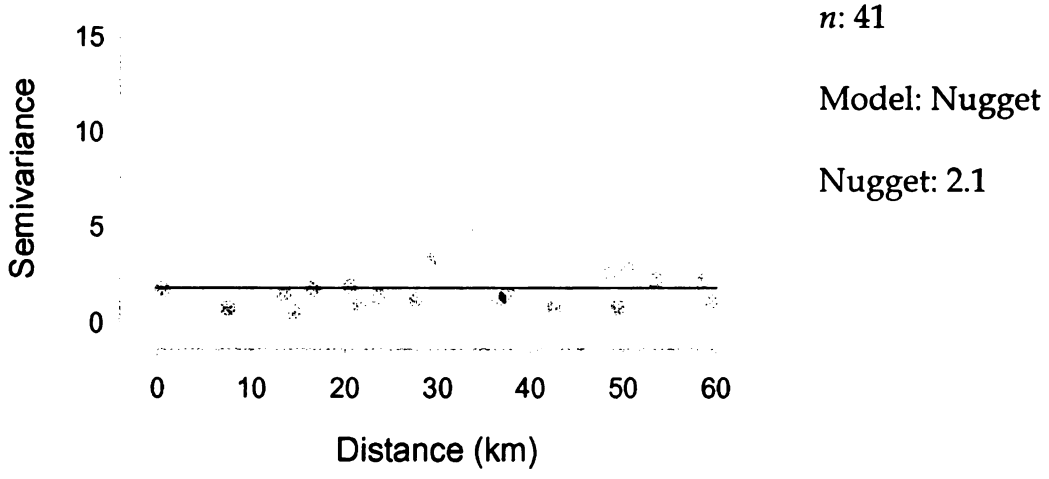
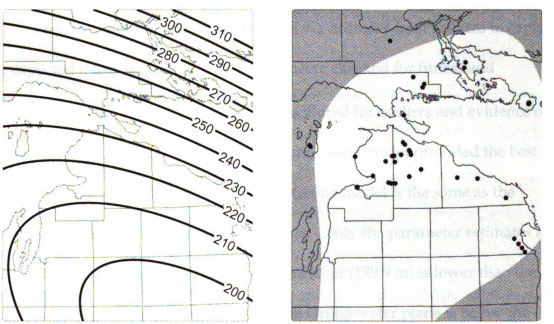


Figure 5.7: Empirical variogram model fitted to the spatial structure of Ardtrea water plane residuals generated during ordinary least squares.

The Ardtrea model was assessed via cross-validated universal kriging, which generated a set of residuals with characteristics similar to those generated via least squares, albeit with a larger range. Cross-validated residuals do not evince bias, extreme values, spatial structure or any warning sign that might suggest either the trend component or the noise component should be refined further. The average magnitude of error (RMSE = 1.55 m) is small. So, I accepted the ad-hoc division of trend and aspatial noise and moved forward.

I reconstructed the Ardtrea water plane from paleoshoreline data via universal kriging and included a pure nugget model of aspatial noise. Figure 5.8a shows the final prediction surface, which illustrates the uplift trend toward the northeast. Figure 5.8b shows the surface of confidence intervals (at the 95% confidence level) about the predictions. The spatial pattern of uncertainty reflects the distribution of available data for confidence intervals tend to increase with distance from sampled locations. Locations in the southwestern portion of the study area suffer the greatest uncertainties because they are situated farthest from data.



(a) Predicted elevations (b) Uncertainty in the predictions

Figure 5.8: The Ardtrea phase water plane: a) predicted elevations are contoured with a 10-meter interval; and b) greater uncertainties are expressed with darker gray tones. Sample sites are shown as black dots.

Upper Orillia phase

The spatial distribution of Upper Orillia water plane elevations is modeled by a random field $\{H_{ori}(\mathbf{u}_i), \mathbf{u}_i \in R\}$, which is a set of spatially-structured random variables $\{H_{ori}(\mathbf{u}_i), i = 1,..., N\}$ each defined at the center of one of N grid cells in the region of interest R. The set of paleoshoreline elevations associated with the Upper Orillia phase of glacial Lake Algonquin $\{h_{ori}(\mathbf{u}_a), a = 1,..., n\}$ is considered one possible joint realization of n corresponding random variables. The specific set of 33 samples I collected $\{h_{ori}(\mathbf{u}_a), a = 1,...,33\}$ is considered a joint realization of 33 corresponding random variables.

Trend surface models were fit to data via ordinary least squares to capture the expected trend $m_{ori}(\mathbf{u})$. Trend models were checked for fitness and statistical significance, and residuals were explored for outliers and evidence of undue leverage. Ultimately, a reduced second-order model provided the best fit (Table 5.5). The general form of the Upper Orillia model is the same as the general form of the Main and Ardtrea models - only the parameter estimates are different. For example, the Upper Orillia intercept (199.9 m) is lower than the Main intercept (208.3 m), which suggests the Orillia water plane is below the Ardtrea water plane at Traverse City. Also, each rate of uplift in the Orillia trend model is less than its respective counterpart in the Ardtrea trend model, which

indicates the Upper Orillia water plane is warped less than the Ardtrea (and hence Main) water plane. A summary of residuals is listed in Table 5.6.

OLS residuals behaved well (e.g., non-normality not evident, not correlated with either sets of predicted values or independent variables), but they exhibited spatial structure. I conducted a variography to explore the apparent autocorrelation, which exposed a substantial anisotropic spatial structure. And, unlike the variograms calculated for the Main and Ardtrea residuals, these reveal a lot of scatter. After iteration, reasonable variogram models were fit by eye (Figure 5.9).

I did not fit a trend surface model to data via generalized least squares because I could not build a suitable anisotropic covariance matrix for use in a generalized linear model. Again, I relied on the tools available in the *gstat* package, which can accommodate such anisotropic structures. I assessed two water plane models via cross-validated universal kriging. The first employed the global trend and an aspatial noise component (pure nugget). The other employed the global trend, an anisotropic spatial component, and an aspatial noise component. Comparing sets of residuals generated by these two universal kriging models allowed me to asses whether or not the anisotropic spatial component served to better the prediction process.

Table 5.5: Upper Orillia phase trend parameters estimated via ordinary least squares.

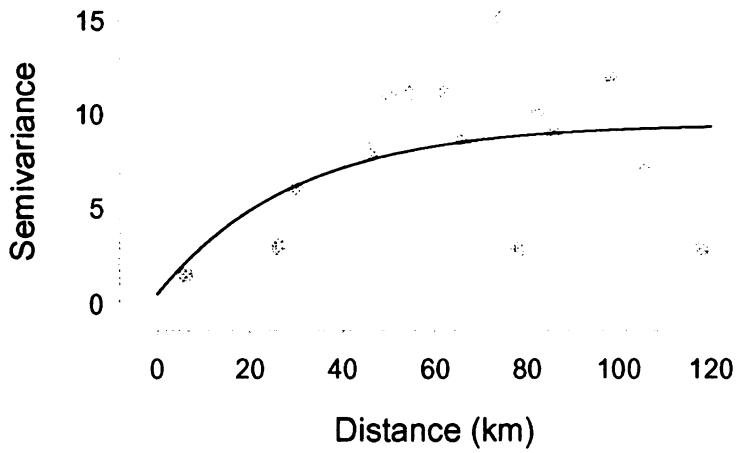
OLS	Estimate	Standard error	Probability
Intercept	199.9	1.5	< 0.0001
x_{km}	-0.1442	0.0412	0.0002
x_{km}* y_{km}	0.001433	0.0009	< 0.0001
x_{km}^2	0.000917	0.0002	0.0001
y_{km}^2	0.001623	< 0.0001	< 0.0001
		Adjusted R^2	0.9900
		F-statistic	793.4
		p-value	< 0.0001
		Residual standard error	2.69 m

Table 5.6: Summary statistics for residuals (n=33) obtained from Upper Orillia elevation trend models obtained via ordinary least squares (OLS), cross-validated universal kriging with pure nugget model (CV.NUG) and cross-validated universal kriging with anisotropic covariance model (CV.MAT).

Residuals	OLS	CV.NUG	CV.MAT
minimum	-4.76 m	-5.07 m	-3.81 m
median	0.34 m	0.42 m	0.54 m
mean (bias)	0.00 m	0.09 m	0.11 m
RMSE	2.48 m	2.95 m	1.88 m
maximum	4.50 m	6.01 m	4.28 m

Neither universal kriging model generated residuals that evince bias, extreme values, or other warning signs that suggests the trend model should be refined further. The model that employed only an aspatial noise component generated the largest residuals. The model that employed both anisotropic covariance and aspatial noise components, however, performed best and

generated residuals smaller than those generated via OLS, which suggests the model compensated for missing data and offers good predictive ability.



n: 33

Model: Matern

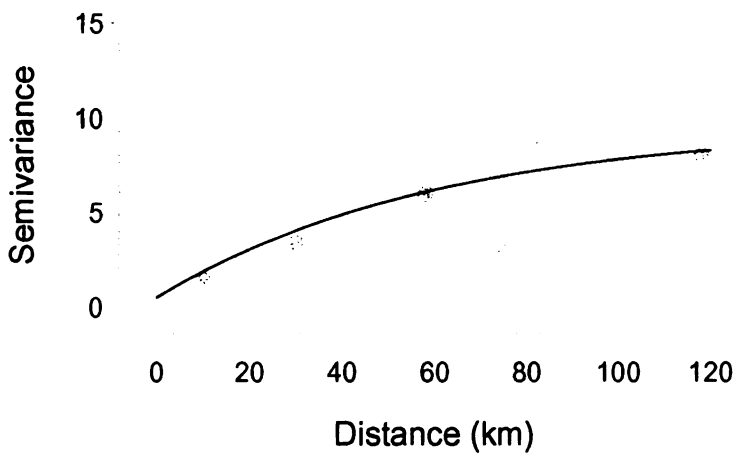
Sill: 9.5 m^2

Range: 30 km

Kappa: 0.5

Nugget: 0.5 m^2

a) 20 degrees azimuth



n: 33

Model: Matern

Sill: 9.5 m^2

Range: 60 km

Kappa: 0.5

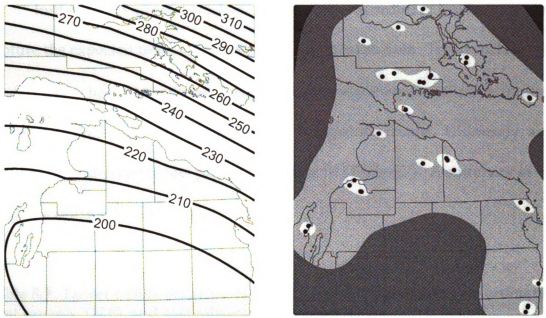
Nugget: 0.5 m^2

b) 110 degrees azimuth

Figure 5.9: Spatial structure of residuals obtained during attempts to model the Upper Orillia water plane via ordinary least squares.

I reconstructed the Upper Orillia water plane from paleoshoreline data via universal kriging using the anisotropic variogram model described above. Figure 5.10a shows the final prediction surface, which shows the expected pattern of increasing elevation toward the former center of ice loading. Figure 5.10b shows the surface of confidence intervals about the predictions (at the 95% confidence level). Again, darker tones express confidence larger intervals and, hence, greater uncertainties.

It is worth noting the Upper Orillia water plane is supported by fewer data than those that support the Main or Ardtrea water planes, but Upper Orillia data span a greater geographic extent. Perhaps that is why, of the three, the Upper Orillia model is noisiest, least precise, and subject to the greatest uncertainties. Also, possible classification errors regarding closely-spaced Upper Orillia and Lower Orillia features might play a role. Nevertheless, the Upper Orillia water plane model is the best model I can build with these data.



(a) Predicted elevations (b) Uncertainty in the predictions

Figure 5.10: The Upper Orillia phase water plane: a) predicted elevations are contoured with a 10-meter interval; and b) greater prediction uncertainties are expressed with darker gray tones. Sample sites are shown as black dots.

Lower Orillia phase

The spatial distribution of Lower Orillia water plane elevations is modeled as a random field $\{H_{low}(\mathbf{u}_i), \mathbf{u}_i \in R\}$, which is a set of spatially-structured random variables $\{H_{low}(\mathbf{u}_i), i = 1,...,N\}$ each defined at the center of one of N grid cells in the region of interest R. The set of paleoshoreline elevations associated with the Lower Orillia phase $\{h_{low}(\mathbf{u}_a), a = 1,...,n\}$ is considered one possible joint realization of n corresponding random variables. The specific set of 16 samples I assembled $\{h_{low}(\mathbf{u}_a), a = 1,...,16\}$ is considered a joint realization of 16 corresponding random variables.

Initial trend surface models were fit to data via ordinary least squares to capture the expected trend component $m_{low}(\mathbf{u})$ in these data. Trend surface models were checked for fitness and significance, significant coefficients, outliers and observations that might have unduly leveraged the results. Ultimately, a reduced second-order model provided the best fit (Table 5.7). A summary of residuals is listed in Table 5.8.

Table 5.7: Lower Orillia phase trend model parameters estimated via ordinary least squares (OLS), and generalized least squares (GLS).

OLS		Estimate	Standard error	Probability
	Intercept	194.4	0.8	< 0.0001
	x_{km}	-0.3614	0.0434	<0.0001
	$x_{km}*y_{km}$	0.001463	< 0.0001	< 0.0001
	x_{km}^2	0.002026	0.0002	< 0.0001
	y_{km}^2	0.001862	< 0.0001	< 0.0001
			Adjusted R^2	0.9979
			F-statistic	1760
			p-value	< 0.0001
			Residual standard error	1.42 m

GLS		Estimate	Standard error	Probability
	Intercept	194.4	1.0	< 0.0001
	x_{km}	-0.3614	0.0531	<0.0001
	$x_{km}*y_{km}$	0.001463	< 0.0001	< 0.0001
	x_{km}^2	0.002026	0.0003	< 0.0001
	y_{km}^2	0.001862	< 0.0001	< 0.0001
			Adjusted R^2	0.9979
			F-statistic	1760
			p-value	< 0.0001
			Residual standard error	1.42 m

Table 5.8: Summary statistics for residuals (n=16) obtained from Lower Orillia water plane models predicted via ordinary least squares (OLS), generalized least squares (GLS) and cross-validated universal kriging (CV.UK).

Residuals	OLS	GLS	CV.UK
minimum	-2.37	-2.37	-3.43
median	-0.03	-0.03	-0.05
mean (bias)	0.00	0.00	-0.01
RMSE	1.18	1.18	1.83
maximum	2.10	2.10	3.98

The initial set of OLS residuals behaved well (e.g., non-normality not evident, not correlated with either set of predicted values or independent variables), which is not surprising given that a five-term surface model was fit to 16 points. A variography revealed no pattern of spatial autocorrelation among residuals (Figure 5.11). The small number of observations made variography difficult, but a pure nugget model was fit by eye to capture the apparent noise.

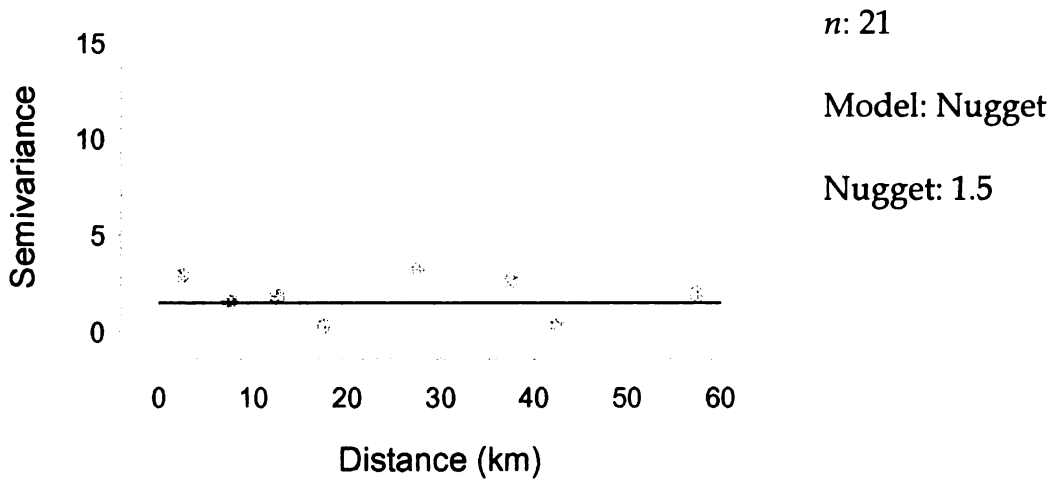
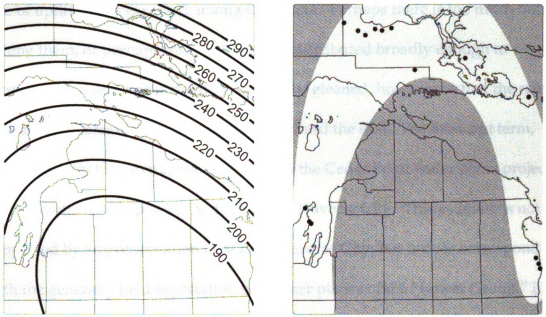


Figure 5.11: Spatial structure of OLS residuals generated during attempts to model the Lower Orillia water plane.

I calculated an inter-distance matrix and used the pure nugget variogram model to transform it into a covariance matrix. The trend surface model was then re-fit to data via generalized least squares; the inverse of the covariance matrix was used as a spatial weights matrix. Model parameters are organized in Table 5.7 and a summary of residuals is given in Table 5.8. As expected, the generalized model provides a fit identical to the ordinary model. The pure nugget component does not alter the overall fit or significance of the model; rather, it inflates the standard error associated with each parameter estimate. Nevertheless, all coefficients remain significant at the 95% confidence level.

The Lower Orillia model was assessed via cross-validated universal kriging, which generated a set of residuals with characteristics similar to those generated via least squares, albeit with a larger range. A larger range was expected given the relative paucity of data and extent they cover. Cross-validated residuals do not evince bias, extreme values, spatial structure or any other warning sign that might suggest the trend component should be refined. I accepted the ad-hoc division of trend and aspatial noise and moved forward.

I reconstructed the Lower Orillia water plane from paleoshoreline data via universal kriging and using only a pure nugget model of aspatial noise. Figure 5.12a shows the final prediction surface, which illustrates the uplift trend toward the northeast. Figure 5.12b shows a surface of uncertainty in the predictions. The spatial pattern of uncertainty reflects the distribution of available data for uncertainty increases with distance from sampled locations.



(a) Predicted elevations (b) Uncertainty in the predictions

Figure 5.12: The Lower Orillia phase water plane: a) predicted elevations are contoured with a 10-meter interval; and b) greater prediction uncertainties are expressed with darker gray tones. Sample sites are shown as black dots.

Cedar Point phase

Fourteen relict bluffs are associated with the Cedar Point water plane and all are located in the northern reaches of the study area. The number and geographic distribution of these data are insufficient to support a water plane reconstruction that covers the entire study area. Nevertheless, I was curious to explore all that these data might allow.

Trend surface models were fit to data via ordinary least squares in an attempt to capture the expected trend. Trend models and their residuals were assessed in the usual way. Ultimately, a first-order trend provided the best fit (Table 5.7). A first-order trend model cannot and does not reflect the increasing

rate of uplift that is expected among these data. Perhaps there is too much noise among them, or perhaps these data are not distributed broadly enough to capture such a non-linear trend. What can be gleaned, however, it that the rate of uplift is greater toward the north than toward the east. The intercept term, albeit a far-reaching extrapolation, suggests the Cedar Point water plane projects far below the contemporary land surface at Traverse City. This estimate is not supported by any observation at or near Traverse City, but is does correspond with the generally held expectation that water planes of the "Lower Group," like the Cedar Point water plane, represent phases in the transition from high glacial Lake Algonquin waters to the Chippewa lowstand.

Table 5.7: Cedar Point phase trend parameters estimated via ordinary least squares (OLS).

OLS	Estimate	Standard error	Probability
Intercept	47.2	6.0	< 0.0001
x_{km}	0.3879	0.0164	<0.0001
y_{km}	0.8485	0.0261	< 0.0001
		Adjusted R^2	0.9872
		F-statistic	538.8
		p-value	< 0.0001
		Residual standard error	1.57 m

Models of errors in the digital elevation model

A digital elevation model (DEM) contains errors in elevation that are results of imprecise sampling, measurement and interpolation processes (see e.g., Shortridge, 2001; Fisher, 1998; Bolstad and Stowe, 1994; Brown and Bara, 1994 and Shearer, 1990). The DEM employed in this work has suffered these as well as map projection and resampling processes that have introduced other errors. Interpolation and resampling processes are generally known to reduce variation in elevation data by trimming local extrema (Burrough and McDonnell, 1998). These effects have spatial consequences for they render an artificially smooth surface that underestimates local maxima and overestimates local minima (Diggle and Ribeiro, 2002). This kind of information suggests the distribution of DEM error should exhibit some form of spatial continuity or structure. And indeed, the DEM employed in this work exhibits spatial structure.

I continued to handle the DEM using the three subsets (i.e., Lower Peninsula, Upper Peninsula and Ontario) described in Chapter 4 because each subset exhibits different error characteristics (Table 4.6), each contains data derived from different measurement processes, and doing so facilitated computation within the memory limits of a Microsoft Windows environment. In addition, the central upland region within Michigan's Lower Peninsula was masked from analysis because the region is clearly not associated with glacial Lake Algonquin features, for the land surface rests at elevations much higher than the highest known glacial Lake Algonquin plane, and doing so reduced

further the computer memory requirements associated with manipulating the large subset.

The spatial distribution of surface elevations within the study area is modeled as a random field $\{Y(\mathbf{u}_i), \mathbf{u}_i \in R\}$, which is a set of spatially-structured random variables $\{Y(\mathbf{u}_i), i = 1,\ldots,N\}$ each defined at the center of one of N grid cells $\{\mathbf{u}_i, i = 1,\ldots,N\}$ in the region of interest R. A DEM $\{y(\mathbf{u}_i), i = 1,\ldots,N\}$ is considered one possible realization of the random field $\{Y(\mathbf{u}_i), \mathbf{u}_i \in R\}$, or one possible joint realization of N random variables $\{Y(\mathbf{u}_i), i = 1,\ldots,N\}$. Specifically, the DEM described in Chapter 4 $\{y(\mathbf{u}_a), a= 1,\ldots,25718215\}$ is considered one possible joint realization of 25,718,215 corresponding random variables.

The spatial distribution of control point elevations is modeled by a second random field $\{Z(\mathbf{u}_i), \mathbf{u}_i \in R\}$, which is a set of spatially structured random variables $\{Z(\mathbf{u}_i), i = 1,\ldots,N\}$ with each defined at the center of one of N grid cells $\{\mathbf{u}_i, i = 1,\ldots,N\}$ in the region of interest R. In general, a set of n control point elevations $\{z(\mathbf{u}_a), a = 1,\ldots,n\}$ is considered a joint realization of n random variables. Specifically, the set of 529 control point elevations described above $\{z(\mathbf{u}_a), a = 1,\ldots,529\}$ is considered one possible joint realization of 529 corresponding random variables.

The relation between these two random fields $\{Y(\mathbf{u}_i), \mathbf{u}_i \in R\}$ and $\{Z(\mathbf{u}_i), \mathbf{u}_i \in R\}$ can be expressed (following the example given by Kyriakidis et al, 1999) by:

$$Y(\mathbf{u}_i) = Z(\mathbf{u}_i) + B(\mathbf{u}_i), \qquad \forall\, \mathbf{u}_i \in R \qquad \text{[Eq. 22]}$$

where $\{B(\mathbf{u}_i), \mathbf{u}_i \in R\}$ is a third random field that is used to model the spatial distribution of error in the DEM. In this case, it is a set random variables $\{B(\mathbf{u}_i), i = 1,\ldots,N\}$ and each is defined at the center of one of N DEM grid cells $\{\mathbf{u}_i, i = 1,\ldots,N\}$ in R. In general, a set of n elevation errors estimated at control point locations $\{b(\mathbf{u}_a), a = 1,\ldots,n\}$ is considered a joint realization of n random variables. Specifically, the set of 529 error values described above $\{b(\mathbf{u}_a), a = 1,\ldots,529\}$ is considered a joint realization of 529 corresponding random variables.

The spatial distribution of DEM error $B(\mathbf{u})$ can then be expressed in terms of a random field:

$$B(\mathbf{u}) = m_B(\mathbf{u}) + \varepsilon_B'(\mathbf{u}) + \varepsilon_B'' \qquad \forall\, \mathbf{u} \in R \qquad \text{[Eq. 23]}$$

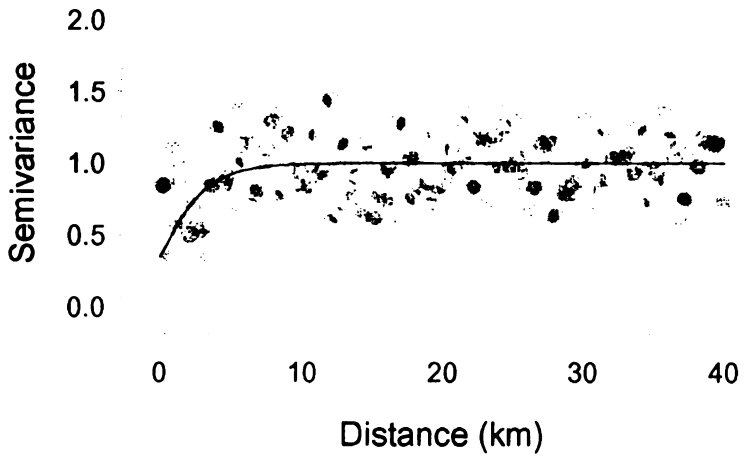
where $B(\mathbf{u})$ is the random field, $m_B(\mathbf{u})$ is the expected value or trend component, $\varepsilon_B'(\mathbf{u})$ is the random and spatially structured error component, ε_B'' is the random and spatially unstructured error component, and $\mathbf{u}$ is the set of all locations in R.

Variography

DEM errors exhibit apparent spatial structure (Figure 4.8). A semi-variogram is a measure of variability and useful for exploring spatial structure in data. Semi-variogram calculations require data that are distributed as Normal (Goovaerts, 1998). Non-normal data can be transformed to normally-distributed standard scores, analyzed, and then back-transformed when original units are required. Results of Shapiro-Wilk tests for normality indicated the distributions

of error in the Lower Peninsula and Upper Peninsula subsets do not fit a Normal distribution. So, power transformations were applied to both subsets and each was transformed again into standard normal scores. Results of a Shapiro-Wilk test for normality indicated the distribution of error in Ontario does resemble a Normal distribution, so these values were simply transformed once to standard normal scores.

Semi-variogram calculations are "unacceptable" for "distances larger than half the extent of the area" of interest (Omre, 1984:107), so I plotted my calculations accordingly. Figure 5.13 shows empirical omni-directional semi-variograms and the models I chose to capture spatial structure in each subset. I chose to fit all models from the Matern class of correlation functions (Minasny and McBratney, 2005 and Stein, 1999). Unlike the more familiar function classes found in textbooks (e.g., Gaussian, spherical, exponential or linear), the Matern class offers flexibility for fitting spatial covariance structures because it utilizes a fourth smoothing parameter (kappa) in addition to the standard sill, range and nugget parameters.



n: 348

Model: Matern

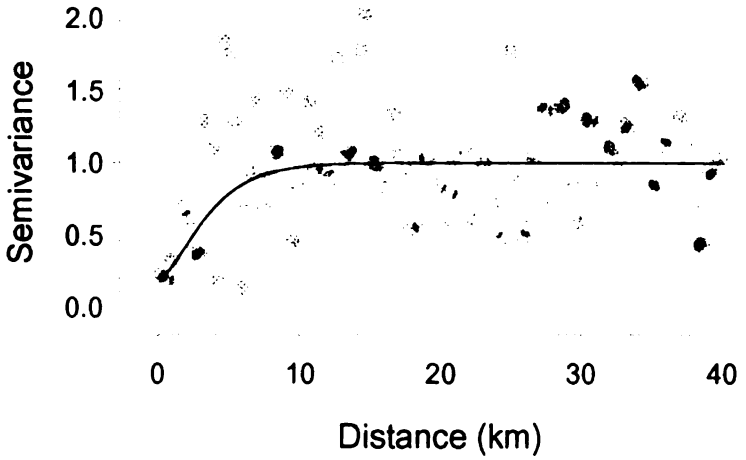
Sill: 1.00

Range: 2.0 km

Nugget: 0.35

Kappa: 0.7

(a) Lower Peninsula subset



n: 108

Model: Matern

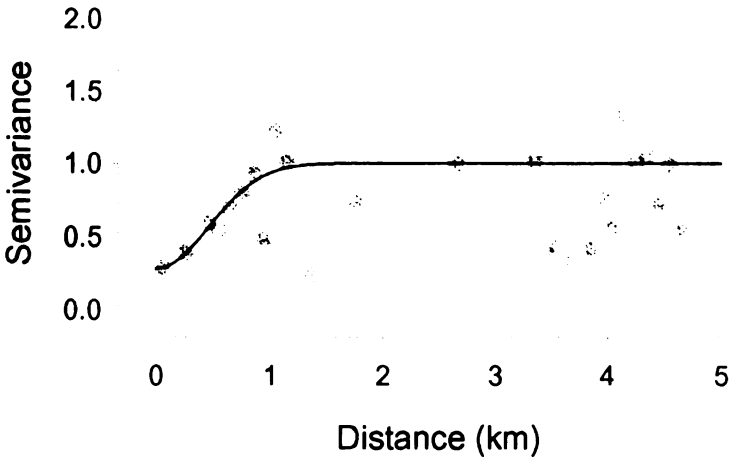
Sill: 1.00

Range: 2.0 km

Nugget: 0.20

Kappa: 1.4

(b) Upper Peninsula subset



n: 73

Model: Matern

Sill: 1.00

Range: 0.15 km

Nugget: 0.28

Kappa: 5.0

(c) Ontario subset

Figure 5.13: Empirical semi-variograms and variogram models for DEM subsets.

I calculated directional semi-variograms for each subset (not shown), but they provided no evidence of either geometric or zonal anisotropy. Moreover, directional variogram calculations yielded erratic results that were difficult to interpret consistently - especially at shorter distances, so I relied on omni-directional calculations only. Not incidentally, Isaaks and Srivastava (1989) warned that spatial continuity analysis is "very frustrating, sometimes seemingly hopeless" (p140), rarely straightforward and can often require several iterations. I am satisfied with my results, but found no reason to believe Isaaks and Srivastava's were crying "wolf."

A semi-variogram of errors in the Lower Peninsula region (Figure 5.13a), which is supported by a relatively large number of observations (n = 348), exhibits a pattern of decreasing correlation (increasing semi-variance) at relatively short distances (< 7 km) and no apparent correlation structure at distances greater than 10 km. A Matern variogram model (nugget = 0.35, sill = 1.0, range = 2.0 km and kappa = 0.7) was fit by eye. Efforts to better model semi-variance using small bins (< 300 m) and short distances (< 1 km) proved futile because I could not capture sufficient numbers of paired observations or obtain stable and interpretable results.

A semi-variogram of errors in the Upper Peninsula region (Figure 5.13b), which is supported by 108 observations, exhibits a pattern of increasing semi-variance at relatively short distances (< 10 km) and no apparent correlation structure at distances greater than 10 km. A single Matern variogram model

(nugget = 0.2, sill = 1.0, range = 2.0 km and kappa = 1.4) was fit by eye to capture the observed spatial structure in the region. As is obvious from Figure 5.13b, semi-variogram calculations at relatively short distances scatter rapidly and, so, are relatively difficult to model. Efforts to better model semi-variance at short distances again proved futile because I could not capture sufficient numbers of paired observations within small bins or obtain suitably stable and interpretable results. The apparent nugget effect (0.2) is, however, lower than that observed in the Lower Peninsula (0.35), probably because much of the Upper Peninsula exhibits flatter terrain.

Error observations in Ontario are relatively few (n = 73) and highly clustered, which facilitated efforts to model spatial structure among short separation distances but impeded attempts to model spatial structure among longer distances. The semi-variogram of error in the Ontario region (Figure 5.13c) exhibits a pattern of increasing semi-variance at relatively short distances (< 1 km). A single Matern variogram model (nugget = 0.28, sill = 1.0, range = 0.15 km and kappa = 5.0) was fit by eye to best capture the observed spatial structure. The large kappa parameter allowed for the best fit between model and empirical data, but required use of a range parameter (150 m) that underestimates the apparent effective range (~1 km).

Making predictions

I used the error samples and variogram models described above, and the ordinary kriging tools available in *gstat* (Pebesma, 2004), to predict error distributions and generate error surfaces for the Lower Peninsula, Upper Peninsula, and Ontario regions. I then used GIS software to build a composite surface of predicted DEM errors for the study area (Figure 5.14).

Visualizing the composite error surface can reveal differences among subsets that have been described already with prose and statistic. For example, the spatial structure among sampled errors in the Lower Peninsula subset has a lesser effective range than that which was observed among sampled errors in the Upper Peninsula. The quantitative difference is expressed visually as relatively small zones of influence around sampled benchmark locations in the Lower Peninsula and relatively large zones of influence in the Upper Peninsula. Differences among mean error values are also evident. Mean errors in the Lower Peninsula (-0.06 m) and Upper Peninsula (-0.50 m) subsets are near zero. Ordinary kriging tends toward the sample mean when predicting values at unsampled locations that are situated far from sampled locations and beyond the effective range of spatial dependence. Such predictions are symbolized in Figure 15.3 with a pale gray tone. The average magnitude of error in the Ontario subset (-1.58 m) is larger, which is why locations in Ontario that are situated far from sampled locations and beyond the modeled range of spatial dependence are shown conspicuously, in Figure 5.14, with a pinkish hue.

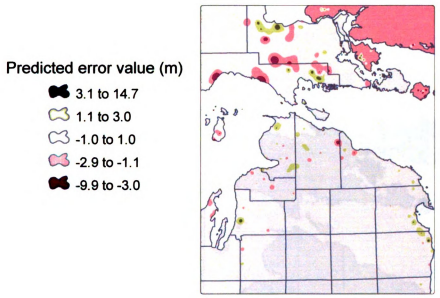


Figure 5.14: Composite surface of predicted DEM errors. The image in this dissertation is presented in color.

I built a composite surface of ordinary kriging variances, which ultimately I transformed into a surface of confidence intervals (Figure 5.15). This surface illustrates large uncertainties associated with error predictions in Ontario and lesser uncertainties in Michigan. The tightest confidence intervals are near NGS benchmark locations, where I have the best estimates of DEM error. As described in Chapter 4, relatively few benchmarks were available to assess elevations in the Ontario region, but of those that were, many revealed large errors. In sum, average DEM error magnitudes in the Michigan subsets tend to be smaller than those in the Ontario subset; more is known about the spatial structure of DEM errors in the Michigan subsets than is known for the Ontario subset; and, consequently, error predictions in the Michigan subsets are made

with greater certainty than those made at unsampled locations in the Ontario subset.

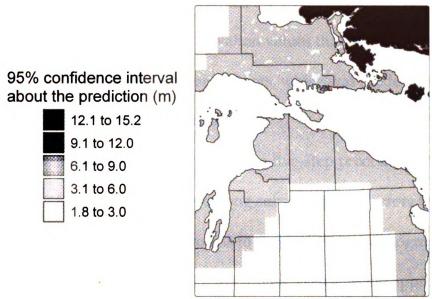


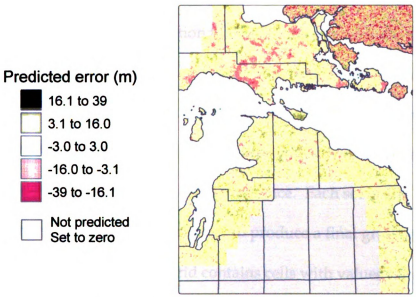
Figure 5.15: Uncertainty in the surface of predicted DEM errors. Darker tones are associated with larger confidence intervals and hence greater uncertainties. Areas shown in white were masked from analysis to facilitate computation.

Running the spatial model

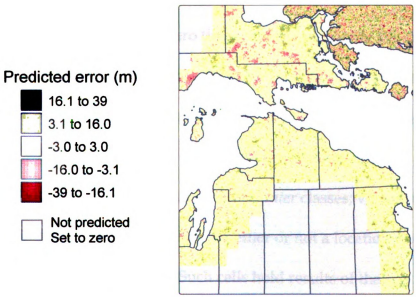
Monte Carlo simulation is a computer-intensive framework that is useful for revealing contributions of random input data errors, differences among uncertainties across a geographic region of interest (Burrough and McDonnell, 1998) and uncertainties that lurk in spatial model results. In essence, a typical simulation consists of evaluating a spatial model many times, each time using input data that have been modified randomly via a model that expresses an error distribution or makes assumptions about error behavior.

I ran my spatial model 100 times for each lake phase (i.e., Main, Ardtrea, Upper Orillia, and Lower Orillia). Specifically, I used the appropriate model of differentially-upwarped water plane elevations and one of a hundred realizations of ground surface elevations (i.e., the DEM) as inputs. Each DEM realization consisted of original DEM elevation values that were perturbed by a model of random and spatially-structured errors, which was made conditional to errors measured at NGS benchmark locations.

DEM realizations were generated using a five-step procedure. As described above, the spatial structures among subsets of DEM errors were modeled by fitting three variogram models to three empirical variograms. Second, I used errors measured at NGS benchmark locations, the appropriate variogram model and ordinary kriging to predict error distributions at every cell location within each subset. Third, I employed sequential Gaussian simulation (sGs) to draw randomly error values from each predicted distribution at every cell location within a subset. Fourth, I appended the three regional error surfaces to create a composite realization of DEM error for the entire study area. I included maps of two of one hundred error simulations (Figure 5.16) below. And fifth, I subtracted the composite error surface from the original DEM, thereby generating an alternate possible realization of the original DEM. I generated one hundred such realizations for the study area. Alternate DEM realizations are visually indistinguishable from the original DEM, so I have not included figures to show them.



a) Results of error simulation #26.



b) Results of error simulation #87.

Figure 5.16: Composite surfaces of DEM errors. Cells shown in gray were masked from analysis to facilitate computation, but later set to zero. The image in this dissertation is presented in color.

Shorelines were interpolated, in effect, by comparing spatially-coincident elevation values in each DEM realization to those along a modeled water plane. Grid cell locations with DEM elevations greater than water plane elevations were classified as *above water* (1); the balance was classified as *not above water* (0). Boundaries between cells coded with 1's and those coded with 0's represent paleoshorelines - the former land and water interface. Each set of 100 binary results was then summed using grid algebra to produce a final grid; one final grid for each lake phase. Each final grid contains cells with values ranging between 0 and 100 and each value indicates the number of times a cell was classified as *above water*. For example, a cell with a value of 0 indicates a location that was predicted to be *above water* zero times, or zero percent of the time, despite errors in the DEM. A cell with a 100 value indicates a location that was predicted to be *above water* 100 times, or 100 percent of the time, despite errors in the DEM. Cells with intermediate values express uncertainty and thus possible membership in both the *above water* and *not above water* classes; values near 50 express the greatest uncertainty regarding whether or not a location was above or not above the ancient water plane. Such cells hold results of the spatial model have been rendered uncertain by errors in input data. The set of four final grids are presented and discussed in Chapter 6.

Summary

In this chapter I described the components of a spatial model used for reconstructing five glacial Lake Algonquin water planes and interpolating each respective set of shorelines. Initial reconstructions of differentially-upwarped water planes were supported by paleoshoreline position data and parameters that describe rates of uplift were estimated via ordinary or generalized least squares. Water planes were reconstructed ultimately via universal kriging, which yielded both a surface of predicted elevations and an estimate of uncertainty at each location within the study area.

The Main, Ardtrea, Upper Orillia, and Lower Orillia water plane surfaces generated during this work (Figures 5.6a, 5.8a, 5.10a, and 5.12a) look similar to the water plane surfaces derived from paleoshoreline data by Schaetzl et al. (2002). The water plane models reported in this work, however, are superior to the water plane models presented by Schaetzl et al. (2002) in five important ways. First, each of my models is supported by more paleoshoreline data that cover larger geographic extents. Recall, the geographic distribution of the original glacial Lake Algonquin dataset was oriented roughly along the expected trend and no normal to it. New paleoshoreline data were collected along an axis normal to expected uplift trends to better capture these trends. Second, each of my models incorporates data taken from Ontario, where Lake Algonquin shorelines have long been recognized. Accordingly, bluff sites that were misclassified by Schaetzl et al. (2002) and Farrand and Drexler (1985) were

reclassified (Chapter 3) and have been integrated into the findings reported by Sly and Lewis (1969), Cowan (1985), and Karrow (1987). Third, I used a reduced second-order trend model to capture the uplift trend; all model parameters were found to be statistically significant. Schaetzl et al. (2002) used a full second-order model that retained a statistically insignificant term, which renders their model as less meaningful. Fourth, my geostatistical rebound models take into account both the broad regional uplift trend and localized deviations from that trend that likely result from differences among site conditions; Schaetzl et al. (2002) focused on the trend only. And fifth, before geostatistical analysis, I rescaled all location coordinate values from the meter to the kilometer unit of measure, and translated the planar coordinate system origin from a location outside the State of Michigan to Traverse City, Michigan to reduce coordinate magnitudes. This coordinate transformation mitigated rounding errors created during trend surface analysis and by computer word overflows (Burrough and McDonnell, 1998) - especially when coordinate values were raised to powers greater than one for use in second- or higher-order trend models. The full second-order trend surface models reported by Schaetzl et al. (2002) were surely influenced by such rounding errors and, therefore, the parameter coefficients obtained from them cannot be considered accurate. Also, my trend model coefficients express rates of uplift in m/km, which is more user-friendly than the rates they reported in m/m. In these five ways, the water plane models reported in this work are superior to the water plane models presented by Schaetzl et al. (2002).

The Lake Algonquin water plane surfaces generated during this work (Figures 5.6a, 5.8a, 5.10a, and 5.12a) also look similar to postglacial rebound surfaces derived from lake gauge data (e.g., Coordinating Committee, 1977, 2001; Tushingham, 1992; Mainville and Craymer, 2005), and others derived from a geophysical model (e.g., Tushingham and Peltier, 1991). Figure 5.17 shows a surface of uplift rates derived by Tushingham and Peltier (1991) and Figure 5.18 shows the latest surface of uplift rates created by Mainville and Craymer (2005). Like these surfaces, Lake Algonquin water planes are continuous, smooth, and show a general pattern of uplift that tends to increase in Michigan from the southwest to the northeast and towards the former centers of ice loading.

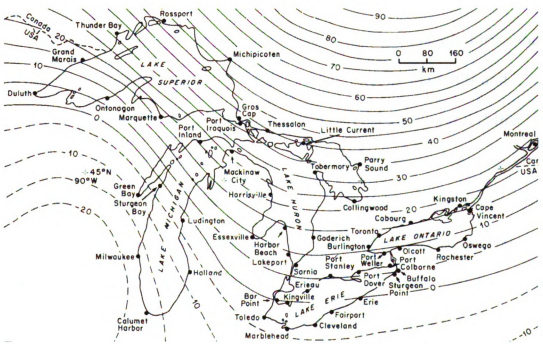


Figure 5.17: Contemporary uplift rates (cm/century) derived from the ICE-3G geophysical model (Tushingham and Peltier, 1991). Figure adapted from Tushingham (1992: 445).

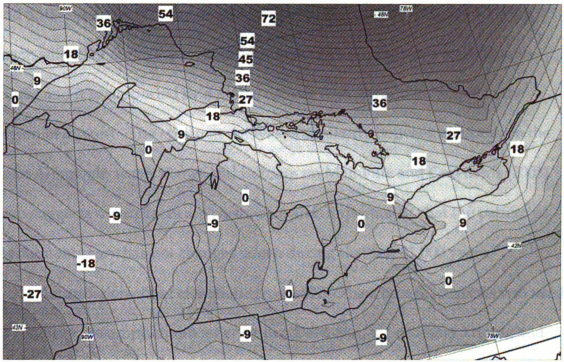


Figure 5.18: Contemporary uplift rates (cm/century) derived from historical lake gauge data. Figure adapted from Mainville and Craymer (2005: 1077).

With respect to the study area, the water plane surfaces built during this work share more similarities with the uplift surface built by Mainville and Craymer (2005) than with the uplift surface built by Tushingham and Peltier (1991). For example, as elevation contours pass through northern Michigan from east to west, they tend to bend more toward the west and less toward the north – just like the isobases depicted in Mainville and Craymer's (2005) map. The isobase pattern in Figure 5.18 is supported by 55 gauge stations and was derived via a least-squares adjustment method; it depicts a regional uplift pattern and what appear to be localized deviations from that pattern – similar to the regional and local patterns depicted in my Main and Upper Orillia surfaces (Figures 5.6

and 5.10, respectively). By comparison, the ICE-3G surface (Figure 5.17) is a much smoother surface, probably because it does not rely on a least-squares model and it is supported by a global dataset with fewer data points in the region of interest. The apparent degrees of similarity between contours on the Lake Algonquin water planes and isobases on Mainville and Craymer's (2005) map suggests my surfaces are reasonable and, importantly, that the pattern of isostatic recovery has not changed much during that last 11,000 years.

Information about elevation errors at NGS benchmark locations was used to condition assumptions about error in a DEM and, via ordinary kriging and Monte Carlo simulation techniques, generate alternate possible realizations of contemporary ground surface elevations. Finally, results of the two components (a predicted water plane and a DEM realization) were used as inputs to the spatial model. Inputs were combined to allow locations within the area of interest to be characterized as: *above water*; *not above water*; or, *possibly either* (i.e., the classification was uncertain). In sum, ancient landscapes associated with the Main, Ardtrea, Upper Orillia, and Lower Orillia phases of glacial Lake Algonquin have been digitally reconstructed. Their shorelines occur within the bands of uncertainty that exist between *above water* and *not above water* areas.

CHAPTER 6: MAPPING THE RESULTS

Introduction

This chapter summarizes results of the four shoreline interpolation models described in Chapter 5 and presents two maps for each modeled lake phase. The first indicates where ancient shorelines *probably* occurred. Shorelines are not represented by lines drawn with a constant width; rather as bands of varying widths. I refer to these bands as *bands of uncertainty* because the exact location of the former land and water interface is indeterminate given errors and uncertainties in the datasets I employed. The second map offers a similar view of the landscape as well as a fog that, ironically, reveals the spatial pattern of uncertainty associated with the reconstructed water plane. Revealing two kinds of uncertainty in maps of glacial Lake Algonquin shorelines, those associated with errors in the DEM and others associated with the spatial pattern of imprecision along the reconstructed water plane, provides the map reader with information that he or she can use to assess the quality of these results in terms of his or her intended use. I believe these maps are useful for locating shorelines and targeting areas that require additional inquiry.

Summary of results obtained from the spatial model

I used a spatial model to reclassify cells in a digital elevation model to reveal the extents of four ancient lake phases (see Chapter 5, this volume). Output cells contain values ranging from 0 to 100; each value indicates the

number of times a cell was classified as *above water*. For example, a cell with a value of 0 was predicted, despite the range of possible errors in the DEM at that location, to be *above water* zero times, or zero percent of the time. A cell with a 100 value was predicted, despite the range of possible errors in the DEM at that location, to be *above water* 100 times, or 100 percent of the time. Cells with intermediate values express uncertain memberships in the *above water* and *not above water* classes; values near 50 express the greatest uncertainty regarding whether or not a location was above the water plane because input data errors have upset the classification process.

The number of uncertain cells that separate *above water* areas from *not above water* areas varies with location. The width of each *band of uncertainty* is generally sensitive to two factors: the vertical distance between a ground surface elevation and the expected water plane elevation; and the beach slope where the ground surface and water plane intersect. The precision with which the vertical distance between an indeterminate ground surface elevation and an expected water plane elevation can be measured, however, is sensitive to the horizontal distance between a DEM grid cell and the nearest ground control point used to condition the DEM error simulation model.

I used a set of errors measured at 529 ground control points to condition a computer simulation that generated 100 alternate possible realizations of DEM error and, subsequently, 100 alternate possible realizations of the original DEM. The spatial structure of error was modeled on a regional basis by one of three

variogram models, each with a nugget parameter that specified the small amount of noisy variance expected at control point locations, a sill parameter that specified the larger amount of variance expected at locations far from control points, and other parameters that specified how covariance increases with distance. According to these models, the precision of DEM elevations tends to decrease with distance from control points because information is known about the errors that occur at control points and less is known about errors that occur at locations far from control points. The precision of measured ground elevations, in turn, directly influences the precision of vertical distances measured between expected DEM elevations and glacial Lake Algonquin water planes. As a water plane approaches the DEM it enters the tails of larger elevation distributions, which are generally situated far from control point locations and subjected to larger error distributions, sooner than it enters the tails of smaller elevation distributions, which are generally situated near control points and subjected to smaller error distributions. Consequently, DEM cell locations are typically classified with greater certainty as the horizontal distance between DEM grid cells and control points decreased.

The second factor, the beach slope at the expected shoreline, is related to shorezone morphology. As beach slope decreases, the surf zone widens and the width of the band of uncertainty tends to increase. For example, if the slope gradient is 90 degrees (e.g., waters lapping against a vertical cliff or wall), then the ground surface will, setting erosion aside, yield little landward movement of

the shoreline as water level changes. Many relict wave-cut bluffs have long and steep slopes that constrained the landward movement of water, which is one reason they are good indicators of former shorelines. As beach slope decreases toward 0 degrees (e.g., waters swashing over a flat beach), however, variations in water level (in this case, uncertainty about ground surface elevation) will force greater horizontal shoreline movements and, hence, greater uncertainty regarding the exact location of the shoreline along the horizontal plane. Low-gradient beaches do not confine variations in water level, but allow the water surface to extend landward or retreat lakeward with changes in water level (or, in this case, with uncertainty about ground surface elevations).

The range of possible interactions among beach slope and data precision might become clearer with two more examples. First, consider a neighborhood of four DEM grid cells that represents the edge of a morainic upland and is situated near a benchmark. Two cells have elevations that tower above the expected water plane and the others have elevations that rest far below, thus implying a steep slope among them. Moreover, the magnitude of error at each cell is estimated with tight precision because the benchmark is proximate and the variogram model provides good information about the amount of error in the neighborhood. The spatial model can classify these cells consistently over 100 runs because the vertical distance between each cell and the water plane can also be estimated with tight precision. Ultimately, the area of uncertainty is mapped as a very narrow band.

Consider another neighborhood of four DEM grid cells that represent an area situated in a wetland and far from any benchmark; all four cells have similar elevations that are near the water plane. The magnitude of error at each cell can be estimated with loose precision only because the nearest benchmark is situated beyond the range of observed spatial structure and the variogram model can provide no helpful information other than the variance of errors. Consequently, the spatial model is unable to classify cells in this neighborhood consistently over 100 runs given the wide range of simulated elevations at each cell. Ultimately, the entire neighborhood is mapped within a broad band of uncertainty.

Using these two examples as "straw men," it is easy to imagine spatial patterns of beach slope (from flat to steep) and data precision (from tight to loose) and how they might interact across space and differentially perturb the classification process from one grid cell to a next.

To put these uncertainties into some perspective, the amount of area (within the study area) that was submerged by each lake phase was determined under three different scenarios. Using the classification results described above, the liberal scenario involved summing the areas of cells that were not classified as *above water* at least ninety percent of the time, which should yield a relatively large estimate of submerged area. The moderate scenario involved summing the areas of cells that were not classified as *above water* at least fifty percent of the time. The conservative scenario involved summing the areas of cells that were not classified as *above water* at least ten percent of the time, which should yield

the smallest or most conservative estimate of submerged area. Percentages were calculated to express the relative amount of area in the study area that was under water during each lake phase. Today, 14,446 km^2 (31%) of the study area (46,468 km^2) is covered by contemporary Great Lakes water. Table 6.1 lists these results. As expected, the smallest submerged areas are associated with the lowest water plane (Lower Orillia). The largest submerged areas are associated with the highest water plane (Main phase), which covered nearly twice as much area as do the contemporary Great Lakes. Submerged area values increased by 300 to 500 km^2 as the selection criterion was relaxed and more cells with less certain classifications were counted. These results show that these area calculations were sensitive to the uncertainties that propagated through the spatial model.

Table 6.1: Estimates of total land area under water during each lake phase. Percentages of contemporary land area under water are indicated in parentheses.

	Estimates of area under each water plane		
	Conservative	Moderate	Liberal
Lake phase	km^2 (%)	km^2 (%)	km^2 (%)
Main	27,957 (60)	28,556 (61)	29,146 (63)
Ardtrea	27,012 (58)	27,662 (60)	28,300 (61)
Upper Orillia	25,775 (55)	26,357 (57)	27,119 (58)
Lower Orillia	24,284 (52)	24,785 (53)	25,420 (55)
Contemporary	14,466 (31)	14,466 (31)	14,466 (31)

Maps of glacial Lake Algonquin shorelines

To prepare each final grid for display, I reclassified grid cells into one of three map categories. Cells predicted to be above water fewer than 10 percent of

the time were reclassified as *probably below water* and symbolized with a light gray tone. Cells predicted to be above water more than 90 percent of the time were reclassified as *probably above water* and symbolized with a medium gray tone. Cells with intermediate values were reclassified as *uncertain* (i.e., indeterminate) and highlighted with black. Grid cells associated with the contemporary Great Lakes are symbolized with white.

I symbolized map categories using a four-tone grayscale and established a visual hierarchy to draw the map reader's attention to the shorelines. I use black to emphasize shoreline locations and white to serve as background and provide contrast. I selected the balance of gray tones to also contrast well with black and allocated them in a way that establishes land as figure and water as ground. For example, I use a medium gray tone to represent *probably above water* areas. When mapped, these homogenous-looking uplands attain figure because they are distinguishable and surrounded by shorelines (Robinson et al., 1995). Yet, the shapes of land areas during glacial Lake Algonquin times were much different than they are today; many readers might not recognize the region, or specific places within the region. So, I added contemporary county boundaries to provide a frame of reference. I used a light gray fill to ensure the political units were distinguishable from all other categories, but less distinguishable from the background and more so from objects in the foreground. Figure 6.1, 6.2, 6.3 and 6.4 illustrate the Main, Ardtrea, Upper Orillia, and Lower Orillia shorelines, respectively.

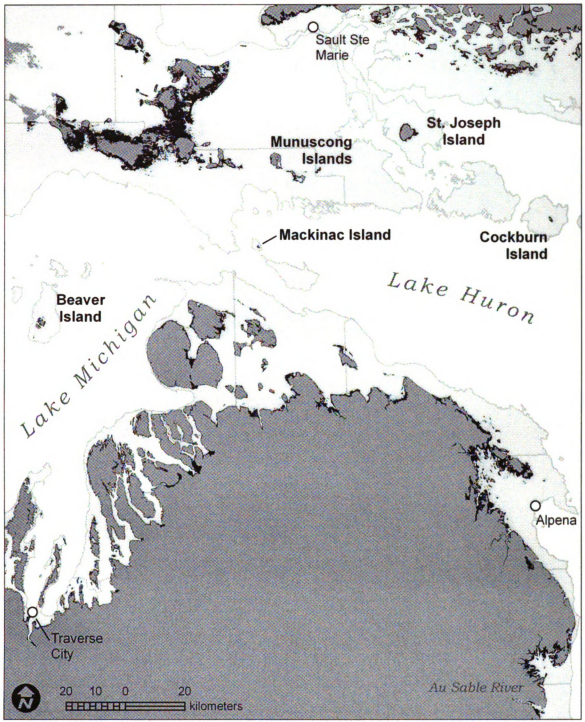


Figure 6.1: Predicted shorelines of the Main phase of glacial Lake Algonquin in the study area. Shorelines are represented as blackened areas; greater widths imply greater uncertainty about shoreline location.

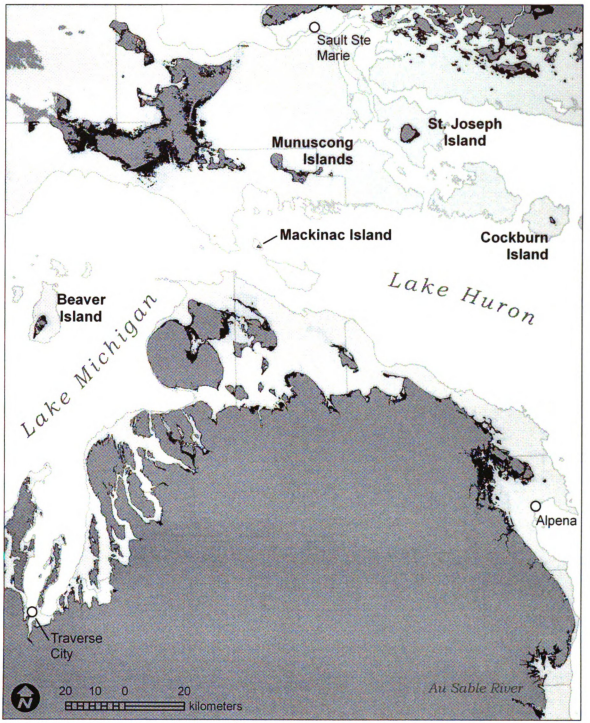


Figure 6.2: Predicted shorelines of the Ardtrea phase of glacial Lake Algonquin in the study area. Shorelines are represented as blackened areas; greater widths imply greater uncertainty about shoreline location.

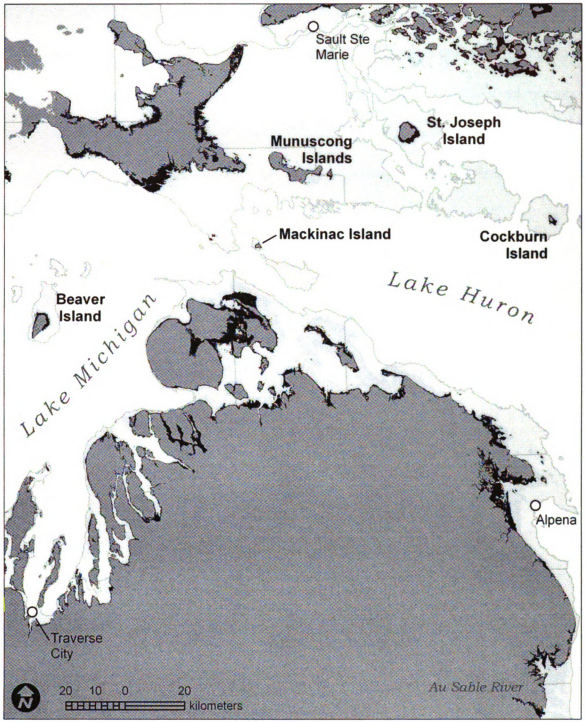


Figure 6.3: Predicted shorelines of the Upper Orillia phase of glacial Lake Algonquin in the study area. Shorelines are represented as blackened areas; greater widths imply greater uncertainty about shoreline location.

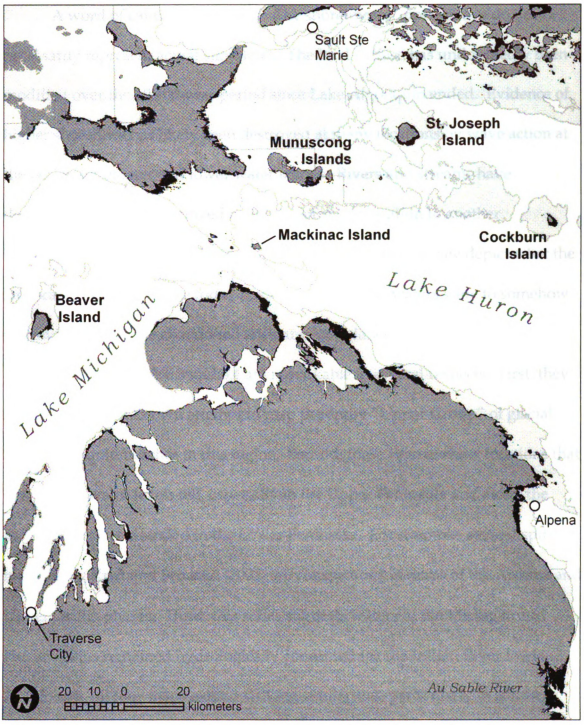


Figure 6.4: Predicted shorelines of the Lower Orillia phase of glacial Lake Algonquin in the study area. Shorelines are represented as blackened areas; greater widths imply greater uncertainty about shoreline location.

A word of caution is required. The shorelines mapped above do not necessarily represent actual shorelines. The land surface has undoubtedly been modified over the 10,400-year period since Lake Algonquin ended. Evidence of higher shorelines has likely been destroyed at many locations by wave action at the perimeter of later and lower water planes. Rivers and streams have deepened channels and moved materials form one location to another. Therefore, the best that can be said about these maps is that they depict what the landscape would look like today if contemporary lake waters were to somehow rise and reoccupy the abandoned ancient water planes.

Figures 6.1, 6.2, 6.3 and 6.4 are remarkable in several respects. First, they represent the first known attempt to map the entire "Upper Group" of glacial Lake Algonquin beaches in this region. Second, these figures show locations that emerged as water levels fell, especially in the Upper Peninsula and along the archipelago now stranded in the Lower Peninsula. For example, several spits reported by Krist and Schaetzl (2001) are conspicuous in maps of the Ardtrea and Upper Orillia phases. Third, this series suggests waters in the Michigan and Huron basins remained hydrologically connected via the Indian River lowland. And fourth, all four maps exhibit striking similarities, particularly in southern portions of the region where water plane models tend to converge.

Similarities among Figures 6.1, 6.2, 6.3, and 6.4 are greatest in areas north of Traverse City and south of Alpena, where water planes tend toward convergence. Karrow reported the Main Algonquin shoreline between

Kincardine and Port Elgin, Ontario, along the eastern shore of Lake Huron, "has been entirely removed by later shore erosion ... by lower water levels after the Main Algonquin level" (Karrow, 1987: 161). I believe the same kind of bluff removal processes have occurred north of Traverse City and south of Alpena. Consequently, I also believe it makes better sense to attribute observable shorelines in these areas to the last phase to act upon them; not the first or the highest. Therefore, I can agree with Larsen's claims that Main and Ardtrea shorelines of eastern Lake Huron predate the highest stranded shorelines in northern Lake Michigan, and the apparent "Main" shoreline of Lake Michigan "may correlate with the Orillia shoreline of Ontario" (Larsen, 1987: 21).

The Main phase

The Main phase was the highest and longest-lasting phase of the glacial Lake Algonquin sequence. I used a sample of 59 features to reconstruct the Main water plane; all but one are located north of an imaginary line connecting Alpena and Charlevoix, Michigan. Contours along the uplifted water plane (Figure 5.6a) reveal a deformation pattern of uplift and curvature that is similar to others patterns mapped by Goldthwait (1910), Schaetzl et al. (2002), and Mainville and Craymer (2005). Clarke et al. (1994) built numerical models of glacio-isostatic recovery to estimate the thickness of the ice sheet in this region. The pattern of deformation shown in Figure 5.6 is more closely aligned with the pattern of

deformation predicted via their thin ice sheet model than with the pattern predicted via their thick ice sheet model.

Figure 6.1 highlights areas over which shorelines probably occurred. Narrow bands of uncertainty (~100 to 200 m) are often associated with large bluffs, steep-gradient shorezones, and an ample supply of nearby ground control points. For example, one narrow band is situated south of Alpena and along the base of "the old lake bluff ... cut sharply into high morainic ground. For 10 miles ... the bluff is high and bold" (Leverett and Taylor, 1915: 420). US Highway 23 follows the base of this high bluff and ten NGS benchmarks situated along this stretch of road were used to condition simulations of the DEM. The combination of steep ground slope and good ground control enabled the spatial model to classify cells in the region consistently.

As expected, shorelines mapped as relatively wide bands of uncertainty (~ 1 to 2 km) are often situated in what were low-gradient shorezones and/or areas that contain few ground control points. For example, the area on the map associated with the "great sand plain west of Alpena" (Leverett and Taylor, 1915:421) is peppered with uncertainty, which implies the classification process was sensitive to errors in the digital elevation model and the relatively flat topography of the region. Only one NGS benchmark (QJ0289) provides ground control for much of this region. And, Leverett and Taylor described the area as "a wide plain of sandy gravel" that runs "for considerable distances", and claimed the exact location of the shoreline "is difficult to determine" (Leverett

and Taylor, 1915: 420). My fieldwork and these results support that claim. Nevertheless, these results offer what previous research has not - a probabilistic surface that indicates, based on the data and information available, where shorelines likely occur and where evidence of shorelines might be found.

I am always amazed by the extent of land in the Upper Peninsula that was once submerged by glacial Lake Algonquin waters. The Munuscong Islands and several morainic features were all that stood above the highest lake surface. Shorelines around the Munuscong Island complex are mapped as narrow bands of uncertainty. Much of the area northwest of the Munuscong Islands occurs at elevations at or near the water surface, and it seems the classification process was sensitive to errors in the digital elevation model and the relatively flat topography of the region. Many shorelines here are mapped as wide bands of uncertainty.

The Ontario portion of the digital elevation model suffers the largest range of error compared to the other portions that represent the Upper and Lower Peninsulas of Michigan. It also contains over-represented elevations that were likely derived from 50-foot contour lines printed on topographic maps (Chapter 4). A consequence of including oversampled contour elevations in a DEM is the fabrication of flat areas or benches in the digital model that do not exist on the real landscape. In the context of the spatial model employed in this work, artificial benches that have surface elevations close to predicted water plane elevations can negatively impact spatial model performance because such

benches would have introduced greater uncertainties into the final results. For example, a cell that holds a contour elevation that over represents actual elevation will tend to be classified as *above water* more often than it should. Conversely, a cell that holds a contour elevation that under represents actual elevation will tend to be classified as *above water* less often than it should. Paradoxically, cells with contour elevations that are over classified as *above water* will tend to be situated lakeward (down slope) of the contour line, and cells with contour elevations that are under classified as *above water* will tend to be situated landward (up slope) of the contour line! Nevertheless, it seems that the substantial relief that exists between Ontario's high bedrock uplands and low lake plains was more than enough to overcome both the artificial benching problem and the propagation of uncertainty about DEM error through the spatial model, for, surprisingly, most shorelines in the Ontario region are mapped as relatively narrow bands of uncertainty. The Ontario portion of the study area, therefore, contains many bedrock hills that might have existed as islands in Main Lake Algonquin. I use the word "might" because Karrow (1987) claims the ice sheet uncovered the area for only a brief time toward the end of the Lake Algonquin sequence.

The Ardtrea phase

Deane described the Ardtrea phase as a "brief period of quiescence", because the character of Ardtrea features in his study area was relatively weak

and indicated relatively little wave action. He also claimed the "[Main] Algonquin and Ardtrea beaches tend to converge toward the south" (Deane, 1950: 73). I used relative differences in character and elevation to distinguish 41 stranded Ardtrea features from the many higher features of Main; all but four are located north of an imaginary line connecting Alpena and Charlevoix, Michigan. Contours along the uplifted water plane (Figure 5.8a) show a deformation pattern of uplift and curvature that is similar to the pattern exhibited in Figure 5.6a. Of all the water plane models built in this work, the Ardtrea model provides the best statistical fit to data.

Figure 6.2 highlights areas over which shorelines probably occurred. Again, narrow bands of uncertainty are often associated with large bluffs, steep-gradient shorezones, and an ample supply of nearby ground control points. Shorelines mapped as relatively wide bands of uncertainty are often situated in what were once low-gradient shorezones and contain few ground control points.

Spurr and Zumberge (1956) identified relict shoreline features in Cheboygan and Emmet Counties, Michigan, that occur 5 to 8 meters below Main Algonquin. The authors interpreted them as evidence of a pre-Lake Algonquin lake. Earlier and later work, however, (Leverett and Taylor, 1915, Krist and Schaetzl, 2001, respectively) characterized the same features as belonging to spits formed in glacial Lake Algonquin. I accepted the later interpretation and correlated several bluffs in the area with the Ardtrea phase, and lower ones with

the Upper Orillia. Figure 6.2 reveals the footprints of several large features that clearly look like spits that formed at, or just beneath the Ardtrea surface.

The footprint of Leverett and Taylor's "morainic tract" (Leverett and Taylor, 1915:425) on Beaver Island is visible. And, as expected, only the northern, higher portion was consistently classified as *above water*.

Distances between successive water plane elevations are greatest in the north, which explains why so much land area in the Upper Peninsula emerged between the Main and Ardtrea phases and so little emerged in more southerly locations. For example, the Munuscong Islands coalesced into one large island while a fourth and smaller island emerged to the east. Although many Ardtrea shorelines are depicted as relatively wide bands of uncertainty in the Upper Peninsula (~2 to 4 km), they are narrower than those associated with the Main phase (~3 to 6 km).

The Upper Orillia phase

Deane characterized evidence of the Upper Orillia phase as the "most conspicuous ... between the Wyebridge and the [Main - *author's inclusion*] Algonquin" (Deane, 1950: 74). Yet, to my knowledge, the Upper Orillia phase has never been mapped. I used a sample of 33 features to reconstruct the Upper Orillia water plane, which includes a massive bluff at Cockburn Island, Ontario. The Upper Orillia water plane is supported by fewer data than supports the Main or Ardtrea water planes, and Upper Orillia data span a greater extent than

both. Perhaps that is why, of the three, the Upper Orillia water plane model is the noisiest, least precise, and subject to the greatest statistical uncertainties. Nevertheless, contours along the uplifted water plane (Figure 5.10a) show a deformation pattern of uplift and curvature that is similar to the patterns revealed in the Main and Ardtrea water planes and similar to the patterns expressed in previous research. Figure 6.3 highlights areas over which Upper Orillia shorelines probably occurred given all the information that is available.

Figure 6.3 shows many interesting features. For example, the footprints of the Riggsville Island, Owens Island, and the Ocqueoc spits (Krist and Schaetzl, 2001) are revealed quite clearly. Proto-Beaver, Cockburn and Mackinac Islands are conspicuous. And, many of the largest islands in the Lower Peninsula archipelago, via the bands of uncertainty that connect them, show signs of emergence and coalescence.

The embayment that holds contemporary Walloon Lake (Lower Peninsula near Charlevoix) is mapped as a band of uncertainty during Upper Orillia times, which suggests the ancient water plane is close to the contemporary water surface. From these results, it is reasonable to hypothesize that waters in the Walloon Lake embayment were last connected to glacial Lake Algonquin during the Upper Orillia phase. Today, the surface of Walloon Lake rests (209 m) higher than the surface of Lake Michigan (177 m).

The most interesting aspect of the predicted Upper Orillia water plane model is that it intersects the predicted Ardtrea plane at the mouth of the Au

Sable River; the two converge at 196.3 m. Convergence suggests transgression by the later lake phase. The line of intersection, or axis, should be connected to a controlling outlet. According to Larsen (1987: 7), "North of the axis the shorelines descend from the oldest to youngest, but to the south the evidence is submerged with the oldest shoreline at the bottom of the sequence." The Upper Orillia plane is supported by data at this location, but the Ardtrea plane is not.

The Lower Orillia phase

I had difficulty identifying features related to the Lower Orillia phase, just as Cowan (1985) did in his work at Sault Ste. Marie, Ontario, and Deane (1950) at Lake Simcoe, Ontario. The features I used to model the Lower Orillia water plane are few (n=16) and far between; they share little commonality other than having elevations too low to be correlated with the Upper Orillia and too high to be correlated with one of the "Lower Group" beaches. Contours along the reconstructed water plane (Figure 5.12a) show a deformation pattern of uplift and curvature that is unlike the patterns exhibited in Figures 5.6a, 5.8a, or 5.10a; the degree of warping is severe and the pattern of deformation does not resemble any previously-mapped pattern, particularly in the Lower Peninsula. Therefore, I believe these results are merely speculative, perhaps provisional in the Upper Peninsula where most of the data are located, even though the Lower Orillia water plane model is fit reasonably well to data that support it.

Figure 6.4 highlights areas over which shorelines probably occurred given available data. By comparison with the others, it reveals the continued emergence, expansion, and coalescence of upland areas in the Upper Peninsula. And, it reveals areas in the Lower Peninsula, particularly along the archipelago and the mouth of the Au Sable River, where new lands emerged.

Maps of glacial Lake Algonquin shorelines that reveal uncertainty

Figures 6.1, 6.2, 6.3, and 6.4 reveal the extents of four former lake phases in the area of interest. Shorelines widths indicate the amount of uncertainty generated by DEM errors that propagated through the spatial model. What Figures 6.1, 6.2, 6.3, and 6.4 do not reveal, however, are uncertainties about the water plane models that were used to derive these results.

Figures 6.1, 6.2, 6.3, and 6.4 were built using water plane surfaces that were fit statistically through point samples via universal kriging. These models respect the points that support them, but do not always predict well in locations removed from data. In addition to prediction surfaces, the universal kriging tools I employed allowed me to generate surfaces of mean square prediction errors, sometimes called kriging variances. Kriging variances provide the basis for deriving confidence intervals at locations where elevations values were predicted (Bailey and Gatrell, 1995). Using a specified level of confidence, 95% is typical, a single confidence interval can indicate the precision with which a single value was predicted, or stated another way, uncertainty about the prediction.

Greater uncertainty is associated with lesser precision, and vice versa. When confidence intervals are mapped over space they can reveal the spatial pattern of uncertainty in the prediction model.

A common approach to represent uncertainty in static maps is to start with Bertin's (1967/1983) visual variables and manipulate them using traditional cartographic techniques (MacEachren, 2005). MacEachren suggests using a gray fog that hovers over the mapped area and "obscures the map theme in proportion to the uncertainty in data about the theme" (MacEachren, 1995: 276). He prefers a gray fog because, according to him, grayness is associated with uncertainty: "more 'gray' equals more uncertain" (MacEachren, 1995: 441). Yet, there is little agreement in the literature about the best method of representing uncertainty, which visual variables are the best to manipulate, or how visual variables should be used. Hengl (2003), for example, manipulated color saturation to indicate relative differences in uncertainty. In his work, more white equals more uncertain; more hue equals more certain. Alternatively, Leitner and Buttenfield (2000) found variations in color value were most effective in depicting variation in uncertainty; lighter values represent greater certainty and darker values represent greater uncertainty.

I employed MacEachren's cartographic concepts of fog and *transparency* (MacEachren, 1992, 1995, 2005) to reveal the spatial pattern of uncertainty in each water plane model, but chose a black fog instead of a grey one. The fog was made completely transparent at locations associated with relatively small

confidence intervals (less than 3 m with 95% confidence), thereby revealing completely the underlying data. I reduced transparency to 33% at locations where the size of the confidence interval about the predicted water plane elevation exceeded 3 meters but was less than 6 meters. I reduced transparency to 67% at locations where the size of the confidence interval about the predicted water plane elevation exceeded 6 meters but was less than 7 meters. And, at every location where the water plane could not be predicted with better than 9 meters of precision (95% confidence), transparency was reduced to 0% to obscure the underlying results completely. In general, the opacity of the black fog of uncertainty increases with distance from sampled bluff locations at a rate determined by the geometry of sampled bluffs and covariance structure specified by the supporting variogram model.

Superposing a layer of black fog over areas already mapped in tones of gray produced unwanted visual effects. Specifically, areas mapped as *probably below water* and symbolized with a light gray tone were rendered darker at locations where the water plane elevation was not predicted precisely; these areas could not be distinguished easily from others mapped as *probably above water* with tight precision. Ultimately, I abandoned my original grayscale and employed two hues: brown to represent locations above the water plane and blue to represent locations below water. Superposing a layer of black fog over areas mapped with different color hues achieved the desired visual effect.

Figures 6.5, 6.6, 6.7, and 6.8 reveal the extents of glacial Lake Algonquin lake phases. Shorelines are again represented as black bands of varying width over which ancient shorelines *probably* occurred. Wide band widths imply greater uncertainty regarding the former location of the land and water interface; uncertainty that results from DEM errors that propagated through the spatial model. In addition, uncertainty in the water plane surface model is depicted as a black fog of apparent varying density. Areas with denser fogs imply greater uncertainties regarding the water plane predictions and typically occur in areas far from sampled locations.

Composite maps of Main Lake Algonquin and the Upper Group

I prepared one final map, without any fog, to represent all four sets of shorelines. I selected and mapped all areas that were predicted by my spatial model to be above water 90 times out of 100 runs. Figure 6.9 shows locations that stood above Main Lake Algonquin waters (dark gray), and locations that emerged during the Upper Group sequence. Locations below all water planes and above the contemporary land surface are symbolized with a light gray tone. Large areas in the Upper Peninsula and small areas in the Lower Peninsula, the sand plain near Alpena for example, exhibit the greatest change over time. I then created Figures 6.10, 6.11, 6.12, 6.13, 6.14, and 6.15 to focus attention on selected areas where field campaigns were conducted (Chapter 3). These figures can be referenced using the index map shown in Figure 3.4.

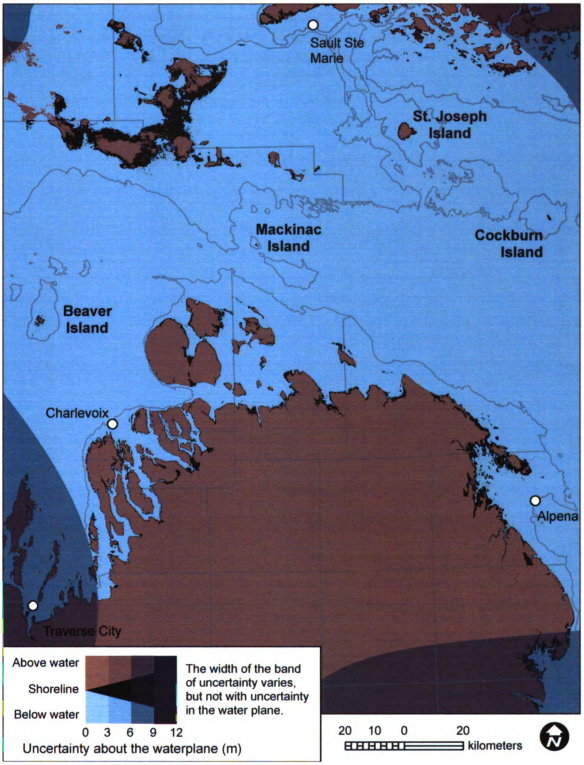


Figure 6.5: The Main phase of glacial Lake Algonquin. Darker tones indicated greater uncertainties about the predicted water plane. The image in this dissertation is presented in color.

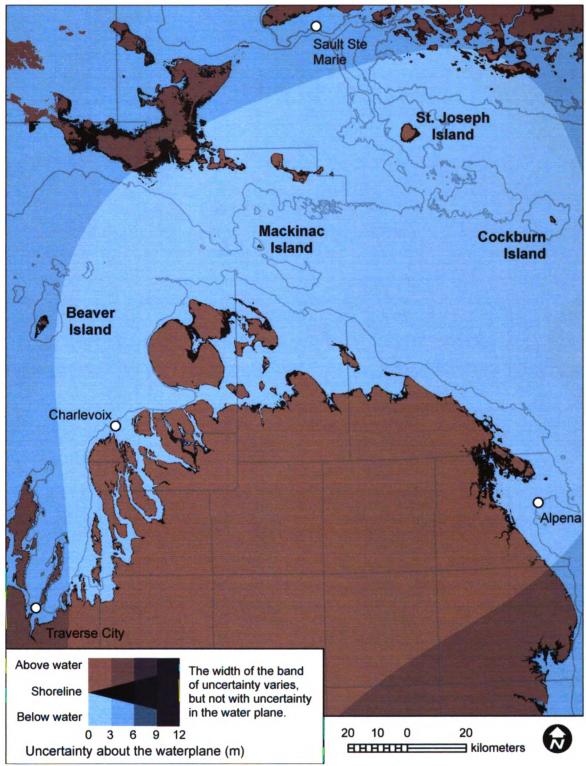


Figure 6.6: The Ardtrea phase of glacial Lake Algonquin. Darker tones indicated greater uncertainties about the predicted water plane. The image in this dissertation is presented in color.

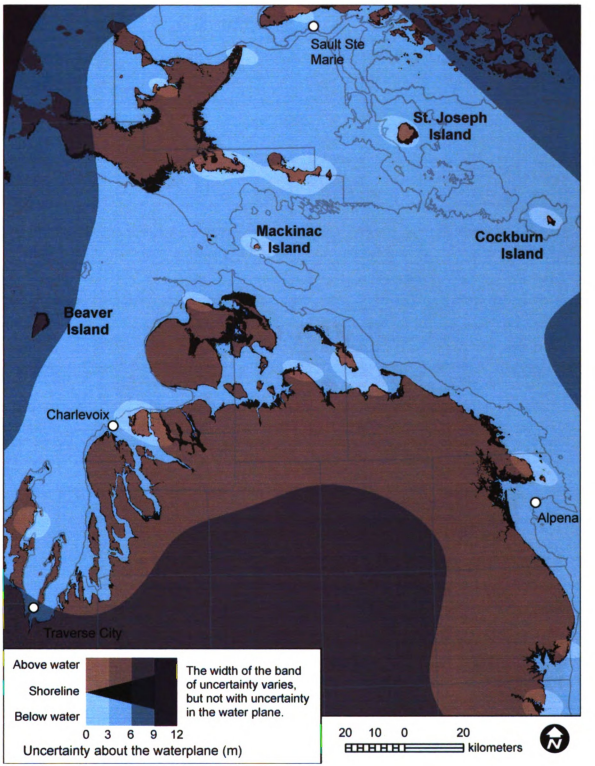


Figure 6.7: The Upper Orillia phase of glacial Lake Algonquin. Darker tones indicated greater uncertainties about the predicted water plane. The image in this dissertation is presented in color.

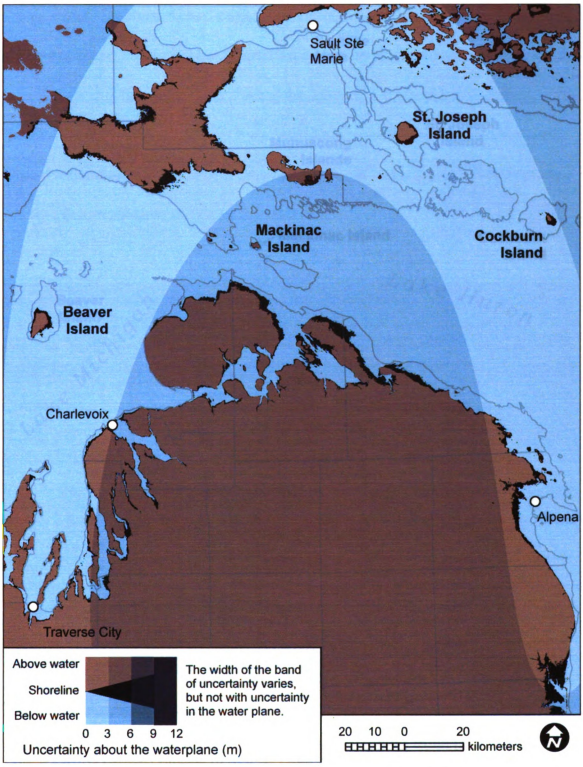


Figure 6.8: The Lower Orillia phase of glacial Lake Algonquin. Darker tones indicated greater uncertainties about the predicted water plane. The image in this dissertation is presented in color.

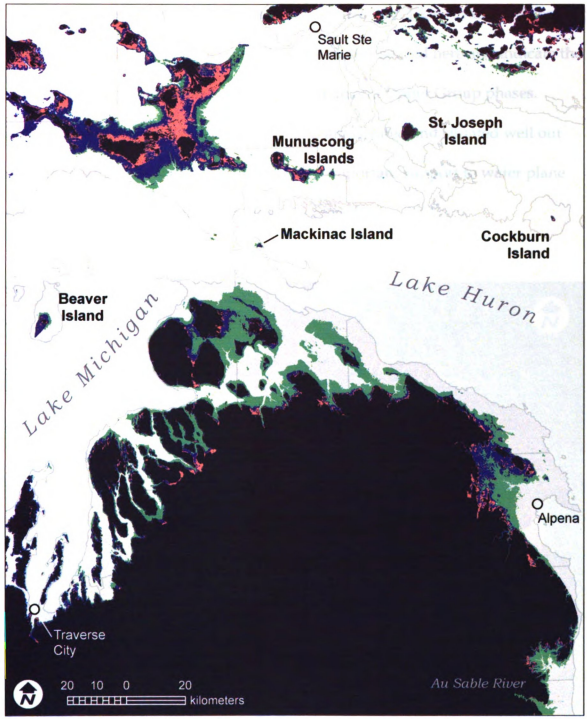


Figure 6.9: The Main (dark gray), Ardtrea (pink), Upper Orillia (purple), and Lower Orillia (green) phases of glacial Lake Algonquin. The image in this dissertation is presented in color.

Proto-Cockburn Island began as an islet less than 1 km^2 in size (Figure 6.10). Main and Upper Group shorelines are closely spaced here and indicate the island grew only slightly larger during the Main and Upper Group phases. Relict shoreline features on Cockburn Island are isolated and situated well out from the mainland. These features provided important support to water plane reconstructions in this portion of the study area.

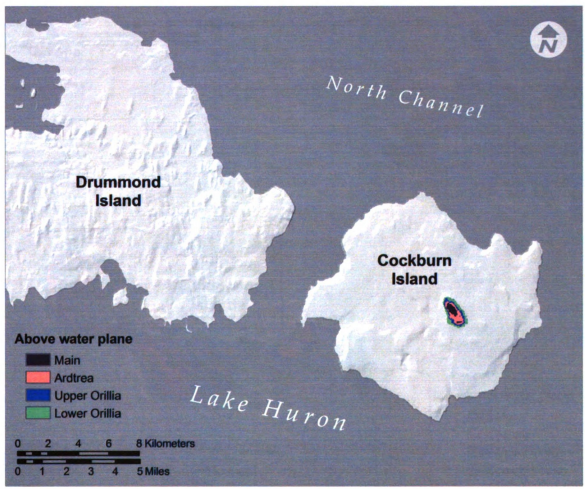


Figure 6.10: Areas on Cockburn Island that were predicted to be above glacial Lake Algonquin water levels. The extent of this figure corresponds with the extent of Figure 3.5. The image in this dissertation is in color.

Figure 6.11 shows the Munuscong Islands region. Four small islands appear to have emerged and coalesced through the Main and Upper Group sequence. Also, two new islands emerged to the east as lake levels fell. The irregular outline of the islands that Taylor (1895) first described is clear to see as is the "sweep of low ground" between the islands and Hessel that "has the appearance of a recently deserted lake bottom" (Taylor, 1985: 26).

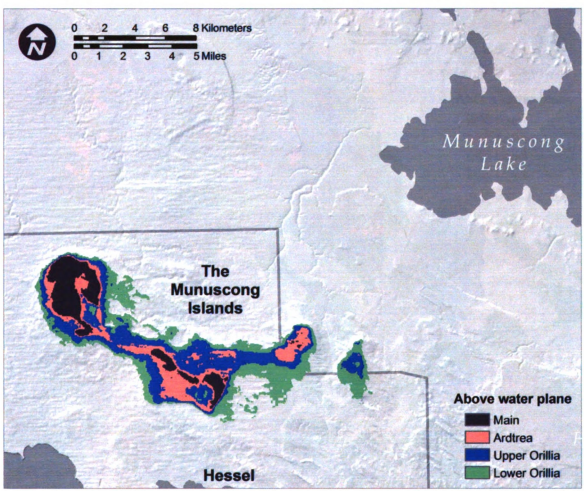


Figure 6.11: Areas in the Munuscong Island region that were predicted to be above glacial Lake Algonquin water levels. The extent of this figure corresponds with the extent of Figure 3.11. The image in this dissertation is in color.

Figure 6.12 highlights the Douglas Lake area. Old shorelines were abandoned, new lands emerged, and new shorelines were cut as water levels fell. The Riggsville Island spit that Krist and Schaetzl (2001) described is evident in the north-central portion of the figure. Main, Ardtrea, and Upper Orillia shorelines tend to be closely spaced, which suggests Upper Orillia waters were the last to erode many shorelines in this area.

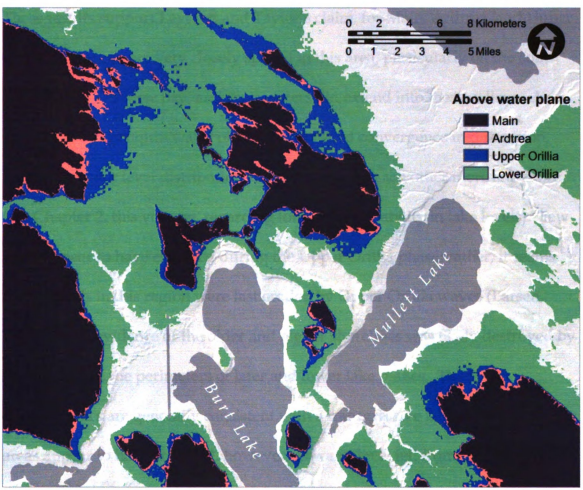


Figure 6.12: Areas in the Douglas Lake area that were predicted to be above glacial Lake Algonquin water levels. This extent of this figure corresponds with the extent of Figure 3.13. The image in this dissertation is presented in color.

The terrain near Charlevoix, Michigan, (Figure 6.13) is complex and relatively difficult to interpret. Recall, Little Traverse Bay served as an outlet for glacial Lake Chicago as water passed into the Indian River Lowlands and drained into the Huron basin (Hansel et al., 1985). Leverett and Taylor (1915:426) speculated glacial Lake Algonquin "probably" extended up these valleys and left "distinct shorelines around Pine Lake" (now called Lake Charlevoix) that "mark the highest Algonquin beach and some lower members of the upper group." These results support Leverett and Taylor's claim, for Main, Ardtrea, and Upper Group shorelines are very closely spaced in this area, particularly on the south side of Little Traverse Bay, and their waters did extend into these valleys. As glacial Lake Algonquin water planes tend toward convergence in this region, long-term water level distributions begin to overlap each other more and more (see Chapter 2, this volume, regarding long-term variability in lake levels). Few areas appear to have emerged during the Upper Orillia phase; rather, it seems that uplands in this region were last eroded by Upper Orillia waves (Larsen, 1987). Thus, evidence of the older and higher shorelines was likely destroyed by wave action at the perimeters of later and lower lake planes. These characteristics are generally consistent with a transgressive lake sequence. Large areas appear to have emerged, however, as water level fell from the Upper Orillia level to the Lower Orillia level. Water either withdrew from these valleys and embayments, or left inland lakes behind.

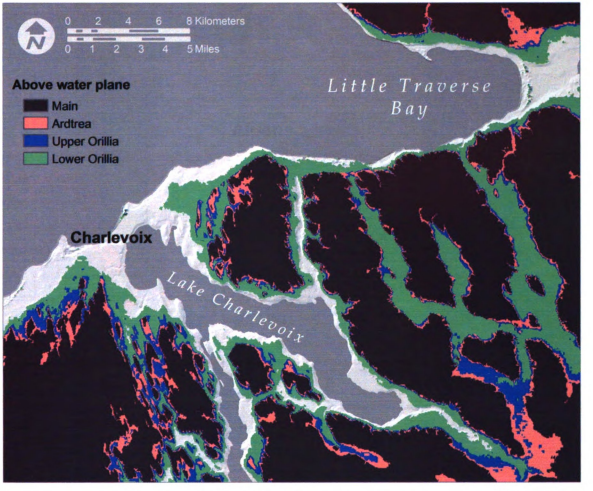


Figure 6.13: Areas near Charlevoix that were predicted to be above glacial Lake Algonquin water levels. This extent of this figure corresponds with the extent of Figure 3.16. The image in this dissertation is presented in color.

The area south of Alpena, Michigan (Figure 6.20) provided similar difficulties. Recall, Leverett and Taylor (1915) expressed great difficulty attempting to identify distinctive water planes along the flat and sandy terrain west of Alpena. Accordingly, glacial Lake Algonquin shorelines appear to separate over vast distances across the sand plain despite close proximities among elevations. The Main and all Upper Group shorelines are compactly spaced and situated, however, at the base of a tall bluff south of Alpena.

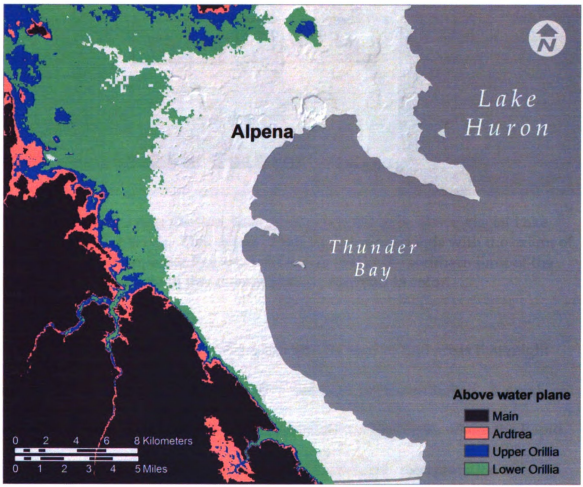


Figure 6.14: Areas south of Alpena, Michigan, predicted to be above glacial Lake Algonquin water levels. This extent of this figure corresponds with the extent of Figure 3.20. The image in this dissertation is presented in color.

Leverett and Taylor (1915) described a "lake cliff and upper ridge" that crosses the Au Sable River "4 miles west of Oscoda" (p.420). The Main, Ardtrea, and Upper Orillia water planes were predicted to have elevations within 3 meters of each other near Oscoda, Michigan (Figure 6.15); the Ardtrea and Upper Orillia were predicted to intersect at 196.3 m. The upland area above the Main water plane is the lower delta Burgis (1977) described that formed at the former mouth of the Au Sable River in glacial Lake Algonquin waters.



Figure 6.15: Areas near Oscoda, Michigan, predicted to be above glacial Lake Algonquin water levels. This extent of this figure corresponds with the extent of Figure 3.22. The apparent line west of Oscoda marks the southern limit of the study area. The image in this dissertation is presented in color.

Maps like those shown above can also be used to find areas that might contain glacial Lake Algonquin features that have been overlooked. A good example is a site in northwestern Kalkaska County, Michigan, where the Rapid River exits the Inner Port Huron moraine (Figure 6.16). Interpretation of topographic maps suggests a large outwash fan and/or delta formed at the mouth of an outwash channel. Figure 6.16 shows a sequence of intersections between the Main and Upper Group water planes and the contemporary ground surface. From these results, it is reasonable to hypothesize that the morphology of this feature might have been last shaped by glacial Lake Algonquin.

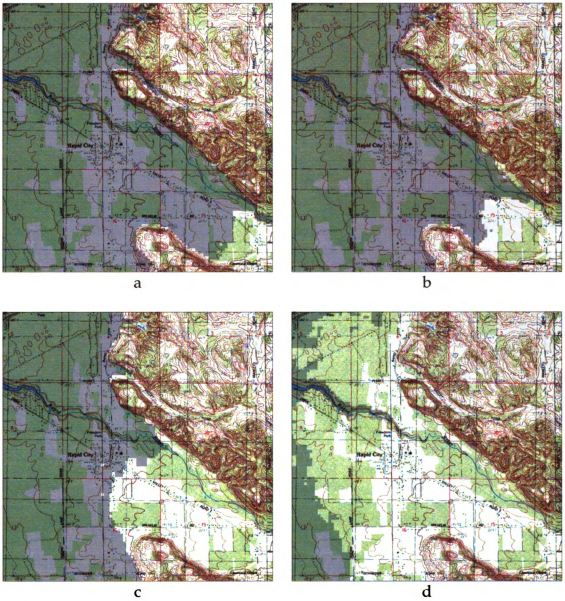


Figure 6.16. The Rapid River outwash fan/delta during the: a) Main; b) Ardtrea; c) Upper Orillia; and d) Lower Orillia phases. Pictured is a portion of the USGS 1:24,000 Torch River 7.5 Minute Series Quadrangle, but rescaled to 1:63,500 for display. Darkened areas are predicted to have been under water at with 90% confidence. The image in this dissertation is presented in color.

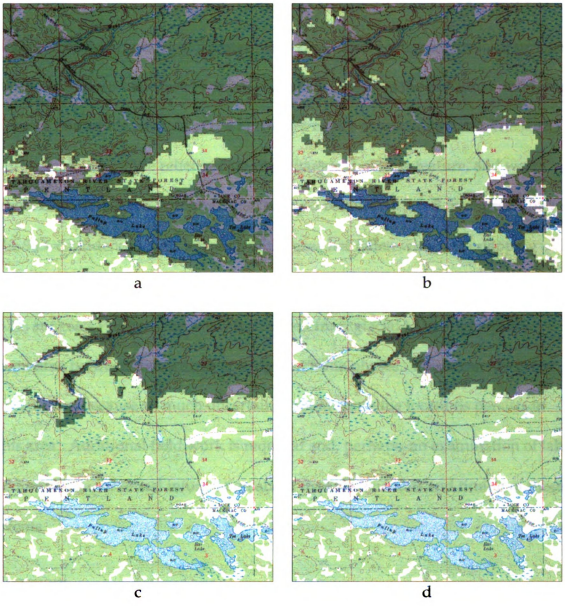


Figure 6.17. Pullup Lake and the surrounding area during the: a) Main; b) Ardtrea; c) Upper Orillia; and d) Lower Orillia phases. Pictured is a composite of the USGS 1:24,000 Gilchrist and Roberts Corner 7.5 Minute Series Quadrangles, but rescaled to 1:63,500 for display. Darkened areas are predicted to have been under water at the 90% confidence level. This image is presented in color.

Other areas simply remain difficult to interpret. For example, the Main and each of the Upper Group water planes apparently intersect the land surface at or near Pullup Lake (see Figure 6.17), which straddles the Mackinac and Luce County line and is situated at the northwest extent of available data. The land surface exhibits gentle relief and no conspicuous shoreline feature, and water plane elevations have been predicted with no better than +/- 3 m of precision (at the 90% confidence level), so much of the area has fallen within overlapping bands of uncertainty. One possible sequence of events, which is shown in Figure 6.17, suggests Pullup Lake was left stranded from glacial Lake Algonquin sometime between the Ardtrea and Upper Orillia phases. This sequence is but speculation because so much uncertainty about shoreline locations persists in this area. Additional field work is required and, perhaps, an examination of lake sediments might reveal information about the true locations and timing of these events.

Summary

In this Chapter I presented maps of four glacial Lake Algonquin lake phases. These maps do not present deterministic answers to the question: where are relict shorelines located? Instead, they summarize a range of possible results and show areas where ancient shorelines probably occurred. Accordingly, I needed to abandon the usual methods for representing shorelines and develop a new and stochastic representation: bands of varying widths over which ancient

shorelines *probably* occurred. I refer to these bands as *bands of uncertainty.* The width of a band of uncertainty is sensitive to two factors: uncertainty about the vertical difference between the ground surface and a water plane; and slope gradient. Uncertainty about the vertical difference between ground surface and water plane elevations is driven by uncertainty about error in the DEM.

Narrow shoreline bands are associated with steep slopes, which retained lake waters, and consistent classification results. Wide bands are associated with gradual slopes and inconsistent classification results. I also mapped uncertainties associated with the water plane models that support landscape reconstructions. In short, I added a layer of 'fog' to indicate where uncertainty about the predicted water plane elevation exceeded certain thresholds.

Maps like those shown in Figures 6.9 to 6.15 can be created when a particular confidence level is selected. For these figures, I selected and mapped all areas that were predicted by my spatial model to be above water 90 times out of 100 runs. Resultant "shorelines" between *above water* and *not above water* areas are then to be interpreted, not as the "water's edge" (Komar, 1998: 47), but as the break between areas that were above water 90 percent of the time and areas that were not above water 90 percent of the time. This probabilistic method is a new way of looking at shorelines.

These results demonstrate the value of assessing spatial data quality, modeling error propagation, and working with uncertainty in work that uses a geographic information system (GIS) because it is the uncertainties, not the

shorelines, that prompt new lines of inquiry. For example, the map of Upper Orillia shorelines indicates the Upper Orillia water plane passes close to the contemporary surface of Walloon Lake. I can tell the two are close because uncertainty about error in the DEM has upset the classification process in this region. Yet, had I used a simpler deterministic model, instead of the cumbersome one I described in Chapter 5, it would have compared the elevations along these two surfaces and rendered only one decision: yes, the surface of Walloon Lake sits above the Upper Orillia water plane; or no, it does not. But the datasets I employed are not perfect, complete, or precise, and my spatial model can deal with that. In the end it is the uncertainty in my results that prompts new line of inquiry: Was Walloon Lake really connected to glacial Lake Algonquin during the Upper Orillia phase and stranded thereafter? If so, does Walloon Lake contain organic materials suitable for radiocarbon dating? If so, would the radiocarbon date help refine the Lake Algonquin chronology? Had Walloon Lake not been mapped as a band of uncertainty, it would not have drawn my attention and I would not have asked these questions.

Aerts et al., claim it is important to understand uncertainty when spatial data and spatial models are used in decision-making processes "where variation in results may have profound implications" (Aerts et al., 2003: 251), particularly decisions that influence human health and safety. Obviously, the variation that exists in these results does not have profound implications for the health and safety of persons living on or near glacial Lake Algonquin shorelines. But the

ideas and methods used in this research can be adapted in work that focuses on contemporary shorelines, where coastal development, population growth, and land use changes occur without regard to the dynamic nature of the coastal zone.

CHAPTER 7: CONCLUSIONS

Introduction

Nearly all forms of data, information, and knowledge are imperfect, so work that relies of geographic information systems should deal with uncertainty. The purpose of this research has been to demonstrate the value of assessing spatial data quality, dealing with uncertainty about errors in input data, and visualizing uncertainties propagated through work conducted in a GIS environment. The additional work required to add uncertainty components to a spatial model is worth any elegance the model might lose because, paradoxically, knowledge gained about uncertainties that propagate into results can reveal valuable insights into the problem under investigation.

The demonstration is accomplished via a thoroughly worked example. In short, I carefully reconstructed four differentially upwarped water planes and four landscapes with isostatic depressions that are associated with glacial Lake Algonquin - a sequence of pro-glacial lakes and a long-standing physiographic and geologic problem. I recognized and modeled uncertainty along the way. In this final chapter I consider the successes and weakness of this demonstration by re-evaluating the research objectives in terms of the work accomplished. I also propose new lines of inquiry and offer some concluding remarks.

Re-evaluation of research objectives

To find and survey relict shoreline features that best serve as indicators of former lake levels; and to conflate new paleoshoreline data with data collected during previous mapping campaign.

I started by inheriting the glacial Lake Algonquin dataset that Schaetzl et al. (2002) had assembled for northern Michigan. I retained most of their data points for further analysis (126 of 146); the balance is stored in a supplemental database. I expanded the study area to include relict shoreline features situated in nearby Ontario and others in Michigan's Upper and Lower Peninsulas; I collected 69 new data points there. Elevation values I obtained at sites in the Munuscong Islands region, near Douglas Lake, and near the Au Sable River compliment the elevation values reported previously by Schaetzl et al. (2002) - so it seems our efforts identified the same features and obtained similar elevation values from them. I conflated data collected previously by Cowan (1985: 10 bluffs at Sault Ste. Marie) and Karrow (1987: 19 bluffs at St. Joseph Island) with my own. The new elements of the glacial Lake Algonquin dataset fill large data gaps (Cowan, 1985) and furnish new points of support for the restoration of glacial Lake Algonquin water planes (Taylor, 1895). Individually, each sample marks a point along a former shoreline. In aggregate, they outline several distinct water planes within the region of interest: Main (57), Ardtrea (41), Upper

Orillia (33), Lower Orillia (16), Wyebridge (12), Penetang (13), Cedar Point (17), Payette (7), Sheguiandah (3), Korah (1) and others (43).

I relied on the Global Positioning System (GPS) to make measurements of paleoshoreline positions. The GPS is being integrated with other forms of technology (e.g., cell-phones, digital cameras, etc.) and used to support location-based services (e.g., recreation, navigation, inventory tracking, etc). Popular conceptions of the GPS, however, include false notions about how consistently it can measure positions with a high degree of accuracy. The accuracy assessment of GPS-derived position data in this work has shown that, yes, the GPS can be used to achieve sub-meter measurement accuracy, but careful planning and execution, and tedious data processing are required to minimize errors. GPS-based position measurements are subject to several error processes that change with location and time.

The features I surveyed at Cockburn Island are particularly important features because they add much needed support near the northern rims of glacial Lake Algonquin water planes. They also provide clues about the deglaciation history of the area. We know that the Superior Lobe of the Laurentide ice sheet retreated northeastwardly after reaching a maximum extent that covered the northern portion of Michigan's Lower Peninsula (Karrow, 1987; Blewett, 1995; Larson and Schaetzl, 2001). Lakes in the Michigan and Huron basins were joined when retreating ice uncovered the Indian River lowlands and, slightly later, the Straits of Mackinac, which Larsen places at approximately 11,200 yr BP (after

Hansel et al., 1985). Water levels in glacial Lake Chicago (Michigan basin) dropped to the glacial Lake Algonquin level (Huron basin) upon joining (Hansel et al., 1985), which left the outlet at Chicago abandoned (Hansel et al., 1985; Larson and Schaetzl, 2001) and directed outflow to the Fenelon Falls outlets near Kirkfield, Ontario (Finamore, 1985). Thus began the Main phase of glacial Lake Algonquin. The presence of Main phase shorelines on Cockburn Island suggests that the ice sheet retreated through Cockburn Island sometime during the early portion of this lake phase; early enough to allow bluff cutting and shoreline development processes to occur. Karrow (1987) concluded that St. Joseph Island was deglaciated "about 11,000 yr BP or shortly thereafter" (p119). Cockburn Island is situated along the same apparent isobase that runs through St. Joseph Island (Figure 3.8), so both islands were likely deglaciated at approximately the same time. Therefore, locations between the Straits of Mackinac and the Cockburn Island-St Joseph Island region must have been deglaciated within, roughly, a 200-year period. Main phase and lower shorelines on Cockburn Island tell us that Cockburn Island was deglaciated before the outlets at North Bay, Ontario, because lower lake phases are associated with falling water levels brought about by deglaciation of the outlets at North Bay (Kaszycki, 1985; Karrow, 1987). Karrow et al. (1975) reported radiocarbon dates that indicate glacial Lake Algonquin, from the Main phase to the lowest, existed between 11,200 yr BP and 10,400 yr BP. Relict shoreline features at Cockburn Island are important features because they help to locate the ice sheet margin, albeit

roughly, as well as the northern extent Main Lake Algonquin within the context of this short time frame.

Karrow (1987) and Larsen (1987) have noted the long-standing controversy regarding whether certain water planes in the glacial Lake Algonquin sequence are parallel, thus implicating changes in outlets were responsible for changes in water levels, or whether they converge toward a single outlet, which would implicate isostatic rebound as the sole cause of shoreline deformation and change. This study has found evidence of convergence between the Main and Ardtrea water planes, which agrees with the earlier findings of Deane (1950) and Schaetzl et al. (2002). Proceeding southwardly: Main and Ardtrea bluffs at Cockburn Island are vertically separated by approximately 8 m (280 and 272 m, respectively); in the Munuscong Islands region they are separated by ~7 m (265 and 258 m, respectively); on Mackinac Island they are separated by ~6 m (242 and 236 m, respectively); and, in the Douglas Lake area, they are separated by ~4 m (225 and 221 m, respectively). Moreover, the Main and Ardtrea shorelines are difficult to differentiate at locations south of Little Traverse Bay (Lake Michigan) and Thunder Bay (Lake Huron) because they either occur within 3 m of each other or they were reworked or destroyed by younger and lower lake phases. Convergence between the Main and Ardtrea water planes suggests differential uplift relative to the Fenelon Falls outlet was the cause of deformation and tilt during the Main and Ardtrea phases.

Areas north of Traverse City and south of Alpena are where the Main and Ardtrea water planes tend toward convergence. In Ontario, Karrow reported the Main Lake Algonquin shoreline between Kincardine and Port Elgin, along the eastern shore of Lake Huron, "has been entirely removed by later shore erosion ... by lower water levels after the Main Algonquin level" (Karrow, 1987: 161). I believe the same kind of bluff removal processes that occurred between Kincardine and Port Elgin, Ontario, also occurred north of Traverse City and south of Alpena, Michigan. Consequently, I also believe it makes good sense to attribute observable shorelines in these areas to the last phase to act upon them; not the first or the highest. Therefore, I can agree with Larsen's claims that Main and Ardtrea shorelines of eastern Lake Huron predate the highest stranded shorelines in northern Lake Michigan, and the apparent "Main" shoreline of Lake Michigan "may correlate with the Orillia shoreline of Ontario" (Larsen, 1987: 21). This does not mean that the Main or Ardtrea water planes did not extend into the Michigan basin, for evidence at Beaver Island suggests they did; it means only that many of the highest remaining glacial Lake Algonquin shorelines in the Michigan basin correlate best with younger lake phases.

Upper Orillia shorelines occur consistently below Ardtrea shorelines at Cockburn Island, the Munuscong Islands, Mackinac Island, and in the Douglas Lake area, but a review of elevation differences between them provides conflicting evidence regarding convergence. Thus, it was somewhat surprising to find that the reconstructed Ardtrea and Upper Orillia water planes intersect

near the mouth of the Au Sable River; the two models converge there at 196.3 m. This finding should be treated as provisional, however, because the Upper Orillia water plane model was supported by fewer data than was the Ardtrea water plane model. Of the two, the Upper Orillia model was noisier, less precise, and subject to the greatest uncertainties. I must also recognize that, after working with these data, there might be some classification errors between the closely-spaced Upper Orillia and Lower Orillia features in Michigan's Lower Peninsula, which would pull the reconstructed Upper Orillia water plane to lower elevations. These features should be revisited.

The embayment that holds contemporary Walloon Lake (Lower Peninsula near Charlevoix) was likely last connected to glacial Lake Algonquin during the Upper Orillia phase. Perhaps future study of the oxygen isotope and pollen records stored in sediments at the bottom of Walloon Lake might reveal information about when the embayment separated from the lake, which could then be used to bracket the time it took glacial Lake Algonquin to transition from the Main to the Upper Orillia phase of its existence at that location.

Few sites contain multiple instances of later and lower water planes. Cockburn Island and the Munuscong Islands region, for example, hold instances of both the Upper Orillia and Penetang shorelines. The vertical difference between these shorelines at Cockburn Island is 36 m, whereas the difference in the Munuscong Islands region is only 30m. A decreasing separating distance with decreasing latitude suggests convergence again, hence the influence of

differential rebound. The difference between two points, however, is not sufficient for characterizing the spatial pattern of difference between two water planes, so no valid conclusion can yet be drawn about the relationship between the Upper Orillia and Penetang water planes.

Evidence of convergence between particular water planes in northern parts of the Huron basin notwithstanding, neither this research or the glacial Lake Algonquin dataset can be used to resolve the question of where glacial Lake Algonquin stood in the southern parts of the Huron and Michigan basins. No data were collected there.

To reconstruct water planes associated with glacial Lake Algonquin lake phases.

This is the first work that has ever attempted to map the entire sequence of "Upper Group" (Deane, 1950) shorelines in this region. I have shown that long-term variation in glacial Lake Algonquin water plane elevations can be expressed as the sum of three components: a spatial trend that represents isostatic recovery across the region; a random and spatially structured component that captures localized effects (e.g., differential subsidence, differential erosion, etc); and a random but spatially unstructured component that captures chaotic variation. From these components, I built geostatistical models to reconstruct four phases of glacial Lake Algonquin. Model parameters quantify the rates at which water plane elevations increase with decreasing distance toward the former center of ice loading. Parameter values decrease over

time and indicate that younger water planes are warped less than older ones. Water planes were reconstructed via universal kriging, which produced surfaces of predicted water plane elevations that passed through supporting data, and estimates of prediction uncertainty at every location. Locations where prediction uncertainty exceeds three meters should be flagged for additional investigation.

The Main, Ardtrea, Upper Orillia, and Lower Orillia water plane surfaces generated during this work (Figures 5.6a, 5.8a, 5.10a, and 5.12a) look similar to the water plane surfaces derived from paleoshoreline data by Schaetzl et al. (2002). The water plane models reported in this work, however, are superior to the water plane models presented by Schaetzl et al. (2002) in five important ways. First, each of my models is supported by more paleoshoreline data that cover larger geographic extents. Recall, the geographic distribution of the original glacial Lake Algonquin dataset was oriented roughly along the expected trend and not normal to it. New paleoshoreline data were collected along an axis normal to expected uplift trends to better capture these trends. Second, each of my models incorporates data taken from Ontario, where Lake Algonquin shorelines have long been recognized. Accordingly, bluff sites that were misclassified by Schaetzl et al. (2002) and Farrand and Drexler (1985) were reclassified (Chapter 3) and have been integrated into the findings reported by Sly and Lewis (1969), Cowan (1985), and Karrow (1987). Third, I used a reduced second-order trend model to capture the uplift trend; all model parameters were found to be statistically significant. Schaetzl et al. (2002) used a full second-order

model that retained a statistically insignificant term, which renders their model as less meaningful. Fourth, my geostatistical rebound models take into account both the broad regional uplift trend and localized deviations from that trend that likely result from differences among site conditions; Schaetzl et al. (2002) focused on the trend only. And fifth, before geostatistical analysis, I rescaled all location coordinate values from the meter to the kilometer unit of measure, and translated the planar coordinate system origin from a location outside the State of Michigan to Traverse City, Michigan to reduce coordinate magnitudes. This coordinate transformation mitigated rounding errors created during trend surface analysis and by computer word overflows (Burrough and McDonnell, 1998) - especially when coordinate values were raised to powers greater than one for use in second- or higher-order trend models. The full second-order trend surface models reported by Schaetzl et al. (2002) were surely influenced by such rounding errors and, therefore, the parameter coefficients obtained from them cannot be considered accurate. Also, my trend model coefficients express rates of uplift in m/km, which is more user-friendly than the rates they reported in m/m. In these five ways, the water plane models reported in this work are superior to the water plane models presented by Schaetzl et al. (2002).

Glacial Lake Algonquin water planes are continuous, smooth, and show a general pattern of uplift that tends to increase in Michigan from the southwest to the northeast and towards the former centers of ice loading. The Lake Algonquin water plane surfaces generated during this work (Figures 5.6a, 5.8a,

5.10a, and 5.12a) also look similar to postglacial rebound surfaces derived by others from lake gauge data (e.g., Coordinating Committee, 1977, 2001; Tushingham, 1992; Mainville and Craymer, 2005), and from a geophysical model (e.g., Tushingham and Peltier, 1991). The apparent similarities between mapped contours that represent elevations along each glacial Lake Algonquin water planes and Mainville and Craymer's (2005) mapped isobases that show contemporary rates of postglacial uplift suggest that my water plane models are reasonable and, importantly, that the pattern of isostatic recovery has not changed much during that last 11,000 years.

It has been customary in past and related research to construct lake-level curves or shoreline diagrams along a line of profile that extends from a recognizable place and is oriented in the expected direction of greatest uplift (e.g., Goldthwait, 1910; Leverett and Taylor, 1915; Stanley, 1936; Farrand and Drexler, 1985; Finamore, 1985; Karrow, 1987; and Larsen, 1987). Although I constructed them, I do not report lake-level curves in this work because I have come to believe such diagrams are inadequate and inappropriate for describing deformation over large *areas*; they cannot depict important and meaningful trends in plan, and they imply the direction of greatest uplift remained constant over time. In my opinion, use of shoreline diagrams should be limited to relatively small areas; those that span roughly no more than one degree of latitude or longitude.

Each of the water plane models presented in this work is a statistical model, with a predicted elevation and variance at each grid cell location. Accordingly, the distribution of elevation values at any location and a statistical *difference of means* test can be used to estimate the probability that a bluff elevation, perhaps one surveyed at a future date, might belong to a modeled lake phase. The test result can be used to reject or fail to reject the null hypothesis of unequal means and, hence, suggest a proper classification for the newly sampled site. Moreover, in the presence of sound physical evidence for a bluff to belong to a particular lake phase, a test result that fails to reject the null hypothesis might indicate the statistical model should be updated to include information obtained from the newly surveyed feature.

And last, co-located elevations along any two statistical lake surfaces can be compared using a spatial version of the *two-sample difference of means test*. For example, an apparent difference between the mean Main and Ardtrea water plane elevations at a given location can be assessed for statistical significance given the respective kriging variance around each predicted mean. Locations where water planes converge should have mean elevations that are not statistically different. Locations where different means are not statistically different should be flagged for additional investigation.

To reconstruct the landscape associated with each lake phases and map the distribution of glacial Lake Algonquin shorelines.

I reconstructed four landscapes within a GIS environment using combinations of digital water plane models and an error-prone digital elevation model. This research has demonstrated that an analysis of elevation errors can reveal artifacts of different DEM production methods, which in turn can be used to partition the dataset into meaningful subsets. Elevation data that covered Ontario, for example, were delivered with scant metadata; hypsometric analysis revealed oversampled elevations that match contours on topographic maps, and undersampled elevations that occur between mapped contours - clues that implicate specific sources materials and interpolation methods. Also, analysis of elevation errors and elevation derivatives, like slope gradient and slope aspect, can be used to identify horizontal shifts in coordinate data. The National Elevation Dataset (Gesch et al., 2002) may be the best available elevation dataset for this region, but this research has shown the meaning of "best" varies with location.

This research has also demonstrated that uncertainty about errors in a DEM can be modeled, incorporated into spatial model design, and used to reveal locations where "the result" is vulnerable to uncertainty and is, therefore, indeterminate. The DEM employed in this work contains 25,718,215 grid cells; only 529 elevations were tested (0.002%) but nearly all contained some amount of error. It is reasonable, rational, even responsible to recognize that most of the

other 25,717,686 elevation values are subject to uncertainty about elevation error. Fortunately, DEM error, like many terrain properties, tends to exhibit spatial autocorrelation. Spatial autocorrelation among data can be exploited; kriging methods can be used to make informed predictions about error at each location; and simulation techniques can be used to generate alternate possible realizations of DEM error surfaces, which in turn can be applied as corrections to the original DEM. The purpose of adding all of this cumbersome complexity to what might otherwise be an elegant spatial model is to determine how vulnerable a particular result is given uncertainty about error in the underlying data. Uncertainty is unavoidable and comes in many forms; its impacts need to be recognized and assessed.

To express the degree of uncertainty with which each glacial Lake Algonquin shoreline location has been mapped.

This research began with the recognition that a linear object is an imprecise representation of a shoreline because linear objects do not represent the volumes of spaces in which natural variability in lake levels and associated shoreline movements occur. Accordingly, this research has adopted a new form of shoreline representation - a stochastic representation -- that embodies uncertainty about shoreline location.

In recent work, MacEachren (2005) identified core challenges associated with visualizing uncertainty in geospatial data; among them is "the challenge of

depicting multiple forms of uncertainty in the same display" (MacEachren, 2005: 156). This work has met that challenge. Glacial Lake Algonquin shoreline maps depict one form of uncertainty that results from the interplay between beach slope and uncertainty about error in the underlying DEM, and another form associated with the spatial distribution of precision with which the underlying water plane elevations had been predicted. Different visual cues express each form of uncertainty and they work in conjunction with the results. Visual cues allow the map reader to focus on the best parts of the map, identify locations on the map where results are vulnerable to uncertainty, and to understand the reasons for why a result at one location might be more or less reliable than at another.

Future research

This research is intrinsically geographic because it synthesizes concepts, knowledge, and tools from multiple disciplines to study a portion of the Earth. It employs methods developed in the field of Geographic Information Science to tackle a long-standing physiographic and geologic problem. Yet, because I was trying to build a bridge between these specialties, I faced the constant challenge of striking the right balance, or maybe the right juxtaposition, between efforts to understand how uncertainty should be incorporated into a GIS environment and efforts to understand a sequence of pro-glacial lakes. A strength of this work is that each field provided a context for reflecting upon the other. A weakness is

that opportunities to follow paths into one field were sometimes abandoned to follow paths into the other. Consequently, I can think of many lines of inquiry worth pursuing in the future.

Glacial Lake Algonquin

Although new data have been collected, relict features in Michigan's Upper Peninsula remain under-represented. More data should be collected to resolve some of the uncertainty that persists regarding relict shorelines in that area. The swampy nature of the terrain, private property, and a sparse road network serve as effective barriers to exploration and data collection, but the maps built during this research can be used to focus future exploration and data collection activities. Data collected in the Upper Peninsula will furnish new and valuable support to water plane reconstructions and can provide better ground control for future DEM simulations.

This research has demonstrated again that a wave-cut bluff is an effective indicator of a former water plane position. Yet, a weakness associated with using bluffs as indictors is that they seldom occur in close proximity to each other wherever water planes converge. The landscapes situated between Petoskey and Traverse City, and between Alpena and the Au Sable River, remain difficult to study because water planes trend toward convergence (the Ardtrea and the Upper Orillia do converge) and each relatively old bluff record has likely been reworked or destroyed by younger lake phases. New and better indicators

are needed to mark glacial Lake Algonquin water planes in these troublesome areas.

Maps of the ancient landscapes reveal several changes that merit study beyond the scope of research presented here. For example, the apparent outwash fan/delta complex at the former mouth of the Rapid River (Kalkaska County, MI) might have a sediment structure that can provide clues about past lake events. The sediment and pollen records at the bottom of Walloon Lake (Charlevoix County), an embayment that separated from glacial Lake Algonquin after the Upper Orillia phase, might hold clues about the timing of that separation and, hence, the timing of the Upper and Lower Orillia phases. And, the cedar swamps that bracket the Penetang and Cedar Point shorelines at Cockburn Island (Ontario) might hold organic materials suitable for radiocarbon dating of those phases.

Like newly sampled bluffs, the elevations of small inland lake surfaces and bottoms can be compared statistically to co-located elevations along the glacial Lake Algonquin water planes. Difference of means tests can be used to assess whether an inland lake is higher (older), lower (younger) or coincident (in both space and time) with a given lake phase. Of course, statistical test results are subject to their own forms of uncertainties, but they provide some grist for rational decision making.

Topographic map analysis

Topographic maps are commonly used to support geographic and geologic explorations. Mapped contours are used to identify landforms and landform assemblages, as they were during the initial stages of this work. The differentially-upwarped water plane models reported in Chapter 5 can be mathematically inverted and used to differentially-depress a DEM. New contour lines can be constructed from the adjusted DEM, which might reveal landform characteristics that are not depicted in the contemporary representation, or slope gradients that suggest, for example, the overland flow of water moved differently than it would today.

Visualizing uncertainty

I invested much effort into understanding, modeling, and depicting uncertainty in my data, models, and results; doing so surely kept me close to the data and prevented me from trusting software. Yet, I do not know whether or not my depictions will actually aide others who are interested in this line of work (another form of uncertainty!). Will the indicators of uncertainty be ignored? Or, will any tinge of uncertainty prompt the reader to reject all results out of hand? The GIScience literature provides little guidance about which depictions of uncertainty are best, or how map readers respond to mapped uncertainties. More cartographic research is needed at the cognitive level to find answers to these questions and provide guidance.

Global climate change and sea-level rise

This research focused on an analysis of ancient shorelines in the upper Great Lakes basin. Yet clearly, the ideas and methods it employs can also be applied in other work that uses GIS to model paleolake sequences (e.g., Lake Agassiz , Lake Barlow-Ojibway, etc.), or to study contemporary issues regarding coastal environments.

A major threat of global climate change is the expected rise in global sea-level. Many human populations and economic infrastructures are situated in low-lying coastal environments and vulnerable to flood and inundation. Much work is already underway to identify flood-prone areas and to prioritize them according to the degree of perceived risk; many are using a GIS and digital elevation models to find locations under elevated water planes (e.g., Titus and Richman, 2001; Simas et al., 2001; Cowell and Zeng, 2003; and Hennecke et al., 2004), but only a few are integrating data quality assessments, uncertainty, or simulation into the work (e.g., Cowell and Zeng, 2003; and Hennecke et al., 2004). The concepts of vulnerability and risk embody the very idea of uncertainty, and so too should related work with spatial data and GIS. Failure to recognize uncertainty in the concepts, data, and models that support analysis of global sea-level rise will surely fail to identify all areas that are at risk.

Final thoughts

At the very beginning of this research I knew that data errors, inaccuracies, or imprecision are customarily absorbed into many analyses. The logic is usually something like -- it is impossible, impractical, or too costly to find and correct every little error in a dataset, so, do your best to recognize pitfalls, but move forward. Yet, of the many lessons I learned during my doctoral research, the one that has made the biggest impression is learning just how sensitive results can be to the slightest error - either in input data or assumptions. For example, in terms of a given glacial Lake Algonquin water plane, a meter of uncertainty in predicted water surface elevation and a co-located meter of uncertainty in ground surface elevation, when combined, might produce a kilometer of uncertainty regarding the location of the former land and water interface. For another, in terms of a 300-kilometer line segment extending S72°E from Mackinac Island (the terminus of which would land on Ontario's Bruce Peninsula), a single degree of uncertainty in the generally accepted direction of maximum isostatic uplift at Mackinac Island would (assuming a linear uplift trend) subtend a 10.47 km (6.5 mi) arc of uncertainty in the terminus location. In both examples, larger uncertainties in the inputs would result in larger uncertainties in the outputs. Of course, uncertainties compound in such ways in part because of the relatively large area covered by glacial Lake Algonquin, but this work is hardly unique in its scale of analysis. Many such uncertainties likely remain unexamined in other work.

In addition to recognizing uncertainty, this research has allowed me to learn methods for dealing with uncertainty. Monte Carlo simulation techniques can be used very effectively to reveal ranges of possible outcomes and I find I employ them more and more frequently, particularly when I undertake any analysis that requires use of a DEM.

This research has provided me with invaluable opportunities to explore landscapes once foreign to me; ancient and contemporary. I found great satisfaction in exploring the Upper Great Lakes, particularly when I entered field sites first described by James Goldthwait, Frank Leverett, or Frank Taylor, and I was still able to see what they observed 100 years ago. I developed a deep respect and appreciation for the detailed work they accomplished at the turn of the twentieth century (although, after reading Lawson's (1898) report, I think the cleared landscapes of the timber-boom era offered them a few vantage points that no longer exist today). Until recently, I did not appreciate the glacial history of my hometown, North Tonawanda, New York. For example, I had always thought a road near my house had been named, perhaps, by a comedic politician, rather than for an actual *beach ridge* that formed along the shore of glacial Lake Tonawanda, which I have begun to study. As a kid I thought I knew the nearest beach was a forty-minute drive away -- I never considered a lake had once covered much of my hometown. I now explore Western New York with a brand new set of eyes.

APPENDICES

APPENDIX A: THE GLACIAL LAKE ALGONQUIN DATASET

Table A.1: The glacial Lake Algonquin dataset.

SID	Longitude	Latitude	H	Phase	Surveyed by:	USGS Quadname
101	-85.63302366	45.00334624	199.5	Upper Orillia	Drzyzga (this work)	Gills Pier MI
102	-85.60231784	45.04332913	199.3	Upper Orillia	Drzyzga (this work)	Omena MI
103	-85.56937309	45.05697549	196.8	Lower Orillia	Drzyzga (this work)	Omena MI
104	-85.58865547	45.07031354	196.4	Lower Orillia	Drzyzga (this work)	Omena MI
105	-85.62899645	45.16615307	198.0	Lower Orillia	Drzyzga (this work)	Northport NW MI
106	-85.66830344	45.12257434	203.0	Supplemental	Drzyzga (this work)	Gills Pier MI
107	-85.73049857	45.01907969	194.2	Supplemental	Drzyzga (this work)	Gills Pier MI
108	-85.09660453	45.35397611	212.9	Ardtrea	Drzyzga (this work)	Bay Shore MI
109	-85.09372479	45.35500076	213.3	Ardtrea	Drzyzga (this work)	Bay Shore MI
110	-85.08827092	45.35584481	213.0	Ardtrea	Drzyzga (this work)	Bay Shore MI
111	-85.06883233	45.28293080	206.4	Upper Orillia	Drzyzga (this work)	Bay Shore MI
112	-85.07880280	45.28504629	208.4	Upper Orillia	Drzyzga (this work)	Bay Shore MI
113	-85.10439545	45.28015334	186.3	Nipissing	Drzyzga (this work)	Bay Shore MI
114	-85.13856504	45.36462996	211.6	Upper Orillia	Drzyzga (this work)	Ironton MI
115	-85.18779164	45.32784476	207.8	Upper Orillia	Drzyzga (this work)	Ironton MI
116	-85.32408926	44.96835341	192.2	Supplemental	Drzyzga (this work)	Alden MI
117	-85.32237124	44.91577464	193.7	Supplemental	Drzyzga (this work)	Alden MI
118	-85.32252291	44.91739619	193.5	Supplemental	Drzyzga (this work)	Alden MI

SID	Longitude	Latitude	H	Phase	Surveyed by:	USGS Quadname
119	-85.32154529	44.91647656	185.5	Nipissing	Drzyzga (this work)	Alden MI
122	-83.45362909	44.40797866	196.5	Upper Orillia	Drzyzga (this work)	Foote Site Village
123	-83.45106651	44.40359657	193.4	Supplemental	Drzyzga (this work)	Foote Site Village
124	-83.43179963	44.44200397	196.3	Upper Orillia	Drzyzga (this work)	Foote Site Village
125	-83.42798820	44.45051694	196.8	Upper Orillia	Drzyzga (this work)	Foote Site Village
126	-83.35134954	45.92652966	257.1	Lower Orillia	Drzyzga (this work)	Alpena-W
127	-83.33455407	45.91880168	270.6	Ardtrea	Drzyzga (this work)	Alpena-W
128	-83.33573016	45.91869340	282.8	Main	Drzyzga (this work)	Alpena-W
129	-83.33781383	45.92006442	287.6	Supplemental	Drzyzga (this work)	Alpena-W
130	-83.34320991	45.92318112	289.4	Supplemental	Drzyzga (this work)	Alpena-W
131	-83.30577735	45.93664500	225.4	Cedar Point	Drzyzga (this work)	Alpena-W
132	-83.29547761	45.93210483	228.3	Penetang	Drzyzga (this work)	Alpena-W
133	-83.29397249	45.92815920	223.9	Cedar Point	Drzyzga (this work)	Alpena-W
136	-83.34183811	45.91501164	278.4	Main	Drzyzga (this work)	Alpena-W
137	-83.34188721	45.91466539	272.9	Ardtrea	Drzyzga (this work)	Alpena-W
138	-83.33962682	45.91334400	274.1	Supplemental	Drzyzga (this work)	Alpena-W
139	-83.33416549	45.91442885	278.7	Main	Drzyzga (this work)	Alpena-W
140	-83.33468861	45.91447228	284.0	Supplemental	Drzyzga (this work)	Alpena-W
141	-83.33508133	45.91237384	281.4	Main	Drzyzga (this work)	Alpena-W
142	-83.33731193	45.92213802	270.3	Ardtrea	Drzyzga (this work)	Alpena-W
143	-83.34322871	45.92317229	291.0	Supplemental	Drzyzga (this work)	Alpena-W

SID	Longitude	Latitude	H	Phase	Surveyed by:	USGS Quadname
144	-83.34363020	45.92164571	281.5	Main	Drzyzga (this work)	Alpena-W
145	-83.34721044	45.91774749	265.8	Upper Orillia	Drzyzga (this work)	Alpena-W
146	-83.31282193	45.88670837	229.8	Penetang	Drzyzga (this work)	Alpena-W
147	-83.30608526	45.89051522	225.8	Cedar Point	Drzyzga (this work)	Alpena-W
148	-83.31027677	45.88818884	225.8	Cedar Point	Drzyzga (this work)	Alpena-W
149	-83.31094088	45.88840274	231.0	Penetang	Drzyzga (this work)	Alpena-W
150	-83.32045596	45.88144630	229.6	Penetang	Drzyzga (this work)	Alpena-W
151	-83.32055222	45.88096144	221.5	Cedar Point	Drzyzga (this work)	Alpena-W
152	-83.34188074	45.91780072	280.4	Main	Drzyzga (this work)	Alpena-W
153	-83.34374321	45.91787262	272.4	Ardtrea	Drzyzga (this work)	Alpena-W
154	-83.33678089	45.92058486	280.0	Main	Drzyzga (this work)	Alpena-W
155	-83.33602752	45.92064461	270.7	Ardtrea	Drzyzga (this work)	Alpena-W
156	-83.35121893	45.92486486	266.6	Upper Orillia	Drzyzga (this work)	Alpena-W
157	-83.35063026	45.92946412	261.3	Lower Orillia	Drzyzga (this work)	Alpena-W
158	-83.35743306	45.86297615	222.1	Cedar Point	Drzyzga (this work)	Alpena-W
159	-85.57144067	45.65039861	223.2	Ardtrea	Drzyzga (this work)	Beaver Island North
160	-85.56099611	45.64079801	225.1	Ardtrea	Drzyzga (this work)	Beaver Island North
161	-85.60102805	45.58783750	212.5	Wyebridge	Drzyzga (this work)	Beaver Island South
162	-85.57687948	45.65082847	229.3	Main	Drzyzga (this work)	Beaver Island North
163	-85.55061430	45.63533858	230.3	Main	Drzyzga (this work)	Beaver Island North
164	-85.59166373	45.59503977	211.4	Wyebridge	Drzyzga (this work)	Beaver Island South

SID	Longitude	Latitude	H	Phase	Surveyed by:	USGS Quadname
165	-85.60005708	45.58858628	214.0	Wyebridge	Drzyzga (this work)	Beaver Island South
166	-84.39957291	46.24582720	222.3	Cedar Point	Drzyzga (this work)	Pickford NW MI
167	-84.40278195	46.25272000	224.5	Cedar Point	Drzyzga (this work)	Dafter MI
168	-84.40771905	46.26127845	223.8	Cedar Point	Drzyzga (this work)	Dafter MI
169	-84.52817275	46.09691993	264.3	Main	Drzyzga (this work)	PontchartrainShores
170	-84.46171093	46.08546835	268.2	Main	Drzyzga (this work)	Hessel MI
171	-84.51391141	46.12579042	259.7	Ardtrea	Drzyzga (this work)	Rudyard MI
172	-84.51522788	46.12571287	266.9	Main	Drzyzga (this work)	Rudyard MI
174	-84.35074705	46.10030093	252.2	Upper Orillia	Drzyzga (this work)	Pickford Se MI
178	-84.67800346	45.56689190	227.4	Main	Drzyzga (this work)	Indianville MI
180	-84.71894887	45.56974785	222.2	Ardtrea	Drzyzga (this work)	Indianville MI
181	-84.73761887	45.56823962	224.1	Ardtrea	Drzyzga (this work)	Indianville MI
182	-84.72269172	45.52825547	223.8	Main	Drzyzga (this work)	Indianville MI
184	-84.69642609	45.52827872	187.6	Nipissing	Drzyzga (this work)	Indianville MI
185	-84.62606253	45.53077935	211.8	Wyebridge	Drzyzga (this work)	Indianville MI
186	-84.62612251	45.52931520	198.8	Supplemental	Drzyzga (this work)	Indianville MI
201	-83.99226000	46.18304000	266.4	Upper Orillia	Karrow (1987)	Blind River-W
202	-83.99161000	46.18330000	272.2	Ardtrea	Karrow (1987)	Blind River-W
203	-83.98939000	46.18425000	279.6	Main	Karrow (1987)	Blind River-W
204	-83.96704000	46.17608000	279.4	Main	Karrow (1987)	Blind River-W
205	-83.94314000	46.14960000	229.4	Cedar Point	Karrow (1987)	Blind River-W

SID	Longitude	Latitude	H	Phase	Surveyed by:	USGS Quadname
206	-83.99543000	46.20719000	231.8	Penetang	Karrow (1987)	Blind River-W
207	-83.97798000	46.22210000	277.4	Ardtrea	Karrow (1987)	Blind River-W
210	-83.99223000	46.21496000	259.2	Lower Orillia	Karrow (1987)	Blind River-W
211	-83.98233000	46.21939000	266.0	Upper Orillia	Karrow (1987)	Blind River-W
212	-84.04024000	46.18748000	282.9	Main	Karrow (1987)	Sault Sainte Marie-E
214	-84.04283000	46.19030000	211.6	Payette	Karrow (1987)	Sault Sainte Marie-E
216	-84.01131000	46.19021000	235.4	Penetang	Karrow (1987)	Sault Sainte Marie-E
217	-84.01152000	46.19052000	231.0	Penetang	Karrow (1987)	Sault Sainte Marie-E
220	-84.00889000	46.19139000	233.2	Penetang	Karrow (1987)	Sault Sainte Marie-E
221	-84.00843000	46.19105000	236.9	Penetang	Karrow (1987)	Sault Sainte Marie-E
223	-83.88658000	46.25011000	229.2	Supplemental	Karrow (1987)	Blind River-W
225	-83.88925000	46.25373000	205.3	Sheguiandah	Karrow (1987)	Blind River-W
226	-83.42700000	46.27742000	257.0	Cedar Point	Karrow (1987)	Blind River-W
229	-83.42293000	46.27994000	242.3	Payette	Karrow (1987)	Blind River-W
230	-83.41440000	46.28120000	216.1	Korah	Karrow (1987)	Blind River-W
301	-84.61732000	45.85397000	226.4	Supplemental	Schaetzl et al. (2002)	Round Island MI
302	-84.61689000	45.85634000	236.3	Ardtrea	Schaetzl et al. (2002)	Round Island MI
304	-84.42874000	46.04946000	244.2	Upper Orillia	Schaetzl et al. (2002)	Hessel MI
305	-84.61326000	45.86035000	227.4	Upper Orillia	Schaetzl et al. (2002)	Round Island MI
306	-84.61430000	45.86105000	229.2	Upper Orillia	Schaetzl et al. (2002)	Round Island MI
307	-84.61673000	45.85712000	242.0	Main	Schaetzl et al. (2002)	Round Island MI

SID	Longitude	Latitude	H	Phase	Surveyed by:	USGS Quadname
308	-84.88870000	45.69295000	233.9	Main	Schaetzl et al. (2002)	Bliss MI
309	-84.88881000	45.69346000	221.2	Upper Orillia	Schaetzl et al. (2002)	Bliss MI
310	-84.91972000	45.70072000	232.7	Main	Schaetzl et al. (2002)	Bliss MI
311	-84.93121000	45.67052000	231.9	Main	Schaetzl et al. (2002)	Bliss MI
312	-84.93156000	45.66732000	230.2	Main	Schaetzl et al. (2002)	Bliss MI
313	-85.11090000	45.56785000	224.4	Main	Schaetzl et al. (2002)	Good Hart MI
314	-85.11102000	45.56797000	221.8	Ardtrea	Schaetzl et al. (2002)	Good Hart MI
315	-85.03678000	45.44465000	222.4	Main	Schaetzl et al. (2002)	Forest Beach MI
316	-84.93290000	45.43185000	215.9	Ardtrea	Schaetzl et al. (2002)	Harbor Springs MI
317	-84.42160000	46.05165000	256.2	Ardtrea	Schaetzl et al. (2002)	Hessel MI
319	-84.50916000	46.13939000	241.4	Lower Orillia	Schaetzl et al. (2002)	Rudyard MI
320	-84.50916000	46.14145000	236.9	Wyebridge	Schaetzl et al. (2002)	Rudyard MI
321	-84.50952000	46.14325000	219.5	Supplemental	Schaetzl et al. (2002)	Rudyard MI
322	-84.56758000	45.60592000	224.6	Ardtrea	Schaetzl et al. (2002)	Mullett Lake MI
323	-84.58870000	45.52021000	212.8	Wyebridge	Schaetzl et al. (2002)	Mullett Lake MI
324	-84.59014000	45.50540000	231.2	Supplemental	Schaetzl et al. (2002)	Mullett Lake MI
325	-84.59833000	45.51805000	225.1	Main	Schaetzl et al. (2002)	Mullett Lake MI
326	-84.65294000	45.53869000	210.6	Wyebridge	Schaetzl et al. (2002)	Indianville MI
327	-84.67479000	45.55726000	229.3	Main	Schaetzl et al. (2002)	Indianville MI
328	-84.71226000	45.52652000	221.6	Ardtrea	Schaetzl et al. (2002)	Indianville MI
329	-84.80139000	45.57997000	225.0	Main	Schaetzl et al. (2002)	Pellston MI

SID	Longitude	Latitude	H	Phase	Surveyed by:	USGS Quadname
330	-84.84149000	45.68009000	232.5	Main	Schaetzl et al. (2002)	Levering MI
333	-84.62920000	45.66410000	226.1	Ardtrea	Schaetzl et al. (2002)	Freedom MI
334	-83.62305603	45.32519387	210.4	Supplemental	Schaetzl et al. (2002)	Thompsons Harbor
335	-83.59894435	45.25779824	219.6	Ardtrea	Schaetzl et al. (2002)	Thompsons Harbor
341	-84.45442644	45.47459575	225.9	Main	Schaetzl et al. (2002)	Legrand MI
342	-84.19049326	45.40898973	225.5	Main	Schaetzl et al. (2002)	Black Lake Bluffs
343	-84.13565017	45.42469734	228.0	Main	Schaetzl et al. (2002)	Black Lake Bluffs
344	-84.13851006	45.42464758	219.0	Upper Orillia	Schaetzl et al. (2002)	Black Lake Bluffs
356	-84.20202880	45.49575522	220.2	Upper Orillia	Schaetzl et al. (2002)	Black Lake Bluffs
357	-84.21784849	45.52079069	227.3	Main	Schaetzl et al. (2002)	Grace MI
358	-84.22302439	45.52256839	229.5	Main	Schaetzl et al. (2002)	Grace MI
359	-84.22880504	45.43421460	209.5	Wyebridge	Schaetzl et al. (2002)	Black Lake Bluffs
360	-84.08819982	45.40879539	222.7	Ardtrea	Schaetzl et al. (2002)	Ocqueoc MI
361	-84.08810804	45.40886362	225.4	Main	Schaetzl et al. (2002)	Ocqueoc MI
362	-84.04832592	45.46319257	218.5	Supplemental	Schaetzl et al. (2002)	Ocqueoc MI
363	-84.04778740	45.46284301	227.5	Main	Schaetzl et al. (2002)	Ocqueoc MI
364	-84.04769782	45.46213165	227.8	Main	Schaetzl et al. (2002)	Ocqueoc MI
367	-83.98904505	45.45278767	229.4	Main	Schaetzl et al. (2002)	Moltke MI
368	-83.88414029	45.39936502	222.9	Ardtrea	Schaetzl et al. (2002)	Moltke MI
369	-83.82380683	45.38785866	225.7	Main	Schaetzl et al. (2002)	Rogers City MI
370	-83.69338766	45.33825394	206.5	Supplemental	Schaetzl et al. (2002)	Posen MI

SID	Longitude	Latitude	H	Phase	Surveyed by:	USGS Quadname
371	-84.67629206	46.44486940	270.2	Upper Orillia	Schaetzl et al. (2002)	Dollar Settlement
372	-84.74021453	46.43716052	259.7	Lower Orillia	Schaetzl et al. (2002)	Dollar Settlement
374	-84.74495853	46.43867465	231.3	Cedar Point	Schaetzl et al. (2002)	Dollar Settlement
375	-84.64920303	45.57800168	224.3	Ardtrea	Schaetzl et al. (2002)	Indianville MI
376	-84.74911461	45.37772823	215.0	Ardtrea	Schaetzl et al. (2002)	Burt Lake MI
377	-84.63313100	45.44144764	211.2	Supplemental	Schaetzl et al. (2002)	Burt Lake MI
378	-84.58903554	45.42530622	207.4	Wyebridge	Schaetzl et al. (2002)	Indian River MI
379	-84.57091213	45.42319758	218.2	Ardtrea	Schaetzl et al. (2002)	Indian River MI
381	-84.71036395	45.37740598	214.4	Ardtrea	Schaetzl et al. (2002)	Burt Lake MI
382	-84.77874610	45.38385287	223.0	Main	Schaetzl et al. (2002)	Alanson MI
383	-84.77755629	45.38321676	217.8	Ardtrea	Schaetzl et al. (2002)	Alanson MI
385	-84.83107870	45.43714322	225.3	Supplemental	Schaetzl et al. (2002)	Alanson MI
386	-84.80538259	45.53183628	222.1	Ardtrea	Schaetzl et al. (2002)	Pellston MI
387	-84.80544307	45.53189694	223.4	Main	Schaetzl et al. (2002)	Pellston MI
388	-84.70242937	45.61685275	229.7	Main	Schaetzl et al. (2002)	Indianville MI
389	-84.40614855	46.25881886	221.2	Cedar Point	Schaetzl et al. (2002)	Dafter MI
390	-84.92605951	45.55080838	223.6	Main	Schaetzl et al. (2002)	Larks Lake MI
391	-84.90655181	46.44482623	234.5	Penetang	Schaetzl et al. (2002)	McNearney Lake MI
392	-84.90681053	46.43164950	261.1	Lower Orillia	Schaetzl et al. (2002)	McNearney Lake MI
393	-84.90723553	46.42600783	281.9	Main	Schaetzl et al. (2002)	McNearney Lake MI
395	-84.21857808	46.48512906	240.2	Payette	Schaetzl et al. (2002)	Baie de Wasai MI

SID	Longitude	Latitude	H	Phase	Surveyed by:	USGS Quadname
396	-84.21825660	46.45945842	228.8	Sheguiandah	Schaetzl et al. (2002)	Baie de Wasai MI
397	-84.45054458	45.47556791	217.2	Upper Orillia	Schaetzl et al. (2002)	Legrand MI
398	-84.45045627	45.47174045	221.8	Ardtrea	Schaetzl et al. (2002)	Legrand MI
399	-83.47505515	45.18305170	213.4	Upper Orillia	Schaetzl et al. (2002)	Long Lake East MI
400	-83.47477603	45.18315549	210.6	Wyebridge	Schaetzl et al. (2002)	Long Lake East MI
401	-84.63595218	46.43961387	240.4	Penetang	Schaetzl et al. (2002)	Dollar Settlement
402	-83.52638080	44.96914845	209.9	Ardtrea	Schaetzl et al. (2002)	Big Ravine Creek
403	-84.82851886	46.43381986	230.2	Cedar Point	Schaetzl et al. (2002)	Pendills Lake MI
404	-84.83609532	46.42109801	259.5	Lower Orillia	Schaetzl et al. (2002)	Pendills Lake MI
406	-84.74408419	46.38566303	272.2	Ardtrea	Schaetzl et al. (2002)	Dollar Settlement
407	-84.21838987	46.48460739	241.2	Payette	Schaetzl et al. (2002)	Baie de Wasai MI
409	-83.32930199	44.78509654	197.7	Lower Orillia	Schaetzl et al. (2002)	Black River MI
410	-83.40495598	45.13449345	214.2	Upper Orillia	Schaetzl et al. (2002)	Long Lake East MI
412	-83.42845631	44.44738975	196.0	Upper Orillia	Schaetzl et al. (2002)	Foote Site Village
415	-83.31709229	44.60621500	199.2	Upper Orillia	Schaetzl et al. (2002)	Greenbush MI
416	-83.30402450	44.74327233	195.6	Lower Orillia	Schaetzl et al. (2002)	Harrisville MI
417	-83.29081057	44.70767625	194.0	Lower Orillia	Schaetzl et al. (2002)	Harrisville MI
418	-83.47441160	45.23744780	157.1	Supplemental	Schaetzl et al. (2002)	Long Lake East MI
419	-83.55748810	45.22256920	217.7	Supplemental	Schaetzl et al. (2002)	Long Lake West MI
420	-83.55755667	45.22479077	201.6	Supplemental	Schaetzl et al. (2002)	Long Lake West MI
421	-83.58602001	45.21953387	221.6	Main	Schaetzl et al. (2002)	Long Lake West MI

SID	Longitude	Latitude	H	Phase	Surveyed by:	USGS Quadname
422	-83.48511400	44.93197274	209.4	Ardtrea	Schaetzl et al. (2002)	Ossineke MI
426	-83.30301677	44.64424244	189.5	Supplemental	Schaetzl et al. (2002)	Harrisville MI
430	-83.42333174	44.87308497	209.0	Ardtrea	Schaetzl et al. (2002)	Spruce MI
431	-83.42505556	44.87319590	214.0	Main	Schaetzl et al. (2002)	Spruce MI
432	-83.45062220	44.90216957	211.9	Ardtrea	Schaetzl et al. (2002)	Ossineke MI
435	-83.42503845	44.87325454	213.9	Main	Schaetzl et al. (2002)	Spruce MI
436	-83.30298278	44.64430982	190.2	Supplemental	Schaetzl et al. (2002)	Harrisville MI
440	-85.19560860	46.09898741	249.2	Main	Schaetzl et al. (2002)	Epoufette MI
441	-85.15435504	46.10454764	250.8	Main	Schaetzl et al. (2002)	Epoufette MI
442	-85.17520487	46.06371179	214.6	Supplemental	Schaetzl et al. (2002)	Epoufette MI
443	-84.97784297	46.17370048	259.1	Main	Schaetzl et al. (2002)	Ozark MI
445	-84.78927924	46.11430390	257.7	Main	Schaetzl et al. (2002)	Ozark SE MI
446	-84.84366807	46.09717148	239.1	Upper Orillia	Schaetzl et al. (2002)	Ozark SE MI
447	-84.72485788	46.11805526	245.4	Upper Orillia	Schaetzl et al. (2002)	Charles MI
448	-84.36269308	46.08904251	249.5	Upper Orillia	Schaetzl et al. (2002)	Pickford SE MI
449	-84.33750218	46.10228830	227.0	Supplemental	Schaetzl et al. (2002)	Pickford SE MI
450	-84.40501602	46.07400022	258.4	Ardtrea	Schaetzl et al. (2002)	Hessel MI
451	-84.44699546	46.07161098	265.7	Main	Schaetzl et al. (2002)	Hessel MI
452	-84.46699744	46.05520906	241.4	Upper Orillia	Schaetzl et al. (2002)	Hessel MI
453	-84.21703213	46.45848640	228.2	Sheguiandah	Schaetzl et al. (2002)	Baie de Wasai MI
454	-85.02418164	46.33678241	276.8	Supplemental	Schaetzl et al. (2002)	Eckerman MI

SID	Longitude	Latitude	H	Phase	Surveyed by:	USGS Quadname
455	-85.03058381	46.35106008	259.7	Upper Orillia	Schaetzl et al. (2002)	Eckerman MI
456	-85.06933171	46.41646149	249.0	Wyebridge	Schaetzl et al. (2002)	Piatt Lake MI
457	-85.08359452	46.42155634	258.0	Lower Orillia	Schaetzl et al. (2002)	Piatt Lake MI
458	-85.09491566	46.49957572	233.6	Penetang	Schaetzl et al. (2002)	Piatt Lake MI
459	-85.11635073	46.47715490	276.7	Supplemental	Schaetzl et al. (2002)	Piatt Lake MI
460	-85.22599496	46.47753561	261.0	Lower Orillia	Schaetzl et al. (2002)	Big Beaver Creek MI
461	-85.00674669	46.38988785	255.7	Lower Orillia	Schaetzl et al. (2002)	Piatt Lake MI
463	-84.27014191	45.55388648	229.7	Main	Schaetzl et al. (2002)	Manning MI
464	-84.20690114	45.50243140	217.2	Supplemental	Schaetzl et al. (2002)	Grace MI
465	-84.21234800	45.50911718	221.7	Upper Orillia	Schaetzl et al. (2002)	Grace MI
466	-84.54980477	45.57589774	225.6	Ardtrea	Schaetzl et al. (2002)	Mullett Lake MI
467	-84.55853828	45.59495159	226.2	Ardtrea	Schaetzl et al. (2002)	Mullett Lake MI
468	-84.61109548	45.64852333	231.2	Main	Schaetzl et al. (2002)	Point Nipigon MI
469	-84.61092475	45.64875361	227.4	Ardtrea	Schaetzl et al. (2002)	Point Nipigon MI
470	-84.60114369	45.63751326	230.6	Main	Schaetzl et al. (2002)	Point Nipigon MI
471	-84.59611067	45.63766964	233.4	Main	Schaetzl et al. (2002)	Point Nipigon MI
472	-84.45442526	45.47459652	225.8	Main	Schaetzl et al. (2002)	Legrand MI
501	-84.35307774	46.58282675	307.3	Main	Cowan (1985)	Sault Sainte Marie-E
507	-84.34384520	46.56875261	247.7	Payette	Cowan (1985)	Sault Sainte Marie-E
508	-84.34392283	46.56983441	254.4	Cedar Point	Cowan (1985)	Sault Sainte Marie-E
516	-84.38323813	46.56642152	247.2	Payette	Cowan (1985)	Sault Sainte Marie-E

SID	Longitude	Latitude	H	Phase	Surveyed by:	USGS Quadname
517	-84.38334252	46.56696391	253.7	Cedar Point	Cowan (1985)	Sault Sainte Marie-E
522	-84.41477525	46.56182938	243.8	Payette	Cowan (1985)	Sault Sainte Marie-E
523	-84.41492481	46.56417276	253.5	Cedar Point	Cowan (1985)	Sault Sainte Marie-E
524	-84.41616848	46.56546089	264.5	Penetang	Cowan (1985)	Sault Sainte Marie-E
525	-84.41719644	46.56854412	275.3	Wyebridge	Cowan (1985)	Sault Sainte Marie-E
526	-84.41759403	46.57116310	290.9	Upper Orillia	Cowan (1985)	Sault Sainte Marie-E
991	-83.35040849	45.92941133	261.4	Supplemental	Drzyzga (this work)	Alpena-W
992	-83.35014286	45.92930711	265.6	Supplemental	Drzyzga (this work)	Alpena-W
993	-83.35018783	45.92904659	267.0	Supplemental	Drzyzga (this work)	Alpena-W
994	-83.35023280	45.92878607	268.4	Supplemental	Drzyzga (this work)	Alpena-W
995	-83.43138274	44.47595453	204.3	Supplemental	Drzyzga (this work)	Foote Site Village
996	-83.43335401	44.47579292	211.4	Supplemental	Drzyzga (this work)	Foote Site Village
997	-83.34475011	45.95382812	222.0	Supplemental	Drzyzga (this work)	Alpena-W
998	-83.37191795	45.94480089	241.9	Supplemental	Drzyzga (this work)	Alpena-W
999	-83.45614737	44.40725030	203.0	Supplemental	Drzyzga (this work)	Foote Site Village

APPENDIX B: SCRIPTS WRITTEN FOR USE WITH R

This appendix contains four scripts that were written for use in the R environment for statistical computing. The first two (i.e., first.R and second.R, supported exploratory data analysis and were used to build initial water plane models via ordinary and generalized least squares, respectively. The third (third.R) supported cross-validated assessment of the generalized model. And the fourth script (i.e., predictWaterplane.R) makes the final predictions and reconstructs the ancient water plane via universal kriging.

These scripts deal specifically with my efforts to model the Main phase of Lake Algonquin. They were not written to be used once only; rather, they were edited and tweaked dozens of times during the lengthy and iterative process of building the final prediction model. Interactive exploratory and diagnostic analyses were usually conducted before and after each run. The general structure of each script was adapted for re-use during subsequent efforts to build water plane models for lower and younger lake phases.

```
#############################################################
#
#       first.R
#
#       Scott A. Drzyzga
#       Summer 2006
#
#       Purpose: to model a differentially-uplifted water plane and estimate
#               parameters that describe rates of uplift.  This script can be adapted
#               for use with other water plane data.
#
#       Dependencies (packages):
#               gstat, geoR, and sp.
#
#       Dependencies (objects):
#               main: a data.frame object that contains paleoshoreline position
#                       data.
#               distance.R: an script that defines an R function to calculate an
#                       interdistance matrix for a sample of points.
#
#############################################################
#
#       Specify the form of the ordinary least squares model.
#
main.formula <- z~x+I(x*y)+I(x^2)+I(y^2)
#
#       Create and format main.xyz for simple and easy use.
#
main.xyz <- as.data.frame(cbind(main$SID, main$E, main$N, main$H))
colnames(main.xyz) <- cbind("SID","E","N","z")
#
#       Scale and transform MIGEOREF coordinates (m) to a local coordinate
#               system (local origin and km units of measure).
#
main.xyz$x <- (main.xyz$E - 532000) / 1000
main.xyz$y <- (main.xyz$N - 468000) / 1000
#
#       Calculate the inter-distance matrix
#
source("C:/rdata/phd/waterplanes/distance.R")
dist.mat <- calc.dist.mat(main.xyz$x, main.xyz$y)
#
```

```
#
#       Initial water plane model estimated via Ordinary Least Squares (OLS)
#       Plot residuals - stop to examine model fit, significance and check run
#               other diagnostics interactively.
#
main.ols <- lm(formula=main.formula, data=main.xyz)
main.xyz$olsr <- main.ols$residuals
qq.plot(main.xyz$olsr)
summary(main.ols$residuals)
#
#       Perform variography of OLS residuals.
#       Distance units are in km, elevation units are in meters.
#       Explore, visualize, and assess interactively.
#
main.geo <- as.geodata(main.xyz, coords.col=5:6, data.col=7)
main.var <- variog(main.geo, option="bin", pairs.min=6, direction=110, ~
tolerance=45, unit.angle="degrees", max.dist=100, breaks=seq(from=0, to=60, ~
by=range))
#
main.var$km <- main.var$u
plot(main.var$km, main.var$v, xlim=c(0,60), ylim=c(0,15), pch=16,col=rgb(0,0,1))
#
abline(v=0, col="gray", lty=2)
abline(h=var(main.xyz$olsr), col="red", lty=3)
#
#       Examine empirical variogram and fit a variogram model by eye.
#               (of the flexible Matern class)
#
my.nug <- 2.2
my.sil <- 3.5
my.ran <- 19
my.kap <- 0.5
lines.variomodel(cov.model="matern", cov.pars=c(my.sil,my.ran), ~
nugget=my.nug, kappa=my.kap, max.dist=60, col="black", lty=1)
#
#       Write positions and residuals to a CSV file to visualize pattern in a GIS.
#
write.csv(main.xyz, file="mainxyz.csv", row.names=FALSE)
#
##########################################################
```

```
#############################################################
#
#       second.R
#
#       Scott A. Drzyzga
#       Summer 2006
#
#       Purpose: to fit polynomial uplift model via generalized least squares.
#
#       Dependencies (packages):
#               gstat, geoR, and sp.
#
#       Dependencies (objects):
#               dist.mat: a matrix object that contains distances between pairs of
#                       paleoshoreline data.
#               my.nug, my.sil, my.ran, and my.kap: parameters of the chosen
#                       variogram model (assuming Matern class).
#               main.xyz: a data.frame object that contains paleoshoreline position
#                       data and OLS residuals - obtained from first.R script.
#               main.formula: formula object that specifies form of the trend model
#
#############################################################
#
#       Build the spatial covariance matrix.
#
main.cov <- cov.spatial(dist.mat, cov.model=c("pure.nugget","matern"),
cov.pars=rbind(c(my.nug,0),c(my.sil,my.ran)), kappa=my.kap)
#
#       Alternate covariance matrix when spatial structure is absent.
#
# main.cov <- cov.spatial(dist.mat, cov.model="pure.nugget", cov.pars=c(4,0))
#
#       Fit model via Generalized Least Squares (GLS).
#       Examine model for fitness and assess residuals for warning signs.
#
main.gls <- lm.gls(formula=main.formula, data=main.xyz, W=main.cov, ~
inverse=TRUE)
#
main.xyz$glsr <- main.gls$residuals
summary(main.gls$residuals)
qq.plot(main.xyz$glsr)
#
```

```
#
#       Examine GLS residuals for signs of any remaining spatial structure.
#       Conduct a variography of GLS residuals.
#       Explore, visualize, and assess interactively.
#
main.gr.geo <- as.geodata(main.xyz, coords.col=5:6, data.col=8)
main.gr.var <- variog(main.gr.geo, option="bin", pairs.min=6, ~
breaks=seq(0,60,range))
#
main.gr.var$km <- main.gr.var$u
write.csv(main.xyz, file="mainxyz.csv", row.names=FALSE)
plot(main.gr.var$km, main.gr.var$v, xlim=c(0,60), ylim=c(0,15), pch=16, ~
col=rgb(0,0,1))
#
abline(v=0, col="gray", lty=2)
abline(h=var(main.xyz$glsr), col="red", lty=3)
# lines.variomodel(cov.model="pure.nugget", cov.pars=c(4,0), nugget=0, ~
max.dist=60, col="black", lty=1)
#
lines.variomodel(cov.model="matern", cov.pars=c(my.sil, my.ran), ~
nugget=my.nug, kappa=my.kap, max.dist=60, col="black", lty=1)#
#
##########################################################
```

```
#############################################################
#
#       third.R
#
#       Scott A. Drzyzga
#       Summer 2006
#
#       Purpose: Assess prediction model via cross-validated universal kriging.
#
#       Dependencies (packages):
#               gstat, geoR, and sp.
#
#       Dependencies (objects):
#               my.nug, my.sil, my.ran, and my.kap: parameters of the chosen
#                       variogram model (assuming Matern class).
#               main.xyz: a data.frame object that contains paleoshoreline position
#                       data and OLS residuals - obtained from first.R script.
#               main.formula: formula object that specifies form of the trend
#                       model.
#
#############################################################
#
#       Build prediction model with trend and aspatial variance components only.
#       Start by establishing a gstat object and the underlying trend component.
#
main.pnug.gstat <- gstat(id="lake", formula=main.formula, locations=~x+y,
data=main.xyz)
#
#       Add aspatial variance component to the gstat object (pure nugget)
#
main.pnug.gstat <- gstat(main.pnug.gstat, id="lake", ~
model=vgm(psill=my.sil+my.nug, model="Nug", range=0, nugget=0))
#
#       Generate residuals via cross-validated universal kriging.
#       Explore, visualize, and assess interactively.
#
main.pnug.cvuk <- gstat.cv(main.pnug.gstat)
main.xyz$pnug <- main.pnug.cvuk$residual
qq.plot(main.xyz$pnug)
summary(main.xyz$pnug)
#
#       Build another prediction model with spatial trend, spatial covariance, and
#               aspatial variance components.
```

```
#       Start by establishing a gstat object and the underlying trend component.
#
main.gstat <- gstat(id="lake", formula=main.formula, locations=~x+y, ~
data=main.xyz)
#
#       Specify a variogram model that describes spatial covariance structure.
#       Add it to the gstat object.
#
main.vgm <- vgm(psill=my.sil, model="Mat", range=my.ran*10, nugget=my.nug,
~ kappa=my.kap, anis=c(110,0.1))
main.gstat <- gstat(main.gstat, id="lake", model=main.vgm)
#
#       Generate residuals via cross-validated universal kriging.
#       Explore, visualize, and assess interactively.
#       Write results to a CSV file for import into a GIS.
#
main.cvuk <- gstat.cv(main.gstat)
main.xyz$cvukr <- main.cvuk$residual
qq.plot(main.xyz$cvukr)
#
write.csv(main.xyz, file="mainxyz.csv", row.names=FALSE)
##########################################################
```

```
#############################################################
#
#       predictWaterplane.R
#
#       Scott A. Drzyzga
#       Summer 2006
#
#       Purpose: to generate prediction and uncertainty surfaces for the Main
#               Algonquin water plane.
#       This specific script can be modified to predict other water planes given an
#               appropriate sample of x,y,z data..
#
#       Dependencies (packages):
#               gstat, geoR, and sp.
#
#       Dependencies (objects):
#               main.gstat: a gstat object that specifies the prediction method and
#                       variogram model.
#               predict.here: a data.frame object with grid cell locations (in local
#                       coordinate system) where predictions should occur.
#
#############################################################
#
#       Load required packages, if not loaded already.
#       Allocate a large chunk of RAM to the process.
#
library(geoR)
library(gstat)
library(maptools)
memory.limit(1700)
#
#       Load file containing coordinates of locations needing predictions
#               (in local coordinate system).
#
load("C:/rdata/phd/waterplanes/predict.here")

#
#       Surface prediction via universal kriging
#
predict <- predict.gstat(main.gstat, newdata=main.grd, BLUE=FALSE, nsim=0)
colnames(predict) <- cbind("x","y","pred","kvar")
#
#       Scale and translate local coordinates back to MIGEOREF coordinates
```

```
#
predict$x <- predict$x * 1000 + 532000
predict$y <- predict$y * 1000 + 468000
#
#       Reformat data.frame for export to ASCII grid format.
#          Undocumented quirk:
#                Setting the na.value to an integer value will create an integer grid.
#                Setting the na.value to a non-integer value will create a floating
#                      point grid.
#
#
coordinates(predict) <- ~x+y
gridded(predict) <- TRUE
write.asciigrid(predict, "mainPred.asc", attr="pred", na.value=-99.9)
write.asciigrid(predict, "mainKvar.asc", attr="kvar", na.value=-99.9)
rm(predict, main.grd)
#
#
#       Garbage collection: returns memory to the operating system after a
#                memory-hogging model run.
#
#
gc()
#
#
############################################################
```

REFERENCES

Andrews JT (1970) Present and postglacial rates of uplift for glaciated northern and eastern North America derived from postglacial uplift curves, *Canadian Journal of Earth Sciences* 7: 703-715.

Angel JR (1995) Large-scale storm damage on the U.S. shores of the Great Lakes, *Journal of Great Lakes Research* 21(3): 287-293.

Argylian EP, Forman SL, Johnston JW and Wilcox DA (2005) Optically stimulated luminescence dating of late Holocene raised strandplain sequences adjacent to Lakes Michigan and Superior, Upper Peninsula, Michigan, USA. *Quaternary Science Reviews* 63: 122-135.

Baedke SJ and Thompson TA (2000) A 4,700-year record of the lake level and isostasy for Lake Michigan, *Journal of Great Lakes Research* 26(4): 416-426.

Baedke SJ, Thompson TA, Johnston JW, and Wilcox DA (2004) Reconstructing paleo lake levels from relict shorelines along the Upper Great Lakes, *Aquatic Ecosystems Health & Management; Special Issue: Emerging issues in Lake Superior Research* 7(4): 435-449.

Bailey TC and Gatrell AC (1995) *Interactive spatial data analysis,* Essex, England: Longman Group Limited.

Bertin J (1983) *Semiology of graphics: Diagrams, networks, maps.* (Translation from a French 1967 edition by W. Berg [Ed]), Madison, WI: University of Wisconsin Press.

Bishop CT (1990) Historical variation of water levels in Lakes Erie and Michigan-Huron, *Journal of Great Lakes Research* 16(3): 406-425.

Bivand R, (2005) *Maptools version 0.4-13.* [URL] http://www.R-project.org, Last viewed on August 10, 2006.

Blake EC (1999) *Where be "Here be Dragons"?* [URL] http://www.maphist.nl/extra/herebedragons.html, Last viewed on July 31, 2006.

Blewett WL (1995) Deglaciation history of the Port Huron moraine in northwestern Lower Michigan. *Great Lakes Geographer* 2(1): 1-15.

Bolstad PV and Stowe T (1994) An evaluation of DEM accuracy: Elevation, slope and aspect, *Photogrammetric Engineering & Remote Sensing* 60(11): 1327-1332.

Bossler JD (1984) *Standards and specification for geodetic control networks*, Rockville, MD: United States National Geodetic Information Branch.

Broecker WS (1966) Glacial rebound and the deformation of the shorelines of proglacial lakes, *Journal of Geophysical Research* 71: 4777-4783.

Broecker WS and Farrand WR (1963) Radiocarbon age of the Two Creeks forest bed, Wisconsin, *Geological Society of America Bulletin* 74: 795-802.

Brown DG and Bara TJ (1994) Recognition and reduction of systematic error in elevation and derivative surfaces from 7.5-minute DEMs, *Photogrammetric Engineering & Remote Sensing* 60(2): 189-194.

Burgis WA (1977) Late-Wisconsinan history of northeastern lower Michigan, *Ph.D. Dissertation*, University of Michigan, 396 pages.

Burrough PA (1991) Sampling designs for quantifying map unit composition. In Mausbach MJ and Wilding LP (Eds) *Spatial variabilities of soils and landforms,* Madison, WI: Soil Science Society of America, Inc.

Burrough PA (1992) Development of intelligent geographic information systems, *International Journal of Geographic Information Systems* 6(1): 1-11.

Burrough PA and McDonnell RA (1998) *Principles of Geographical Information Systems,* Oxford: Oxford University Press.

Buttenfield BP (1993) Representing data quality, *Cartographica* 30(2/3): 1-7.

Carter JR (1992) The effect of data precision on the calculation of slope and aspect using gridded DEMs, *Cartographica* 29(1): 22-34.

Cashman WJ and Wojan EB (1977) *The Wojan-Cashman Map of Beaver Island Charlevoix County, Michigan* [Map: nominal scale 1:31,680], Lansing, Michigan: Wellman Press, Inc.

Changnon SA (2004) Temporal behavior of levels of the Great Lakes and climate variability, *Journal of Great Lakes Research* 30(1): 184-200.

Chapman LJ and Putnam DF (1966) *The physiography of southern Ontario,* Toronto, Ontario: Ontario Research Foundation.

Christakos G (2000) *Modern spatiotemporal geostatistics,* Oxford: Oxford University Press.

Clark JA, Hendriks M, Timmermans TJ, Struck C and Hilverda KJ (1994) Glacial isostatic deformation of the Great Lakes region, *Geological Society of America Bulletin* 106: 19-31.

Clark RH and Persoage NP (1970) Some implications of crustal movement in engineering planning, *Canadian Journal of Earth Science* 7:628-633.

Clark JA, Pringer II HS, Walsh JK, Primus JA (1990) A numerical model of glacial isostasy in the Lake Michigan basin, in Schneider AF and Fraser GS (Eds) *Late Quaternary history of the Lake Michigan basin*, Boulder, Colorado: Geological Society of America, Special Paper 251.

Coordinating Committee on Great Lakes Basic Hydraulic and Hydrologic Data (2001) *Apparent vertical movement over the Great Lakes: Revisited,* Chicago, IL.

Coordinating Committee on Great Lakes Basic Hydraulic and Hydrologic Data (1977) *Apparent vertical movement over the Great Lakes,* Chicago, IL.

Couclelis H (1992) People manipulate objects (but cultivate fields): beyond the raster-vector debate in GIS, In Frank AU, Campari I and Formentini U (eds) *Theories and methods of spatio-temporal reasoning in geographic space,* p65-77. Berlin: Springer Verlag.

Couclelis H (2003) The certainty of uncertainty: GIS and the limits of geographical knowledge, *Transactions in GIS* 7(2): 165-175.

Cova TJ and Goodchild MF (2002) Extending geographical representation to include fields of spatial objects, *International Journal of Geographical Information Science* 16(6):509-532.

Cowan WR (1985) Deglacial Great Lakes shorelines at Sault Ste. Marie, Ontario, In Karrow PF and Calkin P (Eds) Quaternary Evolution of the Great Lakes, *Geological Association of Canada Special Paper 30,* St. Johns, Newfoundland: Geological Association of Canada, p.33-37.

Cowell PJ and Zeng TQ (2003) Integrating Uncertainty Theories with GIS for Modeling Coastal Hazards of Climate Change: Special Issue on Marine and Coastal GIS, *Marine Geodesy* 26(1-2): 5-18.

Deane RE (1950) *Pleistocene geology of the Lake Simcoe district, Ontario,* Geological Survey of Canada, Memoir 256, 108p.

Dietrich RV (1978) Post-Valders Geological History of Beaver Island, Michigan, *Michigan Academician* 10(3):283-297.

Diggle PJ and Ribeiro Jr. PJ (2002) Bayesian inference in Gaussian model-based geostatistics, *Geographical & Environmental Modelling* 6(2): 129-146.

Drzyzga SA, Shortridge A, and Schaetzl RJ (2002) Revealing uncertainty in maps of Glacial Lake Algonquin, In Richardson D and van Oosterom P (Eds) *Advances in Spatial Data Handling,* Berlin: Springer-Verlag, p. 377-390.

Eshman DF and Karrow PF (1985) Huron Basin glacial lakes: A review, in Karrow PF and Calkin P (Eds) Quaternary evolution of the Great Lakes. *Geological Association of Canada Special Paper 30,* St. Johns, Newfoundland: Geological Association of Canada, p.79-93.

Fairchild H (1926) Changing levels of the Great Lakes, *Scientific Monthly* 22(3): 193-199.

Farrand WR (1967, revised 1998) The glacial lakes of Michigan, *Michigan Department of Natural Resources Bulletin 4,* Lansing, Michigan: Michigan Department of Natural Resources.

Farrand WR and Bell DL (1982) *Quaternary Geology of Southern Michigan* [Map: nominal scale 1:500,000], Lansing, Michigan: State of Michigan Department of Natural Resources.

Farrand WR and Drexler CW (1985) Late Wisconsinan and Holocene history of the Lake Superior basin, in Karrow PF and Calkin P (Eds) Quaternary Evolution of the Great Lakes, *Geological Association of Canada Special Paper 30.* St. Johns, Newfoundland: Geological Association of Canada, p.33-37.

Farrand WR and Eschman DF (1974) Glaciation of the southern peninsula of Michigan; A review, *Michigan Academician* 7(1): 31-56.

Finamore PF (1985) Glacial Lake Algonquin and the Fenelon Falls outlet, in Karrow PF and Calkin P (Eds) Quaternary Evolution of the Great Lakes, *Geological Association of Canada Special Paper 30.* St. Johns, Newfoundland: Geological Association of Canada, p.125-132.

Firth CR, Smith DE and Cullingford RA (1993) Late Devensian and Holocene glacio-isostatic uplift patterns in Scotland, In Owen LA, Stewart I and Vita-Finzi C (eds) Neotectonics: Recent advances, *Quaternary Proceedings No. 3.* Cambridge: Quaternary Research Association.

Fisher P (1998) Improved modeling of elevation error with geostatistics, *GeoInformatica* 2(3): 215-233.

Flannery JJ (1956) The graduated circle: A description, analysis, and evaluation of a quantitative map symbol. *Unpublished PhD Dissertation*. Department of Geography, University of Wisconsin.

Foody GM (2003) Uncertainty, knowledge discovery and data mining in GIS, *Progress in Physical Geography* 27(1): 113-121.

Futyma RP (1981) The northern limits of glacial Lake Algonquin in upper Michigan, *Quaternary Research* 15: 291-310.

Gabriel AO, Kreutzwiser RD, and Stewart CJ (1997) Great Lakes Flood thresholds and impacts, *Journal of Great Lakes Research* 23(3): 286-296.

Gesch D, Williams J and Miller W (2001) A comparison of US Geological Survey seamless elevation models with Shuttle Radar Topography Mission data, In Milne T (ed) *Proceedings of IGARSS 2001, v.2*. International Geoscience and Remote Sensing Symposium, p 754-756.

Gesch D, Oimoen M, Greenlee S, Nelson C, Steuck M and Taylor D (2002) The National Elevation Dataset, *Photogrammetric Engineering & Remote Sensing* 68(1): 1327-1332.

Gilbert GK (1898) Recent earth movements in the Great Lakes region, US *Geological Survey 18th Annual Report, Part 2* pages 601-647.

Goldthwait JW (1908) A reconstruction of water planes of the extinct glacial lakes in the Michigan basin, *Journal of Geology* 16: 459-476.

Goldthwait JW (1910) An instrumental survey of the shore-lines of the extinct Lakes Algonquin and Nipissing in southwestern Ontario, *Canada Geological Survey Branch Memoir* 10:1-57.

Goodchild MF and Gopal S (1989) *The accuracy of spatial databases,* London: Taylor & Francis.

Goovaerts P (1998) Impact of simulation algorithm, magnitude of ergodic fluctuations and number of realizations on the spaces of uncertainty of flow predictions, *Unpublished Annul Report No. 11.* Stanford Center for Reservoir Forecasting, Stanford University.

Government of Canada, Natural Resources Canada, Centre for Topographic Information (1994) Meldrum Bay, Edition 3 [Map] *1:50,000 National Topographic Series of Maps for Canada,* Ottawa, Ontario: Natural Resources Canada.

Government of Canada, Natural Resources Canada, Geodetic Survey Division (2003) *Canadian Spatial Reference System Online Database,* Ottawa, Ontario: Natural Resources Canada.

Graham D, Sault M, and Captain Bailey J (2003) National Ocean Service Shoreline - Past, Present, and Future, *Journal of Coastal Research, Special Issue 38*: 14-32.

Gringarten E and Deutsch CV (2001) Teacher's aide: Variogram interpretation and modeling. *Mathematical Geology* 33(4): 507-534.

Hansel AK, Mickelson DM, Schneider AF and Larsen CE (1985) Late Wisconsinan and Holocene history of the Lake Michigan basin, , In Karrow PF and Calkin P (Eds) Quaternary evolution of the Great Lakes. *Geological Association of Canada Special Paper 30,* St. Johns, Newfoundland: Geological Association of Canada, p.39-53.

Hartmann HC (1988) Historical basis for limits on Lake Superior water level regulations, *Journal of Great Lakes Research* 14(3): 316-324.

Hennecke WG, Greve CA, Cowell PJ, and Thom BG (2004) GIS-Based Coastal Behavior Modeling and Simulation of Potential Land and Property Loss: Implications of Sea-Level Rise at Collaroy/Narrabeen Beach, Sydney (Australia), *Coastal Management* 32(4): 449-470.

Heuvelink GBM (1998) *Error propagation in environmental modeling with GIS,* Bristol, PA: Taylor & Francis.

Heuvelink GBM and Burrough PA (2002) Developments in statistical approaches to spatial uncertainty and its propagation, *International Journal of Geographic Information Science* 16(2): 111-113.

Holmes KW, Chadwick OA and Kyriakidis PC (2000) Error in a USGS 30-meter digital elevation model and its impact on terrain modeling, *Journal of Hydrology* 233: 154-173.

Hough JL (1958) *Geology of the Great Lakes,* Urbana, IL: University Illinois Press.

Hunter GJ and Goodchild MF (1997) Modeling the uncertainty of slope and aspect estimates from spatial databases, *Geographical Analysis* 29: 35-49.

Hutchinson MF and Gallant JC (2000) Digital elevation models and representation of terrain slope, Chapter 2 in Wilson JP and Gallant JC (Eds) *Terrain analysis: Principles and applications,* New York, NY: John Wiley & Sons, Inc. p.29-50.

Isaaks EH and Srivastava RM (1989) *Applied geostatistics,* New York, NY: Oxford University Press.

Johnston JW (2004) Changes in water level, vertical ground movement, shoreline behavior and climate in the Lake Superior Basin during the last 5,000 years. *Ph.D. Dissertation,* Department of Geological Sciences, Indiana University.

Journel AJ and Huijbregts CJ (1978) *Mining geostatistics,* London: Academic Press.

Karrow PF (2002) Comment on "Formation of large beaches in an area of rapid differential isostatic rebound: the three-outlet control of Lake Agassiz" by J.T. Teller, *Quaternary Science Reviews* 21: 2115-2118.

Karrow PF (1988) The Lake Algonquin shoreline, Kincardine - Port Elgin, Ontario, *Canadian Journal of Earth Science* 25: 157-162.

Karrow PF (1987) Glacial and glaciolacustrine events in northwestern Lake Huron, Michigan and Ontario, *Geological Society of American Bulletin* 98:113-120.

Karrow PF, Anderson TW, Clarke AH, DeLorme LD, and Sreenivasa MR (1975) Stratigraphy, paleontology, and age of Lake Algonquin sediments in southwestern Ontario, Canada, *Quaternary Research* 5: 49-87.

Kaszycki CA (1985) History of glacial Lake Algonquin in the Haliburton region, south central Ontario, in Karrow PF and Calkin P (Eds) Quaternary evolution of the Great Lakes. *Geological Association of Canada Special Paper 30,* St. Johns, Newfoundland: Geological Association of Canada, p.109-123.

Kincare KA and Larson GJ (2002) Surficial geology of northern Leelanau County; Michigan Geological Survey [Map: nominal scale 1:100,000], *Open File Report 2002-3.* Lansing, Michigan: State of Michigan Geological Survey.

Kite GW and Adamowski K (1973) Stochastic analysis of Lake Superior elevations for computation of relative crustal movement, *Journal of Hydrology* 18: 163-175.

Komar PD (1998) *Beach processes and sedimentation, 2nd edition,* Upper Saddle River, NJ: Prentice Hall.

Komar PD (1976) *Beach processes and sedimentation,* Upper Saddle River, NJ: Prentice Hall.

Krist Jr, F and Schaetzl RJ (2001) Paleowind (11,000 BP) directions derived from lake spits in Northern Michigan, *Geomorphology* 38:1-18.

Kumler MP (1994) An intensive comparison of triangulated irregular networks (TINs) and digital elevation models (DEMs), *Cartographica* 31(2):1-99.

Kyriakidis PC, Shortridge AM and Goodchild MF (1999) Geostatistics for conflation and accuracy assessment of digital elevation models, *International Journal of Geographical Information Science* 13(7): 677-707.

Larsen CE (1987) Geological history of Glacial Lake Algonquin and the upper Great Lakes, *U.S. Geological Survey Bulletin* 1801, 36 p.

Larsen CE (1994) Beach ridges as monitors of isostatic uplift in the upper Great *Lakes, Journal of Great Lakes Research* 20: 108-134.

Larson G and Schaetzl RJ (2001) Review: Origin and evolution of the Great Lakes, *Journal of Great Lakes Research* 27(4): 518-546.

Lawson AC (1891) Sketch of the coastal topography of the north side of Lake Superior with special reference to the abandoned strands of Lake Warren (the greatest of the late Quaternary lakes of North America), In Winchell NH (ed) *The Geological and Natural History Survey of Minnesota, The Twentieth-Annual Report for the Year 1891*, The Geologic and Natural History Survey of Minnesota, Minneapolis, pp. 183-289.

Lee DH and Southam C (1994) Effect and implications of differential isostatic rebound on Lake Superior's regulation limits, *Journal of Great Lakes Research* 20(2): 407-415.

Lenters JD (2001) Long-term trends in the seasonal cycle of Great Lakes water levels, *Journal of Great Lakes Research* 27(3): 342-353.

Leverett F (1913) Notes concerning the features of St. Joseph Island, Lake Huron, Ontario, in Geological Survey of Canada (Ed) Summary report of the Geological Survey, *Sessional Paper No. 26*, p.271-274.

Leverett F (1897) The Pleistocene features and deposits of the Chicago area, *Chicago Academy of Science Bulletin* 2.

Leverett F and Taylor FB (1915) The Pleistocene of Indiana and Michigan and the history of the Great Lakes, *US Geological Survey Monograph* 53.

Leverington DW, Teller JT and Mann JD (2002) A GIS method for reconstruction of late Quaternary landscapes from isobase data and modern topography, *Computers and Geosciences* 28:631-639.

Leverington DW and Teller JT (2003) Paleotopographic reconstructions of the eastern outlet of glacial Lake Agassiz, *Canadian Journal of Earth Sciences* 40(9): 1259-1278.

Lewis CFM (1969) Late Quaternary history of lake levels in the Huron and Erie basins. In *Proceedings of the 12th Conference of Great Lakes Research*, p250-270. International Association for Great Lakes Research.

Lewis CFM and Anderson TW (1985) Early Holocene lake levels in the Huron Basin: Comparative uplift histories of basins and sills in a rebounding glacial margin depression, in Karrow PF and Calkin P (Eds) Quaternary evolution of the Great Lakes. *Geological Association of Canada Special Paper 30*, St. Johns, Newfoundland: Geological Association of Canada, p.147-148.

Loope W L and Arbogast AF (2000) Dominance of a ~150-Year cycle of sand-supply change in Late Holocene dune building along the eastern shore of Lake Michigan, *Quaternary Research* 54: 414-422.

MacEachren AM (2005) Visualizing geospatial information uncertainty: What we know and what we need to know, *Cartography and Geographic Information Science* 32(3): 139-160.

MacEachren AM (1995) *How Maps Work: Representation, Visualization, and Design*, New York: The Guilford Press.

MacEachren AM (1992) Visualizing uncertain information, *Cartographic Perspectives* 13: 10-19.

Mainville A and Craymer MR (2005) Present-day tilting of the Great Lakes region based on water level gauges, *Geological Society of America Bulletin* 117(7/8): 1070-1080.

Maune DF (1996) Chapter 6: DEM Extraction, editing, matching and quality control techniques, In Greve CW (ed) *Digital Photogrammetry: An addendum to the manual of Photogrammetry*, Bethesda, MD: American Society for Photogrammetry & Remote Sensing.

McQuarrie H (2000) *Cockburn Island, Ontario* [Map: nominal scale 1:40,000].

Minasny B and McBratney AB (2005) The Matern function as a general model for soil variograms, *Geoderma* 128:192-207.

Mothersill JS and Schurer PJ (2004) Paleomagnetic Logs: A Tool for Dating Lake Erie's Past, *Studia Geophysica et Geodaetica* 47(2): 289-300.

Moore LJ (2000) Shoreline mapping techniques, *Journal of Coastal Research* 16(1): 111-124.

Morton RA and Speed FM (1998) Evaluation of shorelines and legal boundaries controlled by water levels on sandy beaches, *Journal of Coastal Research* 14(4): 1373-1384.

Motro A (1993) Sources of uncertainty in information systems. *Proceedings of the 2nd Workshop on uncertainty management and information systems: From needs to solutions*, Catalina Island, CA.

National Oceanic & Atmospheric Administration, Center for Operational Oceanographic Products and Services (2006) *Great Lakes water level data - Station selection*, [URL] http://tidesandcurrents.noaa.gov/station_retrieve.shtml?type=Great+ Lakes+Water+Level+Data, Last viewed on August 7, 2006.

National Geodetic Survey (2004) *Horizontal and vertical control data*, Silver Spring, MD: National Geodetic Survey.

National Geodetic Survey (1998) N*ational Geodetic Survey strategic plan*, Silver Spring, MD: National Geodetic Survey. Available online at: http://www.ngs.noaa.gov/INFO/NGSStratPlan98.html.

National Imaging and Mapping Agency, US Geological Survey and National Geographic Data Committee (1997) *30"-gridded DEM from DTED, precursors and derivatives*, Boulder, CO: National Geophysical Data Center.

Omre, H (1984) The variogram and its estimation, in Verly G, David M, Journel AG and Marechal A (Eds) *Geostatistics for Natural Resources Characterization, Part I*, Dordrecht: Reidel Publishing Company. p 107-125.

Openshaw S (1989) Learning to live with errors in spatial databases, In Goodchild MF and Gopal S (Eds) *The accuracy of spatial databases*. London: Taylor & Francis, p263-276.

Pang A (2001) *Visualizing uncertainty in geo-spatial data*, [URL] http://www.spatial.maine.edu/~worboys/SIE565/papers/pang%20viz%20uncert.pdf, Last viewed on July 1, 2006.

Parker BB (2003) The difficulties in measuring a consistently defined shoreline - The problem of vertical referencing, *Journal of Coastal Research, Special Issue 38*: 44-56.

Parsons S (1996) Current approaches to handling imperfect information in data and knowledge bases, *IEEE Transactions on Knowledge and Data Engineering* 8(3): 353-372.

Pebesma EJ (2004) Multivariable geostatistics in S: the gstat package, *Computers and Geosciences* 30: 683-691.

Pebesma E, Bivand R, Rowlinson B and Gomez-Rubio V (2005) *sp - version 0.7-10*, [URL] http://www.R-project.org, Last viewed on August 10, 2006.

Pengelly JW, Tinkler KJ, Parkins WG, and McCarthy FM (1997) 12600 years of lake level changes, changing sills, ephemeral lakes and Niagara Gorge erosion in the Niagara Peninsula and Eastern Lake Erie basin, *Journal of Paleolimnology* 17: 377-402.

Poole MA and O'Farrell PN (1971) The assumptions of the linear regression model, *Transactions of the Institute of British Geographers* 52:145-158.

Quinn FH (2002) Secular changes in Great Lakes water level seasonal cycles, *Journal of Great Lakes Research* 28(3): 451-465.

Quinn FH (1999) Paleo lake levels - The last four-thousand years, in Sellinger CE and Quinn FH (Eds) *Proceedings of the Great Lakes paleo-levels workshop: The Last 4000 years*. Ann Arbor, MI: Great Lakes Environmental Research Laboratory.

Quinn FH and Sellinger CE (2006) A reconstruction of Lake Michigan-Huron water levels derived from tree ring chronologies for the period 1600-1961, *Journal of Great Lakes Research* 32(1): 29-39.

Quinn FH and Sellinger CE (1990) Lake Michigan record levels of 1838, a present perspective, *Journal of Great Lakes Research* 16(1): 133-138.

R Development Core Team (2005). *R: A language and environment for statistical computing*, Vienna, Austria: R Foundation for Statistical Computing, [URL] http://www.R-project.org, Last viewed on August 10, 2006.

Reilly JP (2002) The GPS Observer: Dilution of Precision, *Point of Beginning*, February, [URL] http://www.pobonline.com, Last viewed on August 10, 2006.

Ribeiro Jr. PJ and Diggle PJ (2001) geoR: A package for geostatistical analysis, *R-News* 1(2): 15-18.

Robinson AH, Morrison JL, Muehrcke PC, Kimerling AJ, and Guptill SC (1995) *Elements of Cartography, Sixth Edition*, New York: John Wiley & Sons, Inc.

Roman DR, Wang YM, Henning W and Hamilton J (2004) Assessment of the new national geoid height model, GEOID03. 2004 ACSM/TAPS Conference and Technology Exhibition, Nashville, TN, 14pp. Available online: http://www.ngs.noaa.gov/GEOID/geolib.html (Last viewed on November 1, 2005).

Schaetzl RJ (2001) Late Pleistocene ice-flow directions and the age of glacial landscapes in northern Lower Michigan, *Physical Geography* 22:28-41.

Schaetzl RJ, Drzyzga SA, Weisenborn BN, Kincare KA, Lepczyk XD, Shein KA, Dowd CM, and Linker J (2002) Measurement, Correlation and Mapping of Glacial Lake Algonquin shorelines in Northern Michigan, *Annals of the Association of American Geographers* 92(3):399-415.

Schlather M (2001) Simulation and analysis of random fields, *R-News* 1(2): 18-20.

Shearer JW (1990) The accuracy of digital terrain models, In Petrie G and Kennie TJM (eds) *Terrain modeling in surveying and civil engineering*, New York: McGraw Hill, p315-336.

Shortridge AM (2001a) Topics on uncertainty in Geographic Information Science, *PhD Dissertation*, University of California, Santa Barbara.

Shortridge AM (2001b) Chapter 11: Characterizing uncertainty in digital elevation models, in Hunsaker CT, Goodchiled MF, Friedl MA and Case TJ (Eds) *Spatial uncertainty in ecology: implications for remote sensing and GIS applications*, New York, New York: Springer, p238-257.

Simas T, Nunes JP, and Ferreira JG (2001) Effects of global climate change on coastal salt marshes, *Ecological Modeling* 139: 1-15.

Smith DA and Milbert DG (1999) The GEOID96 high resolution geoid height model for the United States, *Journal of Geodesy* 73(5): 219-236.

Smith DE, Cullingford RA and Firth CR (2000) Patterns of isostatic land uplift during the Holocene: evidence from mainland Scotland, *The Holocene* 10(4): 489-501.

Smithson M (1989) *Ignorance and uncertainty: Emerging paradigms,* New York, New York: Springer Verlag.

Sly PG and Lewis CFM (1972) The Great Lakes of Canada - Quaternary geology and limnology: *International Geological Congress 24th Field Excursion A43 Guidebook.*

Spencer JW (1891a) Deformation of the Algonquin beach and birth of Lake Huron, *American Journal of Science* 41: 11-21.

Spencer JW (1891b) Origin of the basins of the Great Lakes of America, *American Geologist* 7: 86-97.

Spencer JW (1888) The St. Lawrence Basin and the Great Lakes (Abstract), *Proceedings of the American Association for the Advancement of Science* 37:197-199.

Spurr SH and Zumberge JH (1956) Late Pleistocene features of Cheboygan and Emmet Counties, Michigan, *American Journal of Science* 254:96-109.

Stanley GM (1945) Prehistoric Mackinac Island, *Michigan Geological Survey Publication 43.*

Stanley GM (1936) Lower Algonquin beaches of the Penetanguishene Peninsula, *Geological Society of America Bulletin* 47(12): 1933-1960.

Stein ML (1999) *Interpolation of spatial data: Some theory for Kriging,* New York: Springer.

Taylor FB (1897) Notes on the abandoned beaches of the north coast of Lake Superior, *American Geologist* 20: 111-128.

Taylor FB (1895) The Munuscong Islands, *The American Geologist* 15:24-33.

Taylor FB (1894) A reconnaissance of the abandoned shore lines of the south coast of Lake Superior, *American Geologist* 13: 365-383.

Teller TJ (2002) Reply of the comment by P.F. Karrow, *Quaternary Science Reviews* 21: 2119-2122.

Thompson TA (1992) Beach-ridge development and lake-level variation in southern Lake Michigan, In Donoghue JF, Davis RA, Fletcher CH, and Suter JR, Quaternary Coastal Evolution, *Sedimentary Geology* 80: 305-318.

Thompson TA and Baedke SJ (1999) Strandplain evidence for reconstruction late Holocene lake-levels in the Lake Michigan basin, In Sellinger CE and Quinn FH (Eds) *Proceedings of the Great Lakes Paleo-Levels Workshop: The last 4000 years, NOAA Technical Memorandum ERL GLERL-113*, p.30-34.

Thompson TA and Baedke SJ (1997) Strandplain evidence for late Holocene lake-level variations in Lake Michigan, *Geological Society of America Bulletin* 109: 666-682.

Thompson TA and Baedke SJ (1995) Beach-ridge development in Lake Michigan: shoreline behavior in response to quasi-periodic lake-level events, *Marine Geology* 129: 163-174.

Thompson TA, Fraser GS, and Hester NC (1991) Lake-level variation in southern Lake Michigan: Magnitude and timing of fluctuations over the past 4,000 years, *Illinois-Michigan NOAA Sea Grant Special Report, IL-IN-SR-91-2*, 19p.

Tinkler KJ and Pengally JW (1995) Great Lakes response to catastrophic inflows from Lake Agassiz: some simulations of a hydraulic geometry for chained lake systems, *Journal of Paleolimnology* 13(3): 251-266.

Titus JG and Richman C (2001) Maps of lands vulnerable to sea level rise, *Climate Research* 18(3): 205-228.

Trimble Navigation Limited (2002) *Pathfinder Office Software v2.7.* Trimble Navigation LTD: Sunnyvale, CA.

Tushinghan AM (1992) Postglacial uplift predictions and historical water levels of the Great Lakes, *Journal of Great Lakes Research* 18(3): 440-455.

Tushingham AM and Peltier WR (1991) ICE-3G: A new global model of late Pleistocene deglaciation based upon geophysical predictions of post-glacial relative sea level change, *Journal of Geophysical Research* 96: 4497-4523.

US Coast Guard Navigation Center (2004) *GPS Status message archives.* Alexandria, VA: US Coast Guard Navigation Center, [URL] http://www.navcen.uscg.gov/gps/status_and_outage_info.htm.

US Geological Survey (2004) *National Elevation Dataset,* Sioux Falls, SD: USGS National Center for Earth Resources Observation and Science, [URL] http://ned.usgs.gov/Ned/

Veregin H (1997) The effects of vertical error in digital elevation models on the determination of flow-path direction, *Cartography and Geographic Information Systems* 24: 67-79.

Weibel R and Heller M (1991) Chapter 19: Digital terrain modeling, In Goodchild MF and Rhind D (eds) *Geographic Information Systems, Principles and Applications*, New York: Taylor & Francis.

Wolf D (1985) An improved estimate of lithospheric thickness based on a reinterpretation of tilt data from Pleistocene Lake Algonquin, *Canadian Journal of Earth Sciences* 22: 768-773.

Wolf PR and Dewitt BA (2000) *Elements of photogrammetry with applications in GIS, 3rd edition*, Boston, MA: McGraw Hill.

Wood J (1996) The Geomorphological characterisation of digital elevation models, *PhD Dissertation*, University of Leicester, England.

Wood WL, Stockberger MT, and Madalon LJ (1994) Modeling beach and nearshore profile response to lake level change, *Journal of Great Lakes Research* 20(1): 206-214.

Zurek PJ, Nairn RB, and Thieme SJ (2003) Spatial and temporal considerations for calculating shoreline change rates in the Great Lakes basin, *Journal of Coastal Research, Special Issue 38*: 125-146.